7-15-2020 5:00 PM

The Migration and Wear of Reverse Total Shoulder Arthroplasty

Madeleine L. Van de Kleut, *The University of Western Ontario*

Supervisor: Teeter, Matthew G., *The University of Western Ontario*
A thesis submitted in partial fulfillment of the requirements for the Doctor of Philosophy degree in Biomedical Engineering
© Madeleine L. Van de Kleut 2020

Abstract

Reverse total shoulder arthroplasty (RTSA) inverts the ball and socket geometry of the shoulder. Though projected to become the most common shoulder replacement in the next decade, RTSA suffers from a high complication and revision rate, with implant loosening requiring revision. As the number of indications and demand from younger patients for RTSA continues to grow, there is the need to identify implant fixation techniques that promote longevity.

Radiostereometric analysis (RSA) is the current standard for measuring implant migration, which, if continuous in the first year postoperatively is highly predictive of later loosening and failure. RSA has also been used to measure polyethylene wear, known to contribute to implant loosening through periprosthetic bone resorption. The objectives of this thesis were to compare early implant migration between different RTSA fixation techniques, and to assess the in vivo polyethylene wear rate of RTSA at mid-to-long-term follow-up.

To accomplish these objectives, the use of RSA for RTSA was first validated using a phantom setup. Subsequently, patients were prospectively randomized to compare cemented to press-fit humeral stems, and bone graft to porous metal-augmented glenosphere baseplates. Imaging was acquired postoperatively through one year. Separately, patients with an implant term-of-service greater than five years were recruited and imaged at a single timepoint. All migration analyses were performed in model-based RSA, with the addition of an in-house software for wear analysis.

Significantly greater migration was observed with press-fit compared to cemented stems six months and one year postoperatively, though both groups demonstrated stability from six months onward. There were no differences at any time point between glenosphere lateralization groups. Polyethylene wear was measurable and multidirectional, with values comparable to simulation studies.

The primary contribution of this work is the first-ever clinical RSA for RTSA study, the results of which provide the best possible evidence on the predicted longevity of cemented vs. press-fit humeral fixation, and bony vs. porous metal glenosphere lateralization. The secondary contribution is the first evaluation of in vivo RTSA polyethylene wear; the results from both studies influencing clinical care and the design of next-generation shoulder implants.

Keywords: reverse total shoulder arthroplasty, radiostereometric analysis, implant migration, glenosphere augmentation, polyethylene wear, patient-reported outcome measures

Summary for lay audience

One in five Canadians suffers from arthritis, a progressive joint disease. With no cure, many patients opt for joint replacement, whereby the ends of the damaged bones are replaced with metal implants and separated with a plastic liner. Over time, artificial joints can become loose, causing pain and reduced function. Loosening can result from initially poor attachment between the implant and bone, and made worse by wear of the plastic liner. It is best to remove and replace loose implants, though this procedure is expensive and patient satisfaction decreases each time it is performed. For this reason, it is important to identify implant designs and materials with strong initial attachment. It is known that implant movement in the first year after surgery is predictive of later loosening requiring reoperation. By identifying implants that move more than others, they can be removed from the orthopedic market prior to widespread use. The objectives of this thesis were to use a three-dimensional x-ray technique to compare the early movement of implant components in reverse total shoulder replacement (RTSR), as well as wear of the plastic liner. Patients were recruited and randomized into implant groups comparing the use of bone cement to no bone cement with the metallic stem inserted into the upper arm bone, and the use of either bone graft or porous metal structural enhancement with the metallic hemisphere attached to the shoulder blade. A separate group of patients, with at least five years of use of their joint replacement, were recruited to investigate mid-to-long-term wear of the plastic liner. Results show that stems with bone cement had less movement than stems without, though neither group moved appreciably after six months, suggesting long-term stability. There were no differences in metal hemisphere movement using either bone graft or porous metal structural enhancement. The observed liner wear was measurable and comparable to estimates from simulation studies. Overall, this work is the first to compare different implant-bone attachment techniques in RTSR, and first to measure wear of the plastic liner inside the body. Results from this work will influence future implant design and clinical care.

Co-authorship statement

Chapter 3:   Madeleine L. Van de Kleut, Xunhua Yuan, George S. Athwal, Matthew G. Teeter

MLV: Study design, data acquisition and analysis, manuscript preparation. XY: Study design, phantom preparation, critical manuscript review. GSA: Phantom preparation, critical manuscript review. MGT: Study design, critical manuscript review. Percent of work conducted solely by the student MLV: 90%.

Publication status: Published

> Van de Kleut ML, Yuan X, Athwal GS, Teeter MG. Validation of radiostereometric analysis in six degrees of freedom for use with reverse total shoulder arthroplasty. J Biomech. 2018;68:126–131. doi:10.1016/j.jbiomech.2017.12.027

Chapter 4:   Madeleine L. Van de Kleut, Xunhua Yuan, George S. Athwal, Matthew G. Teeter

MLV: Patient recruitment and communication, data acquisition and analysis, manuscript preparation. XY: Data analysis, critical manuscript review. GSA: Surgeon, study design, critical manuscript review. MGT: Study design, critical manuscript review. Percent of work conducted solely by the student MLV: 85%.

Publication status: Not submitted for publication

Chapter 5:   Madeleine L. Van de Kleut, Xunhua Yuan, Matthew G. Teeter, George S. Athwal

MLV: Patient recruitment and communication, data acquisition and analysis, manuscript preparation. XY: Data analysis, critical manuscript review. MGT: Study design, critical

manuscript review. GSA: Surgeon, study design, critical manuscript review. Percent of work conducted solely by the student MLV: 85%.

Publication status: Not submitted for publication

Chapter 6: Madeleine L. Van de Kleut, Xunhua Yuan, George S. Athwal, Matthew G. Teeter

MLV: Study design, phantom modeling and preparation, data acquisition and analysis, manuscript preparation. XY: Critical manuscript review. GSA: Phantom preparation, critical manuscript review. MGT: Study design, critical manuscript review. Percent of work conducted solely by the student MLV: 90%.

Publication status: Published

Van de Kleut ML, Yuan X, Athwal GS, Teeter MG. Validation of in vivo linear and volumetric wear measurement for reverse total shoulder arthroplasty using model-based radiostereometric analysis. J Orthop Res. 2019;37(7):1620–1627. doi:10.1002/jor.24294

Chapter 7: Madeleine L. Van de Kleut, George S. Athwal, Kenneth J. Faber, Matthew G. Teeter

MLV: Study design, patient recruitment and communication, data acquisition and analysis, manuscript preparation. GSA: Surgeon, study design, critical manuscript review. KJF: Surgeon, critical manuscript review. MGT: Study design, critical manuscript review. Percent of work conducted solely by the student MLV: 95%.

Publication status: In Press

Van de Kleut ML, Athwal GS, Faber KJ, Teeter MG. In vivo volumetric and linear wear measurement of reverse shoulder arthroplasty at minimum 5-year follow-up. J Shoulder Elb Surg. 2020. doi:10.1016/j.jse.2019.11.031. [Epub ahead of print]

Acknowledgements

The completion of this thesis was only possible thanks to the support from a number of people and organizations. First and foremost, I would like to thank my primary supervisor Dr. Matthew Teeter. Matt is prolific in all he does, and approaches research and problem solving with a tenacity that has contributed immensely to my graduate education. His guidance and encouragement have supported my development as a scientist, collaborator, and author, balancing direction with the freedom to pursue my research interests.

I would like to thank Dr. George Athwal, the collaborating surgeon in our shoulder studies, and the team of nurses and administration – especially Andrea Cullen and Katrina Munro – at the Hand and Upper Limb Center for their clinical and research ethics expertise. Despite his celebrity status in the world of shoulder arthroplasty, Dr. Athwal always has the time to meet and discuss the clinical impact of our research, providing new ideas for research questions and the motivation to realize them. The opportunity to conduct a clinical trial, from recruitment, to observing surgery, and communicating with patients through follow-up has provided me with multiple perspectives of healthcare, inspiring a continued interest in everything biomedical.

A special thank you to Dr. Xunhua Yuan, a renowned leader in radiostereometric analysis, for his endless patience and perseverance in helping me with the technique. Without his effort, much of the migration data (Chapters 4 and 5) would not be complete. I would also like to thank Rudy Baronette as x-ray technician for our clinical studies, and for always teaching me something new about the imaging modality. Additionally, Drs. Jim Johnson and Ana Luisa Trejos have been dedicated members of my advisory committee, and I thank them for providing expertise in engineering, biomechanics, and for always asking questions that enhance my research methods and improve my communication.

I thank Jenna, Jonathan, Shawn, Kevin, and everyone at Wright Medical for their continued interest and support, providing implants and CAD models that allow us to

conduct studies furthering orthopedic research. To Matt and Tom at ADEISS, thank you for helping with our additive manufacturing needs.

I am grateful for the opportunities I have had as a graduate student at Western, presenting my research at regional, provincial, national, and international conferences thanks to funding from the Ontario Graduate Scholarship, Queen Elizabeth the II Scholarship in Science and Technology, Canadian Institutes of Health Research Canada Graduate Scholarship (Master's), and the Transdisciplinary Bone and Joint Training Award (Western's Bone and Joint Institute). The Bone and Joint Institute's Collaborative Training Program in Musculoskeletal Health Research was a highlight of my graduate studies, and in particular the workshops and Health Research Journal Club held in collaboration with the Ivey International Center for Health Innovation.

I would like to recognize all the brilliant minds and smiles I have met along this journey – to my lab mates, the Biomedical Engineering Graduate Student Committee, and the fifth floor of Robarts – thank you for keeping me sane and never being too busy for an extra cup of coffee. To my incredible friends, these past four years would not have been as joyful without you. To my family, thank you for being there and supporting me, and my Science Fair projects, from day one.

Table of Contents

List of tables

List of figures

List of appendices

List of abbreviations

ANOVA	Analysis of variance
ALARA	As low as reasonably achievable
BIO-RSA	Bony increased offset reverse shoulder arthroplasty
CAD	Computer-aided design
CONSORT	Consolidated standards of reporting trials
CN	Condition number
CT	Computed tomography
FDA	Food and Drug Administration (United States)
HXLPE	Highly cross-linked polyethylene
CTA	Cuff tear arthropathy
MBRSA	Model-based radiostereometric analysis
MC	Million cycles
MCID	Minimal clinically important difference
MLWD	Maximum linear wear depth
MTPM	Maximum total point motion
PROM	Patient-reported outcome measure
RE	Reverse engineered
RSA	Radiostereometric analysis
RTSA	Reverse total shoulder arthroplasty
UHMWPE	Ultra-high molecular weight polyethylene

Nomenclature

Δ	Change
°	Degree
μ	Micro
2D	Two-dimensional
3D	Three-dimensional
CI	Confidence interval
cm	Centimeter
eV	Electronvolt
kg	Kilogram
kVp	Kilovolt-peak
mAs	Milliamp-second
mm	Millimeter
SD	Standard deviation

1 Introduction

Note a glossary is provided in Appendix A defining the clinical terms used in this thesis.

As the Canadian population ages and the incidence of osteoarthritis continues to grow, so too does the demand for joint replacement surgery. While hip and knee replacement account for the majority of procedures, advances in surgical technique and implant design have led to exponential growth in the demand for shoulder replacement, with demand projected to increase by approximately 750% in patients older than 55 by 2030.[25,112] For patients suffering from shoulder osteoarthritis without rotator cuff injury, anatomic shoulder replacement effectively relieves pain and restores arm elevation. The subset of the population with rotator cuff deficiency, however, achieves little functional benefit from an anatomic implant design (§ 2.2.2). By inverting the shoulder's ball and socket configuration, the humerus is medialized and distalized, increasing the deltoid muscle's mechanical advantage. This enables the patient to elevate their arm without the need for an intact rotator cuff.

Initially proposed as a salvage procedure for elderly patients with limited functional demand, indications for 'reverse' total shoulder arthroplasty (RTSA) have expanded over the past decade, making it the most common primary shoulder replacement.[29] Despite short-to-midterm clinical success, RTSA has a relatively high complication and reoperation rate, at approximately 13 and 9% for primary procedures, respectively.[176] With the cost of revision surgery approximately 80% higher than primary procedures and resulting in poorer clinical outcomes, the failure rate of RTSA poses a burden not only to the patient, but also the healthcare system.[14,25,93] As younger patients face potentially multiple revision surgeries in their lifetime, there is the need for primary implant longevity.

1.1   Motivation

In efforts to address the complications frequently observed with RTSA, and in particular, aseptic implant loosening, a number of in vitro and in silico studies have been conducted, leading to design changes observed in the new implants brought to market.[40,74,79,83,85,89] While these studies have the advantage of being relatively cost-effective, fast, and repeatable, the intricacy of the in vivo environment is simplified during simulation, likely underrepresenting the variability of bone quality, muscle tone, and less objective measures such as lifestyle and actual use of the joint by individual patients. Traditionally, without long-term clinical and radiographic outcomes, it is unclear whether these new designs are superior to the current standards.

Having undergone similar design iterations previously, the lower limb literature has shown that early migration of implant components is predictive of later gross loosening and failure. Early migration can be measured in the first year postoperatively, where implants that stabilize in their position and orientation within the bone are likely to remain well-fixed, and those that demonstrate continuous migration are likely to require revision.[119,120,129] The gold standard for assessing early implant migration is radiostereometric analysis (RSA) – a calibrated, dual-focus x-ray technique. In addition to implant migration, RSA has more recently been used to measure the linear and volumetric wear of polyethylene bearing surfaces in the hip and knee, providing an estimate for in vivo wear rates.[36,37,46,123] Excessive polyethylene liner wear can lead to an inflammatory response in the surrounding tissue, initiating bone resorption around the implant and compromising fixation. Using RSA, it is possible to identify implant designs, materials, and fixation techniques that exhibit inferior performance and withdraw them from clinical practice prior to widespread market distribution and use. Presently, to the best of our knowledge, no studies have investigated the in vivo migration and wear of RTSA components, leaving the question of 'what is normal' unanswered.

1.2 Research and specific thesis objectives and hypotheses

The purpose of this research as a whole was to determine the typical pattern and magnitude of humeral stem and glenosphere migration, as well as the ultra-high molecular weight polyethylene wear rate, in vivo, in reverse total shoulder arthroplasty using radiostereometric analysis. The thesis is structured as follows:

Chapter 1:   *Introduction.*

Chapter 2:   *Literature review* – an overview of relevant background and the current state of the art.

Chapter 3:   *Validation of radiostereometric analysis in six degrees of freedom for use with reverse total shoulder arthroplasty* – validate the use of model-based radiostereometric analysis for use with reverse total shoulder arthroplasty in a phantom setup.

Chapter 4:   *Cemented versus press-fit humeral stem migration in reverse total shoulder arthroplasty: a prospective, randomized clinical trial* – using model-based radiostereometric analysis, evaluate the fixation between cemented and press-fit humeral stems in reverse total shoulder arthroplasty in the first year postoperatively. It is hypothesized that press-fit stems will migrate more than cemented stems in the first six months postoperatively, then stabilize.

Chapter 5:   *BIO-RSA versus augmented glenosphere migration in reverse total shoulder arthroplasty: a prospective, randomized clinical trial* – using model-based radiostereometric analysis, evaluate the fixation between BIO-RSA and porous metal augmented glenospheres in reverse total shoulder arthroplasty in the first year postoperatively. It is hypothesized

that both glenosphere lateralization techniques will demonstrate immediate fixation.

Chapter 6: *Validation of in vivo linear and volumetric wear measurement for reverse total shoulder arthroplasty using model-based radiostereometric analysis* – validate the use of model-based radiostereometric analysis for in vivo volumetric and linear polyethylene wear measurement in the reverse shoulder.

Chapter 7: *In vivo volumetric and linear wear measurement of reverse shoulder arthroplasty at minimum 5-year follow-up* – assess the in vivo polyethylene wear rates of reverse total shoulder arthroplasty using model-based radiostereometric analysis. It is hypothesized that polyethylene wear is measurable and correlated with term-of-service.

Chapter 8: *Conclusions and future directions.*

2 Literature review

2.1 The shoulder

2.1.1 Anatomy

Composed of three bones and a series of muscles, tendons, and ligaments, the shoulder has the greatest range of motion of any joint in the body and is also one of the most complex. The scapula, also known as the shoulder blade; the clavicle, also known as the collar bone; and the upper humerus are the bones that make up the shoulder, each with a dense outer layer of cortical bone, and a spongy interior of cancellous, or trabecular bone (Figure 2.1).
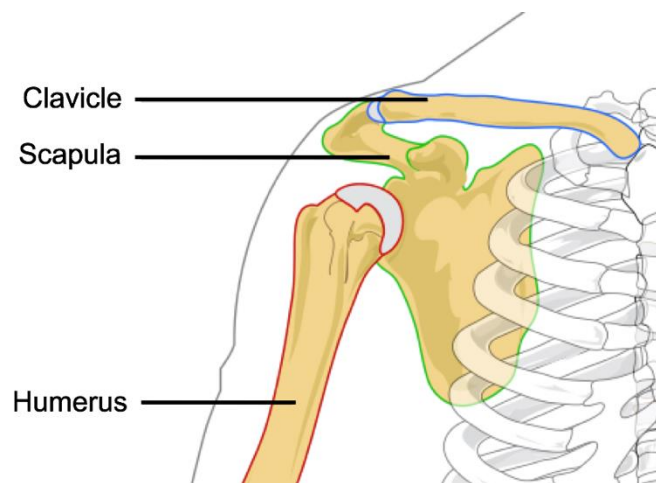
Figure 2.1 Anterior view of the three bones comprising the shoulder: the humerus, scapula, and clavicle. Figure under license to use and modify.

The superior-most scapular process, referred to as the acromion, meets with the clavicle creating the acromioclavicular joint. Similarly, the inferior-lateral scapula fossa, referred to as the glenoid, meets with the humeral head to create the glenohumeral joint. The articulating components are separated by a layer of articular cartilage to reduce friction during shoulder movement (Figure 2.2).
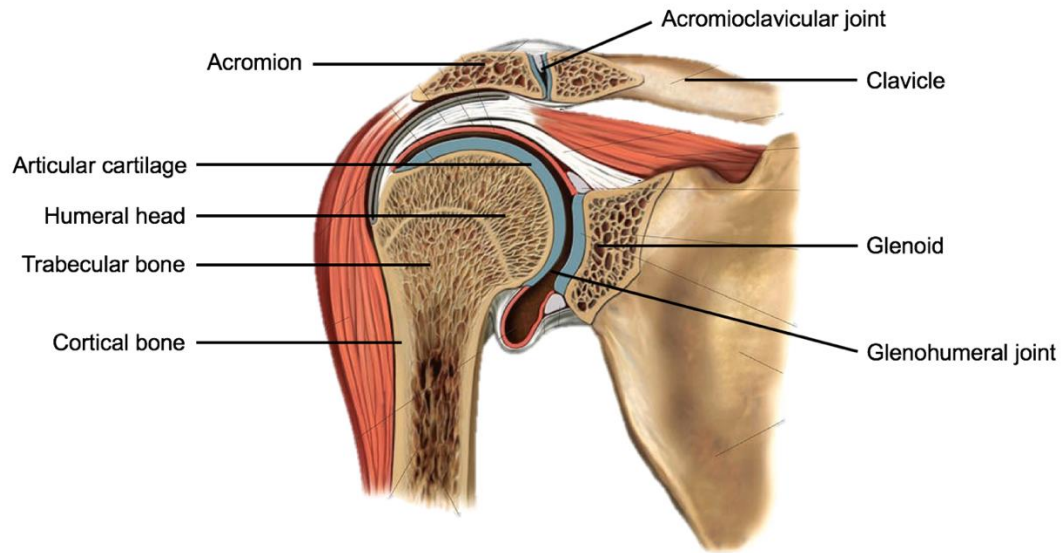
Figure 2.2 Anterior cross-section of bony anatomy of the shoulder joint. Figure under license to use and modify.

The focus of this work is the glenohumeral joint, hereafter referred to as the shoulder. The shoulder is commonly thought of as a ball-and-socket joint, like the hip, and while the articular surface of the humeral head is approximately spherical,[54] the glenoid is only slightly concave and has a greater radius of curvature than the humeral head.[57] This lack of congruency in articulating surfaces enables the six degrees of motion capable by the shoulder, but also means it is susceptible to injury. In order to prevent injury and joint degeneration, the shoulder has a number of muscles, tendons, and ligaments to enhance stability during motion.

Working from the inside out, the joint is filled with synovial fluid, a lubricating agent that reduces friction between the glenoid and humeral head and nourishes the articulating cartilage. The glenoid labrum, a fibrocartilaginous rim that extends the circumference of the glenoid cavity, deepens the shoulder's 'socket' and increases stability. The synovium and glenoid labrum are enclosed by a joint capsule made of strong connective tissue, which extends from the glenoid neck and inserts into the neck of the humeral head. The glenohumeral joint is further protected by the coracohumeral, glenohumeral, and transverse humeral ligaments (Figure 2.3).
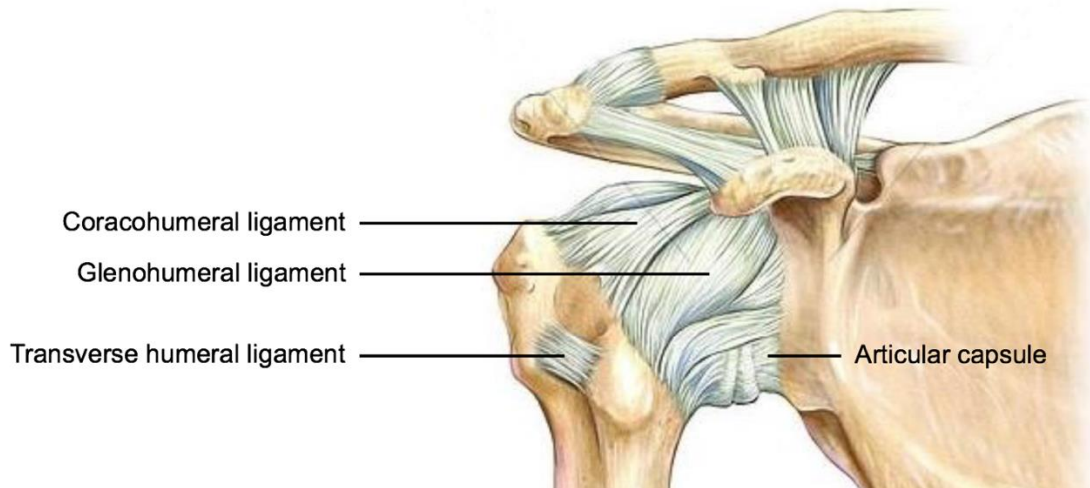
Figure 2.3 Anterior view of glenohumeral ligaments and articular capsule. Figure under license to use and modify.

The outermost components of the shoulder are the muscles and their respective tendons (inelastic cords of strong fibrous tissue that connect muscle to bone). The rotator cuff, composed of the subscapularis, supraspinatus, infraspinatus, and teres minor, connects the scapula to the humerus, with muscle tendons inserting on the humerus, and is responsible for the primary strength and stability of the shoulder (Figure 2.4a-d).
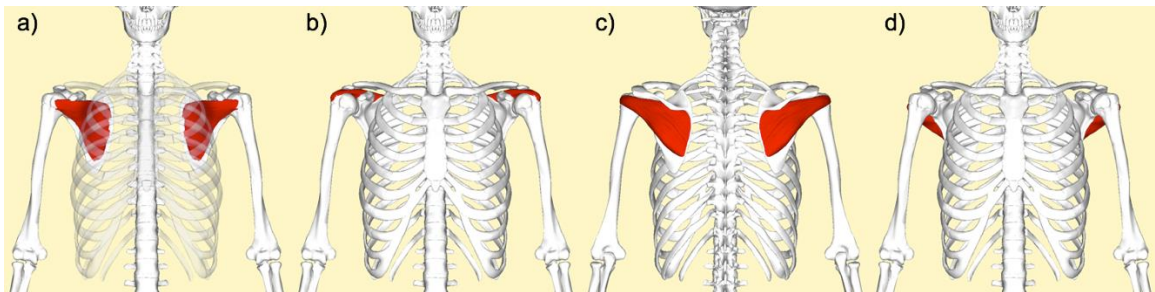
Figure 2.4 Anterior views of the (a) subscapularis and (b) supraspinatus, posterior view of the (c) infraspinatus, and anterior view of the (d) teres minor. Figures under license to use and modify.

The subscapularis is responsible for internal rotation of the arm, the supraspinatus helps in arm abduction, the infraspinatus adducts and rotates the arm externally, and the teres minor extends, adducts, and externally rotates the arm. Compressive forces applied by the rotator cuff muscles help keep the humeral head centered within the glenoid regardless of

the natural movement performed.[53] The deltoid, in addition to the rotator cuff, is also responsible for abduction, forward flexion, extension, and internal/external rotation of the arm (Figure 2.5a-c), with shoulder planes of motion depicted in Figure 2.6.
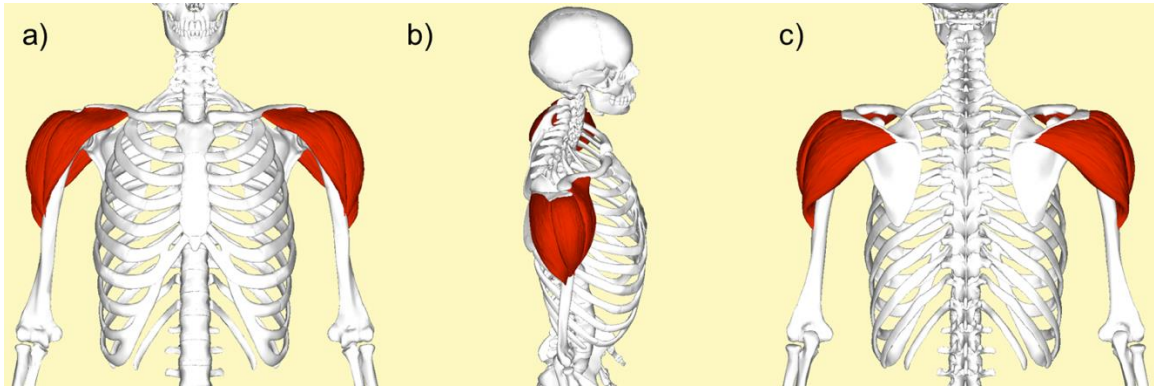
Figure 2.5 (a) Anterior, (b) lateral, and (c) posterior views of the deltoid. Figures under license to use and modify.
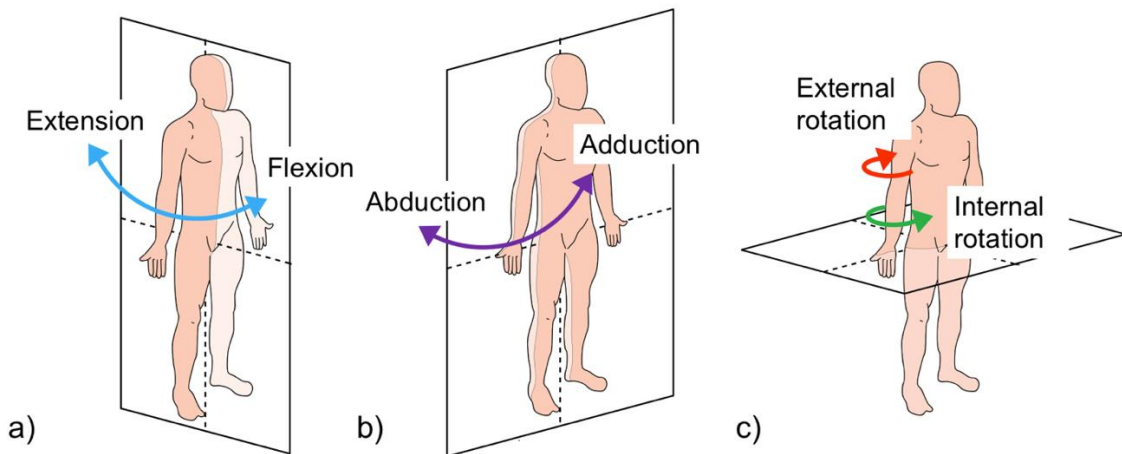
Figure 2.6 Motion along the (a) sagittal, (b) coronal, and (c) transverse planes of the body. Figures under license to use and modify.

2.1.2 Shoulder arthrosis

2.1.2.1 Osteoarthritis

Osteoarthritis (OA) is a progressive joint disease affecting one in five Canadians.[173] Commonly found in weight-bearing joints such as the hip and knee, OA can also affect

other joints of the body. The disease can be idiopathic (primary) or subsequent to trauma (secondary) and is characterized by the loss of articular cartilage, identified as joint space narrowing on radiographs.[66] With no cure, OA can lead to excessive pain and loss of function in the affected joint.[49] Osteoarthritis is increasingly being diagnosed in the shoulder, where the articular cartilage has degenerated on either the glenoid, humeral head, or both. These changes in the articular surface can lead to biomechanics that differ from a healthy shoulder joint. Consequently, atypical joint loading may result in focal stresses and bony glenoid deformity which inhibits joint movement.[87,163] The most effective solution for end-stage osteoarthritis is a joint replacement, whereby one or both sides of the joint are replaced with metal and plastic (§ 2.2).

2.1.2.2 *Rotator cuff tear*

Rotator cuff tears (RCT) are specific to the shoulder and occur when the tendon of one or more of the rotator cuff muscles is no longer fully attached to the humeral head. Rotator cuff tears can be further classified into massive rotator cuff tears (MRCT) and irreparable rotator cuff tears (IRCT). MRCTs are defined as complete tears in two or more tendons, where at least one of the tendons is retracted medially beyond the proximal humeral head.[110] What is defined as "irreparable" continues to change with advances in surgical technique, anchors, and suture strength, though it has been proposed that muscle degeneration in the form of fatty infiltration is prognostic of poorer functional outcomes postoperatively and the recurrence of RCTs.[50]

Tears can be partial-thickness or full-thickness and are most common in the supraspinatus tendon.[131] Approximately 25-50% of the population, increasing with age, has a full-thickness tear in at least one of their rotator cuff tendons, though they may not always be symptomatic.[148] Symptomatic RCTs account for more than 4.5 million physician visits in the United States each year, and are the most common reason for upper extremity pain and disability.[105]

Conservative treatment, in the form of physical therapy and rehabilitation, has been shown to alleviate symptoms in atraumatic partial and full-thickness tears and is promoted as the first line of treatment.[75] Should nonoperative therapies be insufficient, the rotator cuff can be repaired surgically in appropriate candidates,[3] though there remains limited evidence that surgical intervention improves outcomes to a greater degree than conservative treatment in the general population.[126]

2.1.2.3   Cuff tear arthropathy

In 1977, Charles S. Neer, an American orthopedic surgeon, described a series of unique clinical and pathologic findings specific to the shoulder, coining the term *cuff tear arthropathy* (CTA).[96] Neer sought to distinguish CTA from other shoulder pathologies in order to enhance physicians' understanding of its etiology and treatment. The proposed pathomechanics include both mechanical and nutritional factors. Mechanically, following massive rotator cuff tear, the humeral head becomes unstable and migrates upward. This upward migration is frequently associated with posterior dislocation and subsequent acromion, acromioclavicular, and coracoid wear. The tendon tears and atypical loading patterns lead to pain, reduced shoulder motion and loss of function. By reducing loads on the shoulder altogether, bone in the proximal humerus and glenoid becomes osteoporotic and the articular cartilage composition changes and atrophies. Nutritionally, a massive rotator cuff tear introduces a gap in the joint space, reducing internal pressure. This decreases the internal pressure gradient and quantity of joint fluid, and consequently nutrients are not perfused into the articular cartilage. The cartilage then atrophies, contributing to disuse arthritis. The result is cuff tear arthropathy – simply described as shoulder arthritis with associated rotator cuff tear – and treatment options were limited until the adoption of reverse total shoulder arthroplasty (§ 2.2.2).

2.1.2.4   Glenoid bone defects

Atypical loading patterns and focal stresses associated with cuff tear arthropathy can lead to glenoid deformity. In 1999, Walch et al. classified glenoid erosion in the transverse

plane into types A, B, or C based on 2D transverse computed tomography (CT) scans.[163] In 2016, an amendment was made to include types B3 and D to improve inter- and intra-observer reliability of the classification, as 3D CT reconstructions became the gold standard and undescribed glenoid morphologies were identified with increasing frequency.[12] Type A, the most common comprising more than half of cases, is characterized by the humeral head centered within the glenoid, with an average glenoid retroversion of 11.5°. Type A can be subdivided into A1, minor erosion, and A2, major erosion, leading to a centered glenoid concavity (Figure 2.7a). Major erosion was more prominent with increased age. Type B, present in approximately a third of cases, occurs when the humeral head is subluxated posteriorly and loads are distributed unevenly. Type B is subdivided into three subgroups, B1, B2, and B3, where B1 exhibits posterior joint space narrowing, osteophyte formation, and subchondral bone hardening; B2 exhibits posterior erosion, giving the glenoid a biconcave appearance; and B3 exhibits posterior erosion with a severity that results in a single concavity, at least 15° of retroversion, 70% posterior humeral head subluxation, or both (Figure 2.7b). Type C, occurring in approximately 9% of cases, is expressed as glenoid retroversion of greater than 25° and hypothesized as congenital (Figure 2.7c). Type D is defined as any glenoid exhibiting anteversion, or with humeral head anterior subluxation of less than 40% – a pathology that does not occur in normal shoulders (Figure 2.7d). Presently, the frequency of Type D glenoid has not been reported.
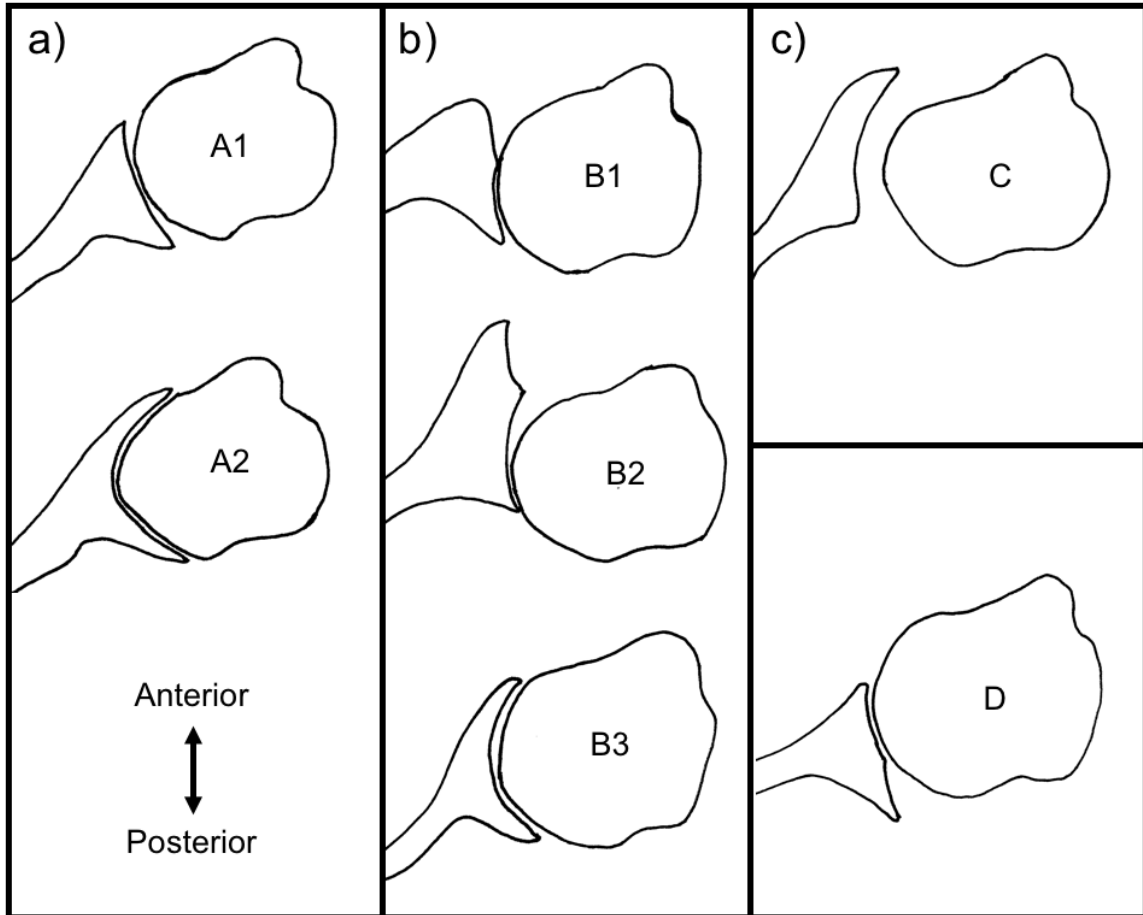
Figure 2.7 Walch glenoid erosion patterns: (a) Type A1-2, (b) Type B1-3, (c) Type C, and (d) Type D.

In 2001, the Favard classification for glenoid erosion in the coronal plane was established, based on radiographic evaluation from the true anteroposterior view in neutral rotation. Five types were described: E0, no erosion, E1, concentric erosion, E2, erosion limited to the superior aspect of the glenoid, E3, erosion extending to the inferior aspect of the glenoid, and E4, erosion limited to the inferior portion of the glenoid (Figure 2.8a-e).[84]

Both Walch and Favard classifications are used to evaluate glenoid erosion, as they describe erosion in orthogonal planes. The Walch classification describes erosion patterns typical to primary glenohumeral osteoarthritis, while the Favard classification describes erosion patterns most common in CTA, though it should be noted that erosion patterns

are highly variable.[84,163] Because glenoid bone defects vary widely between patients, there does not exist a one-size-fits-all joint replacement. For this reason, thoughtful preoperative assessment is necessary for an optimized surgical outcome.
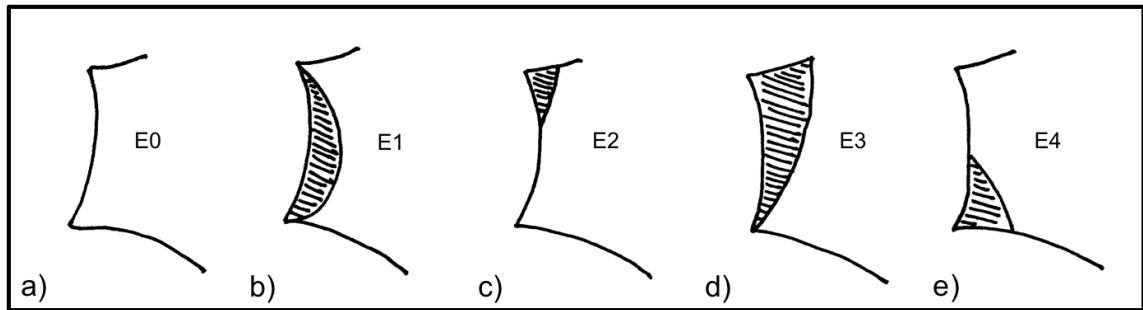
Figure 2.8 Favard glenoid erosion classification: (a) no erosion, (b) concentric erosion, (c) superior erosion, (d) erosion through inferior aspect, and (e) erosion restricted to inferior aspect of glenoid.

2.2 Shoulder replacement

2.2.1 Anatomic

The first modern-day shoulder replacements were presented in the 1950s by Charles S. Neer, the same surgeon responsible for the description of cuff tear arthropathy.[95] The earliest version of the prosthesis, an articular replacement for the humeral head, was intended for proximal humerus fracture. In the decades that followed, shoulder replacement design and surgical techniques improved, expanding indications to include osteo- and inflammatory arthritis, in addition to complex proximal humerus fractures.[8,108]

Anatomic, also known as conventional shoulder arthroplasty, can take the form of hemi-arthroplasty, where only one side of the joint is replaced, or total shoulder arthroplasty, where both sides of the joint are replaced. The humeral head is typically replaced with a cobalt-chrome articular surface and fixed within the metaphysis of the proximal humerus with either a titanium or cobalt-chrome cemented or press-fit stem. The glenoid articular cartilage is replaced with a polyethylene dish, usually fixed within the glenoid using pegs

or keels and bone cement. These artificial components mimic native shoulder anatomy (Figure 2.9). Advances in implant design have introduced short-stemmed and stemless humeral components, with the goal of salvaging as much bone as possible while maintaining fixation.[65]
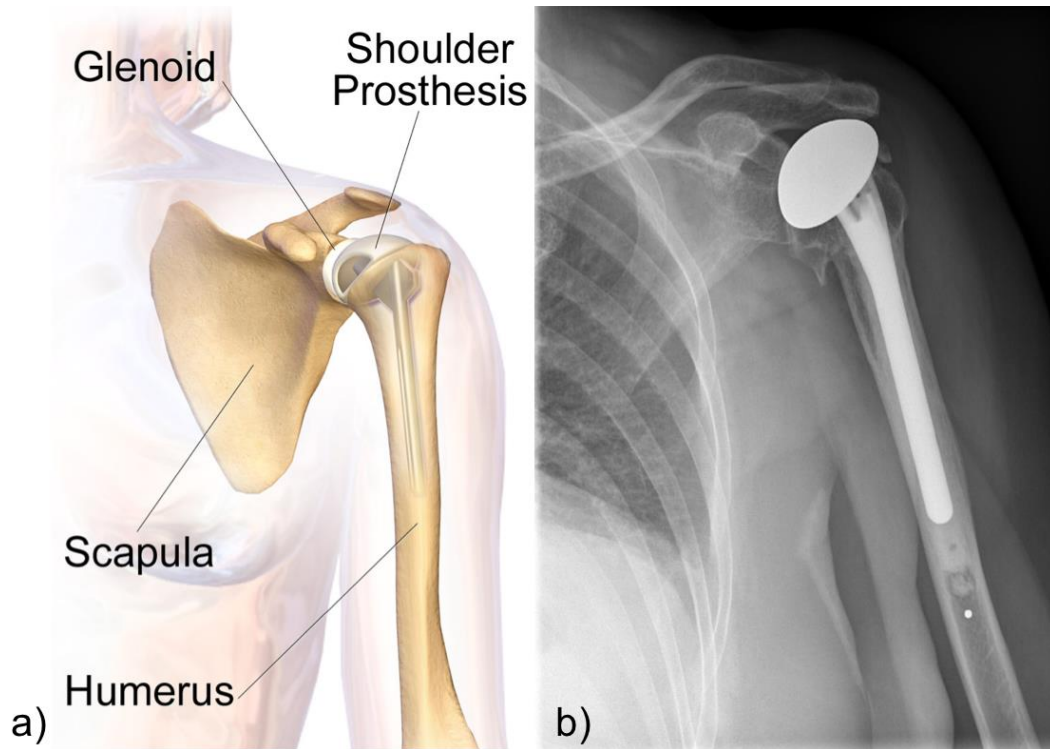
Figure 2.9 (a) Anatomic total shoulder replacement and (b) its corresponding x-ray (note the polyethylene glenoid component is radiolucent and does not show up on x-rays). Figures under license to use and modify.

While anatomic shoulder arthroplasty improves the functional outcome and reduces pain in patients with appropriate indications, its success is limited to patients with an intact rotator cuff.[68,137] This constraint on anatomic shoulder replacement emphasized the need for an alternative surgical approach appropriate for patients suffering from a variety of rotator cuff pathologies.

2.2.2 Reverse

Understanding that the rotator cuff plays an important role in glenohumeral stabilization, initial attempts to enhance stabilization without rotator cuff repair focused on fixed-fulcrum designs, with limited success – shoulder motion remained poor and the implants would loosen.[97] The 1970s saw the introduction of the 'reverse' shoulder arthroplasty configuration as we know it today, inverting native shoulder anatomy by placing a ball on the glenoid, and socket within the proximal humerus. By inverting the ball and socket, the deltoid lever arm is lengthened, and patients are able to elevate their arm more easily. These first-generation constrained prostheses, however, introduced a joint center of rotation lateral to the scapula (in a native shoulder joint, the center of rotation is within the humeral head (Figure 2.10a)). This lateralization meant that joint loads would be transferred to the glenoid with not only a compressive line of action, but with significant torque about the joint's center of rotation. This excessive torque eventually led to implant loosening and the failure of many of these components.[40] It wasn't until 1985 that the future of reverse shoulder arthroplasty really started showing promise, its modern design credited to Paul Grammont, a French orthopedic surgeon.[15]

2.2.2.1   Grammont reverse prosthesis

As mentioned, the supraspinatus, used in active arm elevation, is also the most frequently torn part of the rotator cuff. The purpose of reverse total shoulder arthroplasty (RTSA), therefore, was to compensate for the lack of supraspinatus contractile potential by changing the biomechanics of surrounding accessory arm elevators – primarily, the middle deltoid. Grammont proposed a semi-constrained system that medialized the reverse's fixed center of rotation and distalized the humerus, thereby both lengthening the deltoid moment arm, increasing muscle tension, and improving prosthesis stability (Figure 2.10b). This prototype featured a concave polyethylene humeral component and two thirds of a sphere made of an alumina ceramic as the glenoid component, hereafter referred to as the glenosphere. Both components were cemented into the bone.[9] It should be noted that while the joint's center of rotation was now medialized, it was still lateral to the glenoid-implant interface and glenosphere loosening remained a problem (Figure 2.10c).
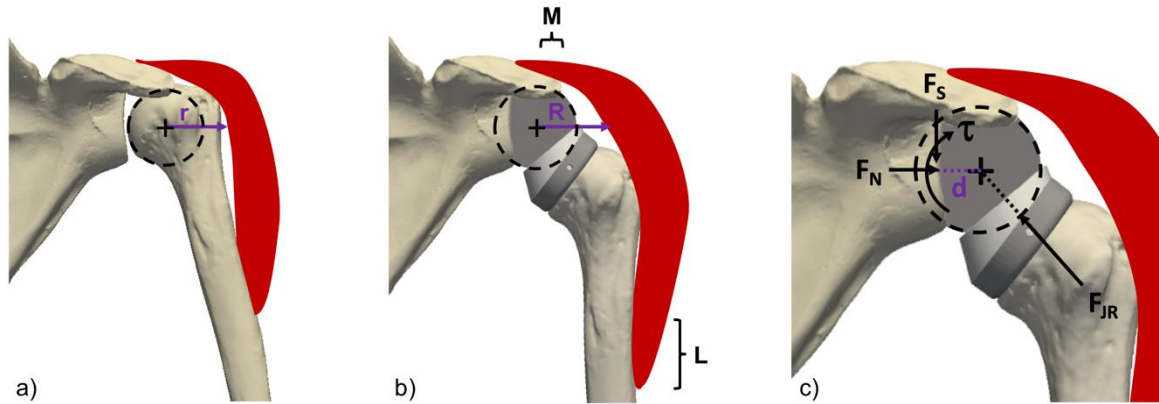
Figure 2.10 Biomechanics of the deltoid in (a) the native shoulder, and (b) the reverse shoulder. Medializing the joint's center of rotation (black plus) a distance M, we lengthen the deltoid lever arm R, where R = r + M. Distalizing the humerus a length L increases tension in the deltoid muscle fibers and their contractile potential. A center of rotation lateral to the bone-implant interface (c) introduces a torque $\tau = d \times F_S$, where d, the moment arm, is the distance from the center of rotation to the bone-implant interface and F_S are baseplate shear forces parallel to the bone-implant interface. F_{JR} is the joint reaction force, resisted by baseplate normal (F_N) and shear (F_S) forces.

2.2.2.2   Delta III reverse prosthesis

To address glenosphere loosening, Grammont's second generation reverse shoulder design, the Delta III (named after the deltoid muscle), introduced by DePuy in 1991, reduced the glenosphere from two thirds to half of a sphere, placing the joint's center of rotation at the glenoid-glenosphere interface. By placing the joint center of rotation at the bone-implant interface, the moment arm, and subsequent torque about the center of rotation, was significantly reduced. Further design alterations included the addition of a central peg and two divergent screws to resist shear forces at the bone-implant interface.[19] The Delta III easily became the most popular surgical solution for treating cuff tear arthropathy, and remained essentially unchanged – comprising of a metal humeral stem, polyethylene liner, metal glenosphere, glenoid baseplate, and glenoid screws – until the early 2000s (Figure 2.11).[51,94,139,170]
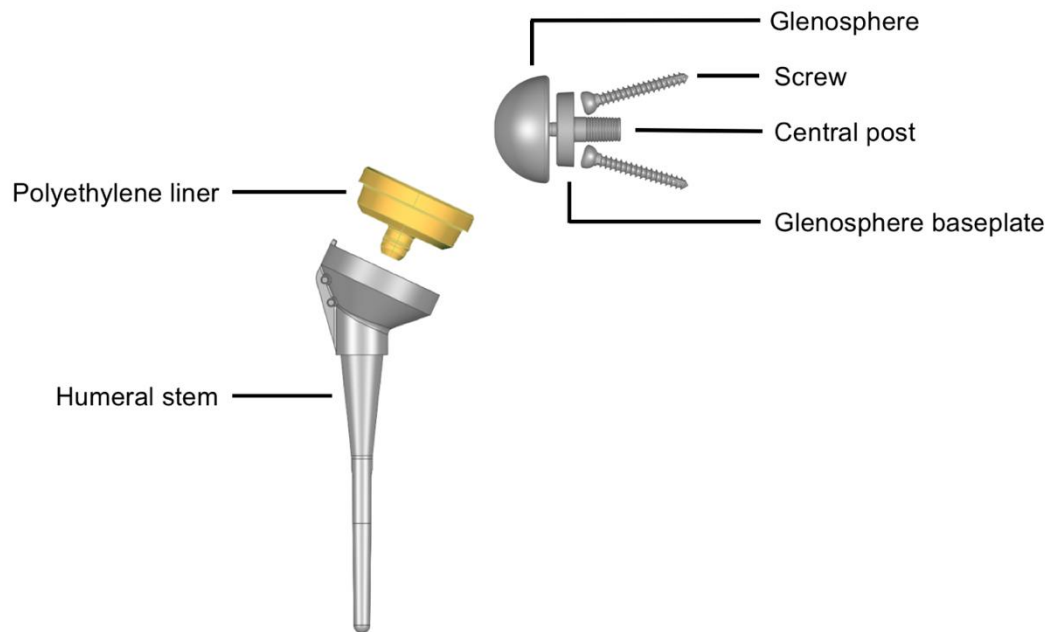
Figure 2.11 Standard reverse total shoulder components (Aequalis™ Reversed II, Tornier; similar to the Delta III).

2.2.2.3 Complications

Reverse total shoulder arthroplasty was approved by Health Canada in 2003 and the United States Food and Drug Administration (FDA) in 2004. Initially reserved as a salvage procedure for the elderly, the procedure has quickly become the most common primary shoulder arthroplasty, with its use projected to more than triple by 2020 (since 2014).[28,83] Increased growth rates are not without concern, however, as complications and revision burden remain a problem from both an economic and patient perspective.[31] Further, as demand for the procedure grows, it is likely that low-volume shoulder surgeons will perform a portion of these surgeries, contributing to increased revision rates.[11]

The reported complication rate for RTSA varies greatly, in part due to different definitions of 'complication' and recent advances in implant design and surgical technique.[16,30,39] A systematic review published in 2011 assessed 782 RTSAs, from 21 studies, and found a reintervention rate of 13.4%, a problem rate of 44%, and a

complication rate of 24% following the procedure. Reintervention included both reoperation and revision, a problem was defined as 'an intraoperative or postoperative event that was not likely to affect the patient's final outcome,' and a complication as 'any intraoperative or postoperative event that was likely to have a negative influence on the patient's final outcome.'[172] Examples of problems were heterotopic ossification, scapular notching, and radiographic lucent lines of the glenoid. Examples of complications were fracture, infection, dislocation, aseptic loosening, polyethylene disassociations, and nerve palsies. When considering only primary procedures (where RTSA was not performed as a revision for any reason), the frequency of reintervention reduced to 9.3%, problems to 6.0%, and complications to 13.4%. As a percent of all cases, the most frequently observed problems and complications were scapular notching at 35%, instability at 5%, infection at 4%, aseptic glenoid loosening at 4%, hematoma at 3%, humeral fracture at 3% and humeral loosening at 1%.[172] While some of these are a biologic response to surgery, such as hematoma and infection, those of a mechanical nature are described in greater detail below.

2.2.2.3.1   Scapular notching

In the late 1990s and early 2000s, the first mid- to long-term follow-ups with the Delta III started being reported. There was widespread observation of notching on the lateral aspect of the scapula.[84] This bony erosion was believed to result from impingement of the inferior portion of the polyethylene liner with the inferior scapular neck during internal/external rotation and flexion/extension with the arm in adduction.[78] Erosion patterns were subsequently classified by Sirveaux et al. into five grades: grade 0 representing no scapular defect, grade 1 affecting the lateral pillar of the scapula, grade 2 extending to the inferior screw, grade 3 extending beyond the inferior screw, and grade 4, extending to the glenosphere baseplate (Figure 2.12).[139] Extreme scapular notching, either grade 3 or 4, has been associated with glenoid component loosening, and remains an area of investigation.[122,161] A prognostic study of the Delta III found that glenosphere positioning, specifically superior glenosphere inclination, is highly predictive of scapular notching and associated with poorer outcomes.[138] Other studies have debated whether

scapular notching affects outcomes, though they agree that its incidence should be mitigated.[84,170]
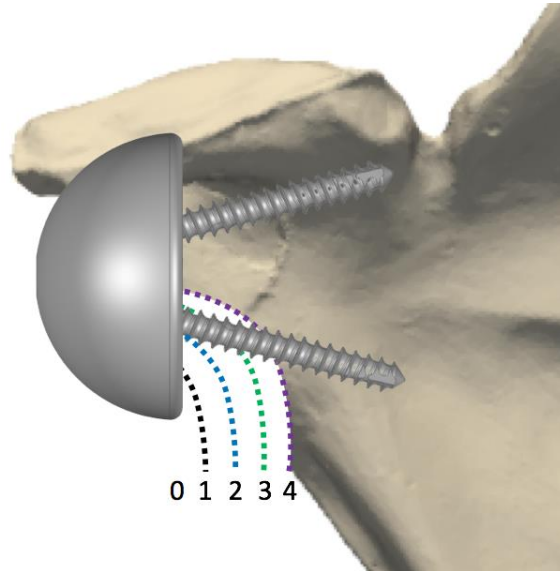
Figure 2.12 Sirveaux's scapular notching grading, from 0-4.

Proposed design modifications to reduce the incidence of scapular notching include reducing the polyethylene neck-shaft angle and cup depth, increasing glenosphere size, and lateralizing the glenosphere, increasing its distance from the scapular neck. All of these methods theoretically increase impingement-free range of motion, and have been successfully implemented in recent RTSA designs with complementing clinical outcomes.[17,67,156]

2.2.2.3.2 Instability

The modern reverse shoulder prosthesis is semi-constrained, meaning that only rotation, not translation, occurs about the joint's center of rotation. This design prevents the humerus from migrating superiorly in the absence of a functional rotator cuff and maintains the lengthened deltoid moment arm and appropriate muscle tensioning. In efforts to increase impingement-free range of motion, standard polyethylene cup depth is typically ~25% of the glenosphere diameter.[52] Biomechanical studies have shown that

standard cup depths are sufficient to prevent dislocation under normal loading conditions, however, dislocation and recurrent instability remain common and incompletely understood.[27,73] A case series published in 2017 evaluated early (within three months postoperatively) and late dislocations, showing that 68% of patients had inadequate soft-tissue tensioning, some due to partial axillary nerve injury perioperatively, and that remaining patients had asymmetric polyethylene wear (accounting for 60% of late dislocations), polyethylene mechanical failure, or impinging heterotopic ossification. Perhaps more concerning, however, was that approximately a third of patients, regardless of either early or late dislocation, suffered from recurrent instability following closed reduction or revision.[71]

Closed reduction, realigning the joint without surgery, is the most common initial treatment for dislocation. If disloction or instability is recurrent, however, it is recommended that the patient undergo revision surgery.[152] During revision, the polyethylene liner can be replaced with either a thicker offset (Figure 2.13a), increasing soft-tissue tensioning, or with a more constrained liner (Figure 2.13b), increasing the joint constraint. Increasing glenosphere size can also increase soft-tissue tensioning in the case where liner exchange is deemed insufficient.

Figure 2.13 Instability is frequently treated by (a) increasing polyethylene offset d → D, or (b) increasing constraint h → H.

2.2.2.3.3   Aseptic glenosphere loosening

Aseptic glenosphere loosening occurs when fixation between the glenosphere baseplate and glenoid itself is compromised without infection, and is assessed on x-rays as areas of 'radiolucency' – dark lines between the implant and bone. As the glenosphere is rigidly fixed to the baseplate, glenosphere loosening is synonymous with baseplate loosening for the purpose of this thesis. Physiologically, patients with rotator cuff arthropathies frequently present with varying degrees of glenoid bone loss and bone quality, and

therefore obtaining sufficient seating of the implant and stable fixation remains a challenge.[41] Biomechanically, we know that the first generation Delta III suffered from high rates of glenosphere loosening due to the joint's lateralized center of rotation, introducing a moment arm and subsequent torque at the bone-implant interface, but that medializing this center of rotation introduced high rates of scapular notching. A proposed solution to increase impingement-free range of motion while maintaining a center of rotation at the bone-implant interface is the use of augmented baseplates, discussed in length in § 2.2.3.1. Additional efforts to improve glenosphere fixation include the use of porous coatings to promote bony ingrowth, fixed-angle peripheral locking screws to maintain baseplate orientation, and bone-preserving augments specific to different glenoid defects.[70,109,143,154]

2.2.2.3.4   Aseptic humeral stem loosening

Aseptic humeral stem loosening, like glenosphere loosening, occurs without infection. Unlike the glenosphere baseplate, which is never cemented to the glenoid, the humeral stem can be fixed with or without bone cement. For this reason, loosening can be in the form of the stem separating from the bone, the stem separating from cement, or cement separating from the bone. In cases of humeral stem loosening, revision is typically to either a cemented standard-length stem, if sufficient bone stock remains, or a cemented long-stemmed implant otherwise. Humeral stem loosening is relatively uncommon, thanks in part to prior observations in successes and failures from the hip arthroplasty community, however, periprosthetic bone resorption is prevalent, occurring in ~86% of standard-length cases.[58] While not a direct cause for humeral stem loosening, bone resorption, its pathology reported as stress shielding in both the shoulder and the hip, has been established as a risk factor for periprosthetic fracture and potential failure in the case of revision surgery in the hip.[92,119,142] To reduce the incidence of periprosthetic bone resorption in the proximal humerus, humeral stem designs have been modified to reduce the effects of stress shielding, governed by Wolff's Law.[42] The most obvious design changes have been the introduction and adoption of both short-stemmed and stemless humeral components, though for the time being stemless components are restricted to

anatomic shoulder arthroplasty.[34] The comparative loosening rates for these novel short-stemmed and stemless implants has yet to be evaluated in vivo with mid- to long-term follow-up.

2.2.2.3.4.1 Wolff's Law

In the late 19th century, Julius Wolff, a German surgeon, established the relationship between bone loading and bone architecture. In its simplest form, Wolff's Law is essentially 'use it or lose it' – bone is a dynamic tissue that responds to its environment, remodeling according to mechanical demand. In a healthy joint, internal and external loads send mechanical signals to bone remodeling cells, promoting resorption of old bone and formation of new strong bone.[29] Stress shielding is a phenomenon that occurs when loads that would typically be transferred to bone are transferred to something stiffer, such as a metal joint replacement. Without a mechanical stimulus, bone remodeling is less active, resulting in weaker, more brittle bone and overall decreased bone mineral density. By introducing bone preserving shorter humeral stems, the effects of stress shielding are thought to be reduced, as more load will be transferred to surrounding bone.[33]

2.2.3 Modern reverse prosthesis design

2.2.3.1 Glenosphere augmentation

2.2.3.1.1 Bony increased offset reverse shoulder arthroplasty

A solution to maintaining the reverse shoulder's joint center of rotation at the bone-implant interface while reducing the incidence of scapular notching came in 2011, when Pascal Boileau, a French orthopedic surgeon, published his method on bony increased offset reverse shoulder arthroplasty (BIO-RSA).[17] This surgical technique involves harvesting a humeral head bone graft with a diameter matching that of the intended glenosphere baseplate diameter and depth of approximately 10 mm, prior to humeral head resection. The cylindrical autograft of cancellous bone is then placed between the reamed

glenoid and the baseplate, fixed using a long central post and four peripheral screws. A 2017 update by the same group suggested "angling" the bone graft to a trapezoidal shape, more accurately correcting patient-specific glenoid deformity and erosion (Figure 2.14).[18]
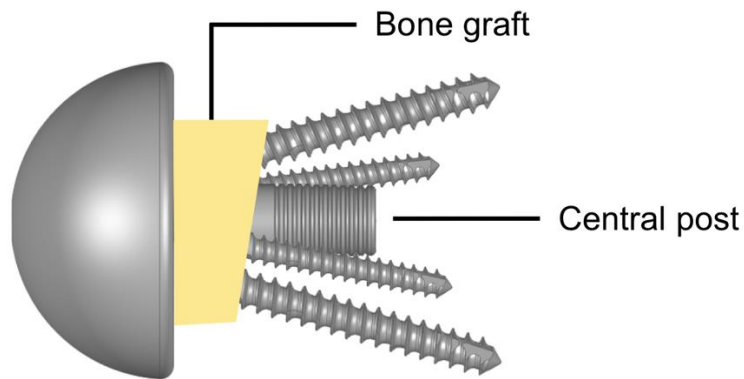
Figure 2.14 Bony increased offset reverse shoulder arthroplasty glenosphere augmentation technique.

Over the course of approximately six months, the bone graft then integrates with the bone of the reamed glenoid, effectively lateralizing the glenosphere without introducing greater torque at the 'new' glenoid-baseplate interface. Based on radiographic assessment, the initial study by Boileau et al. found a 98% incorporation rate of the bone graft two years postoperatively, with a scapular notching rate of 19%; the follow-up study found a graft incorporation rate of 94% and scapular notching in 25% of cases. A retrospective cohort study published in 2015 compared BIO-RSA to standard glenoid fixation, finding no difference in clinical outcomes between cohorts, but that scapular notching was significantly reduced in the BIO-RSA group at 40%, compared to 75%.[7]

While short-term outcomes are promising, there is the potential for graft resorption over time, potentially leading to glenosphere loosening or abnormal contact mechanics. The technique is also limited to primary shoulder procedures and is reliant on appropriate humeral head bone quality, which in the setting of shoulder arthrosis is not always the case. In salvage or revision cases, structural iliac bone crest or cadaveric allograft may also be used, at the risk of donor site morbidity, infection, and potential graft rejection.

2.2.3.1.2 Porous metal augments

More recently, the use of augmented metal baseplates has been proposed as a solution for correcting glenoid deformity, with the benefit of reducing time in the operating room and without the associated potential complications of bone grafting.[59] A number of different designs exist, each for specific glenoid erosion patterns, and these are an attractive alternative to BIO-RSA as they reduce the volume of bone reaming required to correct glenoid version and achieve adequate baseplate seating. By preserving as much dense cortical bone as possible and improving bone-implant contact, there is the potential for greater long-term fixation.[45,70]

Many of these components feature a porous metal-bone interface, with structural properties similar to trabecular bone. Zimmer Biomet's Trabecular Metal™ (Zimmer, Warsaw, IN, USA) has an average pore size of 440 μm and porosity up to 80%, comparable to native trabecular pore size of ~50-300 μm and porosity of 40-90%.[13,61,91] This high porosity promotes bony ingrowth and results in an implant stiffness close to that of native bone, leading to more normal physiological loading and a reduction in stress shielding.[14]

Few studies have been conducted investigating the use of porous metal augments in the shoulder. One study with 10 patients used porous metal in the setting of anatomic shoulder replacement and found no complications or hardware failure, with good incorporations of the augment at 24 months postoperatively.[130] A larger retrospective review of 125 patients receiving a primary reverse shoulder replacement with Zimmer's Trabecular Metal™ augmented baseplate found a 96.7% survivorship at five years, with three revisions (2.4%) for aseptic glenoid failure within 11 months.[154]

2.2.3.1.2.1 Aequalis™ Perform™+ Reversed

The focus of this thesis, in terms of glenoid baseplate augmentation, is the Tornier Aequalis™ Perform™+ Reversed glenoid augment (Wright Medical-Tornier Group, Memphis, TN, USA) (Figure 2.15a). The Aequalis™ Perform™+ Reversed was approved by the U.S. FDA in 2016 and Health Canada in 2017, based on substantial equivalence (K161742) to Zimmer's Trabecular Metal™ and the Equinoxe Reversed Augmented Shoulder Prosthesis (Exactech Inc, Gainesville, FL, USA).[2] The Aequalis™ Perform™+ Reversed has an average porosity of 66% and average pore size of 471-512 µm. The augment is fabricated using a 3D printed titanium alloy (Figure 2.15b), with demonstrated bony ingrowth by four weeks postoperatively. Because this device was approved based on substantial equivalence, to the best of our knowledge no clinical testing of the augment has been completed to date.
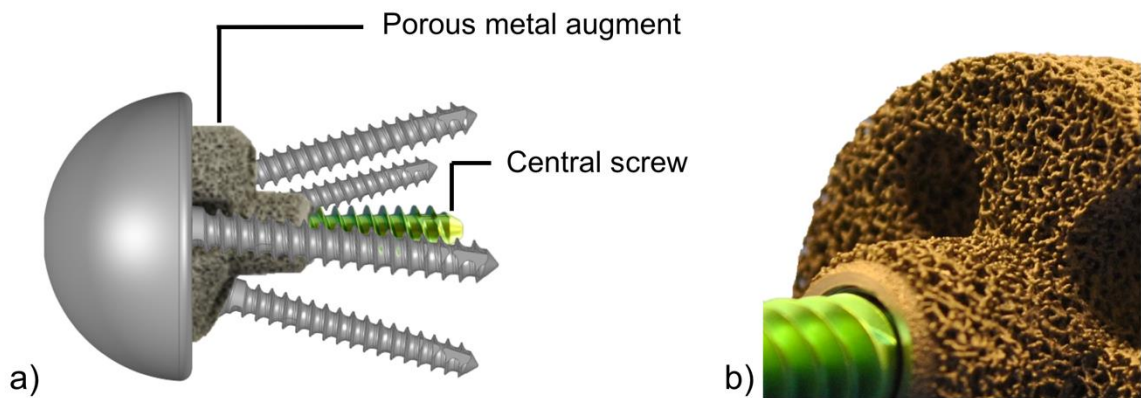
Figure 2.15 (a) The 'full wedge' Tornier Aequalis™ Perform™+ Reversed glenoid porous metal augment, and (b) closeup of the 3D-printed porous structure.

2.2.3.2   Stem fixation

2.2.3.2.1   Cemented

Polymethyl methacrylate, colloquially known as bone cement, was developed in the 1950s by English orthopedic surgeon Sir John Charnley.[157] The polymer itself has no bonding properties, but can be thought of as a grout that fills spaces and is particularly effective between an implant and bone. Once cured, bone cement provides immediate, stable fixation, necessary in patients with poor bone quality or in the case of revision

procedures where bone quantity and quality is compromised. The evolution of bone cement over the years has led to its use as the gold standard in implant fixation.[141]

While the track record for cemented fixation is impressive, it is not without complications. Polymethyl methacrylate is formed by mixing a liquid monomer with a powdered co-polymer, resulting in an exothermic reaction that can reach temperatures of up to 110° Celsius while the mixture hardens.[38] Under normal conditions, this temperature is dissipated through the implant and surrounding blood flow. Different conditions, such as changes to the mixing protocol, the viscosity of the mixture when it is injected, or simply too much bone cement can induce damage to the surrounding bone tissue.[38] Over time, a layer of soft fibrous tissue comprised of macrophages and giant cells can develop between the cement and bone, observed as a radiolucent line on x-rays. This tissue layer develops due to the release of toxic cement monomers in the first few years after implantation and is a concern for later prosthetic loosening.[128] Further down the line, revision surgery following primary cemented fixation can be challenging, as removal of the initial implant can also remove remaining bone stock or lead to periprosthetic fracture and neurovascular injury.

2.2.3.2.2 Press-fit

To address some of the disadvantages of using bone cement, cementless, also known as press-fit, fixation techniques have been introduced. These typically feature a rough surface coating such as hydroxyapatite or a plasma spray titanium to promote bony ingrowth, similar to the porous metal glenoid augments (Figure 2.16). In short stems, the coating is generally limited to the proximal portion of the humeral stem, where it is fit snugly within the humeral metaphysis. Metaphyseal fixation has been proposed to have good vascularity (more rapidly promoting ingrowth), reduced stress shielding, and reduced rates of periprosthetic fracture, compared to diaphyseal fixation which is achieved with cementation of standard-length stems.[65] Further, by eliminating cementing, operating room time is reduced – attractive to surgeons and patients alike.
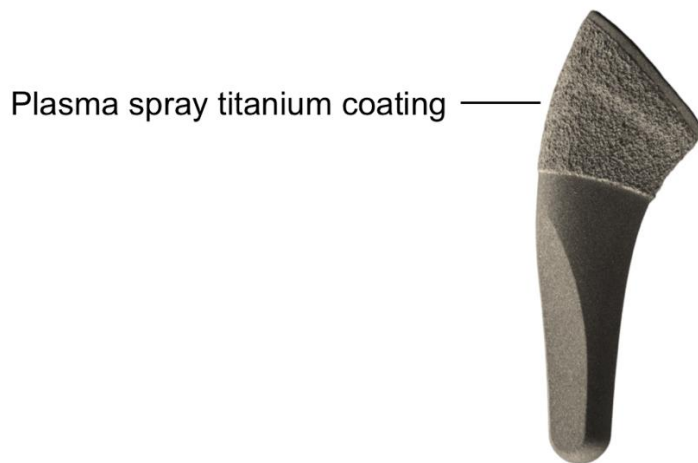
Figure 2.16 Short press-fit stem (Tornier Aequalis™ Ascend™ Flex) with proximal plasma spray titanium coating

A systematic review published in 2016 considered the functional outcome and rate of complications in cemented and press-fit humeral stems in RTSA.[112] They assessed 41 studies comprising of 1455 cemented and 329 press-fit stems, and showed that press-fit stems had a significantly higher incidence of early humeral stem migration and non-progressive radiolucent lines, though lower incidence of postoperative acromion fracture. Cemented stems had increased relative risk of infection, nerve injury, and thromboembolism. There was no difference in the risk of stem loosening or revision, or functional outcome or range of motion between groups.

2.2.3.3 Indications for use

RTSA was initially developed as a salvage procedure for the elderly, a successful outcome being a relative reduction of pain and restoration of sufficient arm function for activities of daily living. The past decade has seen exponential growth in its use, with the most advanced designs and surgical techniques now appropriate for a growing number of conditions in both the elderly and younger populations with good short- to mid-term outcomes.[107,129,136] In addition to treatment for cuff tear arthropathy, RTSA has been used successfully in revision arthroplasty, acute fracture care, glenohumeral instability, severe

glenoid bone wear, non-inflammatory degenerative joint disease, and rheumatoid arthritis.[24,116,164,169] A modern reverse shoulder design is depicted in Figure 2.17.
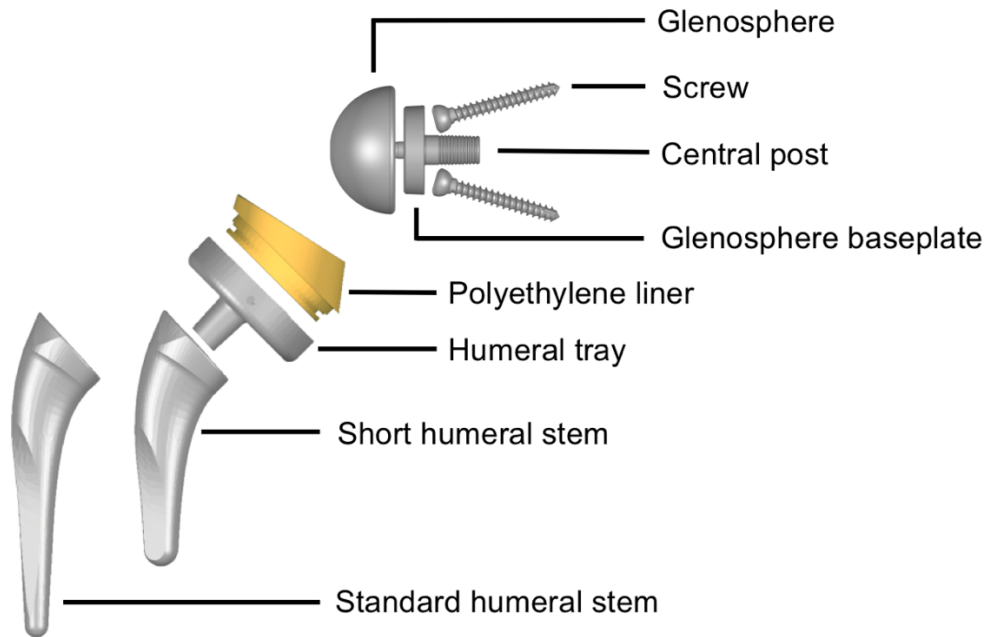
Figure 2.17 The Tornier Aequalis™ Ascend™ Flex reverse total shoulder system.

2.3 Polyethylene Wear

Polyethylene (PE) is a hydrocarbon with the chemical formula $(C_2H_4)_n$ and belongs to the polymer group of thermoplastics, materials that become soft when heated and hard when cooled. Long molecular chains give rise to 'ultra-high molecular weight' polyethylene (UHMWPE), which is used in many medical applications. When UHMWPE is melted and then cooled slowly, the $(C_2H_4)_n$ molecular chains align into ordered strands called lamellae and form a crystalline structure. This ordered structure is what contributes to the hardness of UHMWPE, and what made it the standard bearing surface in artificial joints for many decades, where material integrity is key to implant longevity.[20] Over the years, analysis of hip and knee implant retrievals acquired from revision surgery showed evidence of macroscopic and microscopic UHMWPE volume loss, termed wear, prompting improvements in its wear performance.

2.3.1 Wear mechanism and biologic response

2.3.1.1 Mechanical wear

In the 1950s, John Archard, an English engineer, conducted a series of experiments to describe the wear of materials during contact and rubbing.[4] His simplified wear equation (1), showed that the worn volume of the softer material, *V*, is equal to the product of the sliding distance *s*, applied load *L*, and a proportionality constant, *k*, specific to different materials and derived empirically.[5]

$$V = ksL \tag{1}$$

As we use our joints, there is relative motion and loading between articulations which can lead to abrasive wear and delamination. Loose bone cement, metallic debris, or tiny pieces of bone can become stuck between the PE liner and the metal articulating surface, which can then scratch, through cutting and ploughing, the softer PE. This leads to the release of PE particles via abrasive wear. Delamination can occur as a result of cyclic loading and fatigue failure, through the generation of subsurface cracks which then propagate, separating a thin layer of PE from the rest of the liner.[90,166]

2.3.1.2 Tribochemical wear

Tribology is the science of interacting surfaces in relative motion. While Archard set the foundation for further wear studies, we have come to learn that wear initiation may not be entirely mechanical in nature. There is likely some form of microscopic adhesion between the PE and metal glenosphere which results in material transfer from the plastic to the metal. This results in the removal of the top-most PE layer, leaving a new PE surface behind.[89] This new surface is fibrillar, resulting from the re-organization of the molecular strands at the articulating surface in response to surface traction – the shear forces parallel to the PE surface that occur when the articular surfaces move.[166] The little fibrils are torn off through further joint motion, and can exacerbate abrasive wear.

2.3.1.3   Osteolysis

Over time, these PE debris particles migrate to the tissues surrounding the joint replacement. The introduction of these foreign bodies elicits the recruitment of macrophages, white blood cells that detect and destroy pathogens. The recruitment of macrophages, however, also releases inflammatory cytokines (small proteins) in response. This leads to a chain reaction whereby the inflammatory cytokines stimulate differentiation of bone resorbing cells, leading to periprosthetic osteolysis – the pathologic destruction of bone around the implant.[26]

Polyethylene wear-induced osteolysis has been well established as a mode of aseptic loosening and long-term limitation to an implant's survival.[60] The literature suggests a linear wear rate of less than 0.1 mm/year is acceptable for preventing osteolytic effects in hips (no volumetric threshold exists to date), and changes to the mechanical properties of polyethylene have since taken place for hip and knee prosthesis to meet this threshold.[37]

2.3.2 Highly cross-linked polyethylene

The hardness offered by crystalline lamellae of ultra-high molecular weight polyethylene can be enhanced through crosslinking of its molecules. Polyethylene crosslinking results from the removal of a hydrogen atom from adjacent PE molecules, leaving carbon backbones of the molecules bonded through the sharing of electron pairs. Highly cross-linked PE (HXLPE) used in orthopedic applications is usually cross-linked through gamma or electron beam irradiation, followed by remelting to reduce the number of free radicals (a molecule with an unpaired electron that can react negatively with its environment in vivo), and then cooled and sterilized in an inert gas such as nitrogen.[77]

An interesting property of UHMWPE is that it is highly resistant to wear if the sliding direction is along one path. Its molecules will orient preferentially in the sliding direction, actually increasing its wear resistance along that line. Joint motion, however, is multidirectional, so lamellae don't have the chance to orient themselves in a preferred direction; strength in a direction perpendicular to the lamellae is particularly poor.[165,167]

By introducing cross-linking into polyethylene, the structure becomes stronger and more resistant to wear caused by multidirectional joint motion. Clinical studies comparing wear rates in conventional and highly cross-linked PE show superior wear performance in the highly cross-linked liners.[21,47,48,88,155]

It should be noted that while cross-linking significantly reduces the abrasive wear rate of polyethylene, because it is stiffer, it may be more susceptible to microcracks and delamination.[127] It is also more expensive than conventional polyethylene, and the abrasive particles that *are* generated may be more damaging from a biological perspective. It remains to be seen if this is a clinical concern, and at this time is an active area of research.[10,46] Current research trends also include adding antioxidants such as vitamin E to the polymer to reduce oxidative effects of the liner in vivo.[79,106]

2.3.3 Wear patterns in reverse total shoulder arthroplasty – retrieval and simulation studies

Like hip and knee retrieval analysis, a handful of retrieval studies have quantitatively and qualitatively described wear patterns observed in the reverse shoulder (Table 2.1). Though few in number, these initial retrieval analyses showed that both articular and rim wear are present even in the first few years postoperatively, and that rim wear was likely a result of inferior polyethylene impingement with the scapular neck due to adduction deficit (Figure 2.18).
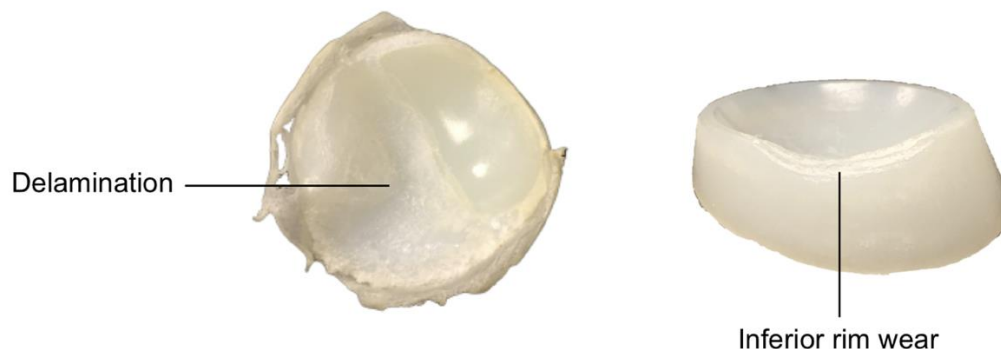
Figure 2.18 Retrieved reverse shoulder polyethylene liners with evidence of delamination and inferior rim wear.

While retrievals can provide a foundation for understanding wear behaviour, a primary limitation of these studies is that they are an evaluation of failed implants with relatively short term-of-service. What is observed upon retrieval may not accurately represent what is observed in well-functioning joint replacements. Quantitative in vitro studies have the potential to fill this gap by providing a controlled environment where many years of wear can be simulated using different bearing materials, motion profiles, and applied loads as a form of preclinical testing. Dedicated simulators and testing protocols have been developed for the hip and knee, though to date there are no established procedures for the reverse shoulder. For this reason, in addition to varying polyethylene geometries, in vitro simulations give a wide range of wear rates, ranging from 14.3 mm^3/million cycles (MC) to 126 mm^3/MC.[25,72,80,111,140,151,162] A recent study investigating the reverse shoulder duty cycle determined that one year of use is equal to approximately 0.75 MC.[81]

Further, in vitro simulations can be expensive and time-consuming, leading many groups to investigate wear through in silico (computer) simulation. Over the past few years, sophisticated wear relationships have been developed, capable of more accurately characterizing wear behaviour than Archard's simple 1956 relationship. This, along with increased computational capacity has led to an increase in the number of numerical and musculoskeletal modeling studies with results comparable to what has been observed in vitro.[1,86,118,147,151]

Table 2.1 RTSA retrieval studies.

Paper	Number of retrievals	Average term-of-service (years)	Method of assessment	Evidence of damage modes	Spatial distribution of damage	Take-home message
Kurdziel et al., 2018[76]	32	2.06 (range 0.3-4.7)	Quantitative: μCT – volumetric and surface deviation changes compared to unworn control Qualitative: Surface damage scored from 0-3 based on proportion of surface area with macroscopic damage in superior, inferior, anterior, posterior quadrants of liner	Not specified	Rim damage present on 62.5% of liners, highest in posterior quadrant (37.5%), followed by inferior (31.3%), superior (21.8%, and anterior (18.8%) Highest damage score present in inferior quadrant, followed by posterior, anterior, then superior	Mean volumetric wear rate: 114.5 ± 160.3 mm^3/year Mean articular surface deviation: 0.084 ± 0.065 mm Mean rim surface deviation: 0.177 ± 0.159 mm Articulation surface deviation positively correlated to term-of-service
Wiater et al., 2015[171]	50	1.67 (range 0-6.8)	Qualitative: Evaluated macroscopically for evidence of damage, confirmed by light microscopy and scanning electron microscopy: • Abrasion, burnishing, dishing, pitting, scratching, embedding, delamination, edge deformation, fracture	All evident, highest incidence: scratching (86%), pitting (72%)	Only articular surface damage on 40% of liners, articular surface and rim damage on remaining 60%	Evidence of both articular and rim wear

Day et al., 2012[32]	7	2.11 (range 1.3-3.3)	Quantitative: μCT – rim deviation changes calculated by multiplying slice thickness with number of slices in which damage was apparent Qualitative: Surface damage scored from 0-3 based on proportion of surface area with macroscopic damage in superior, inferior, anterior, posterior quadrants of liner, graded for: • Burnishing, scratching, embedded debris, pitting, surface deformation, abrasion, delamination	Highest incidence: burnishing, multidirectional scratching, pitting; articular surface abrasion in 3 liners, delamination in 1	All rims had evidence of impingement with scapula, ranging from 87° to 226° of liner circumference (mean, 136°) Depth of impingement ranged from 0.1-4.7 mm (mean, 2.1 mm)	Rim wear due to scapular impingement was primary form of damage
Nam et al., 2010[93]	14	0.46 (range 0-1.92)	Qualitative: Surface damage examined microscopically scored from 0-3 based on proportion of surface area with damage in superior, inferior, anterior, posterior quadrants of liner, graded for: • Burnishing, scratching, embedded debris, pitting, surface deformation, abrasion, delamination, focal damage, fracture	Highest incidence: scratching (100%), abrasion (93%), third-body debris (57%), pitting (43%)	Scratching in all quadrants, abrasion most prevalent and severe in inferior quadrant Inferior quadrant had most damage regardless of damage mode, followed by posterior, then superior, then anterior	Predominant inferior wear due to scapular impingement

The impact of polyethylene wear as a cause for revision is difficult to assess because it is usually a precursor that leads to a more definite form of observable failure, such as implant loosening. Because the shoulder is not weight-bearing in the same obvious way as the hip or knee, reverse shoulder PE wear has not historically been considered a primary cause for concern, and conventional UHMWPE remains the most commonly used bearing material. Simply because the shoulder does not support the weight of the body, however, does not mean it is not load-bearing; loads of up to 0.7 body weight during abduction have been reported in the reverse shoulder.[43] Though retrieval and simulation analysis can accurately tell us what is happening ex vivo, it remains to be determined what is actually going on inside this body. To date, no studies have reported in vivo wear rates, and variations in patient arm use, loading, and range of motion may influence in vivo results.

2.4 Patient-reported outcome measures

The clinician's assessment of disease and treatment on a patient's wellbeing is frequently incomplete. For this reason, patient self-assessment in the form of patient-reported outcome measures (PROMs) have gained popularity within the healthcare and research sector.[99,168] By assessing not only objective, but subjective measures, the clinician can more accurately determine which patients will benefit from specific treatments. Hundreds of PROMs have been developed; however, it is important to choose well-validated, reliable, responsive, and interpretable questionnaires specific to the condition or treatment of interest in order to obtain meaningful results.[22] Validated PROMs will have a threshold for the minimum change in outcome score that is representative of meaningful clinical change – the minimal clinically important difference (MCID).[132] It should be noted that while pre-treatment and post-treatment PROMs may be statistically significantly different, there could be no meaningful clinical change. Common PROMs used in shoulder arthroplasty are highlighted in Table 2.2, a copy of each found in Appendix D.

Table 2.2 Shoulder-specific patient-reported outcome measures

PROM	Description	Scale	MCID
Active forward flexion	Active forward flexion	-	12°[137]
Active lateral abduction	Active lateral abduction	-	7°[137]
Pain (visual analog scale)	Pain	0 (no pain)-10 (most pain)	1.6[137]
American Shoulder and Elbow Surgeons (ASES)	17 questions assessing pain, sleep, and function	0 (worst)-100 (best)	13.6[137]
Disabilities of the Arm, Shoulder and Hand (DASH)	30 questions assessing function, mental, and social wellbeing	0 (best)-100 (worst)	12.7[74]
Subjective Shoulder Value (SSV)	Subjective value of current shoulder as a % of a completely normal shoulder	0 (worst)-100 (best)	Not established
Simple Shoulder Test (SST)	12 yes or no questions assessing comfort and function	0 (worst)-12 (best)	1.5[137]
Constant-Murley Score	8 questions assessing pain, activity, strength, and range of motion	0 (worst)-100 (best)	5.7[137]

While PROMs can improve the understanding of how a disease or treatment impacts patients' daily lives, limitations to their routine use include time, and the need for someone to administer the test and interpret results. Further, emotion, personal bias, missing data, and comorbidities may influence the overall score.[69]

2.5 Radiostereometric analysis

Prefix radi- from the Latin past participle radiiare "to gleam, shine, beam"

2.5.1 X-ray imaging

2.5.1.1 X-ray

X-ray is a high-energy form of electromagnetic radiation, with a wavelength ranging from 0.01 to 10 nanometers and energy in the range of 100 electron volts (eV) to 100

keV. X-rays can be produced using an x-ray tube, where electrons are released by a heated cathode and accelerated to a high velocity before hitting a target anode. The anode is made of metal, usually tungsten in medical applications, and the result of the collision is the release of an x-ray photon in the form of Bremsstruahlung radiation.[134]

2.5.1.2 X-ray in orthopaedic imaging

X-ray is frequently used as a fast and comparatively cheap medical imaging technique, its simplest use in the form of projection radiographs. When acquiring a projection radiograph, the area to be imaged is placed between the x-ray tube and an x-ray detector. The body part of interest will attenuate x-ray photons, with attenuation proportional to the electron density (atomic number) and thickness of the specimen. The fewer the number of x-rays that hit the detector, the brighter that spot will appear on the image. Bones, which are high in calcium (atomic number 20), attenuate x-rays more than soft tissue, composed primarily of hydrogen and carbon (atomic numbers 1 and 12, respectively). Further, joint replacements, frequently made of metals such as titanium (atomic number 22) and cobalt-chrome (atomic numbers 24-27) are also highly attenuating compared to soft tissue and for this reason x-ray is an excellent imaging technique for orthopaedic evaluation.

2.5.1.3 Radiation dose

X-ray is a form of ionizing electromagnetic radiation, meaning that when the photons interact with matter, there is sufficient energy to remove electrons, resulting in a charged, or ionized atom. Interaction of ionizing radiation with the human body is concerning because the body is composed primarily of water. Ionizing water can produce hydroxyl (OH) radicals, which, when they interact with DNA, can break or damage the strands. Sometimes this damage can be misrepaired, leading to cancer.[85] To quantify how much radiation a patient is receiving, an 'effective dose' is used. The effective dose is equal to the absorbed dose (measuring the energy deposited per unit mass) times a radiation weighting factor – which for x-ray is 1.0 – times a tissue weighting factor, and expressed in the unit Sievert. A typical radiostereometric exam of the shoulder has an effective dose

of 0.1 milli-Sievert. For perspective, the average person experiences an effective dose of approximately 3.0 milli-Sievert each year from background sources (e.g. atmospheric radon, cosmic radiation). To minimize the amount of radiation a patient receives during a clinical exam, the "as low as reasonably achievable" (ALARA) principle is applied by qualified x-ray technicians. Techniques such as beam collimating and proper shielding are applied.[55]

2.5.2 Marker-based radiostereometric analysis

The history of radiostereometric analysis (RSA), also known as Roentgen stereophotogrammetric analysis, dates back to the discovery of x-rays in the late 1800s. The dual-plane orthopaedic imaging technique as we know it today, however, was introduced by Swedish mathematician Göran Selvik in 1972.[135] Radiostereometric analysis allows for the reliable three-dimensional localization of a rigid body using x-rays. By using a calibration object and exposing the body of interest from two different views simultaneously, we have the capacity to reconstruct the body's global position and orientation (Figure 2.19).
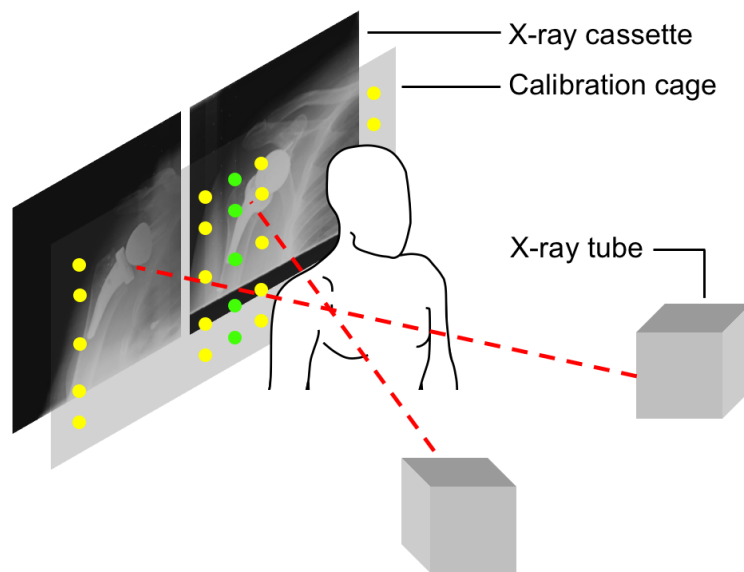
Figure 2.19 Clinical radiostereometric analysis setup using a uniplanar calibration cage and x-ray tubes angled 40° to one another.

The calibration object is placed in front of two x-ray cassettes at the time of exposure, either in a side-by-side configuration (uniplanar) or 90° to one another (biplanar). The calibration object, hereafter referred to as the calibration cage, is marked with a known distribution of radiopaque 'fiducial' and 'control' beads that show up on the patients' x-rays. Analyzing the distribution of known fiducial points on each x-ray, a transformation matrix is generated, whereby the x-ray image is brought into the cage frame of reference. Once in the cage's frame of reference, analysing the distribution of control beads on the x-rays allows us to generate a transformation matrix from which the source (x-ray tube)-to-detector (x-ray cassette) distance can be determined, ultimately defining the global coordinate frame.

In terms of orthopaedics, this allows for precise measurements of implant position and orientation (pose) relative to host bone. Marker-based RSA employs the use of marker beads on both the implant of interest and within the trabeculae of the surrounding bone. Traditionally 0.8-1.0 mm in diameter and made of tantalum, these beads are radiopaque, bioinert, biocompatible, and easily identifiable on x-rays.[6] First calibrating the x-ray images (using the calibration cage fiducial and control beads), the beads on the implant and within the bone can be identified. Back-projecting from the location of these beads on the x-rays to the x-ray source for both images, the line corresponding to the same bead in both images will intersect, this intersection in the global coordinate frame defining its true 3D position. The 3D coordinates of implant beads describe the implant rigid body, while those of the bone beads describe the reference rigid body. It is assumed that the relative position of one bead to another within the respective rigid body will not change over time.

Though the accuracy and precision of marker-based RSA enables implant pose estimates on the order of tens to hundreds of microns,[160] disadvantages of the technique include additional cost and potentially inferior mechanical integrity of the specially-manufactured implants. Further, beads may be obstructed by over-projection of the implant itself, and these radiographs may need to be excluded from analysis.

2.5.3 Model-based radiostereometric analysis

In effort to address the limitations of marker-based RSA, and with the advance of improved computational power, model-based RSA (MBRSA) was proposed by Valstar et al. in the early 2000s.[63,159] In lieu of tantalum beads attached to the implant, MBRSA uses a triangulated surface model, such as the computer-aided design (CAD) model provided by the manufacturer, or a reverse engineered (RE) model from the actual implant, as the implant rigid body geometry. To identify the pose of the implant, rather than identifying markers, as done in marker-based RSA, the contour of the implant is detected on both examination x-rays. Because we know where the x-ray tubes are relative to the x-ray cassettes through calibration, we can create a virtual projection of the surface model onto the x-rays, like shadow puppets. MBRSA software then positions and rotates the surface model in the global coordinate frame until the projected contours match those of the real contours, defining the real position and orientation of the implant in space (Figure 2.20). Mathematically, this is done by minimizing the difference between detected and projected contours.[159] A coarse alignment is completed initially to minimize the risk of the model registering to a local minimum, followed by a fine alignment with a greater number of iterations and smaller step size. Implants with asymmetric geometries are more robust to the MBRSA technique, as different x-ray foci would generate unique projections. Validation of MBRSA with different implant designs have found that virtual projections from RE models typically provide a more accurate match to the true implant contours than CAD models,[63] but the use of CAD models still provides acceptable precision for use in clinical application.[62,133] In all clinical applications, the use of 'double examinations' is suggested, where the patient is imaged twice within a few minutes. In theory, the implant will not have moved within that interval, so any measured change in position and orientation is indicative of the precision of the imaging and analysis technique.[158]
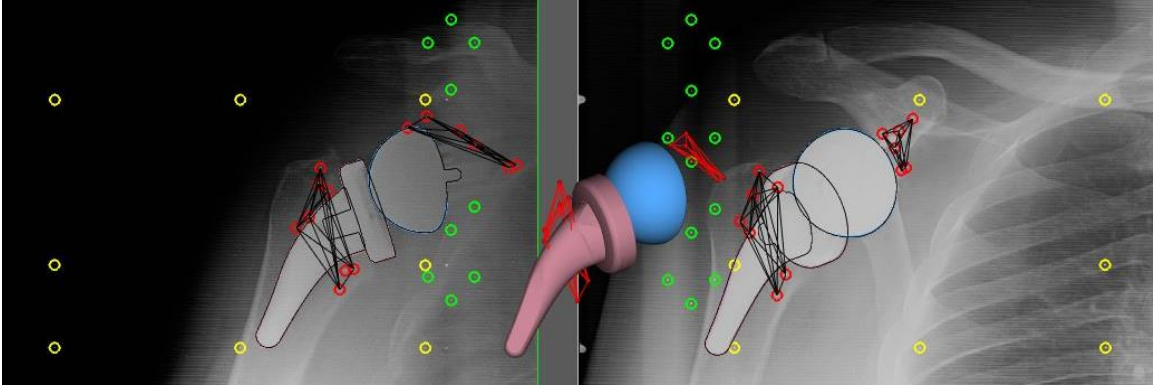
Figure 2.20 Calibration cage fiducial (yellow) and control (green) beads determine the global reference frame. Glenosphere (blue) and humeral stem and tray (pink) contours are detected on x-rays taken 40° to one another, their surface models aligned within the global frame to match. Tantalum beads within the bone are detected (red circles), defining the reference rigid body against which implant migration is measured over time.

There are a two main parameters MBRSA software generates to help the analyzer interpret results. In 2005, a set of guidelines for the standardization of RSA was published and is the source for the following recommendations.[158] The first parameter is condition number. Condition number (CN) refers to the distribution of tantalum beads within the bone and is a function of the number of beads, and the distance between each bead (*d*) and an arbitrary straight line passing through the cluster, calculated in equation (2).

$$CN = 1/(d_1^2 + d_2^2 + d_3^2 + \dots d_n^2)^{1/2} \qquad (2)$$

The condition number is minimized such that the optimal position and orientation of the line is determined.[125] Considering equation (2), we can see that CN is inversely proportional to distance from the line – if the beads are highly collinear, we have small values for *d* and a large CN. The goal is to distribute the beads as far apart from one another as possible in order to maximize distance from the line. Further, increasing the number of beads in the calculation will also reduce the CN. For practical reasons, the number of reference rigid body beads is generally recommended as between six and nine. A minimum of three corresponding beads in each x-ray are required to define the position and orientation of the bone in the global coordinate frame, so by including more than

41

three we increase the chances of reporting reliable measurements. A condition number threshold of 150 has been proposed as the upper limit for acceptable conditioning, with values below 150 providing acceptably reliable migration measurements.

The second parameter is the mean error of rigid body fitting. This is "the mean difference between the relative distances of markers in a rigid body in one examination compared to that in another examination."[158] The mean error of rigid body fitting tells the user whether beads have moved slightly within the bone between timepoints, and therefore subsequent implant migration measurements may not be accurate. The upper limit for rigid body fitting is 0.35 mm.

2.5.4 Applications of radiostereometric analysis in joint replacement

Radiostereometric analysis is the gold standard for measuring orthopaedic implant migration. For the purpose of this thesis, migration is defined as the longitudinal displacement of the implant component relative to its host bone. Micromotion, beyond the scope of this thesis, includes both migration and inducible displacement, the movement of an implant induced by external forces at a single timepoint.[124] Migration has historically been reported in terms of 'maximum total point motion' (MTPM), the three-dimensional vector magnitude of the point on the implant that has moved the most relative to bone between study timepoints.[123] While this definition and interpretation are acceptable for marker-based RSA, where there is a finite number of beads (points) fixed to the implant, the use of MTPM becomes less valuable in model-based RSA. The triangulated surface mesh used in MBRSA offers thousands of surface model points (nodes within the triangulated mesh) to choose from, and it is likely that different nodes will reflect the MTPM at different timepoints, making it difficult to determine whether the reported value is of significance.[158] For this reason, migration in this thesis is reported in terms of its orthogonal vector components, as well as a three-dimensional resultant vector, the square of the sum of squares of cartesian components. Migration of the centroid of the implant is with reference to the center of gravity of the bone fiducials' rigid body.

The high precision afforded by radiostereometric analysis allows for randomized trials to be conducted between different implants and fixation techniques with relatively few patients (~10-20) in each group.[64,100,153] A number of studies have correlated implant migration measured using radiostereometric analysis within the first two years postoperatively to later risk of implant loosening and failure in the lower limb. A systematic review and meta-analysis published in 2012 suggested that for knee arthroplasty, MTPM up to 0.5 mm during the first year is safe, and MTPM greater than 1.6 mm during the first year is unacceptable, with an increase in revision of 7.6% at five years for each mm of MTPM at one year.[115] An update to these thresholds was published in 2018, following the assessment of 2,470 knees with RSA.[114] The results showed very little migration between six months and two years postoperatively (mean migration of 0.04 mm six months through one year, and one year through two years), and therefore MTPM thresholds previously assigned to one-year values could be applied to MTPM at six months. In line with this, historically, tibial components with increases in migration of greater than 0.2 mm between one and two years postoperatively have been classified as "continuously migrating", while those with increases in migration of less than 0.2 mm are stable.[123] Pijls et al. further propose this label of continuous migration can be applied to changes in migration between six months and one year, reducing the previously required radiostereometric study follow-up from two years to one year. Similarly, a systematic review and meta-analysis of the hip literature showed that for every mm increase in 2-year acetabular cup migration, revision rate increased by 10% at ten years postoperatively.[113] To assess the clinical impact of RSA, Nelissen et al. compared the revision rate of total knee replacements that had undergone an RSA study to those that hadn't and observed a 22-35% reduction in revision in knees that had been RSA-tested.[98]

A handful of studies have applied RSA to shoulder replacement, all focusing on the glenoid component in anatomic shoulder arthroplasty, with the exception of one study investigating anatomic humeral stem fixation in rheumatoid patients, and two considering humeral head resurfacing.[101–104,120,121,145,146] As shoulder replacement is relatively new, no thresholds for acceptable migration have been established for these prostheses. Further,

the reverse shoulder experiences different loading patterns than the anatomic shoulder, and thresholds identified for the anatomic geometry may not be directly transferable to the reverse. No studies to date have evaluated reverse total shoulder arthroplasty using RSA.

Model-based radiostereometric analysis has also been used to quantify polyethylene wear in the knee and hip with submillimeter accuracy.[35,36,44,117] The three-dimensionality of RSA enables volumetric measurements of wear, a perhaps more meaningful measure than the traditional 2D maximum linear wear depth, as 3D information can define clinically relevant wear patterns that may be multidirectional in nature.[144] Again, to the best of our knowledge, no studies have applied MBRSA as a technique to evaluate the in vivo wear behaviour of UHMWPE. Assessing in vivo wear can help predict the joint replacement's survivorship.

Expanding beyond migration and polyethylene wear measurement, MBRSA techniques have been used as the foundation for contact assessment between articulating components in the artificial joint. MBRSA enables the investigation of contact differences resulting from different surgical techniques and implant designs,[23,56,149] and whether abnormal contact patterns influence implant migration.[150] To date, only one study has simulated the contact mechanics of the reverse shoulder, and no studies have conducted an in vivo assessment. The finite element study, published by Langohr et al. in 2016, investigated how variations in humeral stem neck-shaft angle, polyethylene cup depth, and glenosphere diameter affect polyethylene contact patch and associated stresses.[82] Langohr observed that reducing neck-shaft angle reduced contact area and increased contact stress; decreasing cup depth reduced contact area and increased contact stress; and decreasing glenosphere diameter decreased contact area but had a negligible effect on contact stress. The contact itself was typically observed in the inferior portion of the polyethylene, with the trend of becoming more inferior as abduction angle increased through 0-120°.[82] These observations are important to understanding how variations in reverse shoulder designs can influence implant longevity – reduced contact areas and increased focal stress may lead to polyethylene wear and/or glenosphere migration. For this reason, future studies

should evaluate the in vivo reverse shoulder contact mechanics under clinically relevant loading conditions.

Overall, model-based radiostereometric analysis allows for a highly accurate, quantitative evaluation of joint replacement in vivo and is the technique of choice in our evaluation of reverse total shoulder arthroplasty.

2.6 References

1. Abdelgaied A, Liu F, Brockett C, Jennings L, Fisher J, Jin Z. Computational wear prediction of artificial knee joints based on a new wear law and formulation. J Biomech. 2011;44(6):1108–1116. doi:10.1016/j.jbiomech.2011.01.027
2. Food and Drug Administration. K161742. 2016.
3. Aleem AW. Outcomes of rotator cuff surgery: What does the evidence tell us? Clin Sport Med. 2012;31:665–674. doi:10.1016/j.csm.2012.07.004
4. Archard JF. Contact and rubbing of flat surfaces. J Appl Phys. 1953;24(8):981–988. doi:10.1063/1.1721448
5. Archard JF, Hirst W, Allibone TE. The wear of metals under unlubricated conditions. Proc R Soc A. 1956;236. doi:https://doi.org/10.1098/rspa.1956.0144
6. Aronson AS, Jonsson N, Alberius P. Tantalum markers in radiography - An assessment of tissue reactions. Skeletal Radiol. 1985;14(3):207–211. doi:10.1007/BF00355566
7. Athwal GS, MacDermid JC, Reddy KM, Marsh JP, Faber KJ, Drosdowech D. Does bony increased-offset reverse shoulder arthroplasty decrease scapular notching? J Shoulder Elb Surg. 2015;24(3):468–473. doi:10.1016/j.jse.2014.08.015
8. Barlow JD, Yuan BJ, Schleck CD, Harmsen WS, Cofield RH, Sperling JW. Shoulder arthroplasty for rheumatoid arthritis: 303 consecutive cases with minimum 5-year follow-up. J Shoulder Elb Surg. 2014;23(6):791–799. doi:10.1016/j.jse.2013.09.016
9. Baulot E, Sirveaux F, Boileau P. Grammont's idea: The story of Paul Grammont's functional surgery concept and the development of the reverse principle. Clin Orthop Relat Res. 2011;469(9):2425–2431. doi:10.1007/s11999-010-1757-y
10. Baxter RM, MacDonald DW, Kurtz SM, Steinbeck MJ. Characteristics of highly cross-linked polyethylene wear debris in vivo. J Biomed Mater Res B Appl Biomater. 2013;101(3):467–475. doi:10.1002/jbm.b.32902
11. Beazley JCS, Evans JP, Furness ND, Smith CD. Comparative learning curves for early complications in anatomical and reverse shoulder arthroplasty. Ann R Coll Surg Engl. 2018;100(6):491–496. doi:10.1308/rcsann.2018.0062
12. Bercik MJ, Kruse K, Yalizis M, Gauci MO, Chaoui J, Walch G. A modification to the Walch classification of the glenoid in primary glenohumeral osteoarthritis using three-dimensional imaging. J Shoulder Elb Surg. 2016;25(10):1601–1606. doi:10.1016/j.jse.2016.03.010

13. Zimmer Biomet. Trabecular Metal Technology [Internet]. 2019 [cited 2019 Nov 5];Available from: https://www.zimmerbiomet.com/medical-professionals/common/our-science/trabecular-metal-technology.html

14. Bobyn JD, Poggie RA, Krygier JJ, Lewallen DG, Hanssen AD, Lewis RJ, et al. Clinical validation of a structural porous tantalum biomaterial for adult reconstruction. J Bone Jt Surg - Ser A. 2004;86(SUPPL. 2):123–129. doi:10.2106/00004623-200412002-00017

15. Boileau P. Biographical Sketch Paul M. Grammont, MD (1940). Clin Orthop Relat Res. 2011;469(9):2422–2423. doi:10.1007/s11999-011-1959-y

16. Boileau P. Complications and revision of reverse total shoulder arthroplasty. Orthop Traumatol Surg Res. 2016;102(1):S33–S43. doi:10.1016/j.otsr.2015.06.031

17. Boileau P, Moineau G, Roussanne Y, O'Shea K. Bony increased-offset reversed shoulder arthroplasty: minimizing scapular impingement while maximizing glenoid fixation. Clin Orthop Relat Res. 2011;469(9):2558–2567. doi:10.1007/s11999-011-1775-4

18. Boileau P, Morin-Salvo N, Gauci MO, Seeto BL, Chalmers PN, Holzer N, et al. Angled BIO-RSA (bony-increased offset-reverse shoulder arthroplasty): A solution for the management glenoid bone loss and erosion. J Shoulder Elb Surg. 2017;26:2133–2142. doi:10.1016/j.jse.2017.05.024

19. Boileau P, Watkinson DJ, Hatzidakis AM, Balg F. Grammont reverse prosthesis: Design, rationale, and biomechanics. J Shoulder Elb Surg. 2005;14:147–161. doi:10.1016/j.jse.2004.10.006

20. Bracco P, Bellare A, Bistolfi A, Affatato S. Ultra-high molecular weight polyethylene: Influence of the chemical, physical and mechanical properties on the wear behavior. A review. Materials (Basel). 2017;10(791). doi:10.3390/ma10070791

21. Bragdon CR, Doerner M, Martell J, Jarrett B, Palm H, Multicenter Study Group, et al. The 2012 John Charnley Award: Clinical multicenter studies of the wear performance of highly crosslinked remelted polyethylene in THA. Clin Orthop Relat Res. 2013;471(2):393–402. doi:10.1007/s11999-012-2604-0

22. Briffa N. The employment of Patient-Reported Outcome Measures to communicate the likely benefits of surgery. Patient Relat Outcome Meas. 2018;9:263–266. doi:10.2147/prom.s132746

23. Broberg JS, Ndoja S, MacDonald SJ, Lanting BA, Teeter MG. Comparison of contact kinematics in posterior-stabilized and cruciate-retaining total knee arthroplasty at long-term follow-up. J Arthroplasty. 2019;74:1–12. doi:10.1016/j.arth.2019.07.046

24. Brorson S, Rasmussen J V, Olsen BS, Frich LH, Jensen SL, Hróbjartsson A. Reverse shoulder arthroplasty in acute fractures of the proximal humerus: A systematic review. Int J Shoulder Surg. 2013;7(2):70–78. doi:10.4103/0973-6042.114225

25. Carpenter S, Pinkas D, Newton MD, Kurdziel MD, Baker KC, Wiater JM. Wear rates of retentive versus nonretentive reverse total shoulder arthroplasty liners in an in vitro wear simulation. J Shoulder Elb Surg. 2015;24(9):1372–1379. doi:10.1016/j.jse.2015.02.016

26. Catelas I, Wimmer MA, Utzschneider S. Polyethylene and metal wear particles:

Characteristics and biological effects. Semin Immunopathol. 2011;33(3):257–271. doi:10.1007/s00281-011-0242-3

27. Chalmers PN, Rahman Z, Romeo AA, Nicholson GP. Early dislocation after reverse total shoulder arthroplasty. J Shoulder Elb Surg. 2014;23(5):737–744. doi:10.1016/j.jse.2013.08.015

28. Chalmers PN, Salazar DH, Romeo AA, Keener JD, Yamaguchi K, Chamberlain AM. Comparative utilization of reverse and anatomic total shoulder arthroplasty. J Am Acad Orthop Surg. 2018;26(24):504–510. doi:10.5435/JAAOS-D-17-00075

29. Chen JH, Liu C, You L, Simmons CA. Boning up on Wolff's Law: Mechanical regulation of the cells that make and maintain bone. J Biomech. 2010;43(1):108–118. doi:10.1016/j.jbiomech.2009.09.016

30. Cheung E, Willis M, Walker M, Clark R, Frankle MA. Complications in reverse total shoulder arthroplasty. J Am Acad Orthop Surg. 2011;19(7):439–449.

31. Day JS, Lau E, Ong KL, Williams GR, Ramsey ML, Kurtz SM. Prevalence and projections of total shoulder and elbow arthroplasty in the United States to 2015. J Shoulder Elb Surg. 2010;19(8):1115–1120. doi:10.1016/j.jse.2010.02.009

32. Day JS, MacDonald DW, Olsen M, Getz C, Williams GR, Kurtz SM. Polyethylene wear in retrieved reverse total shoulder components. J Shoulder Elb Surg. 2012;21(5):667–674. doi:10.1016/j.jse.2011.03.012

33. Denard PJ, Noyes MP, Walker JB, Shishani Y, Gobezie R, Romeo AA, et al. Proximal stress shielding is decreased with a short stem compared with a traditional-length stem in total shoulder arthroplasty. J Shoulder Elb Surg. 2018;27(1):53–58. doi:10.1016/j.jse.2017.06.042

34. Denard PJ, Raiss P, Gobezie R, Edwards TB, Lederman E. Stress shielding of the humerus in press-fit anatomic shoulder arthroplasty: review and recommendations for evaluation. J Shoulder Elb Surg. 2018;27(6):1139–1147. doi:10.1016/j.jse.2017.12.020

35. Digas G, Kärrholm J, Thanner J, Herberts P. 5-Year experience of highly cross-linked polyethylene in cemented and uncemented sockets: Two randomized studies using radiostereometric analysis. Acta Orthop. 2007;78(6):746–754. doi:10.1080/17453670710014518

36. Digas G, Kärrholm J, Thanner J, Malchau H, Herberts P. Highly cross-linked polyethylene in cemented THA: Randomized study of 61 hips. Clin Orthop Relat Res. 2003;(417):126–138. doi:10.1097/01.blo.0000096802.78689.45

37. Dumbleton JH, Manley MT, Edidin AA. A literature review of the association between wear rate and osteolysis in total hip arthroplasty. J Arthroplasty. 2002;17(5):649–661. doi:10.1054/arth.2002.33664

38. Dunne NJ, Orr JF. Curing characteristics of acrylic bone cement. J Mater Sci Mater Med. 2002;13(1):17–22. doi:10.1023/A:1013670132001

39. Familiari F, Rojas J, Nedim Doral M, Huri G, McFarland EG. Reverse total shoulder arthroplasty. EFORT Open Rev. 2018;3(2):58–69. doi:10.1302/2058-5241.3.170044

40. Flatow EL, Harrison AK. A history of reverse total shoulder arthroplasty. Clin Orthop Relat Res. 2011;469(9):2432–2439. doi:10.1007/s11999-010-1733-6

41. Formaini NT, Everding NG, Levy JC, Santoni BG, Nayak AN, Wilson C, et al. The effect of glenoid bone loss on reverse shoulder arthroplasty baseplate fixation.

J Shoulder Elb Surg. 2015;24(11):e312–e319. doi:10.1016/j.jse.2015.05.045

42. Frost HM. A 2003 update of bone physiology and Wolff s law for clinicians. Angle Orthod. 2004;74(1):3–15. doi:10.1043/0003-3219(2004)074<0003:AUOBPA>2.0.CO;2

43. Giles JW, Langohr GDG, Johnson JA, Athwal GS. Implant design variations in reverse total shoulder arthroplasty influence the required deltoid force and resultant joint load. Clin Orthop Relat Res. 2015;473(11):3615–3626. doi:10.1007/s11999-015-4526-0

44. Gill HS, Waite JC, Short A, Kellett CF, Price AJ, Murray DW. In vivo measurement of volumetric wear of a total knee replacement. Knee. 2006;13(4):312–317. doi:10.1016/j.knee.2006.04.001

45. Gilot GJ. Addressing glenoid erosion in anatomic total shoulder arthroplasty. Bull NYU Hosp Jt Dis. 2013;71(SUPPL. 2):51–53.

46. Gioe TJ, Sharma A, Tatman P, Mehle S. Do "premium" joint implants add value?: Analysis of high cost joint implants in a community registry. Clin Orthop Relat Res. 2011;469(1):48–54. doi:10.1007/s11999-010-1436-z

47. Glyn-Jones S, Isaac S, Hauptfleisch J, McLardy-Smith P, Murray DW, Gill HS. Does highly cross-linked polyethylene wear less than conventional polyethylene in total hip arthroplasty? A double-blind, randomized, and controlled trial using Roentgen stereophotogrammetric analysis. J Arthroplasty. 2008;23(3):337–343. doi:10.1016/j.arth.2006.12.117

48. Glyn-Jones S, McLardy-Smith P, Gill HS, Murray DW. The creep and wear of highly cross-linked polyethylene: A three-year randomised, controlled trial using radiostereometric analysis. J Bone Jt Surg Br. 2008;90(B):556–561. doi:10.1302/0301-620X.90B5.20545

49. Glyn-Jones S, Palmer AJR, Agricola R, Price AJ, Vincent TL, Weinans H, et al. Osteoarthritis. Lancet. 2015;386(9991):376–387. doi:10.1016/S0140-6736(14)60802-3

50. Goutallier D, Postel JM, Bernageau J, Lavau L, Voisin MC. Fatty muscle degeneration in cuff ruptures: Pre- and postoperative evaluation by CT scan. Clin Orthop Relat Res. 1994;(304):78–83. doi:10.1097/00003086-199407000-00014

51. Grassi FA, Murena L, Valli F, Alberio R. Six-year experience with the Delta III reverse shoulder prosthesis. J Orthop Surg (Hong Kong). 2009;17(2):151–156. doi:10.1177/230949900901700205

52. Gutiérrez S, Luo ZP, Levy J, Frankle MA. Arc of motion and socket depth in reverse shoulder implants. Clin Biomech. 2009;24(6):473–479. doi:10.1016/j.clinbiomech.2009.02.008

53. Halder a M, Kuhl SG, Zobitz ME, Larson D, An KN. Effects of the glenoid labrum and glenohumeral abduction on stability of the shoulder joint through concavity-compression : an in vitro study. J Bone Joint Surg Am. 2001;83–A:1062–1069.

54. Halder AM, Itoi E, An K-N. Anatomy and biomechanics of the shoulder. Orthop Clin North Am. 2000;31(2):159–176. doi:10.1007/10.1007/978-3-642-36569-0_60

55. Hall EJ, Giaccia AJ. Radiobiology for the radiologist: Seventh edition. 2012.

56. Horsager K, Kaptein BL, Jørgensen PB, Jepsen CF, Stilling M. Oxford medial unicompartmental knees display contact-loss during step-cycle motion and bicycle

motion: A dynamic radiosterometric study. J Orthop Res. 2018;36(1):357–364. doi:10.1002/jor.23625

57. Iannotti JP, Gabriel JP, Schneck SL, Evans BG, Misra S. The normal glenohumeral relationships: An anatomical study of one hundred and forty shoulders. J Bone Joint Surg Am. 1992;74–A(4):491–500.

58. Inoue K, Suenaga N, Oizumi N, Yamaguchi H, Miyoshi N, Taniguchi N, et al. Humeral bone resorption after anatomic shoulder arthroplasty using an uncemented stem. J Shoulder Elb Surg. 2017;26(11):1984–1989. doi:10.1016/j.jse.2017.04.012

59. Jones RB, Wright TW, Roche CP. Bone grafting the glenoid vs Use of augmented glenoid baseplates with reverse shoulder arthroplasty. Bull Hosp Joint Dis. 2015;73(Suppl 1):S129–S135.

60. Kandahari AM, Yang X, Laroche KA, Dighe AS, Pan D, Cui Q. A review of UHMWPE wear-induced osteolysis: The role for early detection of the immune response. Bone Res. 2016;4(16014). doi:10.1038/boneres.2016.14

61. Kapat K, Srivas PK, Rameshbabu AP, Maity PP, Jana S, Dutta J, et al. Influence of porosity and pore-size distribution in Ti6Al4V foam on physicomechanical properties, osteogenesis, and quantitative validation of bone ingrowth by micro-computed tomography. ACS Appl Mater Interfaces. 2017;9:39235–39248. doi:10.1021/acsami.7b13960

62. Kaptein BL, Valstar ER, Stoel BC. Clinical validation of model-based RSA for a total knee prosthesis. Clin Orthop Relat Res. 2007;464:205–209. doi:10.1097/BLO.0b013e3181571aa5

63. Kaptein BL, Valstar ER, Stoel BC, Rozing PM, Reiber JHC. A new model-based RSA method validated using CAD models and models from reversed engineering. J Biomech. 2003;36(6):873–882. doi:10.1016/S0021-9290(03)00002-2

64. Kärrholm J, Gill RHS, Valstar ER. The history and future of radiostereometric analysis. Clin Orthop Relat Res. 2006;448(448):10–21. doi:10.1097/01.blo.0000224001.95141.fe

65. Keener JD, Chalmers PN, Yamaguchi K. The humeral implant in shoulder arthroplasty. J Am Acad Orthop Surg. 2017;25(6):427–438. doi:10.5435/JAAOS-D-15-00682

66. Kellgren JH, Lawrence JS. Radiological assessment of osteo-arthritis. Ann Rheum Dis. 1956;16:494–502.

67. Kempton LB, Balasubramaniam M, Ankerson E, Wiater JM. A radiographic analysis of the effects of prosthesis design on scapular notching following reverse total shoulder arthroplasty. J Shoulder Elb Surg. 2011;20(4):571–576. doi:10.1016/j.jse.2010.08.024

68. Kiet TK, Feeley BT, Naimark M, Gajiu T, Hall SL, Chung TT, et al. Outcomes after shoulder replacement: Comparison between reverse and anatomic total shoulder arthroplasty. J Shoulder Elb Surg. 2015;24(2):179–185. doi:10.1016/j.jse.2014.06.039

69. Kingsley C, Patel S. Patient-reported outcome measures and patient-reported experience measures. BJA Educ. 2017;17(4):137–144. doi:10.1093/bjaed/mkw060

70. Knowles NK, Ferreira LM, Athwal GS. Augmented glenoid component designs for type B2 erosions: A computational comparison by volume of bone removal and

quality of remaining bone. J Shoulder Elb Surg. 2015;24(8):1218–1226. doi:10.1016/j.jse.2014.12.018

71. Kohan EM, Chalmers PN, Salazar D, Keener JD, Yamaguchi K, Chamberlain AM. Dislocation following reverse total shoulder arthroplasty. J Shoulder Elb Surg. 2017;26(7):1238–1245. doi:10.1016/j.jse.2016.12.073

72. Kohut G, Dallmann F, Irlenbusch U. Wear-induced loss of mass in reversed total shoulder arthroplasty with conventional and inverted bearing materials. J Biomech. 2012;45(3):469–473. doi:10.1016/j.jbiomech.2011.11.055

73. Kontaxis A, Johnson GR. The biomechanics of reverse anatomy shoulder replacement – A modelling study. Clin Biomech. 2009;24(3):254–260. doi:10.1016/j.clinbiomech.2008.12.004

74. Koorevaar RCT, Kleinlugtenbelt YV, Landman EBM, van't Riet E, Bulstra SK. Psychological symptoms and the MCID of the DASH score in shoulder surgery. J Orthop Surg Res. 2018;13(246). doi:10.1186/s13018-018-0949-0

75. Kuhn JE, Dunn WR, An Q, Baumgarten KM, Bishop JY, Brophy RH, et al. Effectiveness of physical therapy in treating atrumatic full thicness rotator cufft tears. J Shoulder Elb Surg. 2013;22(10):1371–1379. doi:10.1016/j.jse.2013.01.026

76. Kurdziel MD, Newton MD, Hartner S, Baker KC, Wiater JM. Quantitative evaluation of retrieved reverse total shoulder arthroplasty liner surface deviation and volumetric wear. J Orthop Res. 2018;36(7):2007–2014. doi:10.1002/jor.23849

77. Kurtz SM, Gawel HA, Patel JD. History and systematic review of wear and osteolysis outcomes for first-generation highly crosslinked polyethylene. Clin Orthop Relat Res. 2011;469(8):2262–2277. doi:10.1007/s11999-011-1872-4

78. Lädermann A, Gueorguiev B, Charbonnier C, Stimec B V, Fasel JHD, Zderic I, et al. Scapular notching on kinematic simulated range of motion after reverse shoulder arthroplasty is not the result of impingement in adduction. Medicine (Baltimore). 2015;94(38):e1615. doi:10.1097/MD.0000000000001615

79. Lambert B, Neut D, van der Veen HC, Bulstra SK. Effects of vitamin E incorporation in polyethylene on oxidative degradation, wear rates, immune response, and infections in total joint arthroplasty: a review of the current literature. Int Orthop. 2019;43(7):1549–1557. doi:10.1007/s00264-018-4237-8

80. Langohr GDG, Athwal GS, Johnson JA, Medley JB. Wear simulation strategies for reverse shoulder arthroplasty implants. Proc Inst Mech Eng Part H J Eng Med. 2016;230(5):458–469. doi:10.1177/0954411916642801

81. Langohr GDG, Haverstock JP, Johnson JA, Athwal GS. Comparing daily shoulder motion and frequency after anatomic and reverse shoulder arthroplasty. J Shoulder Elb Surg. 2018;27(2):325–332. doi:10.1016/j.jse.2017.09.023

82. Langohr GDG, Willing R, Medley JB, Athwal GS, Johnson JA. Contact mechanics of reverse total shoulder arthroplasty during abduction: The effect of neck-shaft angle, humeral cup depth, and glenosphere diameter. J Shoulder Elb Surg. 2016;25(4):589–597. doi:10.1016/j.jse.2015.09.024

83. Law TY, Rosas S, George F, Kurowicki J, Formaini N, Levy J. Short-term projected use of reverse total shoulder arthroplasty in proximal humerus fracture cases recorded in Humana's National private-payer database. Am J Orthop. 2017;46(1):E28–E31.

84. Lévigne C, Boileau P, Favard L, Garaud P, Molé D, Sirveaux F, et al. Scapular

notching in reverse shoulder arthroplasty. J Shoulder Elb Surg. 2008;17(6):925–935. doi:10.1016/j.jse.2008.02.010

85. Lin EC. Radiation risk from medical imaging. Mayo Clin Proc. 2010;85(12):1142–1146. doi:10.4065/mcp.2010.0260

86. Liu F, Galvin A, Jin Z, Fisher J. A new formulation for the prediction of polyethylene wear in artificial hip joints. Proc Inst Mech Eng Part H J Eng Med. 2011;225(1):16–24. doi:10.1243/09544119JEIM819

87. Macías-Hernández SI, Morones-Alba JD, Miranda-Duarte A, Coronado-Zarco R, Soria-Bastida M de los A, Nava-Bringas T, et al. Glenohumeral osteoarthritis: overview, therapy, and rehabilitation. Disabil Rehabil. 2017;39(16):1674–1682. doi:10.1080/09638288.2016.1207206

88. Manning DW, Chiang PP, Martell JM, Galante JO, Harris WH. In vivo comparative wear study of traditional and highly cross-linked polyethylene in total hip arthroplasty. J Arthroplasty. 2005;20(7):880–886. doi:10.1016/j.arth.2005.03.033

89. Mckellop H, Campbell P, Park S, Schmalzried T, Grigoris P, Amstutz H, et al. The origin of submicron polyethylene wear debris in total hip arthropasty. Clin Orthop Relat Res. 1995 Mar 1;311:3–20.

90. Medel F, Kurtz S, Sharkey P, Parvizi J, Klein G, Hatzband M, et al. In vivo oxidation contributes to delamination but not pitting in polyethylene components for total knee arthroplasty. J Arthroplasty. 2011;26(5):802–810. doi:10.1016/j.arth.2010.07.010.IN

91. Morgan EF, Unnikrisnan GU, Hussein AI. Bone mechanical properties in healthy and diseased states. Annu Rev Biomed Eng. 2018;20:119–143. doi:10.1146/annurev-bioeng-062117-121139

92. Nagels J, Stokdijk M, Rozing PM. Stress shielding and bone resorption in shoulder arthroplasty. J Shoulder Elb Surg. 2003;12(1):35–39. doi:10.1067/mse.2003.22

93. Nam D, Kepler CK, Nho SJ, Craig E V., Warren RF, Wright TM. Observations on retrieved humeral polyethylene components from reverse total shoulder arthroplasty. J Shoulder Elb Surg. 2010;19(7):1003–1012. doi:10.1016/j.jse.2010.05.014

94. Naveed MA, Kitson J, Bunker TD. The Delta III reverse shoulder replacement for cuff tear arthropathy: a single-centre study of 50 consecutive procedures. J Bone Joint Surg Br. 2011;93(1):57–61. doi:10.1302/0301-620X.93B1.24218

95. Neer CS. Articular replacement for the humeral head. Clin Orthop Relat Res [Internet]. 1955;37–A(2):215–228. Available from: http://www.ncbi.nlm.nih.gov/pubmed/14367414

96. Neer CS, Craig E V, Fukuda H. Cuff-tear arthropathy. J Bone Joint Surg Am. 1983;65–A(9):1232–1244.

97. Neer CS, Watson KC, Stanton FJ. Recent experience in total shoulder replacement. J Bone Joint Surg Am. 1982;64–A(3):319–337. doi:10.1007/978-1-4471-5451-8_81

98. Nelissen RGHH, Pijls BG, Karrholm J, Malchau H, Nieuwenhuijse MJ, Valstar ER. RSA and registries: The quest for phased introduction of new implants. J Bone Joint Surg. 2011;93(3):62–65. doi:10.2106/JBJS.K.00907

99. Nelson EC, Eftimovska E, Lind C, Hager A, Wasson JH, Lindblad S. Patient

reported outcome measures in practice. BMJ. 2015;350(February):1–3. doi:10.1136/bmj.g7818

100. Nilsson KG, Dalén T. Inferior performance of Boneloc® bone cement in total knee arthroplasty. A prospective randomized study comparing Boneloc® with Palacos® using radiostereometry (RSA) in 19 patients. Acta Orthop Scand. 1998;69(5):479–483. doi:10.3109/17453679808997782

101. Nuttall D, Birch A, Haines JF, Trail IA. Radiostereographic analysis of a shoulder surface replacement: Does hydroxyapatite have a place? Bone Jt J. 2014;96 B(8):1077–1081. doi:10.1302/0301-620X.96B8.30534

102. Nuttall D, Birch A, Haines JF, Watts AC, Trail IA. Early migration of a partially cemented fluted glenoid component inserted using a cannulated preparation system. Bone Joint J. 2017;99–B(5):674–679. doi:10.1302/0301-620X.99B5.BJJ-2016-0745.R1

103. Nuttall D, Haines JF, Trail IA. The effect of the offset humeral head on the micromovement of pegged glenoid components: A comparative study using radiostereometric analysis. J Bone Jt Surg Br. 2009;91–B(6):757–761. doi:10.1302/0301-620X.91B6.22060

104. Nuttall D, Haines JF, Trail II. A study of the micromovement of pegged and keeled glenoid components compared using radiostereometric analysis. J Shoulder Elb Surg. 2007;16(Suppl 3):65–70. doi:10.1016/j.jse.2006.01.015

105. Oh LS, Wolf BR, Hall MP, Levy BA, Marx RG. Indications for rotator cuff repair: a systematic review. Clin Orthop Relat Res. 2007;455:52–63. doi:10.1097/BLO.0b013e31802fc175

106. Oral E, Beckos CG, Malhi AS, Muratoglu OK. The effects of high dose irradiation on the cross-linking of vitamin E-blended ultrahigh molecular weight polyethylene. Biomaterials. 2008;29(26):3557–3560. doi:10.1016/j.biomaterials.2008.05.004

107. Padegimas EM, Maltenfort M, Lazarus MD, Ramsey ML, Williams GR, Namdari S. Future patient demand for shoulder arthroplasty by younger patients: national projections. Clin Orthop Relat Res. 2015;473(6):1860–1867. doi:10.1007/s11999-015-4231-z

108. Pandya J, Johnson T, Low AK. Shoulder replacement for osteoarthritis: A review of surgical management. Maturitas. 2018;108:71–76. doi:10.1016/j.maturitas.2017.11.013

109. Parsons BO, Gruson KI, Accousti KJ, Klug RA, Flatow EL. Optimal rotation and screw positioning for initial glenosphere baseplate fixation in reverse shoulder arthroplasty. J Shoulder Elb Surg. 2009;18(6):886–891. doi:10.1016/j.jse.2008.11.002

110. Patte D. Classification of rotator cuff lesions. Clin Orthop Relat Res. 1990;(254):81–6. doi:10.1097/00003086-199005000-00012

111. Peers S, Moravek JE, Budge MD, Newton MD, Kurdziel MD, Baker KC, et al. Wear rates of highly cross-linked polyethylene humeral liners subjected to alternating cycles of glenohumeral flexion and abduction. J Shoulder Elb Surg. 2015;24(1):143–149. doi:10.1016/j.jse.2014.05.001

112. Phadnis J, Huang T, Watts A, Krishnan J, Bain GI. Cemented or cementless humeral fixation in reverse total shoulder arthroplasty? Bone Jt J. 2016;98B(1):65–

74. doi:10.1302/0301-620X.98B1.36336

113. Pijls BG, Nieuwenhuijse MJ, Fiocco M, Plevier JWM, Nelissen RGHH, Valstar ER, et al. Early proximal migration of cups is associated with late revision in THA. Acta Orthop. 2012;83(6):583–591. doi:10.3109/17453674.2012.745353

114. Pijls BG, Plevier JWM, Nelissen RGHH. RSA migration of total knee replacements: A systematic review and meta-analysis. Acta Orthop. 2018;89(3):320–328. doi:10.1080/17453674.2018.1443635

115. Pijls BG, Valstar ER, Nouta K, Plevier JWM, Middeldorp S, Nelissen RGHH, et al. Early migration of tibial components is associated with late revision: A systematic review and meta-analysis of 21,000 knee arthroplasties. Acta Orthop. 2012;83(6):614–624. doi:10.3109/17453674.2012.747052

116. Postacchini R, Carbone S, Canero G, Ripani M, Postacchini F. Reverse shoulder prosthesis in patients with rheumatoid arthritis: a systematic review. Int Orthop. 2016;40(5):965–973. doi:10.1007/s00264-015-2916-2

117. Price A, Short A, Kellett C, Beard D, Gill H, Pandit H, et al. Ten-year in vivo wear measurement of a fully congruent mobile bearing unicompartmental knee arthroplasty. J Bone Joint Surg Br. 2005;87(11):1493–1497. doi:10.1302/0301-620X.87B11.16325

118. Quental C, Folgado J, Fernandes PR, Monteiro J. Computational analysis of polyethylene wear in anatomical and reverse shoulder prostheses. Med Biol Eng Comput. 2015;53(2):111–122. doi:10.1007/s11517-014-1221-3

119. Radl R, Aigner C, Hungerford M, Pascher A, Windhager R. Proximal femoral bone loss and increased rate of fracture with a proximally hydroxyapatite-coated femoral component. J Bone Jt Surg - Ser B. 2000;82(8):1151–1155. doi:10.1302/0301-620X.82B8.11030

120. Rahme H, Mattsson P, Wikblad L, Larsson S. Cement and press-fit humeral stem fixation provides similar results in rheumatoid patients. Clin Orthop Relat Res. 2006;(448):28–32. doi:10.1097/01.blo.0000224007.25636.85

121. Rahme H, Mattsson P, Wikblad L, Nowak J, Larsson S. Stability of cemented in-line pegged glenoid compared with keeled glenoid components in total shoulder arthroplasty. J Bone Joint Surg Am. 2009;91(8):1965–1972. doi:10.2106/JBJS.H.00938

122. Roche CP, Stroud NJ, Martin BL, Steiler CA, Flurin PH, Wright TW, et al. The impact of scapular notching on reverse shoulder glenoid fixation. J Shoulder Elb Surg. 2013;22(7):963–970. doi:10.1016/j.jse.2012.10.035

123. Ryd L, Albrektsson BE, Carlsson L, Dansgard F, Herberts P, Lindstrand A, et al. Roentgen stereophotogrammetric analysis as a predictor of mechanical loosening of knee prostheses. J Bone Joint Surg Br. 1995;77(3):377–383.

124. Ryd L, Lindstrand A, Rosenquist R, Selvik G. Micromotion of conventionally cemented all-polyethylene tibial components in total knee replacements - A roentgen stereophotogrammetric analysis of migration and inducible displacement. Arch Orthop Trauma Surg. 1987;106(2):82–88. doi:10.1007/BF00435419

125. Ryd L, Yuan X, Löfgren H. Methods for determining the accuracy of radiostereometric analysis (RSA). Acta Orthop Scand. 2000;71(August):403–408. doi:10.1080/000164700317393420

126. Ryösä A, Laimi K, Äärimaa V, Lehtimäki K, Kukkonen J, Saltychev M. Surgery

or conservative treatment for rotator cuff tear: a meta-analysis. Disabil Rehabil. 2017;39(14):1357–1363. doi:10.1080/09638288.2016.1198431

127. Sakellariou VI, Sculco P, Poultsides L, Wright T, Sculco TP. Highly cross-linked polyethylene may not have an advantage in total knee arthroplasty. HSS J. 2013;9(3):264–269. doi:10.1007/s11420-013-9352-x

128. Saleh KJ, El Othmani MM, Tzeng TH, Mihalko WM, Chambers MC, Grupp TM. Acrylic bone cement in total joint arthroplasty: A review. J Orthop Res. 2016;34(5):737–744. doi:10.1002/jor.23184

129. Samuelsen BT, Wagner ER, Houdek MT, Elhassan BT, Sánchez-Sotelo J, Cofield R, et al. Primary reverse shoulder arthroplasty in patients aged 65 years or younger. J Shoulder Elb Surg. 2017;26(1):e13–e17. doi:10.1016/j.jse.2016.05.026

130. Sandow M, Schutz C. Total shoulder arthroplasty using trabecular metal augments to address glenoid retroversion: The preliminary result of 10 patients with minimum 2-year follow-up. J Shoulder Elb Surg. 2016;25(4):598–607. doi:10.1016/j.jse.2016.01.001

131. Schmidt CC, Jarrett CD, Brown BT. Management of rotator cuff tears. J Hand Surg Am. 2015;40(2):399–408. doi:10.1016/j.jhsa.2014.06.122

132. Sedaghat AR. Understanding the minimal clinically important difference (MCID) of patient-reported outcome measures. Otolaryngol - Head Neck Surg (United States). 2019;161(4):551–560. doi:10.1177/0194599819852604

133. Seehaus F, Emmerich J, Kaptein BL, Windhagen H, Hurschler C. Experimental analysis of Model-Based Roentgen Stereophotogrammetric Analysis (MBRSA) on four typical prosthesis components. J Biomech Eng. 2009;131(4):041004-1–10. doi:10.1115/1.3072892

134. Seibert JA. X-ray imaging physics for nuclear medicine technologists. Part 1: Basic principles of x-ray production. J Nucl Med Technol. 2004;32(3):139–147.

135. Selvik G. Roentgen stereophotogrammetric analysis. Acta radiol. 1990;31(2):113–126. doi:10.3109/02841859009177472

136. Sershon RA, Van Thiel GS, Lin EC, McGill KC, Cole BJ, Verma NN, et al. Clinical outcomes of reverse total shoulder arthroplasty in patients aged younger than 60 years. J Shoulder Elb Surg. 2014;23(3):395–400. doi:10.1016/j.jse.2013.07.047

137. Simovitch R, Flurin PH, Wright T, Zuckerman JD, Roche CP. Quantifying success after total shoulder arthroplasty: the minimal clinically important difference. J Shoulder Elb Surg. 2018;27(2):298–305. doi:10.1016/j.jse.2017.09.013

138. Simovitch RW, Zumstein MA, Lohri E, Helmy N, Gerber C. Predictors of scapular notching in patients managed with the Delta III reverse total shoulder replacement. J Bone Joint Surg. 2007;89–A(3):588–600. doi:10.2106/JBJS.F.00226

139. Sirveaux F, Favard L, Oudet D, Huquet D, Walch G, Molé D. Grammont inverted total shoulder arthroplasty in the treatment of glenohumeral osteoarthritis with massive rupture of the cuff. Results of a multicentre study of 80 shoulders. J Bone Joint Surg Br. 2004;86–B(3):388–395. doi:10.1302/0301-620X.86B3.14024

140. Smith SL, Li BL, Buniya A, Ho Lin S, Scholes SC, Johnson G, et al. In vitro wear testing of a contemporary design of reverse shoulder prosthesis. J Biomech. 2015;48(12):3072–3079. doi:10.1016/j.jbiomech.2015.07.022

141. Soares D, Leite P, Barreira P, Aido R, Sousa R. Antibiotic-loaded bone cement in

total joint arthroplasty. Acta Orthop Belg. 2015;81(2):184–190.

142. Spormann C, Durchholz H, Audigé L, Flury M, Schwyzer HK, Simmen BR, et al. Patterns of proximal humeral bone resorption after total shoulder arthroplasty with an uncemented rectangular stem. J Shoulder Elb Surg. 2014;23(7):1028–1035. doi:10.1016/j.jse.2014.02.024

143. Stephens BF, Hebert CT, Azar FM, Mihalko WM, Throckmorton TW. Optimal baseplate rotational alignment for locking-screw fixation in reverse total shoulder arthroplasty: A three-dimensional computer-aided design study. J Shoulder Elb Surg. 2015;24(9):1367–1371. doi:10.1016/j.jse.2015.01.012

144. Stilling M, Kold S, de Raedt S, Andersen NT, Rahbek O, Soballe K. Superior accuracy of model-based radiostereometric analysis for measurement of polyethylene wear: A phantom study. Bone Joint Res. 2012;1(8):180–191. doi:10.1302/2046-3758.18.2000041

145. Stilling M, Mechlenburg I, Amstrup A, Soballe K, Klebe T. Precision of novel radiological methods in relation to resurfacing humeral head implants: Assessment by radiostereometric analysis, DXA, and geometrical analysis. Arch Orthop Trauma Surg. 2012;132(11):1521–1530. doi:10.1007/s00402-012-1580-x

146. Streit JJ, Shishani Y, Greene ME, Nebergall AK, Wanner JP, Bragdon CR, et al. Radiostereometric and radiographic analysis of glenoid component motion after total shoulder arthroplasty. Orthopedics. 2015;38(10):e891–e897. doi:10.3928/01477447-20151002-56

147. Strickland MA, Dressler MR, Taylor M. Predicting implant UHMWPE wear in-silico: A robust, adaptable computational-numerical framework for future theoretical models. Wear. 2012;274–275:100–108. doi:10.1016/j.wear.2011.08.020

148. Tashjian RZ. Epidemiology, natural history, and indications for treatment of rotator cuff tears. Clin Sport Med. 2012;31:589–604. doi:10.1016/j.csm.2012.07.001

149. Teeter MG, Perry KI, Yuan X, Howard JL, Lanting BA. Contact kinematic differences between gap balanced vs measured resection techniques for single radius posterior-stabilized total knee arthroplasty. J Arthroplasty. 2017;32(6):1834–1838. doi:10.1016/j.arth.2016.12.054

150. Teeter MG, Perry KI, Yuan X, Howard JL, Lanting BA. Contact kinematics correlates to tibial component migration following single radius posterior stabilized knee replacement. J Arthroplasty. 2018;33(3):740–745. doi:10.1016/j.arth.2017.09.064

151. Terrier A, Merlini F, Pioletti DP, Farron A. Comparison of polyethylene wear in anatomical and reversed shoulder prostheses. J Bone Joint Surg Br. 2009;91–B(7):977–982. doi:10.1302/0301-620X.91B7.21999

152. Teusink MJ, Pappou IP, Schwartz DG, Cottrell BJ, Frankle MA. Results of closed management of acute dislocation after reverse shoulder arthroplasty. J Shoulder Elb Surg. 2015;24(4):621–627. doi:10.1016/j.jse.2014.07.015

153. Thanner J, Freij-larsson C, Kärrholm J, Malchau H, Wesslén B. Evaluation of Boneloc®: Chemical and mechanical properties, and a randomized clinical study of 30 total hip arthroplasties. Acta Orthop Scand. 1995;66(3):207–214. doi:10.3109/17453679508995525

154. Theivendran K, Varghese M, Large R, Bateman M, Morgan M, Tambe A, et al. Reverse total shoulder arthroplasty using a trabecular metal glenoid base plate. Bone Jt J. 2016;98(7):969–975. doi:10.1302/0301-620X.98B7

155. Thomas GE, Simpson DJ, Mehmood S, Taylor A, McLardy-Smith P, Singh Gill H, et al. The seven-year wear of highly cross-linked polyethylene in total hip arthroplasty. J Bone Joint Surg Am. 2011;93(8):716–722. doi:10.2106/JBJS.J.00287

156. Torrens C, Guirro P, Miquel J, Santana F. Influence of glenosphere size on the development of scapular notching: a prospective randomized study. J Shoulder Elb Surg. 2016;25(11):1735–1741. doi:10.1016/j.jse.2016.07.006

157. Vaishya R, Chauhan M, Vaish A. Bone cement. J Clin Orthop Trauma. 2013;4:157–163. doi:10.1016/j.jcot.2013.11.005

158. Valstar ER, Gill R, Ryd L, Flivik G, Börlin N, Kärrholm J. Guidelines for standardization of radiostereometry (RSA) of implants. Acta Orthop. 2005;76(4):563–572. doi:10.1080/17453670510041574

159. Valstar ER, De Jong FW, Vrooman HA, Rozing PM, Reiber JHC. Model-based Roentgen stereophotogrammetry of orthopaedic implants. J Biomech. 2001;34(6):715–722. doi:10.1016/S0021-9290(01)00028-8

160. Valstar ER, Nelissen RGHH, Reiber JHC, Rozing PM. The use of Roentgen stereophotogrammetry to study micromotion of orthopaedic implants. ISPRS J Photogramm Remote Sens. 2002;56(5–6):376–389. doi:10.1016/S0924-2716(02)00064-3

161. Vanhove B, Beugnies A. Grammont's reverse shoulder prosthesis for rotator cuff arthropathy. A retrospective study of 32 cases. Acta Orthop Belg. 2004;70(3):219–225.

162. Vaupel ZM, Baker KC, Kurdziel MD, Wiater JM. Wear simulation of reverse total shoulder arthroplasty systems: Effect of glenosphere design. J Shoulder Elb Surg. 2012;21(10):1422–1429. doi:10.1016/j.jse.2011.10.024

163. Walch G, Badet R, Boulahia A, Khoury A. Morphologic study of the glenoid in primary glenohumeral osteoarthritis. J Arthroplasty. 1999;14(6):756–760. doi:10.1016/S0883-5403(99)90232-2

164. Walker M, Willis MP, Brooks JP, Pupello D, Mulieri PJ, Frankle MA. The use of the reverse shoulder arthroplasty for treatment of failed total shoulder arthroplasty. J Shoulder Elb Surg. 2012;21(4):514–522. doi:10.1016/j.jse.2011.03.006

165. Wang A. A unified theory of wear for ultra-high molecular weight polyethylene in multi-directional sliding. Wear. 2001;248(1–2):38–47. doi:10.1016/S0043-1648(00)00522-6

166. Wang A, Stark C, Dumbleton JH. Mechanistic and morphological origins of ultra-high molecular weight polyethylene wear debris in total joint replacement prostheses. Proc Inst Mech Eng Part H J Eng Med. 1996;210(3):141–155. doi:10.1243/PIME

167. Wang A, Sun DC, Yau S, Edwards B, Sokol M, Essner A, et al. Orientation softening in the deformation and wear of ultra-high molecular weight polyethylene. Wear. 1997;204:230–241.

168. Weldring T, Smith SMS. Article Commentary: Patient-Reported Outcomes (PROs) and Patient-Reported Outcome Measures (PROMs). Heal Serv Insights.

2013;6:HSI.S11093. doi:10.4137/hsi.s11093

169. Werner BS, Böhm D, Abdelkawi A, Gohlke F. Glenoid bone grafting in reverse shoulder arthroplasty for long-standing anterior shoulder dislocation. J Shoulder Elb Surg. 2014;23(11):1655–1661. doi:10.1016/j.jse.2014.02.017

170. Werner CML, Steinmann PA, Gilbart M, Gerber C. Treatment of painful pseudoparesis due to irreparable rotator cuff dysfunction with the Delta III reverse-ball-and-socket total shoulder prosthesis. J Bone Joint Surg Am. 2005;87(7):1476–1486. doi:10.2106/JBJS.D.02342

171. Wiater BP, Baker EA, Salisbury MR, Koueiter DM, Baker KC, Nolan BM, et al. Elucidating trends in revision reverse total shoulder arthroplasty procedures: A retrieval study evaluating clinical, radiographic, and functional outcomes data. J Shoulder Elb Surg. 2015;24(12):1915–1925. doi:10.1016/j.jse.2015.06.004

172. Zumstein MA, Pinedo M, Old J, Boileau P. Problems, complications, reoperations, and revisions in reverse total shoulder arthroplasty: A systematic review. J Shoulder Elb Surg. 2011;20(1):146–157. doi:10.1016/j.jse.2010.08.001

173. The Arthritis Society [Internet]. 2019 [cited 2019 Nov 24];Available from: https://arthritis.ca

3 Validation of radiostereometric analysis in six degrees of freedom for use with reverse total shoulder arthroplasty

A version of this chapter has been published.[14]*

3.1 Introduction

The number of total shoulder replacement procedures is projected to increase by 755% between 2011 and 2030 in the United States.[24] Since its approval by Heath Canada in 2003 and the US Food and Drug Administration in 2004, reverse total shoulder arthroplasty (RTSA) has grown to account for over 30% of all shoulder procedures, with its prevalence expected to increase.[8] For this reason, it is important to understand long-term shoulder implant relative displacement and wear.

Implant displacement relative to its host bone within the first two years post-operatively is a predictive measure of long-term implant failure and subsequent revision in both the hip and knee.[12,26] Radiostereometric analysis (RSA) is a robust dual-focus x-ray imaging technique used for evaluating such relative displacement in vivo.[11,13,18] Currently, two RSA approaches are used in clinical studies: conventional marker-based RSA, and model-based RSA (MBRSA). MBRSA eliminates the need for inserting beads into the implant, instead using the implant's geometry to identify its position and orientation.

RSA has been used to measure glenoid component relative displacement in anatomic shoulder arthroplasty,[19,22,23] though to the best of our knowledge, there are no published studies identifying relative displacement of implant components with RTSA. RSA standardization guidelines recommend that a phantom study be conducted to determine the lower limits of system performance of any new technique prior to implementation in clinical assessment, in order to identify the inaccuracies of MBRSA analysis caused by the dimensional differences between the actual implant and the CAD model.[9,10,31]

---

*This version uses the term 'repeatability' instead of 'bias at zero motion,' as is reported in the published version, for clarity.

Therefore, the objective of this phantom study was to determine the bias and repeatability of both marker- and model-based RSA techniques for RTSA in six degrees of freedom.

3.2 Materials and Methods

A plastic shoulder joint phantom (SKU# 1050-13-2; Sawbones, Pacific Research Laboratories, Vashon, WA, USA) was fitted with an RTSA implant set (Aequalis™ Ascend™ Flex, Wright Medical-Tornier Group, Memphis, TN, USA) by an experienced orthopedic surgeon (Figure 3.1). Thirteen spherical tantalum markers with diameter of 0.8 mm were inserted into the bone surrounding the implants and sealed in place with Loctite adhesive (Loctite, Dusseldorf, Germany). Seven beads were embedded in the proximal humerus, four in the coracoid, and two in the glenoid, at the approach angles available during surgery.
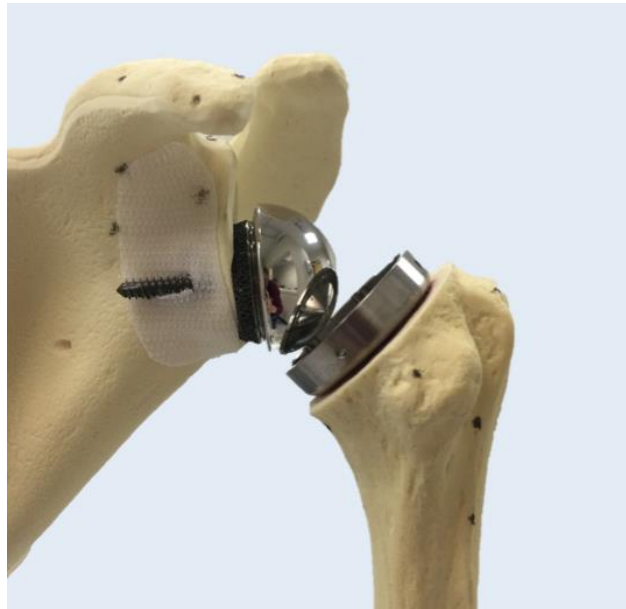
Figure 3.1 The shoulder phantom fitted with reverse total shoulder arthroplasty implants and tantalum beads.

The humerus component of the phantom was attached securely to a composite micrometer stage with manufacturer-stated translation accuracy of $\pm$ 0.002 mm (Model M4434, Parker Hannafin, Irwin, USA) and rotational accuracy of less than 0.02° (Model

TTR001/M, Thorlabs Inc, Newton, USA). The scapula component was rigidly fixed to an acrylic platform using radiolucent nylon screws. The radiographic procedure was completed in a dedicated RSA suite, where two ceiling-mounted x-ray units (Proteus CR/a, GE Medical Systems, Milwaukee, WI, USA) were positioned at 20 degrees to the normal of a uniplanar calibration cage (Cage 43, RSA Biomedical, Umeå, Sweden) mating with 35.5 cm x 43.2 cm imaging plates (Figure 3.2). Radiographs were acquired by a computed radiography system (Capsula XL, FUJIFILM, Tokyo, Japan), producing images with a 3520 x 4280 pixel matrix, 100-micron pixel size, and 10-bit gray-scale mapping. This setup has previously been utilized for phantom validation studies of the hip and knee,[5,15,34] and is the traditional clinical RSA examination setup for large joints, where joint information is recorded together with the calibration cage.[17,20]

Figure 3.2 RSA setup for the shoulder phantom: the phantom is attached to a translation and rotation stage in front of a uniplanar calibration cage.

All captured images were measured using commercial model-based RSA software (RSACore, Leiden, The Netherlands) to determine the two-dimensional bead locations, and contour of the implant's 3D projection (Figure 3.3). Condition numbers for the

humerus bead alignment ranged from 28.3-28.4, and from 32.6-32.7 for the glenoid, indicating very good distribution of tantalum markers within the bone.[27] The threshold for mean rigid body error was 0.200 mm.
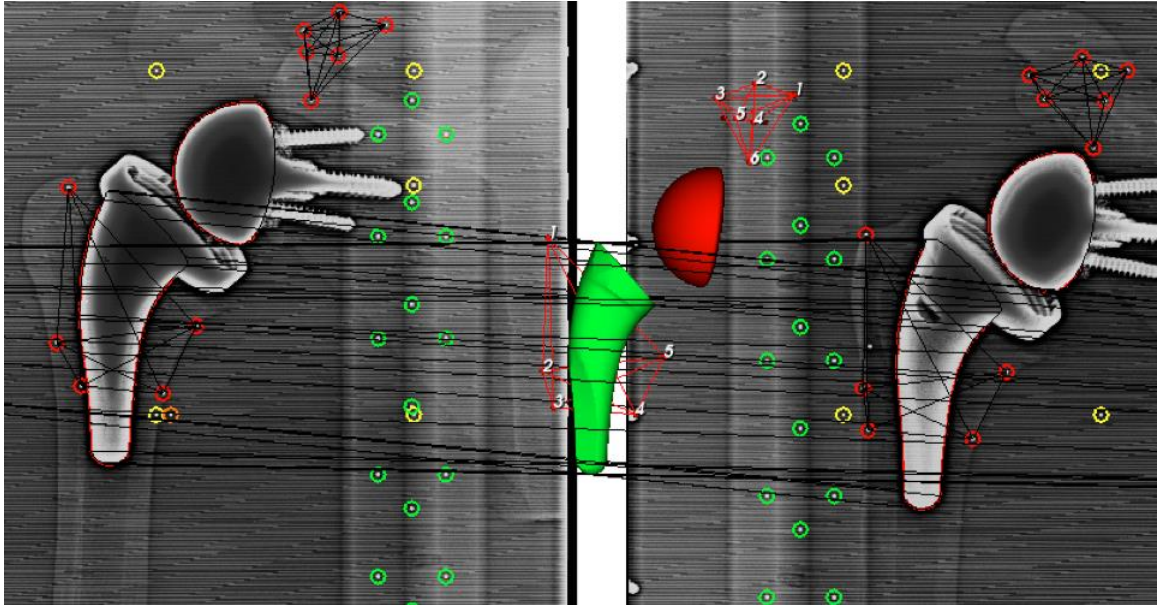
Figure 3.3 The model-based RSA environment showing tantalum beads inserted in the phantom (red circles) and the detected contour of the implants. The 3D surface model of the humeral stem is highlighted in green, and the glenosphere in red.

Translation and rotation studies were conducted independently from one another. In order to evaluate translation bias, simultaneous radiographs were taken at increments of 0.02, 0.05, 0.10, 0.15, 0.20, 0.40, 0.50, 0.60, 0.80, 1.00 1.50, 2.00, 2.50, 3.00, and 5.00 mm in each orthogonal plane, resulting in 15 translation pairs per axis. Displacements were completed sequentially in the X- (medial-lateral), Y- (superior-inferior), and Z- (anterior-posterior) directions. All displacements were calculated in reference to the previous increment examination. Bias in rotation was determined similarly, at increments of 0.11, 0.25, 0.50, 0.75, 1.00, 1.50, 1.99, 2.49, 2.99, 3.99, 5.02, and 6.02 degrees along X- (flexion-extension) and Y- (internal-external rotation) axes (increments limited by rotation stage increments, defined in microns). Angles of rotation along the Z-axis (abduction-adduction) were 0.12, 0.24, 0.51, 0.75, 0.99, 1.50, 2.01, 2.49, 3.00, 3.99, 5.01, and 6 degrees, resulting in 12 rotation pairs per axis. Double examinations, also known as zero-displacement exams, were taken at baseline and each subsequent increment to

provide independent data sets for bias evaluation and to assess the repeatability of the system. The phantom and x-ray foci remained stationary between double exposures.[3,7,28]

For this study, four sets of measurements were obtained. The first was the marker-based RSA gold standard, where relative displacement of the humerus was compared to the glenoid using the tantalum beads in each body (beads vs. beads). The next two sets of measurements are those used in model-based RSA: the comparison of humeral stem relative displacement with respect to the glenoid, and that of the glenosphere with respect to the humerus. In both cases, the relative displacement of a model was calculated in reference to implanted beads (model-beads). The last set of measurements is the relative displacement of the humeral stem with respect to the glenosphere (model-model). Model-model measurements are used predominantly for kinematics analysis and may provide insight into entirely markerless RSA methods.[2,6,29]

Bias along each orthogonal axis, including a resultant vector in translation, was reported as the mean absolute difference between test values and known micrometer increments ± the 95% confidence interval, defined by the most recent ASTM standards (ASTM E177) as recommended by Langlois and Hamadouche.[16] Repeatability was reported as the 95% repeatability limit, also defined by the most recent ASTM standards using the difference between double examinations and a theoretical displacement of zero between exposures. Repeatability was calculated as 1.96 x √2 x SD.

Bias was normally distributed along each translational axis, including the 3D resultant vector, and Rx using the marker-based RSA method. Using the humeral stem vs. glenoid measurements, bias was normally distributed along Ty and Rx. Bias was non-parametric along all translation and rotation axes using the humerus vs. glenosphere and humeral stem vs. glenosphere measurement methods. Repeatability was normally distributed along each translation and rotation axis, excluding Tx for the marker-based RSA measurements; normally distributed along Rx for the humerus vs. glenosphere measurements, and along Tz, 3D, and Rx for the stem vs. glenoid measurements.

Repeatability was non-parametrically distributed along each axis using the model-model humeral stem vs. glenosphere approach.

Statistically significant differences ($P < 0.05$) between the mean absolute error of the four measurement groups along each axis were calculated using the Friedman test for non-parametric comparison, with Dunn's test for multiple comparisons based on at least one measurement method in each comparison following a non-parametric distribution. Statistics were calculated using Prism 7 (GraphPad, La Jolla, CA, USA).

3.3 Results

The measurements are displayed as bias in Table 3.1 and repeatability in Table 3.2, with their statistical differences between measurement methods presented in Tables 3.3 and 3.4, respectively.

Table 3.1 Bias, reported as the mean absolute value ± 95% confidence interval (mm,°) for different measurement methods

	Marker-based	Model-based (humerus vs. glenosphere)	Model-based (glenoid vs. humeral stem)	Model-model (humeral stem vs. glenosphere)
Tx	0.054 ± 0.010	0.027 ± 0.010	0.047 ± 0.011	0.039 ± 0.011
Ty	0.060 ± 0.012	0.023 ± 0.009	0.063 ± 0.012	0.029 ± 0.010
Tz	0.083 ± 0.015	0.062 ± 0.014	0.078 ± 0.017	0.117 ± 0.029
3D	0.129 ± 0.014	0.078 ± 0.017	0.126 ± 0.016	0.135 ± 0.030
Rx	0.126 ± 0.025	0.211 ± 0.095	0.204 ± 0.038	0.243 ± 0.088
Ry	0.076 ± 0.025	N/A	0.794 ± 0.251	N/A
Rz	0.076 ± 0.028	0.239 ± 0.118	0.111 ± 0.033	0.384 ± 0.153

Table 3.2 Repeatability, reported as the 95% repeatability limit (mm,°) for different measurement methods

	Marker-based	Model-based (humerus vs. glenosphere)	Model-based (glenoid vs. humeral stem)	Model-model (humeral stem vs. glenosphere)
Tx	0.120	0.074	0.106	0.069
Ty	0.127	0.083	0.129	0.102
Tz	0.139	0.125	0.134	0.256
3D	0.156	0.149	0.148	0.259
Rx	0.206	0.067	0.356	0.284
Ry	0.131	N/A	1.953	N/A
Rz	0.075	0.141	0.149	1.273

Table 3.3 *P*-values between bias measurement methods (statistical significance set at $P < 0.05$)

	Marker-based & humerus vs. glenosphere	Marker-based & glenoid vs. humeral stem	Marker-based & humeral stem vs. glenosphere	Humerus vs. glenosphere & humeral stem vs. glenoid	Humerus vs. glenosphere & humeral stem vs. glenosphere	Humeral stem vs. glenoid & humeral stem vs. glenosphere
Tx	**< 0.001**	0.096	0.086	0.068	0.077	> 0.999
Ty	**< 0.001**	> 0.999	**0.042**	**< 0.001**	0.725	**0.020**
Tz	0.435	> 0.999	> 0.999	> 0.999	0.068	0.435
3D	**< 0.001**	0.850	0.725	**< 0.001**	**< 0.001**	> 0.999
Rx	> 0.999	0.602	> 0.999	0.064	0.268	> 0.999
Ry	N/A	**0.001**	N/A	N/A	N/A	N/A
Rz	**0.007**	0.064	**< 0.001**	> 0.999	0.135	**0.018**

Table 3.4 *P*-values between repeatability measurement methods (statistical significance set at $P < 0.05$)

	Marker-based & humerus vs. glenosphere	Marker-based & glenoid vs. humeral stem	Marker-based & humeral stem vs. glenosphere	Humerus vs. glenosphere & humeral stem vs. glenoid	Humerus vs. glenosphere & humeral stem vs. glenosphere	Humeral stem vs. glenoid & humeral stem vs. glenosphere
Tx	**< 0.001**	0.945	**0.025**	**< 0.001**	0.066	0.876
Ty	**< 0.001**	> 0.999	0.158	**< 0.001**	0.194	0.115
Tz	0.539	**0.032**	> 0.999	> 0.999	> 0.999	0.454
3D	0.051	0.287	0.074	0.143	0.495	> 0.999
Rx	**< 0.001**	0.352	> 0.999	< 0.001	< 0.001	0.070
Ry	N/A	< 0.001	N/A	N/A	N/A	N/A
Rz	> 0.999	**0.032**	< 0.001	0.184	**< 0.001**	**0.018**

Comparing the four measurement methods, there were no significant differences in the mean absolute error of translation bias along the Z-axis, or rotation bias about the X-axis (Table 3.3). Considering repeatability, there were no observed differences along the 3D translation axis (Table 3.4).

Overall, the mean absolute difference ± 95% confidence interval (bias) for resultant vectors in translation was least for the model-based humerus vs. glenosphere approach, at 0.078 ± 0.017 mm, followed by the model-based glenoid vs. humeral stem, marker-based, and model-model approaches at 0.126 ± 0.016 mm, 0.129 ± 0.014 mm, and 0.135 ± 0.030 mm respectively (Table 3.1). Repeatability measurements show essentially the same value for the resultant vector using each measurement method (ranging from 0.148 to 0.156 mm), excluding the markerless method, which was approximately half as repeatable, at 0.259 mm (Table 3.2).

Variations in bias for rotation were on the order of 0.1 degrees (Table 3.1). The marker-based approach demonstrated the least bias in all axes ($0.076 \pm 0.025°$ to $0.126 \pm 0.025°$), while the Ry axis using the stem and glenoid model-based method presented the most

biased measurement at $0.794 \pm 0.251°$. Greatest repeatability in rotation was achieved when using the humerus and glenosphere model-based technique, where it ranged from 0.067 to 0.141°. The measurement demonstrating least repeatability was obtained with the humeral stem and glenoid model-based method, at 1.953° (Table 3.2).

3.4   Discussion

This study was conducted to validate the use of RSA techniques for RTSA. Both model-based methods presented slightly less bias than the marker-based method in translation, though slightly more bias in rotation. Being relatively cylindrical in shape, very small rotations about the humeral stem's long axis were recorded with greater bias and poorer repeatability, resulting in error on the orders of 0.25° and 2° respectively. This is in agreement with prior model-based rotation studies, where internal/external rotation (Ry) provided the least reliable and repeatable results.[21,32] A systematic review of clinical RSA studies of anatomic total shoulder arthroplasty indicated a mean precision of 0.18 mm for translations and 0.96° for rotations of the glenoid component, and 0.61 mm and 5.34° for the humeral component.[4] Our results coincide with these clinical studies in translation, though provide better results in rotation. Our results show the same trend of humeral components having poorer repeatability measurements.

Variation in bias and repeatability between the measurement methods suggests a dependence on the shape, including symmetry, on the results. A potential source of error for our model-based results is the small dimensional difference between the CAD model of the implant and the implant itself due to casting and hand polishing, making perfect alignment between the detected contour and the actual contour unachievable. Furthermore, the modular tray that connects to the humeral stem was not included in the detected contour. An area of interest in RTSA design is the effect of tray eccentricity on shoulder stability, loading, and range of motion.[1,30] The stem used in this study is offset from the tray's central axis (Figure 3.4), allowing for eccentric alignment of the tray with respect to the stem, if desired by the surgeon. Because of this flexibility in orientation, it would not have been sufficient to claim RSA results from one tray configuration are

applicable to all. Accordingly, the tray component was eliminated from contour detection, and only the common stem considered. This limited contour is likely a significant contributor to the comparatively greater bias and poorer repeatability in internal-external rotation using the stem model. It should also be noted that measurements in internal-external rotation were undetermined when the glenosphere model was used, due its rotational symmetry about that axis.
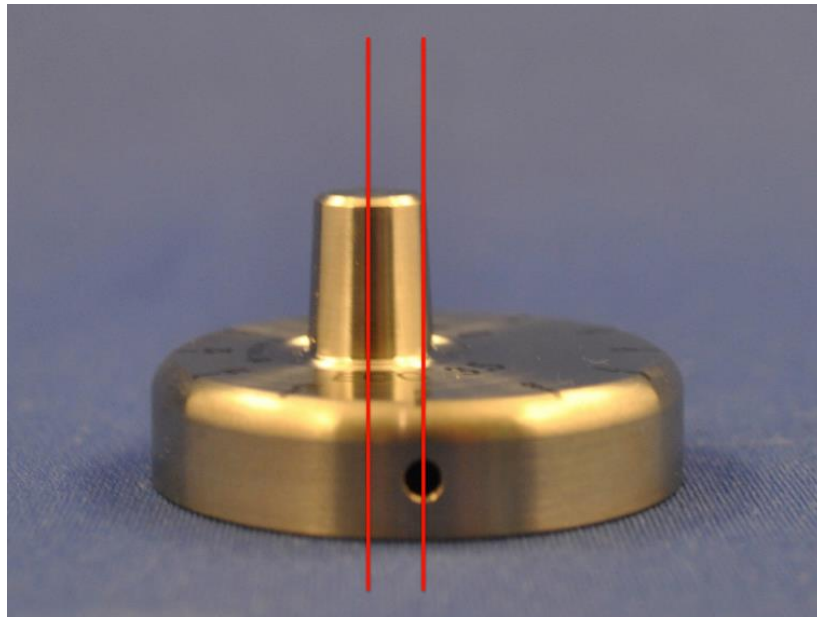
Figure 3.4 Rotation about the non-concentric axis of the humeral tray allows for eccentricity to be varied between patients, as determined by the surgeon.

We would also like to note that relative displacement measurements between the humeral stem and humeral beads, and glenosphere and glenoid beads were not measured directly, but rather bias and repeatability of relative displacement measurements for model-based RSA were measured indirectly (glenosphere to humeral beads; stem to glenoid beads) to accommodate the phantom setup and facilitate image acquisition. Though perhaps not the ideal study setup, we believe the results provide an accurate and reliable description of the capabilities of RSA measurements in terms of RTSA. Another limitation to this study is the use of a phantom model, rather than a cadaver. While the Sawbones phantom is designed to mimic the mechanical and radiographic properties of native bone, patients undergoing shoulder replacement are likely to be older with poorer and more variable

bone quality. Conducting this study in a cadaveric shoulder could have provided greater insight into the feasibility of bead insertion, and subsequent image quality and analysis reflective of the clinical environment.

The bias and repeatability for both model-based methods are well within the ranges of the accepted values for RSA techniques: 0.05 to 0.50 mm in translation, and 0.15 to 1.15° in rotation.[33] Furthermore, it is also important to identify the minimal clinically important difference. A meta-analysis conducted by Pijls et al. determined the upper limit of safe relative displacement for tibial components as 0.5 mm at a one-year postoperative follow-up, and Ryd et al. suggest that relative displacement of greater than 0.2 mm between a one- and two-year post-operative follow-up is indicative of potential implant loosening in the knee.[25,26] For the hip, Kärrholm et al. suggest the upper limit of safe relative displacement is approximately 2.6 mm at two years (95% probability of revision).[12] The critical level of safe relative displacement has not yet been established for reverse total shoulder arthroplasty, and could be much smaller than that for the knee or hip, in which case it is suggested that the RSA method with the least bias and greatest repeatability be used, provided the error in the measurement method is considerably smaller than the expected relative displacement.

3.5   Conclusion

In summary, this phantom study presents the bias and repeatability for both marker- and model-based RSA techniques for RTSA in six degrees of freedom, providing a foundation for future clinical studies in RTSA implant fixation in vivo. All techniques demonstrated system performance limits that fell within accepted range for RSA studies, with the exception of rotations about the Y-axis for model-based measurements due to symmetry of the implant components.

3.6   References

1.   Berhouet J, Kontaxis A, Gulotta LV, Craig E, Warren R, Dines J, et al. Effects of

the humeral tray component positioning for onlay reverse shoulder arthroplasty design: A biomechanical analysis. J Shoulder Elb Surg. 2015;24(4):569–577. doi:10.1016/j.jse.2014.09.022

2.   Bey MJ, Zauel R, Brock SK, Tashman S. Validation of a new model-based tracking technique for measuring three-dimensional, in vivo glenohumeral joint kinematics. J Biomech Eng. 2006;128(4):604–609. doi:10.1115/1.2206199

3.   Bragdon CR, Malchau H, Yuan X, Perinchief R, Kärrholm J, Börlin N, et al. Experimental assessment of precision and accuracy of radiostereometric analysis for the determination of polyethylene wear in a total hip replacement model. J Orthop Res. 2002;20(4):688–695. doi:10.1016/S0736-0266(01)00171-1

4.   Ten Brinke B, Beumer A, Koenraadt KLM, Eygendaal D, Kraan GA, Mathijssen NMC. The accuracy and precision of radiostereometric analysis in upper limb arthroplasty. Acta Orthop. 2017;88(3):320–325. doi:10.1080/17453674.2017.1291872

5.   Broberg JS, Yuan X, Teeter MG. Investigation of imaging magnification in radiostereometric analysis. Proc Inst Mech Eng Part H J Eng Med. 2017;231(1):92–95. doi:10.1177/0954411916676850

6.   de Bruin PW, Kaptein BL, Stoel BC, Reiber JHC, Rozing PM, Valstar ER. Image-based RSA: Roentgen stereophotogrammetric analysis based on 2D-3D image registration. J Biomech. 2008;41(1):155–164. doi:10.1016/j.jbiomech.2007.07.002

7.   Cai R, Yuan X, Rorabeck C, Bourne RB, Holdsworth DW. Development of an RSA calibration system with improved accuracy and precision. J Biomech. 2008;41(4):907–911. doi:10.1016/j.jbiomech.2007.11.012

8.   Day JS, Paxton ES, Lau E, Gordon VA, Abboud JA, Williams GR. Use of reverse total shoulder arthroplasty in the Medicare population. J Shoulder Elb Surg. 2015;24(5):766–772. doi:10.1016/j.jse.2014.12.023

9.   Kaptein BL, Valstar ER, Stoel BC. Clinical validation of model-based RSA for a total knee prosthesis. Clin Orthop Relat Res. 2007;464:205–209. doi:10.1097/BLO.0b013e3181571aa5

10.   Kaptein BL, Valstar ER, Stoel BC, Rozing PM, Reiber JHC. A new model-based RSA method validated using CAD models and models from reversed engineering. J Biomech. 2003;36(6):873–882. doi:10.1016/S0021-9290(03)00002-2

11.   Kärrholm J. Radiostereometric analysis of early implant migration – a valuable tool to ensure proper introduction of new implants. Acta Orthop. 2012;83(6):551–552. doi:10.3109/17453674.2012.745352

12.   Kärrholm J, Borssén B, Löwenhielm G, Snorrason F. Does early micromotion of femoral stem prostheses matter? 4-7-year stereoradiographic follow-up of 84 cemented prostheses. J Bone Joint Surg Br. 1994;76(6):912–917.

13.   Kärrholm J, Gill RHS, Valstar ER. The history and future of radiostereometric analysis. Clin Orthop Relat Res. 2006;448(448):10–21. doi:10.1097/01.blo.0000224001.95141.fe

14.   Van de Kleut ML, Yuan X, Athwal GS, Teeter MG. Validation of radiostereometric analysis in six degrees of freedom for use with reverse total shoulder arthroplasty. J Biomech. 2018;68:126–131. doi:10.1016/j.jbiomech.2017.12.027

15.   Lam-Tin-Cheung K, Yuan X, Nikolov HN, Lanting BA, Naudie DD, Teeter MG.

Marker-based technique for visualizing radiolucent implant components in radiographic imaging. J Orthop Res. 2017;35(9):2017–2022. doi:10.1002/jor.23475

16.   Langlois J, Hamadouche M. Current recommendations for assessing the reliability of a measurement tool: a survival guide for orthopaedic surgeons. Bone Joint J. 2016;98–B(2):166–172. doi:10.1302/0301-620X.98B2.34728

17.   McCalden RW, Korczak A, Somerville L, Yuan X, Naudie DD. Hip: A randomised trial comparing a short and a standard-length metaphyseal engaging cementless femoral stem using radiostereometric analysis. Bone Jt J. 2015;97–B(5):595–602. doi:10.1302/0301-620X.97B5.34994

18.   Molt M, Ryd L, Toksvig-Larsen S. Continued stabilization of Triathlon cemented TKA: A randomized RSA study concentrating especially on continuous migration. Acta Orthop. 2016;87(3):262–267. doi:10.3109/17453674.2016.1166876

19.   Nagels J, Valstar ER, Stokdijk M, Rozing PM. Patterns of loosening of the glenoid component. J Bone Joint Surg Br. 2002;84–B:83–87. doi:10.1302/0301-620x.84b1.11951

20.   Naudie DDR, Somerville L, Korczak A, Yuan X, McCalden RW, Holdsworth D, et al. A randomized trial comparing acetabular component fixation of two porous ingrowth surfaces using RSA. J Arthroplasty. 2013;28(SUPPL 1):48–52. doi:10.1016/j.arth.2013.06.041

21.   Nazari-Farsani S, Finnila S, Moritz N, Mattila K, Alm JJ, Aro HT. Is model-based radiostereometric analysis suitable for clinical trials of a cementless tapered wedge femoral stem? Clin Orthop Relat Res. 2016;474(10):2246–2253. doi:10.1007/s11999-016-4930-0

22.   Nuttall D, Haines JF, Trail IA. The early migration of a partially cemented fluted pegged glenoid component using radiostereometric analysis. J Shoulder Elb Surg. 2012;21(9):1191–1196. doi:10.1016/j.jse.2011.07.028

23.   Nuttall D, Haines JF, Trail II. A study of the micromovement of pegged and keeled glenoid components compared using radiostereometric analysis. J Shoulder Elb Surg. 2007;16(Suppl 3):65–70. doi:10.1016/j.jse.2006.01.015

24.   Padegimas EM, Maltenfort M, Lazarus MD, Ramsey ML, Williams GR, Namdari S. Future patient demand for shoulder arthroplasty by younger patients: national projections. Clin Orthop Relat Res. 2015;473(6):1860–1867. doi:10.1007/s11999-015-4231-z

25.   Pijls BG, Valstar ER, Nouta K, Plevier JWM, Middeldorp S, Nelissen RGHH, et al. Early migration of tibial components is associated with late revision: A systematic review and meta-analysis of 21,000 knee arthroplasties. Acta Orthop. 2012;83(6):614–624. doi:10.3109/17453674.2012.747052

26.   Ryd L, Albrektsson BE, Carlsson L, Dansgard F, Herberts P, Lindstrand A, et al. Roentgen stereophotogrammetric analysis as a predictor of mechanical loosening of knee prostheses. J Bone Joint Surg Br. 1995;77(3):377–383.

27.   Ryd L, Yuan X, Löfgren H. Methods for determining the accuracy of radiostereometric analysis (RSA). Acta Orthop Scand. 2000;71(August):403–408. doi:10.1080/000164700317393420

28.   Seehaus F, Emmerich J, Kaptein BL, Windhagen H, Hurschler C. Experimental analysis of Model-Based Roentgen Stereophotogrammetric Analysis (MBRSA) on

four typical prosthesis components. J Biomech Eng. 2009;131(4):041004-1–10. doi:10.1115/1.3072892

29. Seehaus F, Olender GD, Kaptein BL, Ostermeier S, Hurschler C. Markerless Roentgen Stereophotogrammetric Analysis for in vivo implant migration measurement using three dimensional surface models to represent bone. J Biomech. 2012;45(8):1540–1545. doi:10.1016/j.jbiomech.2012.03.004

30. Tashjian RZ, Burks RT, Zhang Y, Henninger HB. Reverse total shoulder arthroplasty: A biomechanical evaluation of humeral and glenosphere hardware configuration. J Shoulder Elb Surg. 2015;24(3):68–77. doi:10.1016/j.jse.2014.08.017

31. Valstar ER, Gill R, Ryd L, Flivik G, Börlin N, Kärrholm J. Guidelines for standardization of radiostereometry (RSA) of implants. Acta Orthop. 2005;76(4):563–572. doi:10.1080/17453670510041574

32. Valstar ER, De Jong FW, Vrooman HA, Rozing PM, Reiber JHC. Model-based Roentgen stereophotogrammetry of orthopaedic implants. J Biomech. 2001;34(6):715–722. doi:10.1016/S0021-9290(01)00028-8

33. Valstar ER, Nelissen RGHH, Reiber JHC, Rozing PM. The use of Roentgen stereophotogrammetry to study micromotion of orthopaedic implants. ISPRS J Photogramm Remote Sens. 2002;56(5–6):376–389. doi:10.1016/S0924-2716(02)00064-3

34. Yuan X, Lam Tin Cheung K, Howard JL, Lanting BA, Teeter MG. Radiostereometric analysis using clinical radiographic views: Validation measuring total hip replacement wear. J Orthop Res. 2016;34(9):1521–1528. doi:10.1002/jor.23170

4 Cemented versus press-fit humeral stem fixation in reverse total shoulder arthroplasty: A prospective randomized clinical trial

4.1 Introduction

Since approved by Health Canada in 2003 and the United States Food and Drug Administration in 2004, the use of reverse total shoulder arthroplasty has grown exponentially, surpassing the use of anatomic total shoulder arthroplasty.[2,20] Traditionally reserved for an elderly population with low functional demand,[23] expanding indications and increasing surgical experience have extended its use to younger patients with promising early results.[12,19,22] With greater demand, however, is the need by both surgeons and patients for implant longevity.

Cemented humeral stem fixation is the historical gold standard, with advantages being immediate fixation that does not rely on bony ingrowth or ongrowth, the addition of antibiotics, and the ability to fill bony defects in primary or revision surgery.[7] Advances in implant design have led to the introduction of short-stemmed, press-fit humeral stems with a proximal porous coating to encourage bony ingrowth for long-term fixation. Studies comparing cemented and press-fit humeral stem fixation demonstrate comparable functional outcomes, with potentially fewer postoperative complications with press-fit stems, and the added benefit of reduced operating room time, bone stock preservation, and easier removal in the case of revision surgery.[4,13,25]

Though early results of press-fit short-stemmed humeral implants are promising, some studies have suggested they exhibit increased early micromotion and stress shielding compared to cemented stems.[3,5,13,21] Radiostereometric analysis (RSA) is a well-validated x-ray technique capable of identifying early migration of implants not easily observed on clinical radiographs.[6] RSA has been used to evaluate the early migration of hip and knee prostheses, demonstrating a relationship between early implant migration and later loosening in the five-to-ten-year postoperative window.[15,18] For this reason, evaluation of

implant fixation within the first year postoperatively is recommended in order to identify potentially inferior new implant designs and remove them from market prior to their widespread distribution and use.[11]

The purpose of this study was to compare migration between standard-length cemented and short press-fit humeral stems in reverse total shoulder arthroplasty within the first year postoperatively using model-based radiostereometric analysis. It was hypothesized that press-fit stems would migrate more than cemented stems in the first six months postoperatively as biological fixation occurs, and that both groups would demonstrate stability from six months through one year.

4.2 Materials and Methods

4.2.1 Study design

This is a prospective, randomized clinical trial investigating humeral stem fixation in reverse total shoulder arthroplasty. Power analysis was conducted prior to patient enrollment, with 18 patients required per group to assess differences in migration of 0.235 mm or more, with 80% power and alpha = 0.05, assuming a standard deviation within groups of 0.5 mm.[17] Twenty patients were included in each group to account for 10% dropout.

Patients were randomized into study arms using block randomization, with five groups of eight. Two patients, with different stem randomizations, withdrew prior to postoperative radiographic assessment. An additional randomization block of four was added, recruiting three more patients to meet the 20 patients required in for each group (the additional patient included due to randomization order, the first two randomized to the same fixation group). Randomization sequence was generated using the online tool at *sealedenvelope.com*, each treatment allocation printed, concealed and sealed in an opaque envelope, and numbered sequentially. Envelopes were opened three weeks prior to the

scheduled surgery in order to provide time for preoperative templating and instrument preparation.

4.2.2 Patient recruitment

This study was approved by the local ethics board, the Western University Health Sciences Research Ethics Board, protocol #105908. Prior to study enrollment, informed, written consent was obtained by each participant. Forty-one non-consecutive patients (43 shoulders, 22 male) were prospectively enrolled, undergoing primary reverse total shoulder arthroplasty from July 2017 through June 2019. All procedures were performed by GSA, a fellowship-trained shoulder surgeon, at St. Joseph's Health Care, London, Canada. In order to be eligible for study enrollment, patients had to have shoulder arthrosis requiring reverse total shoulder arthroplasty, and a functional deltoid muscle. Patients must also have been able to provide informed, written consent. Patients were excluded if their indication for reverse total shoulder arthroplasty was fracture, avascular necrosis, or revision surgery; they had insufficient bone stock; were pregnant or planning to become pregnant; were unable to read/write English; or had a significant neurologic, gait, or motor control disorder.

4.2.3 Clinical and radiographic outcomes

Secondary to implant migration, active range of motion and validated patient-reported outcomes were acquired preoperatively and one year postoperatively. Active range of motion (forward flexion, lateral abduction, external rotation at 0° abduction, and internal rotation) was measured using a handheld 30 cm goniometer, with internal rotation measured as the highest point along the spine with the thumb extended upward. Recorded outcomes were pain, measured on a visual analog scale from 0-10, the Subjective Shoulder Value (SSV), the American Shoulder and Elbow Surgeons' (ASES) shoulder score, the Simple Shoulder Test (SST), the Disabilities of the Arm, Shoulder and Hand (DASH) score, and the Constant Shoulder Score. A variety of previously validated

outcome measures were chosen to facilitate comparison in outcomes between previously published studies and for future reference.

Anteroposterior radiographs acquired one year postoperatively were assessed for evidence of scapular notching, according to the grading by Sirveaux et al.,[23] and for evidence of humeral stem loosening and stress shielding.

4.2.4 Surgical technique

Patients were brought to the operating suite and placed in the beach chair position. The standard deltopectoral approach was used in each case. All patients received the Aequalis™ Ascend™ Flex reverse shoulder system (Wright Medical-Tornier Group, Memphis, TN, USA), with a 145° neck-shaft angle. Templating was conducted based on preoperative computed tomography scans, though final implant sizes were determined intraoperatively. Prior to implant insertion, eight tantalum beads 1 mm in diameter (Halifax Biomedical Inc., Mabou, NS, Canada) were inserted into the trabeculae of the proximal humerus. Beads were placed as far apart as possible given patient bone size and quality.

Patients randomized to the cemented cohort received a polished standard-length cemented stem, with sizing distributed as size 2 (n = 16), size 4 (n = 3), and size 6 (n = 1). Erythromycin/colistin-loaded bone cement (Antibiotic Simplex®, Stryker, Kalamazoo, MI, USA) was prepared according to its specifications and injected into the humeral canal following irrigation and drying. A distal cement restrictor plug was used in each case. Patients in the press-fit cohort received a short-stemmed implant, the proximal third covered with a plasma spray titanium coating. Sizing was based on achieving appropriate compression between the humeral metaphysis and proximal stem. Press-fit sizing was distributed as size 1 (n = 2), size 2 (n = 9), size 3 (n = 7), size 4 (n = 1), and size 5 (n = 2). Radiographic examples of the Aequalis™ Ascend™ Flex cemented and press-fit stems are illustrated in Figure 4.1. Trial reduction was completed for each patient prior to final polyethylene size selection to ensure stability and mobility. Average

75

humeral retroversion was $24 \pm 8°$ (range = 0-45°). Patients received a glenosphere lateralized with either an autologous bone graft (bony increased offset reverse shoulder arthroplasty) or a porous metal augment.
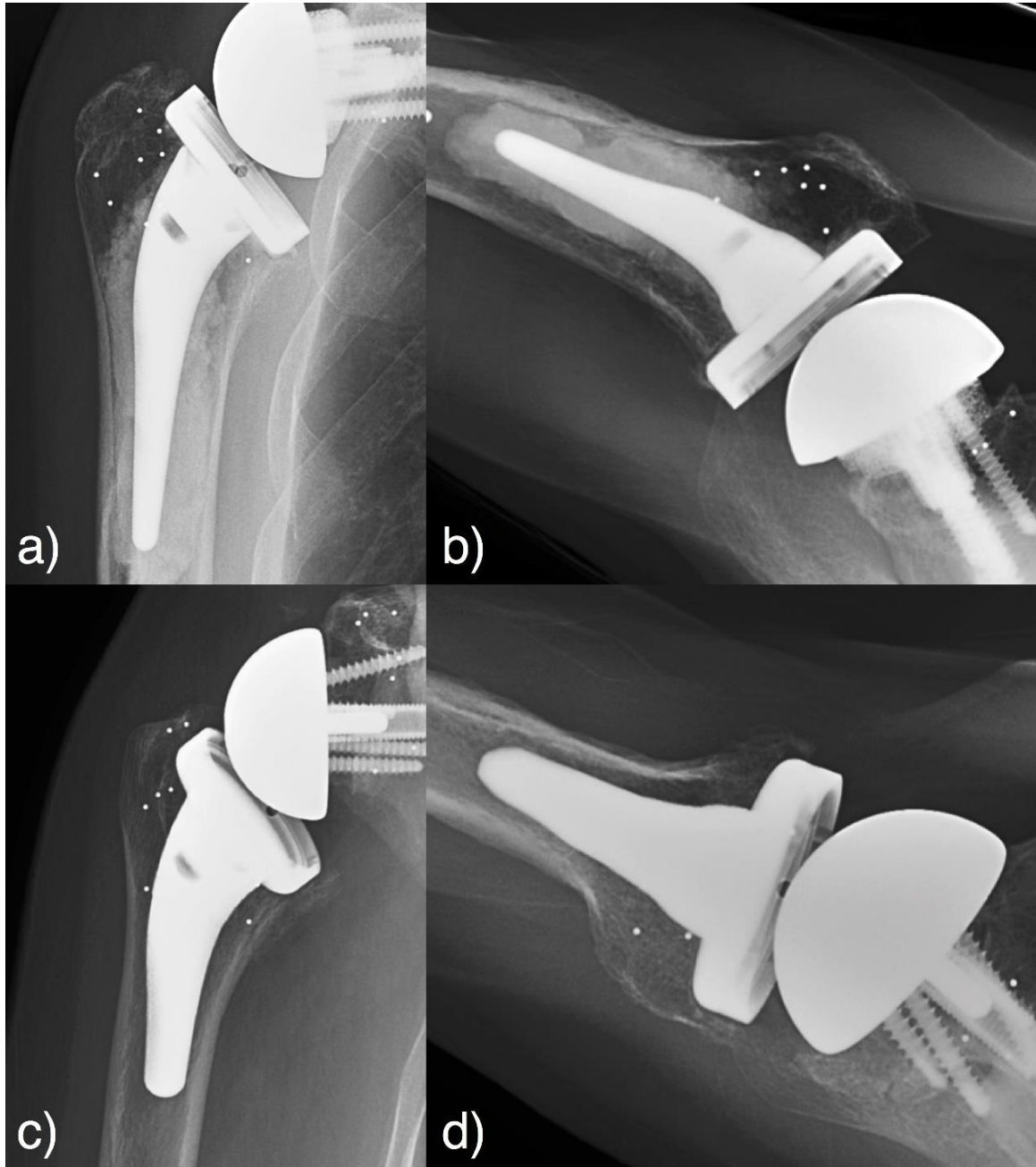
Figure 4.1 Anteroposterior (a) and axial (b) views of a cemented stem (size 2B), and anteroposterior (c) and axial (d) views of a press-fit (size 2B) humeral stem.

4.2.5 Imaging and radiostereometric analysis

A graduated therapy program was initiated immediately. At six weeks postoperatively, the shoulder sling was removed, and full active shoulder motion initiated. For this reason, the baseline radiostereometric exam was taken at six weeks, followed by exams at three and six months, and one year. Patients were imaged in a dedicated radiostereometric analysis suite, seated in front of a uniplanar calibration cage (Cage 43, RSA Biomedical, Umeå, Sweden), with their arm at rest by their side. Two ceiling-mounted x-ray units (Proteus XR/a, GE Medical Systems, Milwaukee, WI, USA) were angled 40 degrees to each other and parallel to the floor during exposure, with x-rays taken at 90 kVp and between 6.3 and 16.0 mAs, depending on patient size. Images were acquired on 35.5 cm x 43.2 cm computed radiography imaging cassettes with 0.1 mm pixel spacing and 10-bit gray scale mapping (Capsula X CR, FUJIFILM, Tokyo, Japan). The effective dose from exposure at all time points, including double examinations, was approximately 0.6 milli-Sievert.

Humeral stem migration was measured in commercial model-based radiostereometric analysis software (RSACore, Leiden, The Netherlands) as migration of the center of gravity of the humeral stem CAD model relative to the centroid of bone markers identified in the proximal humerus. This measurement technique has been previously validated for use with reverse total shoulder arthroplasty, with a reported bias (mean absolute value ± 95% confidence interval) less than, and repeatability greater than, 0.13 ± 0.02 mm and 0.15 mm, and $0.8 \pm 0.3°$ and $2.0°$ in translation and rotation, respectively.[9] Linear translations were recorded along the medial(+)-lateral(-) x-axis, superior(+)-inferior(-) y-axis, and anterior(+)-posterior(-) z-axis. Rotations were recorded about the stem's extension(+)-flexion(-) x-axis, internal(+)-external(-) y-axis, and adduction(+)-abduction(-) z-axis (Figure 4.2).
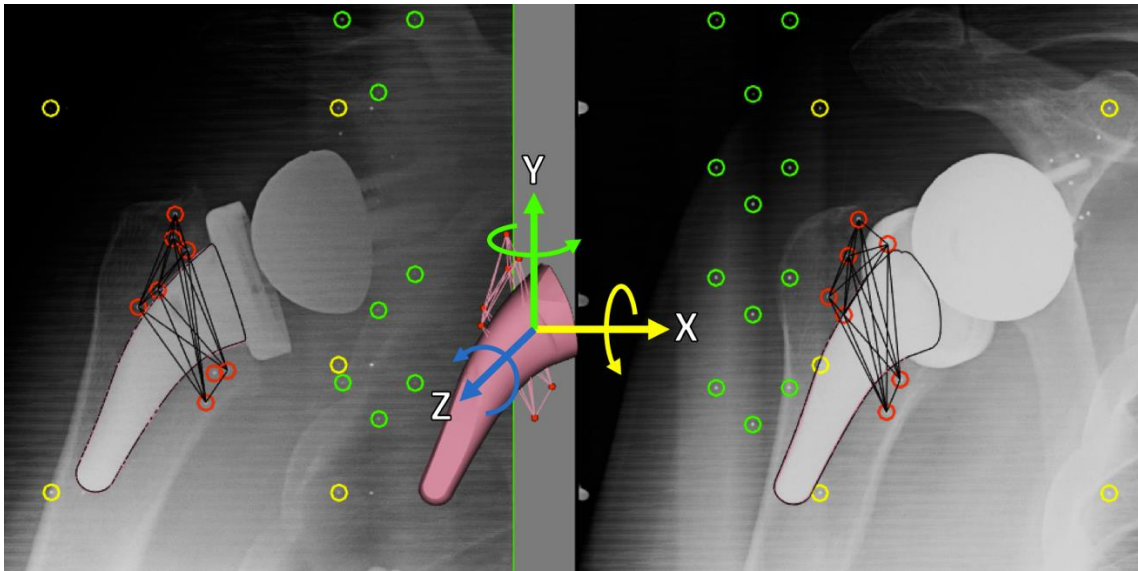
Figure 4.2 Right-handed model-based radiostereometric analysis coordinate system. Tantalum beads are observable within the trabecular bone, highlighted with red circles, surrounding the stem.

Condition number, a unitless measure representing the three-dimensional distribution of tantalum markers within the bone, was recorded for cemented and press-fit measurements. Smaller condition numbers represent good marker distribution, indicating that the recorded migration measurements are reliable. Guidelines for radiostereometric analysis have suggested an upper threshold of 150 as acceptable.[24] In addition to condition number, double exposures with repositioning were taken at three months, or, if unavailable, at one year postoperatively to assess the clinical precision of the radiostereometric technique. Clinical precision was measured as 1.96 x standard deviation of the difference in migration measurements between double exposures.[1] A theoretical perfect precision implies zero migration measurement difference between exposures, as one would expect no migration of the implants in the few minutes between exams. Taking condition number and precision together can help to inform the analyst whether the reported migration value is true. The threshold for rigid body error, used to assess the stability of tantalum markers between subsequent examinations, was set at 0.350 mm.[24]

4.2.6 Statistical analysis

Normality of clinical outcomes was assessed using the Pearson d'Agostino test, with differences in continuous data evaluated using either an unpaired t-test, if normally distributed, or the Mann-Whitney test if not. Categorical data was evaluated using the Chi-square test.

Migration was measured along each translational and rotation axis, in addition to a three-dimensional resultant vector, at each postoperative time point relative to the six-week baseline. Differences in migration between cemented and press-fit stems were assessed using a mixed-effects model to account for any missing values, with Bonferroni's test for multiple comparisons. Assessment of simple effects with Bonferroni's test for multiple comparisons was also applied to determine any differences in migration between time points within each randomization cohort. Statistical analysis was completed in Prism 8 (GraphPad, La Jolla, CA, USA), significance set at $P < 0.05$.

4.3 Results

Preoperatively, there were no significant differences in demographics (Table 4.1) or any patient-reported outcome measure (Table 4.2) between stem fixation groups ($P > 0.334$). Mean age at the time of surgery was 72 ± 9 years. One year postoperatively, all outcomes improved significantly from baseline with a change greater than the minimal clinically important difference (MCID), with the exception of external rotation and internal rotation in the cemented cohort. The MCID for RTSA has previously been reported as 12° of forward flexion, 7° of lateral abduction, 1.6 points for pain, 13.6 points for the ASES score, 1.5 points for the SST, and 5.7 points for the Constant score. There were no significant or clinically important differences in clinical outcomes between cemented and press-fit stems one year postoperatively (Table 4.2). Adverse events include dislocation requiring revision nine months postoperatively in the press-fit group, and an acromion fracture that healed without intervention in the cemented group. Full study flow is illustrated in Figure 4.3. One year postoperatively, no stem showed evidence of

loosening, though two press-fit stems exhibited slight stress shielding (1-2 mm of bone resorption) at the medial calcar (Figure 4.4). There was no evidence of scapular notching with any patient.

Table 4.1 Patient demographics (mean ± SD)

	Cemented (n = 20)	Press-fit (n = 21)	*P*-value
Age	74.0 ± 9.4	71.4 ± 8.0	0.334
Sex	10 M: 10 F	12 M: 9 F	0.758
Indication*	OA: 8 CTA: 7 MRCT: 2 OA + RCT: 2 RA: 1	OA: 9 CTA: 8 MCRT: 4	N/A

*OA = osteoarthritis; CTA = cuff tear arthropathy; MRCT = massive rotator cuff tear;
OA + RCT = osteoarthritis and rotator cuff tear; RA = rheumatoid arthritis

Table 4.2 Patient-reported outcome measures (mean ± SD)

	Preoperative			Postoperative (1 year)			Difference	Difference
	Cemented	Press-fit	*P*-value	Cemented	Press-fit	*P*-value	Cemented	Press-fit
Forward flexion (°)	68 ± 29	74 ± 31	0.519	122 ± 20	119 ± 17	0.670	+54 (*P* < **0.001**)	+45 (*P* < **0.001**)
Lateral abduction (°)	59 ± 25	68 ± 26	0.284	107 ± 24	102 ± 25	0.516	+49 (*P* < **0.001**)	+34 (*P* < **0.001**)
External rotation (°)	27 ± 23	23 ± 20	0.493	35 ± 20	35 ± 16	0.956	+8 (*P* = 0.259)	+12 (*P* = **0.048**)
Internal rotation (1-6)*	3 ± 2	3 ± 2	0.918	4 ± 2	4 ± 1	0.517	+1 (*P* = 0.110)	+1 (*P* = **0.017**)
Pain (0-10)	7.2 ± 2.4	6.7 ± 2.2	0.504	1.8 ± 2.2	1.2 ± 1.2	0.367	-5.4 (*P* < **0.001**)	-5.5 (*P* < **0.001**)
SSV (0-100)	29.7 ± 22.8	33.0 ± 20.7	0.726	86.4 ± 13.3	81.6 ± 16.1	0.505	+56.7 (*P* < **0.001**)	+48.6 (*P* < **0.001**)
ASES (0-100)	32.9 ± 17.0	35.0 ± 15.8	0.681	77.5 ± 18.8	82.2 ± 11.1	0.406	+44.6 (*P* < **0.001**)	+47.2 (*P* < **0.001**)
SST (0-12)	2.2 ± 2.0	2.7 ± 2.0	0.328	7.5 ± 3.0	8.3 ± 2.4	0.413	+5.3 (*P* < **0.001**)	+5.6 (*P* < **0.001**)
DASH (0-100)	55.6 ± 15.4	52.6 ± 16.0	0.545	27.0 ± 20.3	14.7 ± 11.6	0.06	-28.6 (*P* < **0.001**)	-37.9 (*P* < **0.001**)
Constant (0-100)	26.7 ± 13.8	26.0 ± 12.6	0.875	64.2 ± 14.6	63.3 ± 9.5	0.842	+37.5 (*P* < **0.001**)	+37.3 (*P* < **0.001**)

*Based on the landmarks from Constant Shoulder Score: 1 = lateral thigh, 2 = buttock, 3 = lumbo-sacral junction, 4 = waist, 5 = T12, 6 = T7 or interscapular

CONSORT flow diagram – Press-fit vs. cemented humeral stems
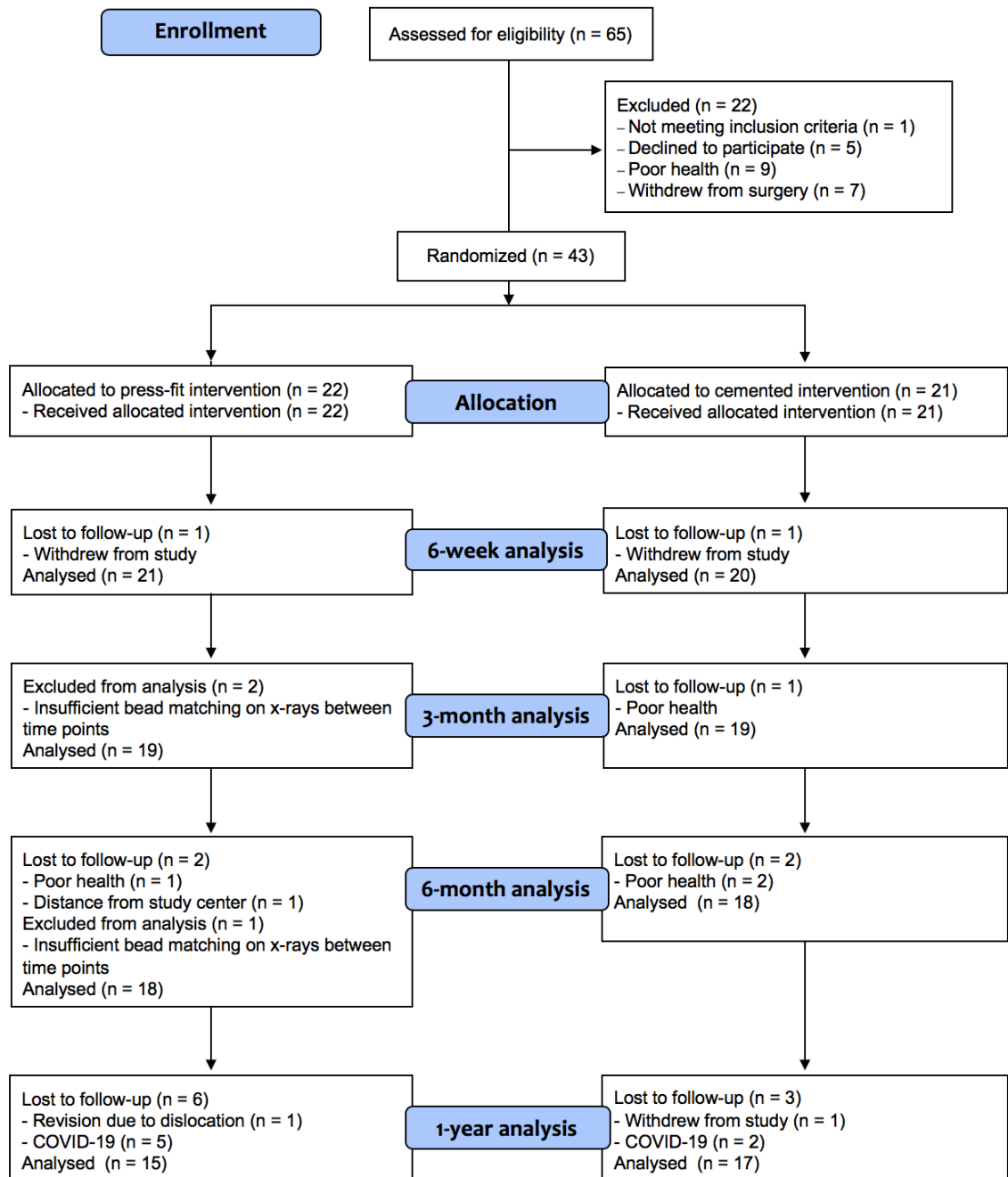
Figure 4.3 CONSORT study flow.
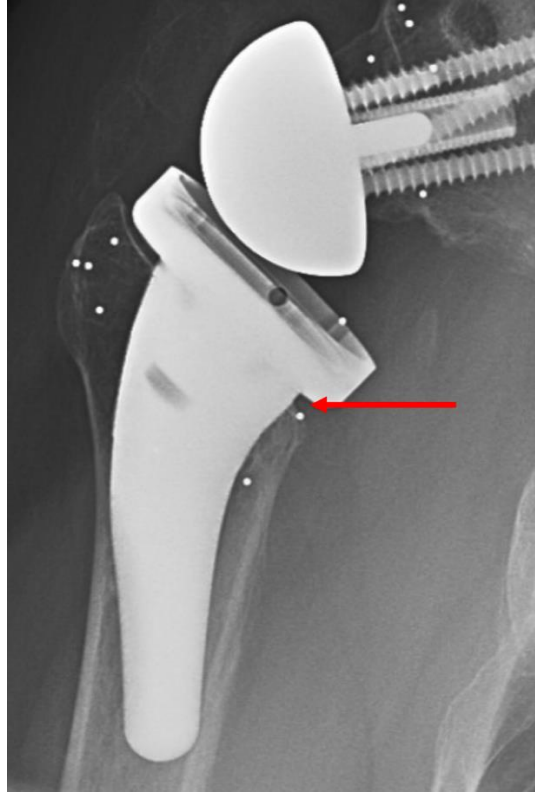
Figure 4.4 Stress shielding at the medial calcar with the use of a press-fit stem.

Clinical precision based on double examinations is recorded in Table 4.3. Out of plane translations and rotations about the long axis of the stem had the poorest precision. Mean condition number for cemented stems was 100 ± 54, and 94 ± 60 for press-fit stems.

Significantly greater total translation was demonstrated by the press-fit stems compared to the cemented stems one year (mean difference $= 0.54$ mm, $P = 0.005$) postoperatively. Press-fit stems showed greater subsidence along the long-axis of the stem at six months (mean difference $= 0.40$ mm, $P = 0.026$) and one year (mean difference $= 0.75$ mm, $P < 0.001$), and greater anterior migration at one year (mean difference $= 0.46$ mm, $P = 0.002$). Migration along translational and rotational axes is recorded in Tables 4.4 and 4.5, respectively, with mean migration along the superior-inferior axis and total translation displayed in Figures 4.5 and 4.6, respectively. Considering the individual patterns of stem migration for each patient, it appears there may be one continuous press-fit migrator, reaching a total translation of 3.05 mm at one year, with increases in

subsidence and total translation of 0.73 mm and 0.71 mm, respectively, from six months to one year (Figure 4.7). Compared to the rest of the cohort, one year postoperatively this patient reported poorer functional outcomes, including increased pain, with values worse than their preoperative performance in all measures of range of motion, the SST, Constant score, and with differences within the minimally clinical important difference for the ASES (13.6) and DASH (12.7) scores. Removing this patient from analysis, press-fit stems continued to show increased subsidence at six months ($P = 0.041$) and one year ($P < 0.001$), and increased total translation at one year ($P = 0.015$), compared to cemented stems.

Table 4.3 Precision, recorded in mm for translation (T) and degrees for rotation (R)

	Medial(+)-Lateral(-) (T_x)	Superior(+)-Inferior(-) (T_y)	Anterior(+)-Posterior(-) (T_z)	Total Translation (T_r)	Flexion(-)-Extension(+) (R_x)	Internal(+)-External(-) (R_y)	Adduction(+)-Abduction(-) (R_z)
Cemented	0.32	0.27	0.43	0.23	1.83	2.41	1.10
Press-fit	0.27	0.20	0.42	0.24	1.73	2.38	0.49

Table 4.4 Translational migration, recorded in mm as mean ± SD

	Medial(+)-Lateral(-) (T_x)			Superior(+)-Inferior(-) (T_y)			Anterior(+)-Posterior(-) (T_z)			Total Translation (T_r)		
	Cemented	Press-fit	*P*-value	Cemented	Press-fit	*P*-value	Cemented	Press-fit	*P*-value	Cemented	Press-fit	*P*-value
3 months	-0.01 ± 0.13	0.09 ± 0.22	> 0.999	-0.06 ± 0.33	-0.24 ± 0.38	0.550	-0.01 ± 0.26	0.11 ± 0.38	0.843	0.36 ± 0.25	0.53 ± 0.35	0.594
6 months	-0.01 ± 0.26	-0.03 ± 0.31	> 0.999	-0.10 ± 0.19	-0.50 ± 0.65	**0.026**	-0.00 ± 0.33	0.18 ± 0.31	0.312	0.41 ± 0.20	0.74 ± 0.58	0.060
1 year	0.06 ± 0.33	-0.05 ± 0.62	> 0.999	0.01 ± 0.25	-0.74 ± 0.82	**< 0.001**	-0.20 ± 0.35	0.26 ± 0.38	**0.002**	0.53 ± 0.20	1.07 ± 0.79	**0.005**

Table 4.5 Rotational migration, recorded in degrees as mean ± SD

	Flexion(-)-Extension(+) (R_x)			Internal(+)-External(-) (R_y)			Adduction(+)-Abduction(-) (R_z)		
	Cemented	Press-fit	*P*-value	Cemented	Press-fit	*P*-value	Cemented	Press-fit	*P*-value
3 months	-0.28 ± 1.14	0.21 ± 0.91	0.638	-0.04 ± 1.08	-0.02 ± 1.25	> 0.999	-0.19 ± 0.69	0.09 ± 0.54	> 0.999
6 months	-0.29 ± 1.27	-0.01 ± 0.73	> 0.999	-0.14 ± 1.36	0.09 ± 1.85	> 0.999	-0.16 ± 1.01	-0.05 ± 0.63	> 0.999
1 year	0.06 ± 1.39	-0.02 ± 1.02	> 0.999	-0.05 ± 1.06	0.25 ± 2.03	> 0.999	-0.14 ± 0.63	-0.22 ± 0.86	> 0.999
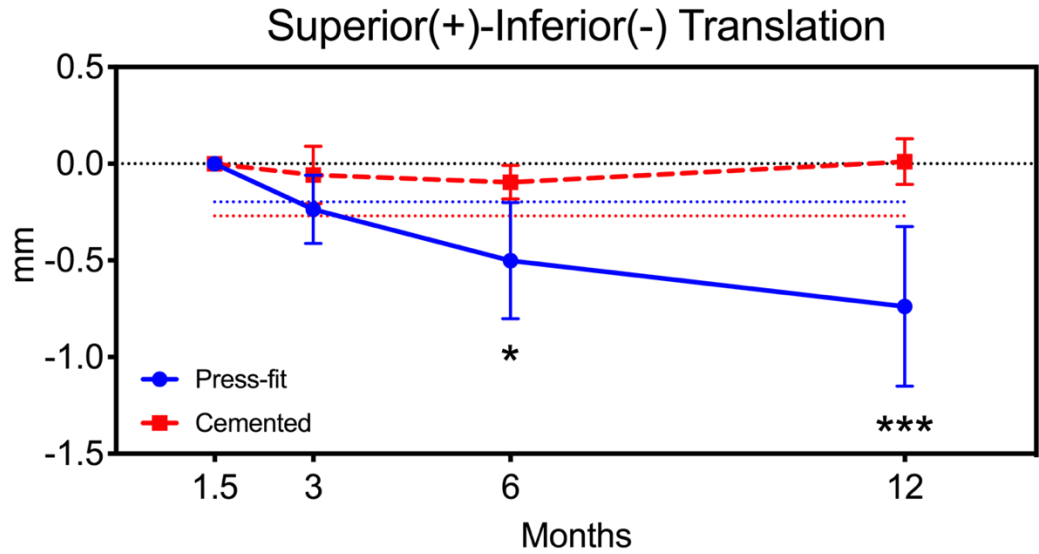
Figure 4.5 Mean migration ± 95% confidence interval at each time point along the superior-inferior axis for press-fit (solid blue) and cemented (dashed red) stems. The precision of RSA for each cohort is indicated by the fine dotted lines (blue, press-fit; red, cemented).
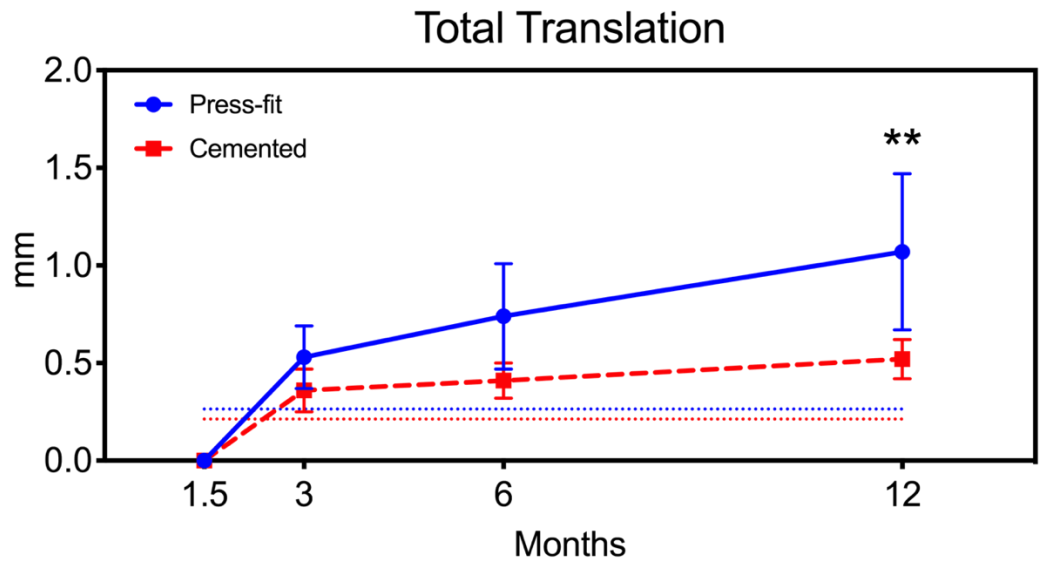
Figure 4.6 Mean total translation ± 95% confidence interval for press-fit (solid blue) and cemented (dashed red) stems through one year. Total translation precision is illustrated as the fine dotted line in blue for press-fit stems and red for cemented stems.
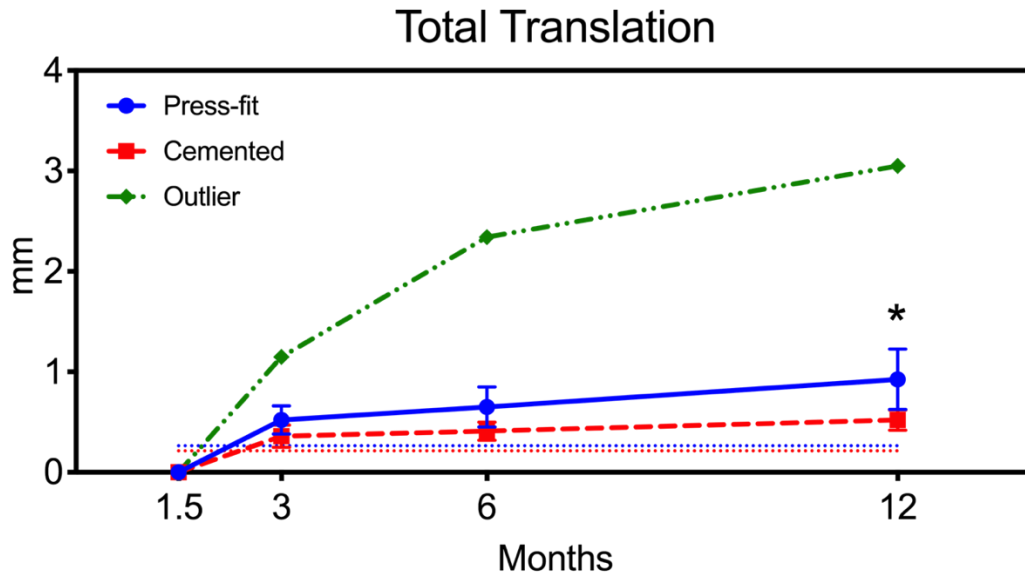
Figure 4.7 One patient in the press-fit cohort (dash-dot green) demonstrated continuous migration between each time point. This outlier has been removed from the mean and confidence intervals of the presented press-fit curve.

Assessing the pattern of migration between contiguous time points within fixation cohorts, the cemented stems showed the greatest increase in total translation from the six-week baseline to three months (mean difference = 0.36 mm), with no significant difference between three and six months, or six months and one year. The press-fit cohort also demonstrated the greatest increase in total translation from baseline to three months (mean difference = 0.53 mm), with a significant difference in total translation observed from six months to one year (mean difference = 0.33 mm, $P = 0.027$). No significant differences were observed between adjacent time points along individual translational or rotational axes with either cemented or press-fit stems (Appendix G).

4.4 Discussion

The use of press-fit humeral stems is an attractive alternative to cementing, as it reduces operating room time, preserves bone stock, and concern about the damaging biological effects of bone cement is eliminated. The purpose of this study was to assess the early migration patterns between cemented and press-fit humeral stems following reverse total shoulder arthroplasty using model-based radiostereometric analysis in a randomized

clinical trial. Our hypothesis was supported, as differences were observed at six months and one year postoperatively, with press-fit humeral stems showing significantly greater inferior migration (subsidence), at -0.50 ± 0.65 mm, and -0.74 ± 0.82 mm, respectively, compared to -0.10 ± 0.19 mm, and 0.01 ± 0.25 mm for the cemented cohort. This increased inferior migration subsequently contributed to increases in total translation at six months and one year. The greater standard deviations observed in the press-fit cohort are reflective of the variation in stem subsidence as the stem settles into the bone, and it appears that most press-fit stems achieve stability from six months through one year. Though significant differences were observed along the anterior-posterior axis at one year, the magnitude of these values was within the clinical precision of the system and therefore of little clinical value.

Previous radiostereometric analysis studies have determined thresholds for acceptable migration in the hip and knee during the first year postoperatively,[13–15] though no such thresholds have been determined for humeral stem migration in the current literature. For this reason, we are unable to conclude whether any of the stems in this study are at risk of later loosening, including the apparent continuous migrator of the press-fit group. Specific to this patient, clinical radiographs showed no evidence of changes to bone quality or stem loosening. The lack of improvement in pain or functional outcomes experienced by this patient suggests that increased early humeral stem migration may be negatively associated with clinical outcomes, though the absence of other continuous migrators within the cohort makes this difficult to conclude.

There were no differences in clinical outcomes between press-fit and cemented cohorts as a whole. As reverse shoulder biomechanics differ from that of anatomic shoulder replacement or the native shoulder joint, targets for postoperative range of motion and strength are more nuanced. The values reported at one year from this patient cohort are comparable to patients with outcomes two years post RTSA, though active range of motion is poorer than in patients with anatomic shoulder arthroplasty.[8] Understanding the limitations of RTSA can help set realistic patient expectations and influence rehabilitation protocols for targeted range of motion and strengthening exercises.

Results from the simple effects analysis highlight that cemented stems showed immediate fixation, with no significant migration between time points after three months. Similarly, press-fit stems migrated most in the first three months postoperatively, though continued to exhibit significant migration from six months through one year, even with the continuous migrator previously addressed removed from statistical analysis. While the magnitude of total translation increased from three months to six months with press-fit stems, this difference was likely not significant due to the comparatively large standard deviations within the group at both time points. These large standard deviations are also the likely reason for no observed statistical differences between adjacent time points along the superior-inferior axis of the stem. These results demonstrate the variability in early stem migration with the use of press-fit fixation, with some patients experiencing prolonged periods of migration prior to stabilization. Compared to studies investigating press-fit fixation in the hip or knee, this period of integration is slightly longer than the previously reported three months, and may be a result of less dense bone in the proximal humerus compared to the tibia or femur.[10,26] Though significant differences were observed in total translation from six months to one year within the press-fit cohort, the mean magnitude of migration, 0.33 mm, was less than that observed from baseline to three months, 0.53 mm, and suggest the implants are stabilizing.

To the best of our knowledge, this is one of the first studies investigating humeral stem migration using model-based radiostereometric analysis, and for this reason we sought to determine the clinical precision of the analysis technique using double exposures. Our reported precision is similar to that of a study using marker-based radiostereometric analysis assessing anatomic shoulder stem migration in rheumatoid patients, with poorest precision along the out-of-plane anterior-posterior translation axis, and along the internal-external rotation axis.[17] The clinical precision is approximately 0.2 mm, and 1° poorer than measurements obtained under ideal in vitro conditions.[9] The use of a uniplanar calibration cage inherently reduces clinical precision compared to that of a biplanar cage, as the projected contours of the humeral stem will only exhibit slight differences from one radiograph to the other. Specifically, x-ray tubes were positioned 40° to one another

for this study. While 60° would have increased the uniqueness of projections, we did not believe this slight difference would merit the increased soft tissue penetration and absorbed dose. Further, the relatively cylindrical shape of the stem is less robust to small differences in projection angle. The condition number for both stems was acceptable as the average was below the recommended threshold of 150.[24]

A limitation to this study is the short follow-up duration. Mid-to-long-term follow-up with the same patients is required to establish any relationships between early migration and later loosening. Strengths of this study are that it was a randomized trial, with each patient receiving the same stem design in either the cemented or press-fit cohort, and the same surgeon performed all procedures. Through randomization it can be assumed that there is likely an equal distribution of bone quality between groups. This could be verified in future studies by placing a known density phantom in the CT scanner while acquiring preoperative scans and calibrating the observed image intensity appropriately, then comparing means between cohorts.

4.5   Conclusion

This model-based radiostereometric analysis study showed that short-stemmed press-fit humeral stems subside more than standard-length cemented stems in the first year postoperatively, but ultimately achieve stability. Clinical outcomes between cohorts were equivalent at one year, though longer follow-up is required to assess the long-term impact of implant migration.

4.6   References

1.   Ten Brinke B, Beumer A, Koenraadt KLM, Eygendaal D, Kraan GA, Mathijssen NMC. The accuracy and precision of radiostereometric analysis in upper limb arthroplasty. Acta Orthop. 2017;88(3):320–325. doi:10.1080/17453674.2017.1291872
2.   Chalmers PN, Salazar DH, Romeo AA, Keener JD, Yamaguchi K, Chamberlain AM. Comparative utilization of reverse and anatomic total shoulder arthroplasty. J Am Acad Orthop Surg. 2018;26(24):504–510. doi:10.5435/JAAOS-D-17-00075

3. Denard PJ, Raiss P, Gobezie R, Edwards TB, Lederman E. Stress shielding of the humerus in press-fit anatomic shoulder arthroplasty: review and recommendations for evaluation. J Shoulder Elb Surg. 2018;27(6):1139–1147. doi:10.1016/j.jse.2017.12.020

4. Giuseffi SA, Streubel P, Sperling J, Sanchez-Sotelo J. Short-stem uncemented primary reverse shoulder arthroplasty: Clinical and radiological outcomes. Bone Jt J. 2014;96 B(4):526–529. doi:10.1302/0301-620X.96B3.32702

5. Harris TE, Jobe CM, Dai QG. Fixation of proximal humeral prostheses and rotational micromotion. J Shoulder Elb Surg. 2000;9(3):205–210. doi:10.1067/mse.2000.105625

6. Kärrholm J, Gill RHS, Valstar ER. The history and future of radiostereometric analysis. Clin Orthop Relat Res. 2006;448(448):10–21. doi:10.1097/01.blo.0000224001.95141.fe

7. Keener JD, Chalmers PN, Yamaguchi K. The humeral implant in shoulder arthroplasty. J Am Acad Orthop Surg. 2017;25(6):427–438. doi:10.5435/JAAOS-D-15-00682

8. Kiet TK, Feeley BT, Naimark M, Gajiu T, Hall SL, Chung TT, et al. Outcomes after shoulder replacement: Comparison between reverse and anatomic total shoulder arthroplasty. J Shoulder Elb Surg. 2015;24(2):179–185. doi:10.1016/j.jse.2014.06.039

9. Van de Kleut ML, Yuan X, Athwal GS, Teeter MG. Validation of radiostereometric analysis in six degrees of freedom for use with reverse total shoulder arthroplasty. J Biomech. 2018;68:126–131. doi:10.1016/j.jbiomech.2017.12.027

10. McCalden RW, Korczak A, Somerville L, Yuan X, Naudie DD. Hip: A randomised trial comparing a short and a standard-length metaphyseal engaging cementless femoral stem using radiostereometric analysis. Bone Jt J. 2015;97–B(5):595–602. doi:10.1302/0301-620X.97B5.34994

11. Nelissen RGHH, Pijls BG, Karrholm J, Malchau H, Nieuwenhuijse MJ, Valstar ER. RSA and registries: The quest for phased introduction of new implants. J Bone Joint Surg. 2011;93(3):62–65. doi:10.2106/JBJS.K.00907

12. Padegimas EM, Maltenfort M, Lazarus MD, Ramsey ML, Williams GR, Namdari S. Future patient demand for shoulder arthroplasty by younger patients: national projections. Clin Orthop Relat Res. 2015;473(6):1860–1867. doi:10.1007/s11999-015-4231-z

13. Phadnis J, Huang T, Watts A, Krishnan J, Bain GI. Cemented or cementless humeral fixation in reverse total shoulder arthroplasty? Bone Jt J. 2016;98B(1):65–74. doi:10.1302/0301-620X.98B1.36336

14. Pijls BG, Nieuwenhuijse MJ, Fiocco M, Plevier JWM, Nelissen RGHH, Valstar ER, et al. Early proximal migration of cups is associated with late revision in THA. Acta Orthop. 2012;83(6):583–591. doi:10.3109/17453674.2012.745353

15. Pijls BG, Plevier JWM, Nelissen RGHH. RSA migration of total knee replacements: A systematic review and meta-analysis. Acta Orthop. 2018;89(3):320–328. doi:10.1080/17453674.2018.1443635

16. Pijls BG, Valstar ER, Nouta K, Plevier JWM, Middeldorp S, Nelissen RGHH, et al. Early migration of tibial components is associated with late revision: A

systematic review and meta-analysis of 21,000 knee arthroplasties. Acta Orthop. 2012;83(6):614–624. doi:10.3109/17453674.2012.747052

17. Rahme H, Mattsson P, Wikblad L, Larsson S. Cement and press-fit humeral stem fixation provides similar results in rheumatoid patients. Clin Orthop Relat Res. 2006;(448):28–32. doi:10.1097/01.blo.0000224007.25636.85

18. Ryd L, Albrektsson BE, Carlsson L, Dansgard F, Herberts P, Lindstrand A, et al. Roentgen stereophotogrammetric analysis as a predictor of mechanical loosening of knee prostheses. J Bone Joint Surg Br. 1995;77(3):377–383.

19. Samuelsen BT, Wagner ER, Houdek MT, Elhassan BT, Sánchez-Sotelo J, Cofield R, et al. Primary reverse shoulder arthroplasty in patients aged 65 years or younger. J Shoulder Elb Surg. 2016;26(1):e13–e17. doi:10.1016/j.jse.2016.05.026

20. Schairer WW, Nwachukwu BU, Lyman S, Craig EV, Gulotta LV. National utilization of reverse total shoulder arthroplasty in the United States. J Shoulder Elb Surg. 2015;24(1):91–97. doi:10.1016/j.jse.2014.08.026

21. Schnetzke M, Coda S, Walch G, Loew M. Clinical and radiological results of a cementless short stem shoulder prosthesis at minimum follow-up of two years. Int Orthop. 2015;39(7):1351–1357. doi:10.1007/s00264-015-2770-2

22. Sershon RA, Van Thiel GS, Lin EC, McGill KC, Cole BJ, Verma NN, et al. Clinical outcomes of reverse total shoulder arthroplasty in patients aged younger than 60 years. J Shoulder Elb Surg. 2014;23(3):395–400. doi:10.1016/j.jse.2013.07.047

23. Sirveaux F, Favard L, Oudet D, Huquet D, Walch G, Molé D. Grammont inverted total shoulder arthroplasty in the treatment of glenohumeral osteoarthritis with massive rupture of the cuff. Results of a multicentre study of 80 shoulders. J Bone Joint Surg Br. 2004;86–B(3):388–395. doi:10.1302/0301-620X.86B3.14024

24. Valstar ER, Gill R, Ryd L, Flivik G, Börlin N, Kärrholm J. Guidelines for standardization of radiostereometry (RSA) of implants. Acta Orthop. 2005;76(4):563–572. doi:10.1080/17453670510041574

25. Wiater JM, Moravek JE, Budge MD, Koueiter DM, Marcantonio D, Wiater BP. Clinical and radiographic results of cementless reverse total shoulder arthroplasty: a comparative study with 2 to 5 years of follow-up. J Shoulder Elb Surg. 2014;23(8):1208–1214. doi:10.1016/j.jse.2013.11.032

26. Winther NS, Jensen CL, Jensen CM, Lind T, Schrøder HM, Flivik G, et al. Comparison of a novel porous titanium construct (Regenerex®) to a well proven porous coated tibial surface in cementless total knee arthroplasty — A prospective randomized RSA study with two-year follow-up. Knee. 2016;23(6):1002–1011. doi:10.1016/j.knee.2016.09.010

5 BIO-RSA versus augmented glenospheres in reverse total shoulder arthroplasty: A prospective, randomized clinical trial

5.1 Introduction

Reverse total shoulder arthroplasty is rapidly being used as the standard surgical procedure for a growing number of shoulder pathologies.[12,22,31] Glenoid preparation remains a technical challenge, as different pathologies present varying glenoid wear patterns.[13] Excessive reaming, in effort to optimize glenosphere baseplate seating, may lead to medialization of the glenohumeral joint's center of rotation and exacerbate scapular notching.[6,30,37] For this reason, augmentation of the glenoid baseplate has been proposed as a method for maintaining glenoid subchondral bone while increasing impingement-free range of motion.[3,4] Bony increased offset reverse shoulder arthroplasty (BIO-RSA) is a structural bone graft method of augmentation.[3–5] Though BIO-RSA provides adequate short-term outcomes in patients with acceptable humeral head bone quality, the procedure is limited to primary joint replacement and adds time to the operative procedure. More recently, porous metal augmented baseplates have been engineered to address varying glenoid deficiencies, without relying on structural bone autograft.[16,34,38]

While baseplate augmentation provides a promising solution to scapular notching and improving impingement-free range of motion, there are concerns about lateralization of the joint's center of rotation and the introduction of bending moments at the bone-implant interface, compromising long-term survivorship.[2,7,17,18] The rationale for using an augmentation technique such as bone grafting or porous metal is that through graft integration or bony ingrowth, the advantages of lateralization are obtained and the joint center of rotation is maintained at the bone-implant interface.

Model-based radiostereometric analysis is a calibrated, dual-plane x-ray technique capable of measuring sub-millimeter implant migration, and is currently the gold standard

for such purposes. The technique has been used in the lower limb, where it has been shown that early implant migration within the first year postoperatively is predictive of later loosening and failure.[25,26] To the best of our knowledge, little to no studies have investigated early glenoid component migration in reverse total shoulder arthroplasty. The purpose of this prospective randomized clinical trial was to compare the migration between BIO-RSA and porous metal augmented glenoid baseplates using model-based radiostereometric analysis in the first year postoperatively. Secondary patient-reported outcome measures and incidence of scapular notching were also recorded. It was hypothesized that there would be no difference in migration between augmentation techniques, and patients would report comparable outcomes.

5.2 Materials and Methods

This study uses the same patients, imaging technique, image analysis, and statistical analysis as Chapter 4. Complete study design is described in Chapter 4, Section 2. While a priori power analysis was calculated to assess differences in humeral stem migration, post hoc power analysis for glenosphere migration using alpha = 0.05, 32 patients, 3 time points, a standard deviation within groups of 0.25 mm, and difference between groups of 0.21 mm for a repeated measures analysis of variance, observed power was reported as 0.80. Forty-three patients were recruited for primary reverse total shoulder arthroplasty, and in addition to humeral stem fixation randomization, were randomized to receive either a BIO-RSA or porous metal wedge augmented glenosphere using block randomization. Two patients withdrew prior to radiographic exposure. Patient-reported outcome measures were acquired preoperatively and one year postoperatively to assess active range of motion, pain, and functional capacity between groups. In addition to scapular notching, anteroposterior radiographs were assessed for glenosphere inclination angle, measured as the angle subtended by tracing the floor of the supraspinatus fossa with a line perpendicular to the back of the glenosphere (Figure 5.1),[21] glenoid lucency, and incorporation of bone graft in the BIO-RSA cohort.[4]

Differences in clinical outcomes between BIO-RSA and metal augment cohorts were assessed using either an unpaired t-test, if normally distributed, or the Mann-Whitney test if not. Categorical data was evaluated using the Chi-square test. Differences in migration between the glenosphere cohorts were assessed using a mixed-effects model with Bonferroni's test for multiple comparisons. Differences in migration between time points within glenosphere cohorts were also examined using Bonferroni's test for multiple comparisons. Pearson's correlation coefficients were assessed to determine any relationship between glenosphere inclination with active external and internal rotation, total glenosphere translation, and glenosphere rotation about the inclination-declination axis at one year. Statistical significance was set at $P < 0.05$ and completed in Prism 8 (GraphPad, La Jolla, CA, USA).
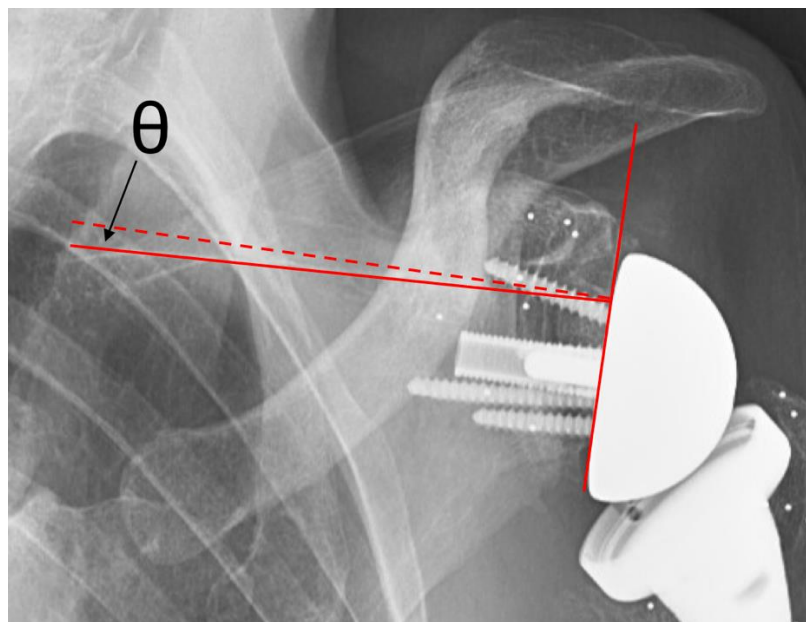
Figure 5.1 The inclination angle θ, measured as the angle between a line tracing the floor of the supraspinatus fossa (solid) and that perpendicular to the back of the glenosphere (dashed). This figure illustrates slight inferior tilt of the glenosphere.

5.2.1 Surgical technique

All procedures were performed by a fellowship-trained shoulder surgeon (GSA), and used the Aequalis™ Ascend™ Flex reverse shoulder system (Wright Medical-Tornier

Group, Memphis, TN, USA). Prior to surgery, computed tomography scans of each patient's glenohumeral joint were assessed for glenoid deficiency and classified according to the Walch and Favard systems as appropriate (Table 5.1).[19,36] Preoperative templating was completed for each patient to optimize implant size and positioning, though final sizes and placement were evaluated intraoperatively. The standard deltopectoral approach was used, with patients in the beach chair position. During surgery, five tantalum beads 1 mm in diameter (Halifax Biomedical Inc., Mabou, NS, Canada) were inserted into the glenoid vault, and three beads in the coracoid, prior to implanting the glenoid baseplate. These beads were spaced as far apart as possible to facilitate subsequent radiostereometric analysis.

For the BIO-RSA cohort, bone graft with a thickness of approximately 10 mm and diameter appropriate to the baseplate was harvested from the humeral head prior to head resection. The graft was then shaped to match each patient's glenoid deficiency, as described by Boileau et al.,[5] and fixed using a long (25 mm) central post, two compression, and two locking screws. A 36 mm glenosphere was used in nine cases, a 39 mm glenosphere in three cases, and a 42 mm glenosphere in eight cases.

For patients in the porous metal wedge cohort, the full wedge (15° slant) augment (Aequalis™ PerFORM™+ Reversed, ADAPTIS™ integrated porous metal) was used, with a diameter of either 25 or 29 mm. The augmented baseplate was seated to the reamed glenoid and fixed using a central screw with diameter either 6.5 or 9 mm, one compression screw, and three locking screws. Eight 36 mm, three 39 mm, and ten 42 mm glenospheres were used. In one case (36 mm) a 9 mm diameter central post was used, as insufficient purchase was achieved using the central screw. Radiographic differences between the two augmentation techniques are illustrated in Figure 5.2.
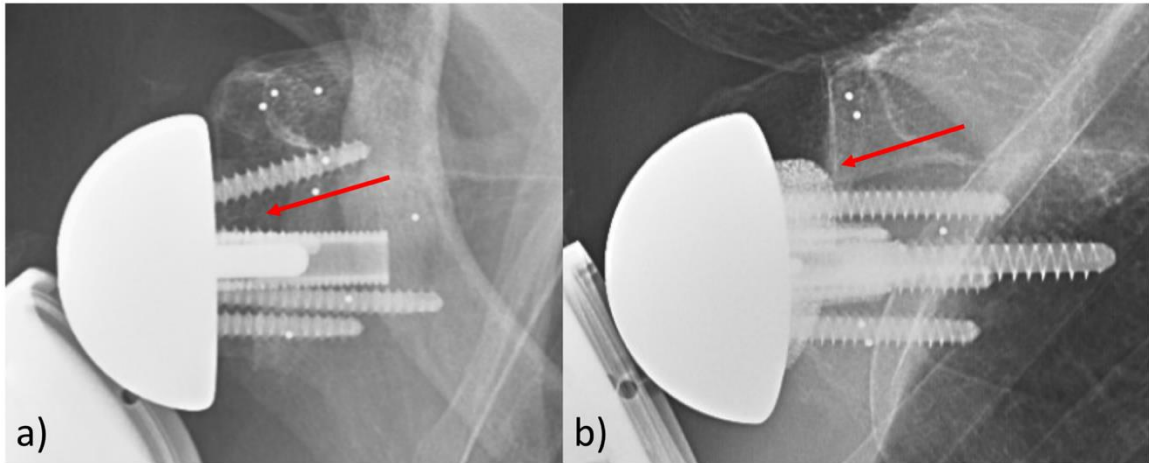
Figure 5.2 Radiographs of glenosphere augmentation (arrow) using (a) BIO-RSA and (b) the porous metal augment. Tantalum beads are also visible in the glenoid vault and coracoid as small radiopaque circles.

Patients received either a cemented or press-fit stem, with either a 1.5 mm (n = 39) or 3.5 mm (n = 2) eccentric tray (Aequalis™ Ascend™ Flex, Wright Medical-Tornier Group, Memphis, TN, USA). Trial reduction was completed prior to final polyethylene selection to ensure stability and mobility of the joint. Polyethylene diameter was matched to glenosphere diameter, with +6 mm poly used in 33 cases and +9 mm poly used in eight cases.

5.2.2 Radiostereometric analysis

Glenosphere migration was measured in commercial model-based radiostereometric analysis software (RSACore, Leiden, The Netherlands). Bias and repeatability of this technique have previously been validated under ideal conditions, with a reported bias (mean absolute value ± 95% confidence interval) less than, and repeatability greater than, 0.08 ± 0.02 mm and 0.15 mm, and 0.3 ± 0.1° and 0.2° in translation and rotation, respectively.[15] The condition number, a value representative of the dispersion of the fiducial markers, was also recorded for each measurement. A well-conditioned marker cluster will be spread out in three dimensions, rather than colinear, and will have a low condition number. It has been generally suggested that measurements with condition numbers less than 150 provide reliable results.[35] Due to the small glenoid and coracoid

area within which tantalum beads could be placed, there is the potential for worse

dispersion and higher condition numbers, and therefore this value has previously

increased to 300 for the glenoid component of the shoulder.[32]

Linear translations were recorded along the medial(+)-lateral(-) x-axis, superior(+)-

inferior(-) y-axis, and anterior(+)-posterior(-) z-axis (Figure 5.3a). A three-dimensional

total translation vector was calculated at each time point as well. Rotations of the

glenosphere were recorded about the anteversion(+)-retroversion(-) x-axis, and

declination(+)-inclination(-) z-axis (Figure 5.3b). The glenosphere is symmetric about its

y-axis and these measurements were consequently indeterminate. Note that rotations

follow Euler rigid body kinematics and therefore are not in line with the model-based

radiostereometric analysis global coordinate frame, as translations are.
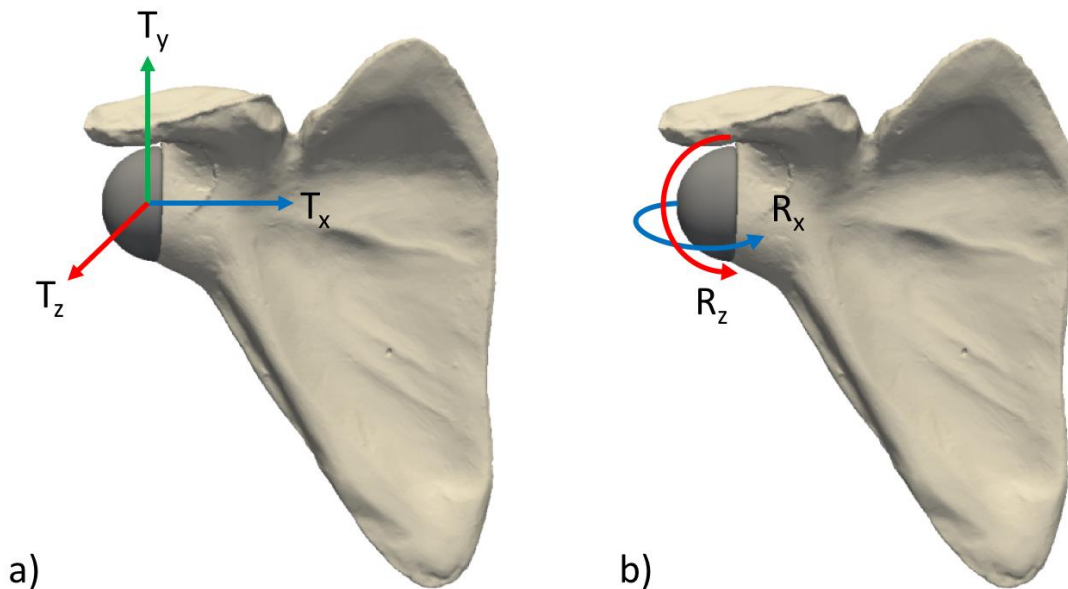
Figure 5.3 Right-handed coordinate system illustrating (a) translational axes and (b) rotational axes.

5.3 Results

Mean age at time of surgery was 72 ± 9 years, with no difference in demographics

between cohorts (Table 5.1). A preoperative difference between groups was observed in

forward flexion (mean difference = 18°, $P = 0.047$), though no other range of motion or

outcome measures were significantly different (Table 5.2). Postoperative patient-reported outcomes are also reported in Table 5.2, along with the mean difference from baseline. All outcomes for each cohort improved significantly one year postoperatively, with the exception of external rotation for both groups, and internal rotation in the augment cohort. Significant and clinically important differences in forward flexion and lateral abduction were observed between groups one year postoperatively, with the metal augment group showing increased flexion and abduction. Adverse events include one revision due to dislocation in the augment cohort nine months postoperatively, and one acromion fracture in the BIO-RSA cohort which healed without intervention. Full study flow is illustrated in Figure 5.3. Mean glenosphere inclination in the BIO-RSA cohort was $1.0 \pm 2.7°$, and $3.5 \pm 5.0°$ in the metal augment cohort. All bone grafts demonstrated structural integrity at the most recent follow-up, with no evidence of glenoid lucency. There was no evidence of scapular notching within either cohort. Mean condition number for patients with BIO-RSA was 145 ± 97, and 138 ± 97 for patients with the metal augment.

Table 5.1 Patient demographics (mean ± SD)

	BIO-RSA (n = 20)	Augment (n = 21)	*P*-value
Age	75.0 ± 8.7	70.3 ± 8.5	0.096
Sex	11 M; 9 F	11 M; 10 F	0.867
Walch classification	A1: 3 A2: 1 B2: 2 B3: 3	A1: 2 A2: 3 B2: 5 D: 1	N/A
Favard classification	E0: 6 E2: 2 E3: 3	E0: 8 E2: 2	N/A
Glenosphere inclination angle (superior(+)-inferior(-))	$1.0 \pm 2.7°$	$3.5 \pm 5.0°$	0.055
Indication*	OA: 7 CTA: 9 MRCT: 2 OA + RCT: 1 RA: 1	OA: 10 CTA: 6 MRCT: 4 OA + RCT: 1	N/A

*OA = osteoarthritis; CTA = cuff tear arthropathy; MRCT = massive rotator cuff tear; OA + RCT = osteoarthritis and rotator cuff tear; RA = rheumatoid arthritis

Table 5.2 Patient-reported outcome measures (mean ± SD)

	Preoperative			Postoperative (1 year)			Difference	Difference
	BIO-RSA	Augment	*P*-value	BIO-RSA	Augment	*P*-value	BIO-RSA	Augment
Forward flexion (°)	62 ± 31	80 ± 26	**0.047**	115 ± 18	128 ± 18	**0.047**	+53 ($P <$ **0.001**)	+48 ($P <$ **0.001**)
Lateral abduction (°)	56± 22	71 ± 26	0.062	95 ± 21	117 ± 23	**0.006**	+39 ($P <$ **0.001**)	+46 ($P <$ **0.001**)
External rotation (°)	24 ± 19	26 ± 23	0.838	34 ± 19	37 ± 17	0.638	+10 ($P = 0.125$)	+11 ($P = 0.121$)
Internal rotation (1-6)*	3 ± 1	3 ± 2	0.281	4 ± 2	4 ± 2	0.665	+1 ($P =$ **0.016**)	+1 ($P = 0.104$)
Pain (0-10)	7.0 ± 2.2	6.9 ± 2.4	0.896	1.7 ± 2.1	1.3 ± 1.5	0.779	-5.2 ($P <$ **0.001**)	-5.6 ($P <$ **0.001**)
SSV (0-100)	33± 21	30 ± 22	0.715	85 ± 11	83 ± 19	0.654	+52 ($P <$ **0.001**)	+56 ($P <$ **0.001**)
ASES (0-100)	33.6 ± 13.7	34.3 ± 18.7	0.895	77.6 ± 17.7	82.1 ± 12.9	0.428	+44.0 ($P <$ **0.001**)	+47.8 ($P <$ **0.001**)
SST (0-12)	1.9 ± 1.4	3.0 ± 2.3	0.075	7.6 ± 2.8	8.3 ± 2.6	0.534	+5.7 ($P <$ **0.001**)	+5.3 ($P <$ **0.001**)
DASH (0-100)	56.6 ± 14.7	51.7 ± 16.3	0.322	27.6 ± 18.0	15.7 ± 16.4	0.129	-29.0 ($P <$ **0.001**)	-36.0 ($P <$ **0.001**)
Constant (0-100)	22.6 ± 9.1	29.9 ± 15.3	0.074	61.6 ± 10.9	66.4 ± 13.5	0.262	+39.0 ($P <$ **0.001**)	+36.5 ($P <$ **0.001**)

***Based on the landmarks from Constant Shoulder Score: 1 = lateral thigh, 2 = buttock, 3 = lumbo-sacral junction, 4 = waist, 5 = T12, 6 = T7 or interscapular

CONSORT flow diagram – BIO-RSA vs. metal augmented glenospheres
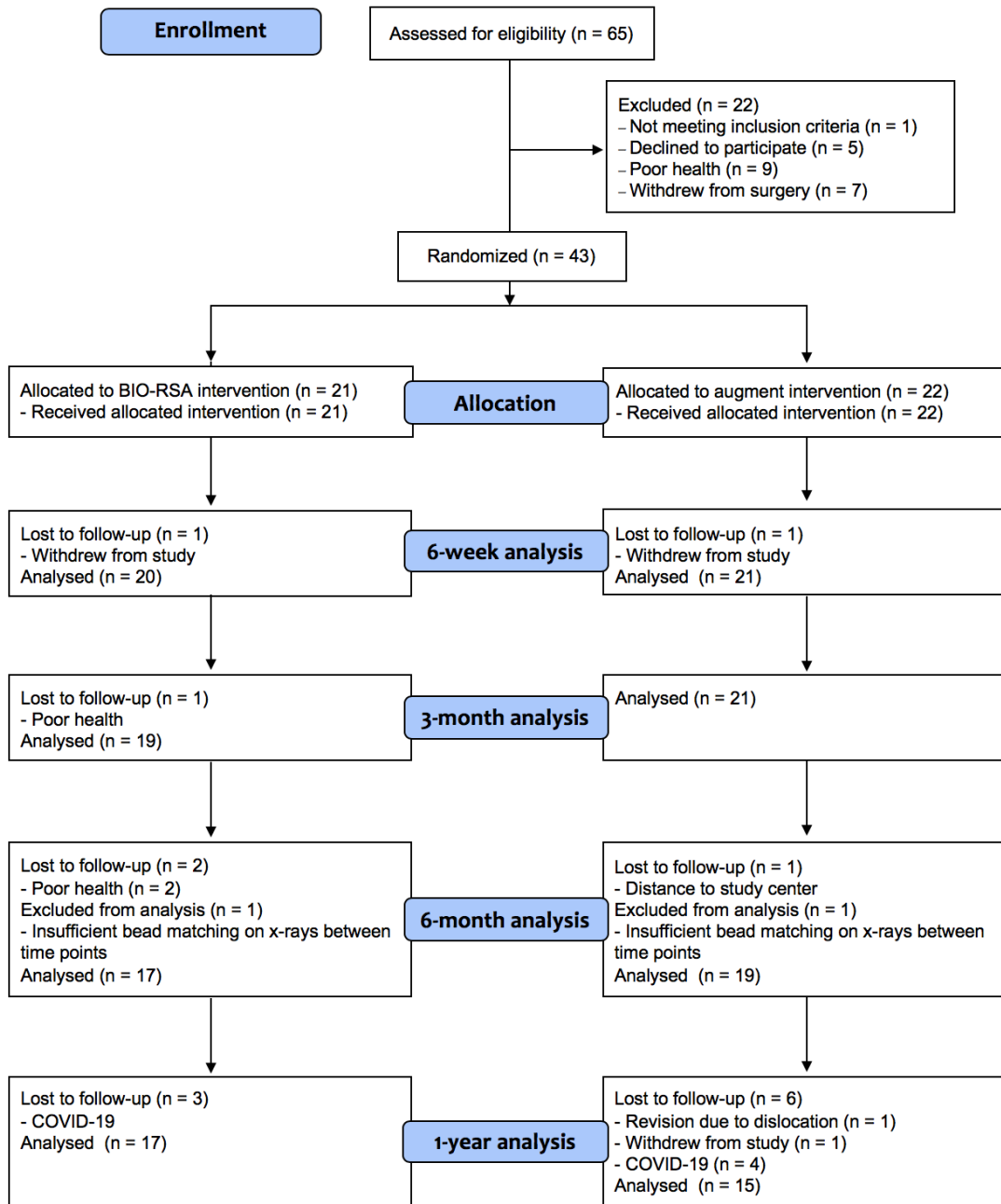
Figure 5.4 CONSORT study flow.

There was no significant difference (mean difference = 0.11 mm, P = 0.611) in total translation between BIO-RSA and porous metal augmented cohorts at one year (Figure 5.5). A significant difference was observed along the medial-lateral axis at one year

(mean difference = 0.23 mm, P = 0.033), with the BIO-RSA cohort showing greater medial translation. No other differences were observed at any time point along any axis between augmentation groups (Tables 5.4, 5.5).

Within cohorts, no differences in total translation were observed from three months to six months, or six months to one year. The porous metal augment cohort demonstrated greater lateral translation from six months to one year (mean difference = 0.18 mm, P = 0.021), and greater superior (mean difference = 0.19 mm, P = 0.002), followed by greater inferior (mean difference = 0.16, P = 0.013) translation from three months to six months, and six months to one year, respectively. The augment cohort also showed increased anteversion (mean difference = 0.51°, P = 0.006) from six months to one year postoperatively. No differences were observed within the BIO-RSA cohort from three months onward along any translation or rotation axis (Appendix G).

There was no correlation between glenosphere inclination angle and total translation (r = 0.138, P = 0.598; r = 0.035, P = 0.902) or rotation about the inclination-declination R_z axis (r = -0.110, P = 0.675; r = -0.029, P = 0.918) for either BIO-RSA or augment cohorts, respectively. The BIO-RSA group demonstrated a significant moderate correlation between active external rotation and superior glenosphere inclination (r = 0.466, P = 0.044), whereas the augment group demonstrated a significant moderate correlation between active internal rotation and inferior glenosphere tilt (r = -0.526, P = 0.044).

Table 5.3 Precision, recorded in mm for translation and degrees for rotation

	Medial(+)-Lateral(-) (T_x)	Superior(+)-Inferior(-) (T_y)	Anterior(+)-Posterior(-) (T_z)	Total Translation (T_r)	Anteversion(+)-Retroversion(-) (R_x)	Inclination(-)-Declination(+) (R_z)
BIO-RSA	0.28	0.18	0.51	0.24	0.84	1.05
Augment	0.29	0.27	0.54	0.31	1.01	1.90

Table 5.4 Translational migration, recorded in mm as mean ± SD

	Medial(+)-Lateral(-) (T_x)			Superior(+)-Inferior(-) (T_y)			Anterior(+)-Posterior(-) (T_z)			Total Translation (T_r)		
	BIO-RSA	Augment	*P*-value	BIO-RSA	Augment	*P*-value	BIO-RSA	Augment	*P*-value	BIO-RSA	Augment	*P*-value
3 months	0.09 ± 0.21	-0.00 ± 0.22	0.787	-0.01 ± 0.21	-0.07 ± 0.19	0.850	0.11 ± 0.36	-0.03 ± 0.36	0.769	0.41 ± 0.26	0.41 ± 0.21	> 0.999
6 months	0.21 ± 0.18	0.05 ± 0.24	0.156	0.00 ± 0.17	0.12 ± 0.18	0.273	0.00 ± 0.29	-0.01 ± 0.40	> 0.999	0.37 ± 0.21	0.45± 0.23	0.580
1 year	0.10 ± 0.21	-0.13 ± 0.25	**0.033**	0.00 ± 0.13	-0.04 ± 0.27	> 0.999	0.08 ± 0.33	-0.02 ± 0.44	> 0.999	0.39 ± 0.16	0.50 ± 0.29	0.611

Table 5.5 Rotational migration, recorded in degrees as mean ± SD

	Anteversion(+)-Retroversion(-) (R_x)			Inclination(-)-Declination(+) (R_z)		
	BIO-RSA	Augment	*P*-value	BIO-RSA	Augment	*P*-value
3 months	-0.09 ± 0.74	-0.06 ± 0.71	> 0.999	0.19 ± 0.61	0.03 ± 0.65	> 0.999
6 months	0.01 ± 0.80	-0.36 ± 0.53	0.535	-0.07 ± 0.66	0.15 ± 0.74	0.921
1 year	-0.21 ± 0.88	0.15 ± 0.44	0.480	0.02 ± 0.37	0.04 ± 0.77	> 0.999
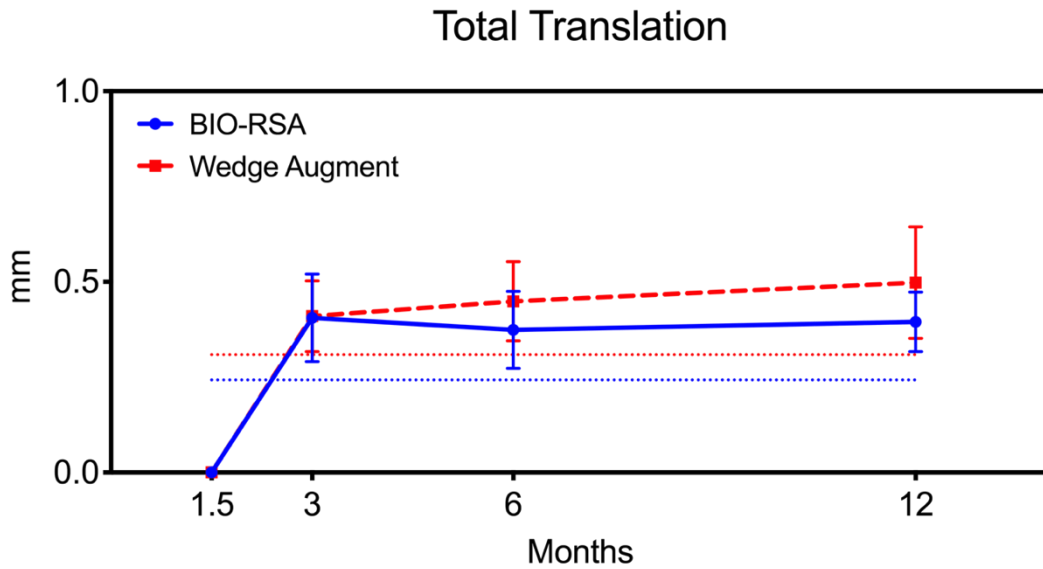
Total Translation

Figure 5.5 Mean ± 95% confidence intervals of total translation migration measurements for BIO-RSA (solid blue) and porous metal wedge augment (dashed red) glenoid lateralization techniques. MBRSA precision is illustrated as the blue dotted line for BIO-RSA and the red dotted line for porous metal wedge augment.

5.4 Discussion

Glenosphere baseplate lateralization in reverse total shoulder arthroplasty is a solution for reducing the incidence of scapular notching and improving impingement-free range of motion. The purpose of this study was to compare implant migration between BIO-RSA and porous metal augmentation techniques in reverse total shoulder arthroplasty using model-based radiostereometric analysis.

No statistically significant differences in migration were observed along any translation or rotation axis at any time point between groups, with the exception of the medial-lateral translation axis at one year. While statistically significant, the magnitude of the observed difference (+0.23 mm for the BIO-RSA cohort) is below the precision of the analysis technique along that plane (0.30 mm), and therefore these results are clinically indeterminate. While it is likely that some minute migration occurred as the implant baseplates integrated with the reamed glenoid in the first few months postoperatively, the

precision of the technique is poorer than the migration values observed, and therefore no distinguishable differences were observed between groups. Similarly, though simple effects analysis demonstrated significant differences in migration between three months and six months, and six months and one year within the porous metal wedge cohort, all observed differences were within the precision of the technique and can be interpreted as noise. Overall, it appears that immediate, stable fixation is achieved with both augmentation techniques.

Both cohorts improved in all functional metrics one year postoperatively, with the exception of external and internal rotation in the porous metal augment cohort and external rotation in the BIO-RSA cohort. The significant improvement in internal rotation with the BIO-RSA cohort not observed with the augment cohort may be a result of augment geometry. While the metal augment is restricted to a predefined geometry, BIO-RSA allows for increased lateralization and shape modification, potentially providing greater patient-specific benefit.[1] Further, while patients in the metal augment cohort showed significantly greater range of motion postoperatively, the relative gain for both groups individually is comparable, with increases in forward flexion of 53° and 48°, and increases in lateral abduction of 39° and 46° for BIO-RSA and metal augment groups, respectively. Outcomes at one year are consistent with those reported at mean 2.8 year follow-up for a cohort with lateralized glenospheres.[3]

A number of studies have investigated the relationship between glenosphere positioning and impingement-free range of motion. Though results are mixed, it is generally proposed that lateral positioning with inferior tilt of the glenosphere results in the greatest range of motion.[11,20,29] While neither lateralization cohort demonstrated any evidence of scapular notching in this study, this is likely attributed to the extent of lateralization achieved, as glenospheres were implanted with a mean neutral tilt as referenced to the floor of the supraspinatus fossa. It is interesting to note that while no differences were observed between groups in active internal or external rotation postoperatively, inferior tilt was moderately correlated with increases in internal rotation within the metal augment cohort. As alluded to previously, patients in this cohort may benefit from greater inferior

tilt, as the extent of lateralization is predefined by the size of the metal wedge. Though the BIO-RSA cohort demonstrated a moderate correlation between external rotation and superior tilt, it has been well established that superior tilt is associated with scapular notching and joint instability, and therefore not recommended.[8,33]

This study has limitations. The first is the use of the glenosphere CAD model as the implant surface model rather than a reverse engineered model. One group has previously evaluated the clinical precision of glenosphere migration measurements in the reverse shoulder using a reverse engineered glenosphere model in the same model-based radiostereometric analysis software, with slightly improved results: $T_x = 0.22$ mm, $T_y = 0.13$ mm, $T_z = 0.25$ mm, $R_x = 0.36°$, $R_z = 0.69°$.[9] This study also changed the imaging position of the patients, having them lie supine, with the calibration cage rotated 90° from our sitting examinations. It has been shown that reverse engineered models improve the clinical precision of model-based radiostereometric analysis compared to CAD models, and this is likely a source of their finer results.[14] Another limitation is that the glenosphere is symmetric about its y-axis, and therefore rotations about this axis could not be measured.

The condition number for both BIO-RSA and metal augment cohorts was comparable, and at the higher end of acceptable, at 145 ± 97 and 138 ± 97, respectively. Traditionally, the upper limit for condition numbers has been set at 150, though our values are within the increased limit of 300 for glenoid components and demonstrate acceptable conditioning.[32] Tantalum beads were inserted into the coracoid in addition to the glenoid vault in order to improve the condition number, but as the results show, the limited surrounding bone volume is still a limitation of acquiring reliably small migration measurements. Lastly, the results of this study are short-term. Further long-term follow-up is required to assess implant longevity and to determine the effect of any potential bone graft resorption or glenoid lucency.

A handful of studies have investigated glenoid component migration in anatomic shoulder arthroplasty, with variable results, though these results are not transferable to the

reverse shoulder glenoid component, as the reverse shoulder undergoes different biomechanics and loading conditions.[10,23,24,27,28,32]

5.5   Conclusion

To the best of our knowledge, this is the first study to report glenosphere migration using model-based radiostereometric analysis. In the short-term, our results indicate both BIO-RSA and the use of porous metal wedge augmented baseplates provide initial, stable fixation, with no difference in clinical outcomes.

5.6   References

1.   Abdic S, Knowles NK, Walch G, Johnson JA, Athwal GS. Type E2 glenoid bone loss orientation and management with augmented implants. J Shoulder Elb Surg. 2020;1–10. doi:10.1016/j.jse.2019.11.009

2.   Ackland DC, Roshan-Zamir S, Richardson M, Pandy MG. Muscle and joint-contact loading at the glenohumeral joint after reverse total shoulder arthroplasty. J Orthop Res. 2011;29(December):1850–1858. doi:10.1002/jor.21437

3.   Athwal GS, MacDermid JC, Reddy KM, Marsh JP, Faber KJ, Drosdowech D. Does bony increased-offset reverse shoulder arthroplasty decrease scapular notching? J Shoulder Elb Surg. 2015;24(3):468–473. doi:10.1016/j.jse.2014.08.015

4.   Boileau P, Moineau G, Roussanne Y, O'Shea K. Bony increased-offset reversed shoulder arthroplasty: minimizing scapular impingement while maximizing glenoid fixation. Clin Orthop Relat Res. 2011;469(9):2558–2567. doi:10.1007/s11999-011-1775-4

5.   Boileau P, Morin-Salvo N, Gauci MO, Seeto BL, Chalmers PN, Holzer N, et al. Angled BIO-RSA (bony-increased offset-reverse shoulder arthroplasty): A solution for the management glenoid bone loss and erosion. J Shoulder Elb Surg. 2017;26:2133–2142. doi:10.1016/j.jse.2017.05.024

6.   Boileau P, Watkinson DJ, Hatzidakis AM, Balg F. Grammont reverse prosthesis: Design, rationale, and biomechanics. J Shoulder Elb Surg. 2005;14:147–161. doi:10.1016/j.jse.2004.10.006

7.   Costantini O, Choi DS, Kontaxis A, Gulotta LV. The effects of progressive lateralization of the joint center of rotation of reverse total shoulder implants. J shoulder Elb Surg. 2015;24(7):1120–1128. doi:10.1016/j.jse.2014.11.040

8.   Duethman NC, Aibinder WR, Nguyen NT V, Sanchez-Sotelo J. The influence of glenoid component position on scapular notching: a detailed radiographic analysis at midterm follow-up. JSES Int. 2020;4(1):144–150. doi:10.1016/j.jses.2019.11.004

9.   Fraser AN, Tsukanaka M, Fjalestad T, Madsen JE, Röhrl SM. Model-based RSA is suitable for clinical trials on the glenoid component of reverse total shoulder arthroplasty. J Orthop Res. 2018;36(12):3299–3307. doi:10.1002/jor.24111

10. Gascoyne TC, McRae SMB, Parashin SL, Leiter JRS, Petrak MJ, Bohm ER, et al. Radiostereometric analysis of keeled versus pegged glenoid components in total shoulder arthroplasty: A randomized feasibility study. Can J Surg. 2017;60(4):273–279. doi:10.1503/cjs.001817

11. Gutiérrez S, Walker M, Willis M, Pupello DR, Frankle MA. Effects of tilt and glenosphere eccentricity on baseplate/bone interface forces in a computational model, validated by a mechanical model, of reverse shoulder arthroplasty. J Shoulder Elb Surg. 2011;20(5):732–739. doi:10.1016/j.jse.2010.10.035

12. Jain NB, Yamaguchi K. The contribution of reverse shoulder arthroplasty to utilization of primary shoulder arthroplasty. J Shoulder Elb Surg. 2014;23(12):1905–1912. doi:10.1016/j.jse.2014.06.055

13. Jean K. Classifications of glenoid dysplasia, glenoid bone loss and glenoid loosening: A review of the literature. Eur J Orthop Surg Traumatol. 2013;23(3):301–310. doi:10.1007/s00590-012-1119-4

14. Kaptein BL, Valstar ER, Stoel BC, Rozing PM, Reiber JHC. A new model-based RSA method validated using CAD models and models from reversed engineering. J Biomech. 2003;36(6):873–882. doi:10.1016/S0021-9290(03)00002-2

15. Van de Kleut ML, Yuan X, Athwal GS, Teeter MG. Validation of radiostereometric analysis in six degrees of freedom for use with reverse total shoulder arthroplasty. J Biomech. 2018;68:126–131. doi:10.1016/j.jbiomech.2017.12.027

16. Knowles NK, Ferreira LM, Athwal GS. Augmented glenoid component designs for type B2 erosions: A computational comparison by volume of bone removal and quality of remaining bone. J Shoulder Elb Surg. 2015;24(8):1218–1226. doi:10.1016/j.jse.2014.12.018

17. Kontaxis A, Johnson GR. The biomechanics of reverse anatomy shoulder replacement – A modelling study. Clin Biomech. 2009;24(3):254–260. doi:10.1016/j.clinbiomech.2008.12.004

18. Kwon YW, Forman RE, Walker PS, Zuckerman JD. Analysis of reverse total shoulder joint forces and glenoid fixation. Bull NYU Hosp Jt Dis. 2010;68(4):273–280. doi:PMID: 21162705

19. Lévigne C, Boileau P, Favard L, Garaud P, Molé D, Sirveaux F, et al. Scapular notching in reverse shoulder arthroplasty. J Shoulder Elb Surg. 2008;17(6):925–935. doi:10.1016/j.jse.2008.02.010

20. Li X, Knutson Z, Choi D, Lobatto D, Lipman J, Craig EV, et al. Effects of glenosphere positioning on impingement-free internal and external rotation after reverse total shoulder arthroplasty. J Shoulder Elb Surg. 2013;22(6):807–813. doi:10.1016/j.jse.2012.07.013

21. Maurer A, Fucentese SF, Pfirrmann CWA, Wirth SH, Djahangiri A, Jost B, et al. Assessment of glenoid inclination on routine clinical radiographs and computed tomography examinations of the shoulder. J Shoulder Elb Surg. 2012;21(8):1096–1103. doi:10.1016/j.jse.2011.07.010

22. Nam D, Kepler C, Neviaser A, Jones K, Wright T, Craig E, et al. Reverse total

shoulder arthroplasty: Current concepts, results, and component wear analysis. J Bone Joint Surg Am. 2010;92–A(2):23–35. doi:10.2106/JBJS.J.00769

23. Nuttall D, Haines JF, Trail IA. The early migration of a partially cemented fluted pegged glenoid component using radiostereometric analysis. J Shoulder Elb Surg. 2012;21(9):1191–1196. doi:10.1016/j.jse.2011.07.028

24. Nuttall D, Haines JF, Trail II. A study of the micromovement of pegged and keeled glenoid components compared using radiostereometric analysis. J Shoulder Elb Surg. 2007;16(Suppl 3):65–70. doi:10.1016/j.jse.2006.01.015

25. Pijls BG, Plevier JWM, Nelissen RGHH. RSA migration of total knee replacements: A systematic review and meta-analysis. Acta Orthop. 2018;89(3):320–328. doi:10.1080/17453674.2018.1443635

26. Pijls BG, Valstar ER, Nouta K, Plevier JWM, Middeldorp S, Nelissen RGHH, et al. Early migration of tibial components is associated with late revision: A systematic review and meta-analysis of 21,000 knee arthroplasties. Acta Orthop. 2012;83(6):614–624. doi:10.3109/17453674.2012.747052

27. Rahme H, Mattsson P, Larsson S. Stability of cemented all-polyethylene keeled glenoid components. J Bone Joint Surg Br. 2004;86–B:856–860. doi:10.1302/0301-620X.86B6.14882

28. Rahme H, Mattsson P, Wikblad L, Nowak J, Larsson S. Stability of cemented in-line pegged glenoid compared with keeled glenoid components in total shoulder arthroplasty. J Bone Joint Surg Am. 2009;91(8):1965–1972. doi:10.2106/JBJS.H.00938

29. Randelli P, Randelli F, Arrigoni P, Ragone V, D'Ambrosi R, Masuzzo P, et al. Optimal glenoid component inclination in reverse shoulder arthroplasty. How to improve implant stability. Musculoskelet Surg. 2014;98(SUPPL. 1):15–18. doi:10.1007/s12306-014-0324-1

30. Roche CP, Stroud NJ, Martin BL, Steiler CA, Flurin PH, Wright TW, et al. The impact of scapular notching on reverse shoulder glenoid fixation. J Shoulder Elb Surg. 2013;22(7):963–970. doi:10.1016/j.jse.2012.10.035

31. Schairer WW, Nwachukwu BU, Lyman S, Craig EV, Gulotta LV. National utilization of reverse total shoulder arthroplasty in the United States. J Shoulder Elb Surg. 2015;24(1):91–97. doi:10.1016/j.jse.2014.08.026

32. Streit JJ, Shishani Y, Greene ME, Nebergall AK, Wanner JP, Bragdon CR, et al. Radiostereometric and radiographic analysis of glenoid component motion after total shoulder arthroplasty. Orthopedics. 2015;38(10):e891–e897. doi:10.3928/01477447-20151002-56

33. Tashjian RZ, Martin BI, Ricketts CA, Henninger HB, Granger EK, Chalmers PN. Superior baseplate inclination is associated with instability after reverse total shoulder arthroplasty. Clin Orthop Relat Res. 2018;476(8):1622–1629. doi:10.1097/CORR.0000000000000340

34. Theivendran K, Varghese M, Large R, Bateman M, Morgan M, Tambe A, et al. Reverse total shoulder arthroplasty using a trabecular metal glenoid base plate. Bone Jt J. 2016;98(7):969–975. doi:10.1302/0301-620X.98B7

35. Valstar ER, Gill R, Ryd L, Flivik G, Börlin N, Kärrholm J. Guidelines for standardization of radiostereometry (RSA) of implants. Acta Orthop. 2005;76(4):563–572. doi:10.1080/17453670510041574

36.   Walch G, Badet R, Boulahia A, Khoury A. Morphologic study of the glenoid in primary glenohumeral osteoarthritis. J Arthroplasty. 1999;14(6):756–760. doi:10.1016/S0883-5403(99)90232-2

37.   Werner CML, Steinmann PA, Gilbart M, Gerber C. Treatment of painful pseudoparesis due to irreparable rotator cuff dysfunction with the Delta III reverse-ball-and-socket total shoulder prosthesis. J Bone Joint Surg Am. 2005;87(7):1476–1486. doi:10.2106/JBJS.D.02342

38.   Wright TW, Roche CP, Wright L, Flurin P-H, Crosby LA, Zuckerman JD. Reverse shoulder arthroplasty augments for glenoid wear: Comparison of posterior augments to superior augments. Bull Hosp Jt Dis. 2015;73 Suppl 1(January 2016):S124–S128.

6 Validation of in vivo linear and volumetric wear measurement for reverse total shoulder arthroplasty using model-based radiostereometric analysis

A version of this chapter has been published.[16]

6.1 Introduction

Material loss of the polyethylene (PE) articulating surface plays a critical role in the longevity of total joint replacements. Polyethylene wear debris, in excess, has been shown to induce an osteolytic response leading to implant loosening and failure.[31,42] This material loss, termed wear, is frequently quantified ex vivo using gravimetric analysis, coordinate measuring machines, or micro-computed tomography.[11,18,33,36] While these methods accurately describe the volume and pattern of wear, they are limited to retrieved components and wear simulations, leaving the majority of implanted components uninvestigated.

With interest in identifying wear rates of typical joint replacements over time, in vivo methods have been developed using radiographic techniques.[2,7,13,24,41] Radiostereometric analysis (RSA) has become the gold standard for such measurements, where the change in minimum separation distance between the two metal components of the joint replacement over time is representative of linear wear.[3,13,32,39]

Though radiostereometric analysis has been used in a number of studies investigating wear in both the hip and knee, in vivo wear measurements remain incomplete for the shoulder.[2,3,6–8,29,39] As the number of total shoulder procedures is expected to grow exponentially within the next decade, it is important to evaluate how new designs and bearing materials interact.[14,27] Of particular interest is reverse total shoulder arthroplasty (RTSA), which features a semi-constrained design and ultra-high molecular weight polyethylene (UHMWPE).[30] Retrieval, in vitro, and in silico studies have demonstrated a large range of wear rates in RTSA, from 14.3 mm^3/million cycles (MC) to 126 mm^3/MC,

with no obvious relationship between wear rate and polyethylene diameter.[5,17,23,25,33,40] With the introduction of new RTSA designs, it is important to evaluate this material loss under the conditions of a well-functioning implant in vivo to determine what can be classified as normal. As such, the purpose of this study was to validate the use of model-based radiostereometric analysis as a measurement tool for in vivo RTSA wear using a phantom setup.

6.2   Materials and Methods

6.2.1   Wear Simulation

Wear patterns representing those typical of reverse total shoulder arthroplasty were generated for use in this study.[5,17,23,25,33,40] The computer-aided design (CAD) models of the polyethylene insert (36 mm diameter) and glenosphere (36 mm diameter) were obtained from an implant manufacturer (Aequalis™ Reversed II, Wright Medical-Tornier Group, Memphis, TN, USA) and manipulated in SolidWorks (Dassault Systèmes, Paris, France). The glenosphere was set in contact with the polyethylene insert in an orientation representative of the arm at the side, at 0° of abduction, and 0° of internal/external rotation. Five wear patterns were simulated by moving the glenosphere into the insert at varying depths and positions, resulting in five inserts with artificial wear. Insert 1 is representative of inferior articular wear, insert 2 of inferior articular and rim wear, insert 3 primarily illustrating inferior rim wear, insert 4 representing large articular wear, and insert 5 representing small inferior rim notching – a phenomenon particular to the reverse shoulder design (Figure 6.1). The five worn inserts, in addition to an unworn control, were fabricated from their three-dimensional computer models using the Stratasys J735 3D printer (Stratasys Ltd, Eden Prairie, MN, USA). Models were printed in proprietary VeroBlackPlus™, a polymerized acrylate (plastic), with 27-micron layer thickness. The printed components had an elastic modulus of 2000-3000 MPa and shore hardness of 83-86 (Scale D), according to the product's material data sheet.[43] The true variation in volume from the control was determined using micro-computed tomography.[37] Inserts 1, 2, and 3 ranged in worn volume from 180 to 239 mm^3, with patterns and volumes based

on retrieval and simulation studies with approximately five years of wear.[5,17,23,25,33,40] Insert 4, simulating large articular wear, was fabricated with 403 mm^3 of material loss, to ensure any measured wear is not just noise and to determine a lower limit of detectability. Insert 5, representing small inferior rim notching, had a notch of 114 mm^3 volume loss and was designed to quantify the system's ability to detect strictly non-articular wear.
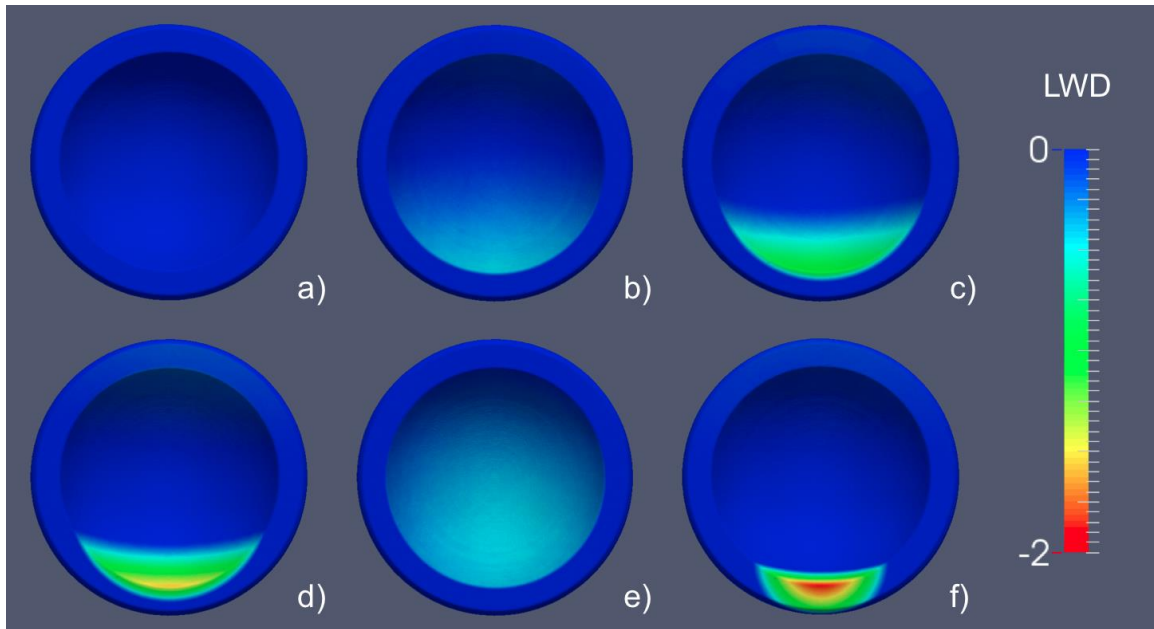
Figure 6.1 Deviation maps representing the linear wear depth (LWD) in mm of each additively manufactured worn insert, using the unworn insert (a) as reference. Insert 1 (b) simulates inferior articular wear, Insert 2 (c) inferior articular and rim wear, Insert 3 (d) inferior rim wear, Insert 4 (e) large articular wear, and Insert 5 (f) simulating small inferior rim notching.

6.2.2 Phantom Setup

A Sawbones shoulder model (SKU# 1050-13-2; Sawbones, Pacific Research Laboratories, Vashon, WA, USA) was implanted with reverse shoulder components (Aequalis™ Reversed II, Wright Medical-Tornier Group, Memphis, TN, USA) by an experienced orthopedic surgeon (GSA). Each additively manufactured polyethylene insert was then independently fixed within the metaphyseal tray for imaging. Proper orientation of the insert was achieved by matching a notch on the model to its

corresponding projection on the metaphyseal tray, as is done clinically with this implant. The humeral component was then rigidly fixed within a PVC tube and positioned using a retort stand. Five arm positions: neutral, 90° of abduction, 90° of flexion in the scapular plane, 30° of external rotation in adduction, and -70° of internal rotation with 40° of abduction were simulated to obtain measurements within the typical active range of motion of RTSA patients (Figure 6.2).[9] Separate retort stands were used for each position to ensure repeatability of positioning between liner trials. When the appropriate glenohumeral position was achieved, the humerus and scapula components were constrained using elastic bands to ensure contact between the insert and glenosphere.
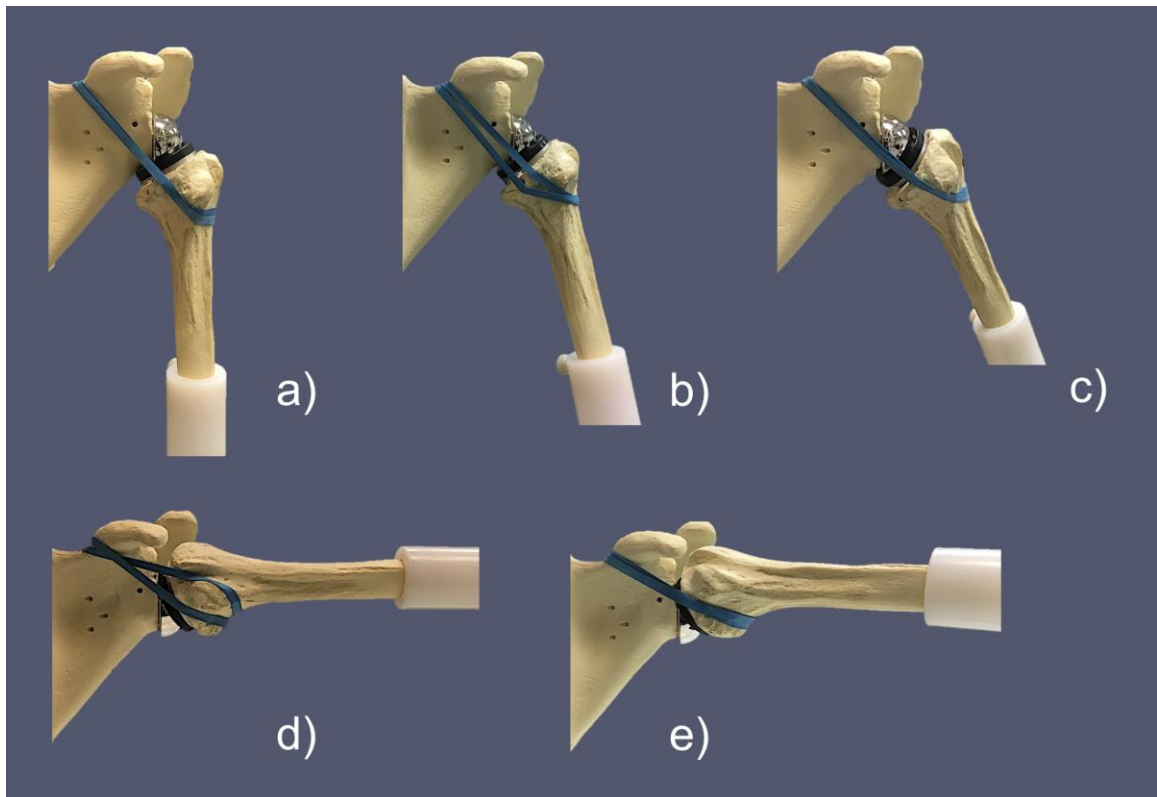
Figure 6.2 Each additively manufactured insert was placed in the RTSA phantom and mounted in a neutral (a), externally rotated (b), internally rotated (c), abducted (d), and flexed in the scapular plane (e) position for imaging.

6.2.3 Imaging Setup and Acquisition

The Sawbones phantom was positioned to mimic a radiostereometric analysis shoulder examination. It was placed in front of a vertical uniplanar calibration cage (Cage 43; RSA Biomedical, Umeå, Sweden) with two ceiling-mounted x-ray units angled 20° to the normal of the cage. Computed radiography imaging cassettes (35.5 cm x 43.2 cm) with 3520 x 4280 pixel matrix, 100-micron pixel size, and 10-bit gray-scale mapping were used for image acquisition. The full imaging system setup has been described and validated previously.[15] Image pairs were acquired for each series of arm positions in two rounds to obtain double exposures, for a total of ten image pairs per insert. The x-ray tubes and calibration cage were moved between exposures to imitate patient movement. The protocol was repeated for each artificially worn and control insert for a total of 60 image pairs.

6.2.4 Wear Analysis

Model-based radiostereometric analysis (MBRSA) was used to determine the position and orientation of glenosphere and humeral stem implants for each image pair, and the transforms recorded. The three-dimensional model of the unworn polyethylene component, obtained through micro-computed tomography (μCT) of the additively manufactured control insert, was virtually inserted into the metaphyseal tray of the humeral stem using Geomagic Studio (3D Systems Inc, Morrisville, NC, USA). This composite model was then transformed, along with the glenosphere, based on the estimation derived from MBRSA (Figure 6.3a).[38] The glenosphere is expected to intersect the unworn polyethylene model in the manner representative of the artificial wear of the worn inserts used during image acquisition. The μCT of the additively manufactured insert was used in lieu of the CAD model for the component to eliminate any error associated with the manufacturing process.

The method used for volumetric and linear wear quantification has previously been described and validated.[38] The unworn polyethylene model is discretized into isotropic voxels of length 0.075 mm (Figure 6.3b). Voxels belonging to the intersection of glenosphere and polyethylene from each image pair are recorded (Figure 6.3c). The sum

of unique polyethylene voxels from the intersection of the glenosphere in the five arm positions is multiplied by the voxel volume to obtain a physical measure of volumetric wear. Identification of unique voxels eliminates the overestimation of wear if the same voxel is marked in more than one image pair.

Maximum linear wear depth (MLWD) was recorded for each polyethylene insert using the same, previously validated method.[38] The 3D Euclidean distance as a surface normal from the articular surface of the polyethylene model to each intersected voxel was recorded, with the largest of these surface normal distances taken as the MLWD (Figure 6.3d). The true MLWD for this validation study was defined as the largest surface normal distance between the μCT model of the unworn insert and the μCT model of the respective insert of investigation. For each of the five artificially worn inserts, in addition to the unworn control, the measured MLWD was the distance recorded following the position and orientation transformations obtained by the model-based RSA software to the polyethylene and glenosphere models, respectively.
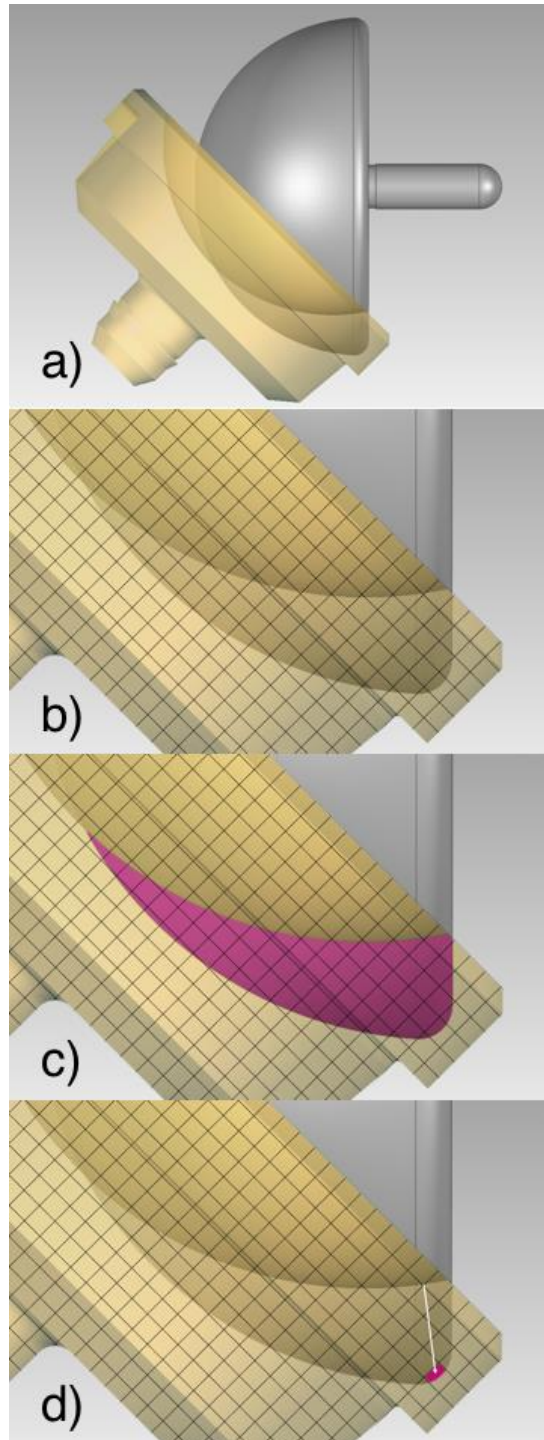
Figure 6.3 The glenosphere and polyethylene surface models are transformed using the position and orientation from model-based RSA (a). The polyethylene is discretized into isotropic voxels of length 0.075 mm (b). Volumetric wear is recorded as those voxels intersected by the glenosphere model (c), and linear wear as the maximum 3D Euclidean distance measured as a surface normal from the polyethylene articulating surface to each intersected voxel (d).

MLWD was also measured as the difference in minimum distance between the glenosphere and metal metaphyseal tray surface models for each worn insert relative to the distance measured with the unworn control in place. This difference in minimum distance between the two metal components has previously been used as a measure of linear wear in the hip,[1,26] and was included to determine whether in vivo wear measurements necessitate the use of the poly model for reverse total shoulder prostheses.

6.2.5 Reporting of Results

The measurement results are reported in terms of both volumetric and linear bias and precision. As per recently published recommendations, bias is reported as the mean absolute difference in known worn volume (or depth) from the measured volume $\pm$ 95% confidence interval.[20] For comparison with previously published studies, precision is reported as 1.96 x SD of the difference in measured volume (or depth) from double exposures.[10]

A one-way ANOVA was applied to determine if precision varies between arm positions, and the Kruskal-Wallis test with Dunn's test for multiple comparisons was used to determine if total observed wear volume from one arm position was different from another.

A paired t-test was used to compare the measured volume to true worn volume, as determined from the μCT scan for both exposures of each insert (n = 10 measurements). Similarly, a paired t-test was used to compare measured and true maximum linear wear depth (n = 10 measurements) between inserts using our novel method, and independently, to compare the true depth and measured separation distance between glenosphere and metaphyseal tray.

6.3 Results

Measurements from insert 5, representative of extra-articular notching, were excluded from the following results, as the proposed method was unable to account for such material loss and we did not want these measurements to influence the aggregate results and statistics. Complete volumetric precision results are recorded in Table 6.1. The overall precision, measured from 30 pairs of double exposures, was 49.3 mm^3. Complete bias results are recorded in Table 6.2. Overall bias, measured from 10 complete volume measurements (five inserts, each measured twice), was 48.9 ± 24.3 mm^3.

Table 6.1 Precision of RSA volumetric wear measurement (mm^3)

	Δ Volume from double exposures (mm^3)					
Phantom arm position	*Insert 0 (control)*	*Insert 1*	*Insert 2*	*Insert 3*	*Insert 4*	*Insert average*
Neutral	5.9	38.0	-6.5	-16.1	52.1	21.1
External Rotation	8.0	17.3	2.6	-0.2	-56.6	-4.8
Internal Rotation	-2.0	-16.5	-4.9	16.7	64.9	9.2
Flexion	-0.1	-0.9	-11.2	0.0	-58.0	-12.3
Abduction	0.0	-28.6	-1.2	6.9	25.6	-8.5
Combined	8.1	9.9	-11.3	7.7	15.9	3.5
Precision	(n = 6) 8.9	(n = 6) 47.0	(n = 6) 10.8	(n = 6) 21.6	(n = 6) 104.1	(n = 30) 49.3

Table 6.2 Bias of RSA volumetric wear measurement (mm^3)

Wear volume (mm^3)	*Insert 0 (control)*	*Insert 1*	*Insert 2*	*Insert 3*	*Insert 4*
True	0	180.5	188.6	239.3	403.4
Measured (1)	37.1	200.7	209.3	115.9	438.9
Measured (2)	45.1	210.6	198.0	123.6	454.8
Difference (1)	37.1	20.1	20.7	-123.4	35.5
Difference (2)	45.1	30.1	9.4	-115.7	51.4
Mean absolute value (n = 10) 48.9			**95% CI (n = 10)** 24.3		

The most precise measurements were obtained with the unworn control insert, at 8.9 mm^3, and the least precise measurements were obtained with Insert 4, large articular

wear, at 104.1 mm^3. Each phantom arm position provided equally precise volumetric wear results ($P = 0.453$). The greatest bias was observed for Insert 3, which underestimated the worn volume by an average of 120 mm^3. The least bias was observed for Insert 2, with an average overestimation of 15 mm^3.

The average percent observed wear volume from double exposures of each arm position compared to the total observed wear volume measured is recorded in Table 6.3. There was no significant difference in the percent of observed wear from different arm positions to the total measured volume ($P = 0.074$), though the greatest average observed volume is from the abducted arm position at 62% of the total volume, and the least from the external rotation arm position at 14% (Table 6.3). Further, considering the observed volume for Insert 0, the unworn insert, the majority of the recorded volume (93%) was from the neutral position. As the known volume is 0 mm^3, it was proposed that measurements from the neutral position contribute to systematic error of the system. From these observations, precision and bias calculations were repeated excluding the measurements from the neutral and external rotation arm positions. Excluding these measurements made no difference in precision measurements ($P = 0.195$) or bias measurements ($P = 0.078$), with modified precision reported as 53.3 mm^3 and modified bias as 35.6 ± 30.8 mm^3.

Table 6.3 % Observed of total wear volume from each arm position

Phantom arm position	*Insert 0 (control)*	*Insert 1*	*Insert 2*	*Insert 3*	*Insert 4*	*Position average*
Neutral	92.6	15.6	4.8	6.9	31.4	30.3
External Rotation	8.9	4.1	13.7	0.1	44.5	14.3
Internal Rotation	4.2	6.1	22.9	7.8	37.7	15.7
Flexion	0.2	0.2	41.2	0	64.3	21.2
Abduction	0.0	81.9	69.9	85.2	71.9	61.8

Table 6.4 Maximum linear wear depth (mm) measured as Glenosphere vs. Insert[a] and Glenosphere vs. Metaphyseal tray[b] compared to true value

Linear Wear Depth (mm)	Insert 0 (control)	Insert 1	Insert 2	Insert 3	Insert 4
True	0	-0.44	-1.06	-1.56	-0.44
Measured[a] (average)	-0.51	-0.98	-1.25	-1.54	-0.97
Precision (n = 5) 0.21 mm			**Mean absolute value ± 95% CI (n = 10)** 0.36 ± 0.13 mm		
Measured[b] (average)	0.00 (baseline)	-0.11	-0.02	0.02	-0.60
Precision (n = 5) 0.09 mm			**Mean absolute value ± 95% CI (n = 10)** 0.62 ± 0.20 mm		

A significant difference was observed between measured and true depth of the inserts using our previously validated novel method ($P = 0.037$), though no difference was observed ($P = 0.164$) when comparing the true depth and depth measured as the change in minimum distance between glenosphere and metaphyseal tray (the current standard for linear hip wear measurements) (Table 6.4).

Similar to volumetric wear calculations, maximum linear wear depth was recalculated excluding the contributions from the neutral and external rotation arm positions. No difference in measured wear compared to that measured with all arm positions was observed ($P = 0.182$). MLWD was also measured using only the position and orientation from the abduction exam, as it was shown that the greatest percent observed wear volume was from this arm position. From the single abduction exposures, MLWD was measured with a precision of 0.09 mm and bias of 0.21 ± 0.13 mm, with no difference from the true measurements ($P = 0.127$).

6.4 Discussion

Recently, model-based radiostereometric analysis has been used to evaluate the precision and accuracy of linear and volumetric wear measurements using hip and knee phantom models. In 2011, van IJsseldijk et al reported an accuracy of 0.1 mm and a precision of

0.2 mm for linear polyethylene wear in the knee.[13] In 2012, Stilling et al used model-based radiostereometric analysis in a simulated hip wear phantom, recording a precision of 2D wear measurement as 0.102 mm, and 3D wear measurement as 0.189 mm, respectively.[34] The precision of these model-based radiostereometric analysis experiments are in line with our results at 0.21 mm for linear wear, and adequate for clinical application.[13]

In 2013, van IJsseldijk et al expanded their measurements to volumetric wear, recording measured wear at varying knee flexion angles and observing that large differences in wear were observed at these different angles, and at most 56% of the true volume was measured, resulting in poor accuracy and precision.[12] The observations and limitations presented by this study in volumetric wear measurement led to our method of recording wear at different arm positions and taking the unique sum of intersecting overlap voxels. As a result, our method provides measurements with a bias of 48.9 ± 24.3 mm^3 and precision of 49.3 mm^3. These results are in good alignment with a previous paper published using a similar technique for the knee and single-plane fluoroscopy, which recorded a precision of 39.7 mm^3.[38]

Unlike the hip or knee, the shoulder is capable of motion in six degrees of freedom, introducing wear patterns that are not as predictable as the former. For this reason, we simulated five patterns emphasizing different aspects of RTSA wear – inserts 1, 2, 3 and 4 focusing on different proportions of articular and rim wear, and 5 on strictly extra-articular inferior notching. Our results show that articular and shallow rim wear is picked up well using model-based radiostereometric analysis, with a lower limit of detection equivalent to the bias of inserts 1, 2, 3, and 4 at a conservative approximate of 50 mm^3. However, notching, a phenomenon thought to be the result of scapular impingement and not the articulation of glenosphere against polyethylene, is not picked up if it is restricted to the rim. This can be observed by considering the surface deviation maps generated using the unworn µCT insert as the reference (Figure 6.1) and comparing them to the wear maps derived from the radiostereometric analysis measurements (Figure 6.4).
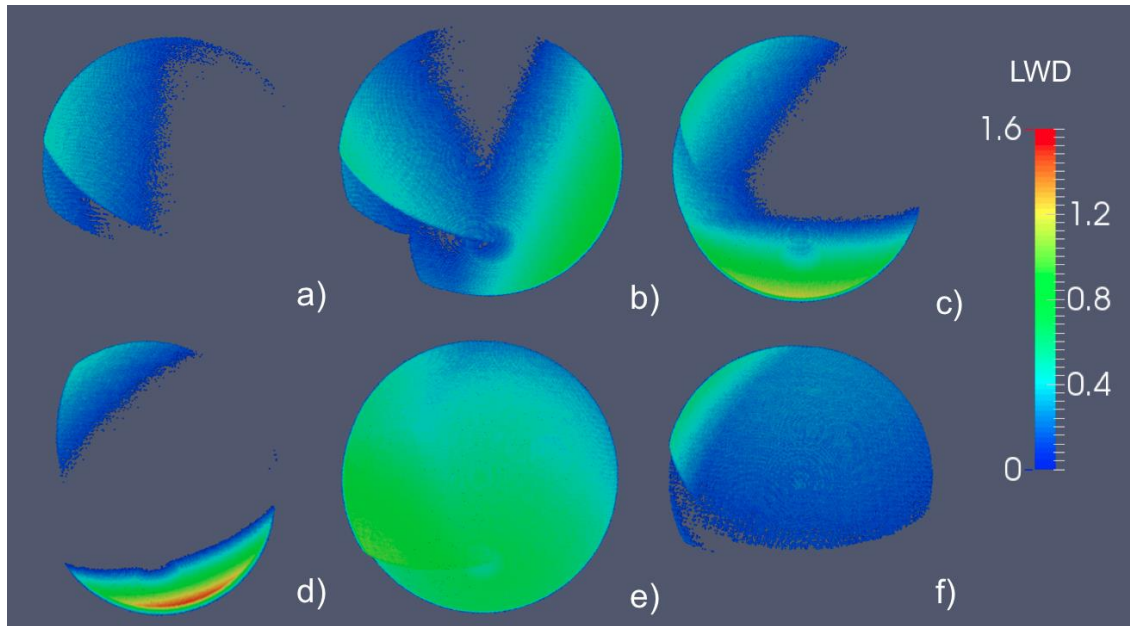
Figure 6.4 Wear maps measured using RSA of Inserts 0 through 5 (a – f), respectively, using Insert 0 (a) as the reference model virtually inserted into the metaphyseal tray.

It was shown in our analysis of the percent observed of total wear volume from different arm positions (Table 6.3) that though there was no significant difference in observed wear from the different positions, there was a trend towards the neutral position contributing wear when the known volume was 0 mm^3, indicating a source of systematic error. Further, the contribution from external rotation was typically within the margin of precision of the system, suggesting that it also may not be critical to the true wear measurement. For this reason, the neutral and external arm positions were eliminated and the precision and bias measurements re-calculated. Excluding these exposures did not significantly change either precision or bias, with differences from the original measures within 15 mm^3 and clinically negligible. Similarly, no difference was observed in maximum linear wear depth between the two calculation methods, though a trend towards slight improvement in precision and bias was observed by excluding the neutral and external rotation arm positions. The measurements using only the abduction arm position exam also showed no difference from the true values. Though these results would suggest an appropriate volumetric and linear wear estimation can be made on the basis of capturing x-rays from a limited number of arm positions, a limitation to this study is that

it does not accurately represent the soft tissue and compression forces at play in vivo, requiring further validation from in vivo studies.

Compared to the hip standard of measuring linear wear as the change in minimum distance between the constrained metal components of the joint replacement, our method performed with improved bias by 0.28 mm, and worse precision by 0.12 mm. Though a statistically significant difference was observed between our proposed novel method measurements and the true measurements, this is likely due to the consistent overestimation bias. It is interesting to note that the minimum separation method severely underestimated the true linear wear in all cases, except for that of large articular wear (insert 4). This is likely a result from the difference in wear patterns between hips and reverse shoulders – the hip has a deeper polyethylene liner, resulting in predominantly articular wear, whereas the modern reverse shoulder is semi-constrained,[4] allowing for greater range of motion and thus greater susceptibility to dislocation and forces applied at the edge of the polyethylene, resulting in more rim-focal wear patterns. It is likely this variation in the nature of implant design that requires a more robust method of wear measurement than simply minimum separation distance for the less constrained device. Further, in the case of the shoulder, where one geometry is spherical (glenosphere) and the other planar (tray), this method will only work if the wear vector is directly through the apex of the polyethylene liner. As such, it is sensitive to the wear vector, and only that component normal to the plane will be recorded. For this reason, the authors discourage the use of minimum separation distance as a measure of linear wear in the shoulder.

As the number of RTSA designs and configurations continue to grow, there are a number of variables that contribute to wear estimations from in vitro and in silico studies, making it difficult to directly compare the results from this study to those that have been previously published. Taking simulation studies using a similar maximum load profile (926.7 N, 926.7 N, and 914 N), wear rates were identified as 125.8 mm^3/MC, 83.6 mm^3/MC, and 42.0 mm^3/MC, respectively, highlighting such variation.[21,28,40] These loads are twice the physiologic loading observed in the RTSA shoulder under unloaded conditions,[19] suggesting the true wear rate is likely less than those observed in these

simulations. As such, with a wear estimate of approximately 40 mm^3/MC, and that one million cycles represents one year of use,[22] from a clinical perspective our results may be capable of identifying articular wear within a year from the true value. It should be noted that for patients with a low arm duty cycle due to lack of strength, range of motion or increased pain, a more conservative annual estimate may be appropriate.

There are several limitations to this study. The necessity of acquiring CAD models for each implant configuration under investigation is a major limitation, as not all implant manufacturers will be open to sharing 3D models or dimensioned drawings of their devices. Further, the study was conducted under ideal conditions and has not considered the manufacturing variability of polyethylene inserts in the results. Previous studies have investigated manufacturing lot variations, with both intra-system surface deviation variability and variability between manufactured inserts and their respective CAD model on the order of tens of microns.[35,36] Such variations are below the limit of detection for our proposed wear measurement method and for this reason would not contribute any additional error to the measurements. Our proposed method does not differentiate between creep and wear, classifying all material intersection as material loss. For this reason, wear, if measured without a postoperative baseline to account for in vivo measurement bias at a state of assumed zero-wear, may be over- or underestimated. If measurements are taken and compared over time, however, this offset from the state of zero wear could be applied to adjust the measurements accordingly. Additionally, the wear pools were artificially modeled based on retrieval and simulation studies, and the result may not be entirely accurate when compared to wear pools observed in vitro or from retrieved components. The artificially modeled wear modes in this study were derived from a single penetration vector of the glenosphere into the polyethylene model. The six degrees of motion allowed by the shoulder joint suggest that true wear modes would likely have multiple principal vectors associated with each predominant motion of daily living. By imaging patients in multiple relevant arm positions, these different principal vectors would be accounted for in vivo, though future validation needs to include models with more than one principal vector.

6.5 Conclusion

In summary, this study has revealed a number of insights into the feasibility of measuring RTSA wear in vivo. Radiographic views from multiple arm positions are required to maximize the accuracy of the measurement technique to a variety of wear patterns, providing a volumetric precision of 49.3 mm^3, with a bias of 48.9 $\pm$ 24.3 mm^3. Linear wear can be measured with a precision of 0.21 mm, and bias of 0.36 $\pm$ 0.13 mm. The technique is limited in its ability to measure inferior rim notching damage, though it is unlikely that any radiographic technique would be able to quantify such material loss as it is not part of the congruent surface between bearing materials. Advantages of this method are that it eliminates the requirement for the insertion of metal beads into the polyethylene at the time of surgery, and it does not require a baseline exam for comparison. Provided CAD models are available for the joint replacement under investigation, the technique can be translated between different prosthesis designs, allowing for a range of retrospective studies on large populations to be conducted. Its application in measuring in vivo articular wear is promising, with the current precision and bias meriting further investigation.

6.6 References

1.   Barrack RL, Lavernia C, Szuszczewicz ES, Sawhney J. Radiographic wear measurements in a cementless metal-backed modular cobalt-chromium acetabular component. J Arthroplasty. 2001;16(7):820–828. doi:10.1054/arth.2001.26589
2.   Bragdon CR, Malchau H, Yuan X, Perinchief R, Kärrholm J, Börlin N, et al. Experimental assessment of precision and accuracy of radiostereometric analysis for the determination of polyethylene wear in a total hip replacement model. J Orthop Res. 2002;20(4):688–695. doi:10.1016/S0736-0266(01)00171-1
3.   Campbell DG, Field JR, Callary SA. Second-generation highly cross-linked X3™ polyethylene wear: A preliminary radiostereometric analysis study. Clin Orthop Relat Res. 2010;468(10):2704–2709. doi:10.1007/s11999-010-1259-y
4.   Clouthier AL, Hetzler MA, Fedorak G, Bryant JT, Deluzio KJ, Bicknell RT. Factors affecting the stability of reverse shoulder arthroplasty: A biomechanical study. J Shoulder Elb Surg. 2013;22(4):439–444. doi:10.1016/j.jse.2012.05.032
5.   Day JS, MacDonald DW, Olsen M, Getz C, Williams GR, Kurtz SM. Polyethylene wear in retrieved reverse total shoulder components. J Shoulder Elb Surg. 2012;21(5):667–674. doi:10.1016/j.jse.2011.03.012

6. Digas G, Kärrholm J, Thanner J, Herberts P. 5-Year experience of highly cross-linked polyethylene in cemented and uncemented sockets: Two randomized studies using radiostereometric analysis. Acta Orthop. 2007;78(6):746–754. doi:10.1080/17453670710014518

7. Gill HS, Waite JC, Short A, Kellett CF, Price AJ, Murray DW. In vivo measurement of volumetric wear of a total knee replacement. Knee. 2006;13(4):312–317. doi:10.1016/j.knee.2006.04.001

8. Glyn-Jones S, McLardy-Smith P, Gill HS, Murray DW. The creep and wear of highly cross-linked polyethylene: A three-year randomised, controlled trial using radiostereometric analysis. J Bone Jt Surg Br. 2008;90(B):556–561. doi:10.1302/0301-620X.90B5.20545

9. Gutiérrez S, Comiskey IV CA, Luo Z-P, Pupello DR, Frankle MA. Range of impingement-free abduction and adduction deficit after reverse shoulder arthroplasty: Hierarchy of surgical and implant-design-related factors. J Bone Joint Surg Am. 2008;90–A(12):2606–2615. doi:10.2106/JBJS.H.00012

10. Van Hamersveld KT, Marang-Van De Mheen PJ, Van Der Heide HJL, Van Der Linden-Van Der Zwaag HMJ, Valstar ER, Nelissen RGHH. Migration and clinical outcome of mobile-bearing versus fixed-bearing single-radius total knee arthroplasty: A randomized controlled trial. Acta Orthop. 2018;89(2):190–196. doi:10.1080/17453674.2018.1429108

11. Hui AJ, McCalden RW, Martell JM, MacDonald SJ, Bourne RB, Rorabeck CH. Validation of two and three-dimensional radiographic techniques for measuring polyethylene wear after total hip arthroplasty. J Bone Jt Surg Am. 2003;85–A(3):505–511.

12. Van Ijsseldijk EA, Lebel B, Stoel BC, Valstar ER, Gouzy S, Vielpeau C, et al. Validation of the in vivo volumetric wear measurement for total knee prostheses in model-based RSA. J Biomech. 2013;46(7):1387–1391. doi:10.1016/j.jbiomech.2013.02.021

13. Van Ijsseldijk EA, Valstar ER, Stoel BC, Nelissen RGHH, Reiber JHC, Kaptein BL. The robustness and accuracy of in vivo linear wear measurements for knee prostheses based on model-based RSA. J Biomech. 2011;44(15):2724–2727. doi:10.1016/j.jbiomech.2011.08.013

14. Jain NB, Yamaguchi K. The contribution of reverse shoulder arthroplasty to utilization of primary shoulder arthroplasty. J Shoulder Elb Surg. 2014;23(12):1905–1912. doi:10.1016/j.jse.2014.06.055

15. Van de Kleut ML, Yuan X, Athwal GS, Teeter MG. Validation of radiostereometric analysis in six degrees of freedom for use with reverse total shoulder arthroplasty. J Biomech. 2018;68:126–131. doi:10.1016/j.jbiomech.2017.12.027

16. Van de Kleut ML, Yuan X, Athwal GS, Teeter MG. Validation of in vivo linear and volumetric wear measurement for reverse total shoulder arthroplasty using model-based radiostereometric analysis. J Orthop Res. 2019;37(7):1620–1627. doi:10.1002/jor.24294

17. Kohut G, Dallmann F, Irlenbusch U. Wear-induced loss of mass in reversed total shoulder arthroplasty with conventional and inverted bearing materials. J Biomech. 2012;45(3):469–473. doi:10.1016/j.jbiomech.2011.11.055

18. Kurdziel MD, Newton MD, Hartner S, Baker KC, Wiater JM. Quantitative evaluation of retrieved reverse total shoulder arthroplasty liner surface deviation and volumetric wear. J Orthop Res. 2018;36(7):2007–2014. doi:10.1002/jor.23849

19. Kwon YW, Forman RE, Walker PS, Zuckerman JD. Analysis of reverse total shoulder joint forces and glenoid fixation. Bull NYU Hosp Jt Dis. 2010;68(4):273–280. doi:PMID: 21162705

20. Langlois J, Hamadouche M. Current recommendations for assessing the reliability of a measurement tool: a survival guide for orthopaedic surgeons. Bone Joint J. 2016;98–B(2):166–172. doi:10.1302/0301-620X.98B2.34728

21. Langohr GDG, Athwal GS, Johnson JA, Medley JB. Wear simulation strategies for reverse shoulder arthroplasty implants. Proc Inst Mech Eng Part H J Eng Med. 2016;230(5):458–469. doi:10.1177/0954411916642801

22. Langohr GDG, Haverstock JP, Johnson JA, Athwal GS. Comparing daily shoulder motion and frequency after anatomic and reverse shoulder arthroplasty. J Shoulder Elb Surg. 2018;27(2):325–332. doi:10.1016/j.jse.2017.09.023

23. Lewicki KA, Bell JE, Van Citters DW. Analysis of polyethylene wear of reverse shoulder components: A validated technique and initial clinical results. J Orthop Res. 2017;35(5):980–987. doi:10.1002/jor.23353

24. Manning DW, Chiang PP, Martell JM, Galante JO, Harris WH. In vivo comparative wear study of traditional and highly cross-linked polyethylene in total hip arthroplasty. J Arthroplasty. 2005;20(7):880–886. doi:10.1016/j.arth.2005.03.033

25. Nam D, Kepler CK, Nho SJ, Craig EV, Warren RF, Wright TM. Observations on retrieved humeral polyethylene components from reverse total shoulder arthroplasty. J Shoulder Elb Surg. 2010;19(7):1003–1012. doi:10.1016/j.jse.2010.05.014

26. Ohlin A, Selvik G. Socket wear assessment: A comparison of three different radiographic methods. J Arthroplasty. 1993;8(4):427–431. doi:10.1016/S0883-5403(06)80043-4

27. Padegimas EM, Maltenfort M, Lazarus MD, Ramsey ML, Williams GR, Namdari S. Future patient demand for shoulder arthroplasty by younger patients: national projections. Clin Orthop Relat Res. 2015;473(6):1860–1867. doi:10.1007/s11999-015-4231-z

28. Peers S, Moravek JE, Budge MD, Newton MD, Kurdziel MD, Baker KC, et al. Wear rates of highly cross-linked polyethylene humeral liners subjected to alternating cycles of glenohumeral flexion and abduction. J Shoulder Elb Surg. 2015;24(1):143–149. doi:10.1016/j.jse.2014.05.001

29. Pineau V, Lebel B, Gouzy S, Dutheil JJ, Vielpeau C. Dual mobility hip arthroplasty wear measurement: Experimental accuracy assessment using radiostereometric analysis (RSA). Orthop Traumatol Surg Res. 2010;96(6):609–615. doi:10.1016/j.otsr.2010.04.007

30. Roy J-S, Macdermid JC, Goel D, Faber KJ, Athwal GS, Drosdowech DS. What is a successful outcome following reverse total shoulder arthroplasty? Open Orthop J. 2010;4:157–163. doi:10.2174/1874325001004010157

31. Schmalzried TP, Jasty M, Rosenberg A, Harris WH. Polyethylene wear debris and tissue reactions in knee as compared to hip replacement prostheses. J Appl

Biomater. 1994;5(3):185–190. doi:10.1002/jab.770050302

32. Short A, Gill HS, Marks B, Waite JC, Kellett CF, Price AJ, et al. A novel method for in vivo knee prosthesis wear measurement. J Biomech. 2005;38(2):315–322. doi:10.1016/j.jbiomech.2004.02.023

33. Smith SL, Li BL, Buniya A, Ho Lin S, Scholes SC, Johnson G, et al. In vitro wear testing of a contemporary design of reverse shoulder prosthesis. J Biomech. 2015;48(12):3072–3079. doi:10.1016/j.jbiomech.2015.07.022

34. Stilling M, Kold S, de Raedt S, Andersen NT, Rahbek O, Soballe K. Superior accuracy of model-based radiostereometric analysis for measurement of polyethylene wear: A phantom study. Bone Joint Res. 2012;1(8):180–191. doi:10.1302/2046-3758.18.2000041

35. Teeter MG, Dawson MT, Athwal GS. Inter and intra-system size variability of reverse shoulder arthroplasty polyethylene inserts. Int J Shoulder Surg. 2016;10(1):10–14. doi:10.4103/0973-6042.174512

36. Teeter MG, Naudie DDR, Bourne RB, Holdsworth DW. How do CAD models compare with reverse engineered manufactured components for use in wear analysis? Clin Orthop Relat Res. 2012;470(7):1847–1854. doi:10.1007/s11999-011-2143-0

37. Teeter MG, Naudie DDR, McErlain DD, Brandt JM, Yuan X, MacDonald SJ, et al. In vitro quantification of wear in tibial inserts using microcomputed tomography. Clin Orthop Relat Res. 2011;469(1):107–112. doi:10.1007/s11999-010-1490-6

38. Teeter MG, Seslija P, Milner JS, Nikolov HN, Yuan X, Naudie DDR, et al. Quantification of in vivo implant wear in total knee replacement from dynamic single plane radiography. Phys Med Biol. 2013;58(9):2751–2767. doi:10.1088/0031-9155/58/9/2751

39. Thomas GE, Simpson DJ, Mehmood S, Taylor A, McLardy-Smith P, Singh Gill H, et al. The seven-year wear of highly cross-linked polyethylene in total hip arthroplasty. J Bone Joint Surg Am. 2011;93(8):716–722. doi:10.2106/JBJS.J.00287

40. Vaupel ZM, Baker KC, Kurdziel MD, Wiater JM. Wear simulation of reverse total shoulder arthroplasty systems: Effect of glenosphere design. J Shoulder Elb Surg. 2012;21(10):1422–1429. doi:10.1016/j.jse.2011.10.024

41. Wan Z, Boutary M, Dorr LD. Precision and limitation of measuring two-dimensional wear on clinical radiographs. Clin Orthop Relat Res. 2006;449:267–274. doi:10.1097/01.blo.0000218758.35181.93

42. Willert HG, Bertram H, Buchhorn GH. Osteolysis in alloarthroplasty of the hip. The role of ultra-high molecular weight polyethylene wear particles. Clin Orthop Relat Res. 1990 Sep;258:95—107.

43. Stratasys Vero^{TM} Family, VeroBlackPlus (Stratasys Ltd, Eden Prairie, MN, USA). Published 2018. Accessed February 14, 2019 (https://www.forecast3d.com/qp-content/uploads/2018/06/PolyJet-Vero.pdf).

7 In vivo volumetric and linear wear measurement of reverse shoulder arthroplasty at minimum five-year follow-up

A version of this chapter has been published.[14]

7.1 Introduction

Reverse total shoulder arthroplasty (RTSA) is an established surgical solution for patients suffering from a number of shoulder pathologies. Historically used as a salvage procedure for massive irreparable rotator cuff disease, indications have expanded to include revision arthroplasty, acute fracture care and their sequelae, glenohumeral instability, severe glenoid bone wear, and rheumatoid arthritis.[2,26,37,39] In response to a growing number of indications, the increased demand for active lifestyles by an older population, and good short-to-midterm clinical outcomes, the use of RTSA has grown exponentially in the past decade and is predicted to become the most frequently performed glenohumeral replacement procedure.[5,28,30]

Excessive polyethylene (PE) wear that creates particulate debris and can induce osteolysis has been identified as a cause of aseptic implant loosening in the hip and knee literature.[29,38] Modern artificial hips and knees typically use highly cross-linked PE, with superior wear properties compared to its ultra-high molecular weight counterpart, to mitigate the risk of osteolysis and implant loosening .[1,11,13,35] Despite the proven efficacy of highly cross-linked PE, however, ultra-high molecular weight PE remains the current standard for RTSA.

Simulation and retrieval studies have shown that abrasive wear of the RTSA PE is common,[3,16,19,24,25,32,34,36] with the reverse shoulder experiencing loads up to 0.7 body weight during abduction and a duty cycle of approximately 0.75 million cycles (MC) per year.[9,18,20] At present, to the best of our knowledge, no studies have investigated in vivo wear rates of the RTSA PE bearing surface, and as these joint replacements age it is important to understand their mid-to-long-term behaviour.

Model-based radiostereometric analysis is a calibrated dual-plane x-ray technique used to identify the three-dimensional (3D) position and orientation of implants in space. Given the relative position and orientation of total joint components, penetration into the PE liner can be measured. This technique has previously been used to quantify three-dimensional PE wear in the knee and hip with submillimeter accuracy, providing a more complete assessment of PE wear than two-dimensional clinical x-rays.[6,7,10,27] The purpose of this study was to measure the in vivo volumetric and linear wear rates of the reverse total shoulder arthroplasty polyethylene using model-based radiostereometric analysis. It was hypothesized that wear would be measurable and correlated with term-of-service.

7.2 Materials and Methods

7.2.1 Patient Recruitment

This is a prospective case series. Following institutional review board approval, a medical chart review was completed to identify potential participants. Inclusion criteria were patients with the Aequalis™ Reversed II (Wright Medical-Tornier Group, Memphis, TN, USA) shoulder system, a term-of-service greater than five years, and patients willing to travel to the Radiostereometric Laboratory for a specific series of radiographs. All procedures were performed by either GSA or KF, board-certified orthopaedic surgeons between January 2008 and January 2013. Patients were excluded if they lived greater than 200 km from the study center, were deceased, pregnant, unable to read/write English, or were unable to provide informed consent due to cognitive decline. Initially, 95 patients were identified that fit the inclusion criteria. Fifty-nine were excluded prior to recruitment due to distance from the study center or because they were deceased. Thirteen refused to participate (9 = poor health, 4 = distance), eight were unable to be reached, leaving 15 providing written, informed consent.

7.2.2 Clinical and Radiographic Outcomes

In addition to radiostereometric imaging, patients were asked to complete the American Shoulder and Elbow Surgeons' score (ASES), rate their subjective shoulder value (SSV), and pain from 0-10. Active forward flexion, lateral abduction, and external rotation in adduction were measured using a handheld long-arm goniometer. Internal rotation was recorded as the highest point along the spine with the thumb pointing upward. Scapular notching was assessed by GSA on the most recent anterior-posterior radiographs based on the grading by Sirveaux et al.[31]

7.2.3 Imaging

Study imaging was completed from November 2018 through July 2019. Radiostereometric analysis exams were taken with the patient sitting in front of a uniplanar calibration cage (Cage 43, RSA Biomedical, Umeå, Sweden). In order to assess multi-vector polyethylene wear patterns, exposures were taken at the limits of patients' active range of motion: in external rotation with the arm at the side, internal rotation with the thumb extended upwards along the spine, lateral abduction, forward flexion, and in a neutral position with the arm at the side (adduction).

To reduce the effect of potential joint distraction, patients were asked to hold a 2.3 kg weight during the neutral examination. The weight was not used during the other four examinations so as not to limit patients' range of motion. Radiograph energies were optimized for contrast while maintaining the "as low as reasonably achievable" principle in each patient, ranging from 8.0-16.0 mAs with 90 kVp.

Radiostereometric images were analyzed using commercial model-based radiostereometric analysis software (RSACore, Leiden, The Netherlands). Computer-aided design (CAD) models of the glenosphere and stem were provided by the manufacturer (Wright Medical-Tornier Group, Memphis, TN, USA) and converted to 3D virtual surface models. Each surface model was aligned to its respective implant contour in the model-based radiostereometric analysis environment, and its global transformation matrix recorded (Figure 7.1).
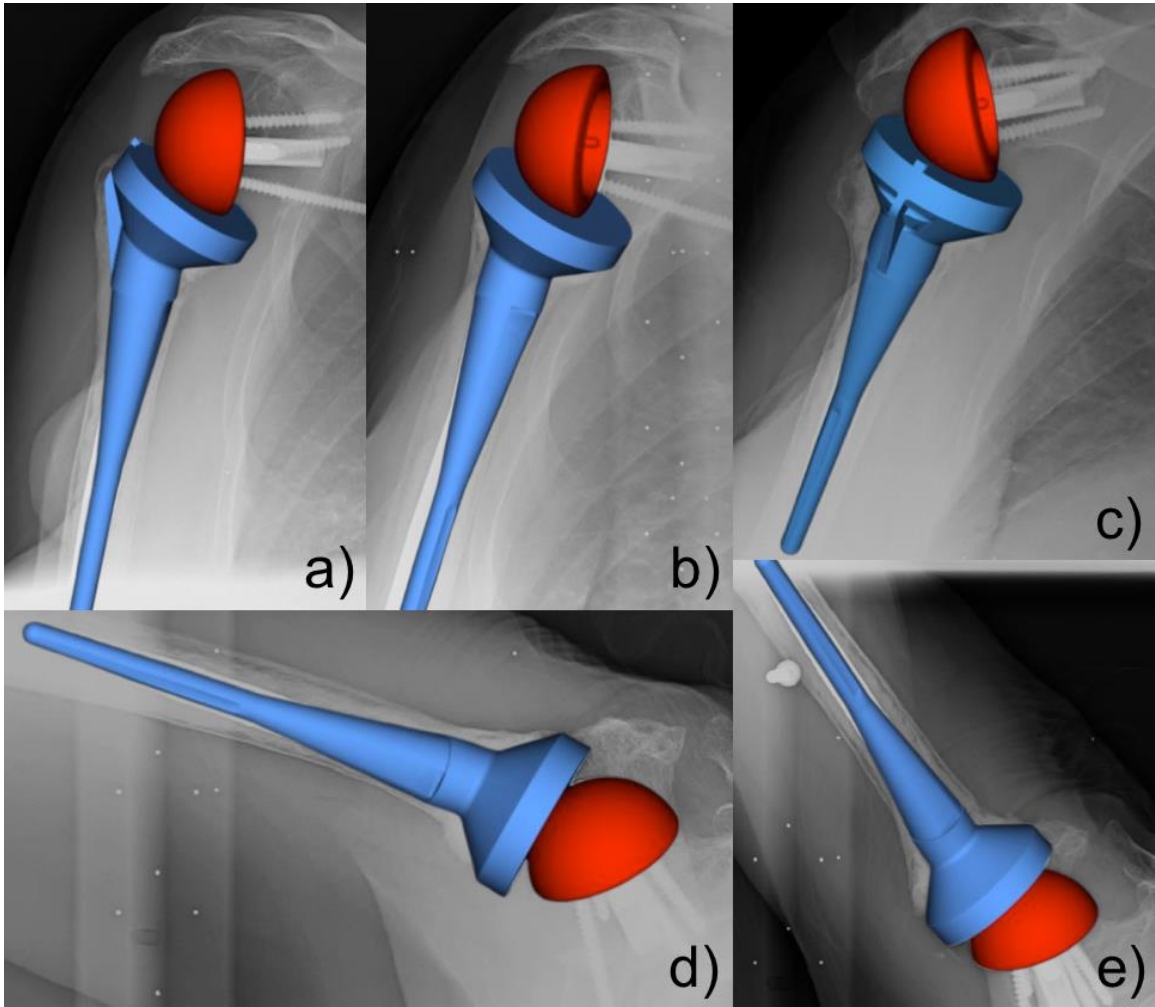
Figure 7.1 Alignment of the glenosphere (red) and stem (blue) in (a) neutral, (b) external rotation, (c) internal rotation, (d) lateral abduction, and (e) forward flexion arm positions using model-based radiostereometric analysis.

7.2.4 Wear Analysis

Our wear measurement methodology has previously been validated in vitro and was used for this in vivo assessment.[15] The CAD model of the appropriately sized polyethylene liner was virtually inserted into the CAD model of the stem using Geomagic Studio (3D Systems Inc., Morrisville, NC, USA). A notch on the polyethylene corresponding to a protrusion on the stem model ensured the virtually inserted polyethylene was in the correct orientation.

A separate, previously validated software, built in-house, applied the transformations recorded from the model-based radiostereometric analysis software to the glenosphere and polyethylene models at each arm position.[33] The polyethylene model was then discretized into isometric voxels of length 0.075 mm, with apparent intersection of the glenosphere into the polyethylene recorded as wear. Each voxel intersection was added to the cumulative wear measurement, though intersections of the same voxel from different arm positions were only recorded once to eliminate over-estimation. Maximum linear wear depth was also measured as the largest surface normal from polyethylene surface to intersected voxel. A wear map example is illustrated in Figure 7.2.
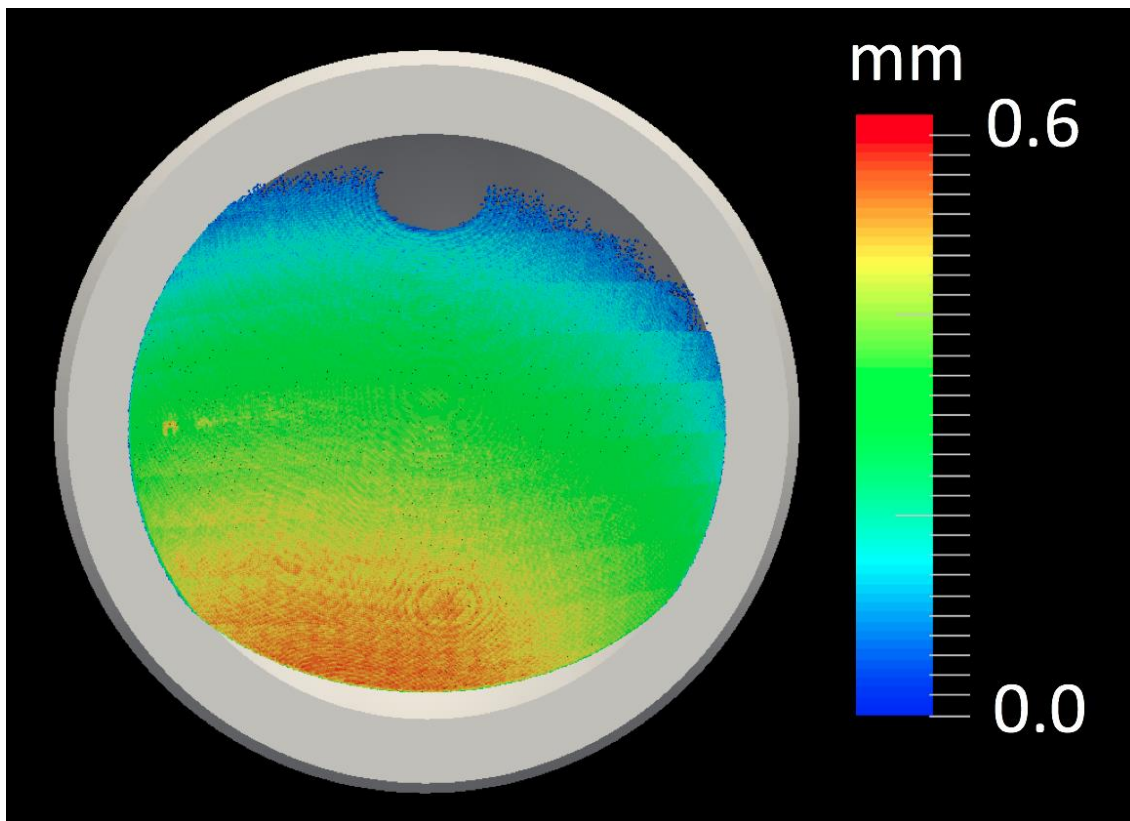

Figure 7.2 Wear map from the neutral arm position (Subject 07). Linear wear depth is visualized by the colour bar, measured in millimetres (mm). The unworn semi-circle in the superior quadrant of the liner is the location of the glenosphere screw hole at the time of imaging.

7.2.5 Statistical Analysis

Polyethylene liners with different diameters were assessed independently. Statistical analysis was not applied to the two 42 mm liners because of the small sample size (n = 2). Volumetric and linear wear rates were recorded as mean ± standard deviation. The Pearson correlation coefficient was determined for volumetric and linear wear of the 36 mm liners to assess respective relationships with term-of-service.

To spatially quantify volumetric and linear wear rates, each polyethylene model was symmetrically divided into its superior, inferior, anterior, and posterior quadrants. The d'Agostino Pearson test was used to assess normality. A one-way analysis of variance (ANOVA) with Tukey post-hoc test for normally distributed data, and the Kruskal-Wallis test with Dunn's test for multiple comparisons for non-normally distributed data, was applied to volumetric and linear wear data independently to determine any difference in wear rate between quadrants.

A one-way ANOVA with Tukey post-hoc test was applied to determine any differences in the proportion of observed wear from each independent arm position to the total wear, and separately, the Kruskal-Wallis test with Dunn's test for multiple comparisons to determine if certain arm positions contribute to wear in specific quadrants. Statistical significance was set at $P < 0.05$.

7.3 Results

The mean term-of-service at the time of study imaging was 8 ± 1 years (range 6-11 years). Patient demographics are reported in Table 6.1. Mean American Shoulder and Elbow Surgeons' score was 77 ± 21, pain was 1.5 ± 2.3, and Subjective Shoulder Value was 74 ± 19. Active forward flexion was 110 ± 18°, lateral abduction 95 ± 20°, external rotation 31 ± 18°, and internal rotation to the posterior waist. Five patients had evidence of grade 1 or 2 scapular notching.

Implant survival analysis from the 95 potential participants indicates a 96.6% survival at 10 years postoperatively (Figure 7.3). Three components were revised for instability, with stability achieved by exchanging polyethylene liners and glenospheres for a larger size. Revisions occurred within 18 months postoperatively.

Table 7.1 Patient demographic characteristics

Subject	Age at surgery	Sex	Indication[a]	Term-of-service at time of imaging (years)	Poly diameter (mm, +offset)	BIO-RSA[b] (1 = yes, 0 = no)	Scapular notching (grade 0-4)	Volumetric wear rate (mm³/year)	Maximum linear wear rate (mm/year)
01	72	F	CTA	6.2	36 +6	1	0	32.1	0.10
02	74	F	CTA	6.7	36 +6	1	1	40.6	0.08
03	75	F	OA + RCT	6.8	36 +6	1	0	39.3	0.09
04	78	F	CTA	6.8	36 +6	1	0	23.8	0.11
05	62	F	PT OA	9.5	36 +6	0	1	54.3	0.13
06	66	F	RA	9.2	36 +6	0	2	31.4	0.10
07	68	F	PT OA	7.4	36 +6	1	1	40.7	0.10
08	75	F	CTA	7.7	36 +9	0	0	20.6	0.11
09	71	F	PT OA	10.5	36 +9	0	0	94.4	0.16
10	59	M	CTA	6.9	36 +9	1	0	58.5	0.12
11	60	M	CTA	6.5	36 +9	1	2	66.6	0.17
12	69	M	CTA	7.1	36 +9	1	0	7.4	0.10
13	69	M	CTA	9.0	36 +9	1	0	41.8	0.09
14	87	M	CTA	6.5	42 +6	1	0	144.6	0.18
15	72	M	CTA	6.9	42 +9	1	0	83.0	0.16

[a]CTA: cuff tear arthropathy; OA: osteoarthritis; RCT: rotator cuff tear; PT: post-traumatic; RA: rheumatoid arthritis
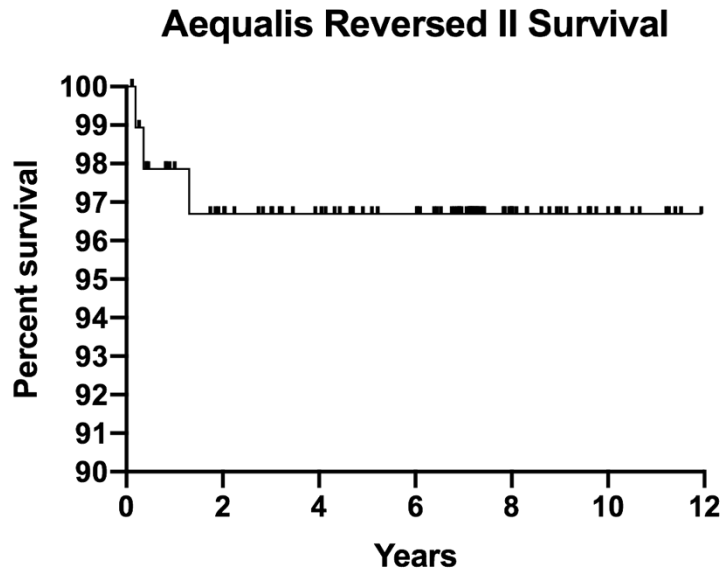[b]BIO-RSA: Bony Increased Offset Reverse Shoulder Arthroplasty

Figure 7.3 Survivorship of the Aequalis™ Reversed II implant system.

For the 36 mm polyethylene liners, mean volumetric and linear wear rates were 42 ± 22 mm^3/year (r = 0.688, $P = 0.009$), and 0.11 ± 0.03 mm/year (r = 0.767, $P = 0.002$), respectively (Figure 7.4). There were no significant differences in wear rates between quadrants for these liners (Table 7.2).
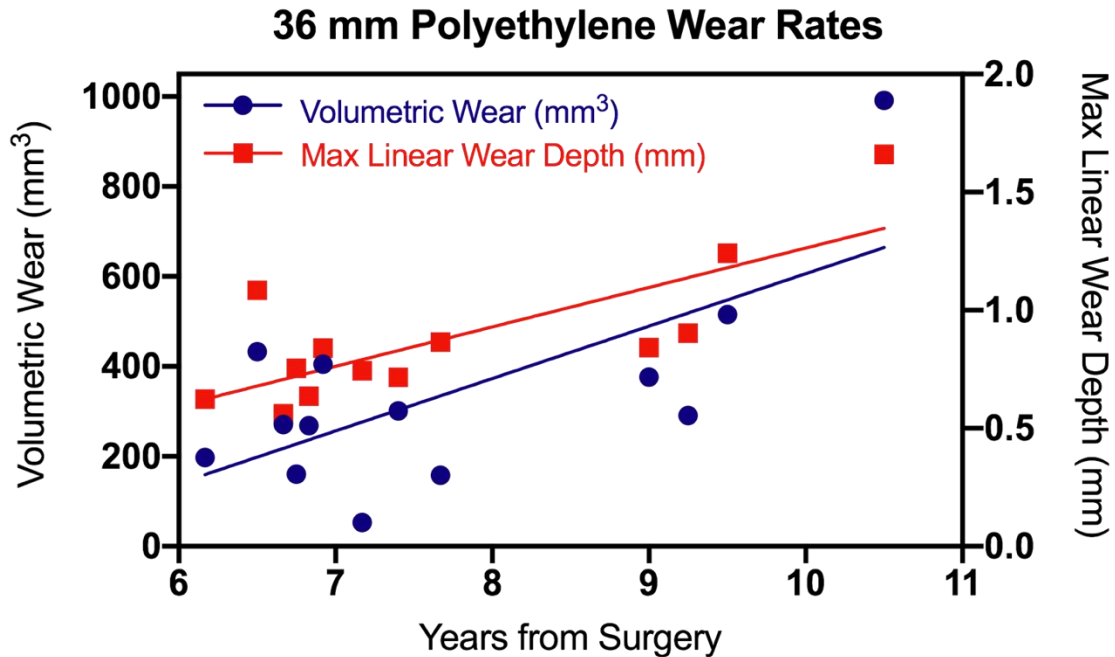
Figure 7.4 Volumetric (blue circles) and linear (red squares) wear measurements for each 36 mm polyethylene.

Table 7.2 Quadrant analysis of 36 mm diameter polyethylene liners

Mean ± SD (n = 13)	Superior	Inferior	Anterior	Posterior	*P*-value
% of total wear volume	22 ± 13	27 ± 22	28 ± 17	23 ± 15	0.743
Volumetric wear rate (mm³/year)	10 ± 8	11 ± 8	13 ± 9	10 ± 5	0.866
Linear wear rate (mm/year)	0.09 ± 0.04	0.10 ± 0.03	0.10 ± 0.04	0.09 ± 0.03	0.947

For the two subjects with 42 mm liners, the mean volumetric wear rate was 114 ± 44 mm³/year, and mean linear wear rate was 0.17 ± 0.01 mm/year. Average wear rates for each quadrant are recorded in Table 7.3, but again, no statistical analysis was applied.

Table 7.3 Quadrant analysis of 42 mm diameter polyethylene liners

Mean ± SD (n = 2)	Superior	Inferior	Anterior	Posterior
% of total wear volume	15 ± 11	33 ± 14	30 ± 1	22 ± 4
Volumetric wear rate (mm³/year)	19 ± 18	35 ± 1	34 ± 12	26 ± 15
Linear wear rate (mm/year)	0.12 ± 0.06	0.17 ± 0.01	0.16 ± 0.02	0.13 ± 0.05

There were no significant differences in terms of the observed wear from each arm position (Figure 7.5) as a percent of the total wear volume (Table 7.4). Similarly, there were no significant differences when comparing different arm positions and their contributions to wear in different quadrants (neutral, $P = 0.294$; external rotation, $P = 0.616$; internal rotation, $P = 0.839$; lateral abduction, $P = 0.783$; forward flexion, $P = 0.809$).
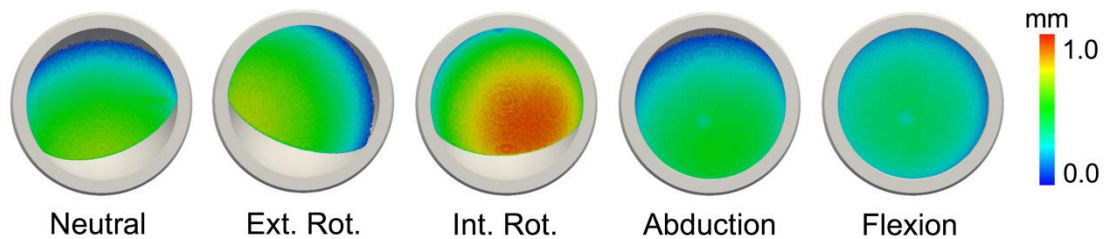
Figure 7.5 Example wear maps from each arm position. Warmer colours are representative of greater penetration of the glenosphere into the polyethylene.

Table 7.4 Observed wear volume as a percent of total wear volume from each arm position

% Observed volume of total volume (mean ± SD)	Neutral	External rotation	Internal rotation	Lateral abduction	Forward flexion	P-value
36 mm (n = 13)	51 ± 33	55 ± 25	32 ± 22	40 ± 26	40 ± 31	0.242
42 mm (n = 2)	39 ± 1	45 ± 3	45 ± 50	57 ± 27	57 ± 18	N/A

7.4   Discussion

The purpose of this study was to investigate the in vivo wear rates of ultra-high molecular weight polyethylene in the reverse shoulder. Though a number of in vitro and in silico studies have simulated RSA wear patterns, there is a lack of biomechanically established test protocols and apparatus that mimic in vivo loading and muscles tensioning. Consequently, the results from these simulations are variable, with wear rates ranging from 14.3mm^3/MC to 126 mm^3/MC.[3,16,19,25,32,34,36] Using a mathematical model, Terrier et al[34] conducted a simulation study on the Aequalis™ Reversed II and estimated a volumetric wear of 44.6 mm^3 and linear wear of 0.13 mm after one year of simulated activity for the 36 mm polyethylene. The in vivo mean volumetric (42 ± 22 mm^3/year) and linear (0.11 ± 0.03 mm/year) wear rates of the 36 mm polyethylene presented in our study are similar to wear rates reported in simulation studies and show a strong correlation between both volumetric and linear wear, and term-of-service.

The osteolytic threshold for linear wear in the hip is set at approximately 0.1 mm/year,[8] reinforcing the notion that with an average wear rate of 0.11 mm/year for 36 mm polyethylenes, and 0.17 mm/year for the 42 mm liners, RSA wear is clinically significant. No patient in our study, however, illustrated humeral stem or glenosphere loosening, suggesting that the observed wear rates are clinically acceptable in the short term.

Results from the 42 mm polyethylene liners must be interpreted cautiously since only two patients were assessed, though both patients had wear rates of approximately double the 36 mm averages. It has been established in the hip literature that though larger femoral head size increases volumetric wear, it decreases linear wear by reducing the contact stress transmitted through the femoral head.[23] This observation was recently supported by an in vitro study comparing wear rates of 32 and 40 mm glenospheres in RSA.[12] Our results challenge these findings, as both volumetric and linear wear rates were higher with the 42 mm glenosphere/polyethylene combination, and further investigation with a

greater number of subjects is merited. Neither 42 mm patient had evidence of component loosening or scapular notching.

The volumetric and linear wear rates from the 36 mm polyethylene liners with evidence of notching (n = 5), to those without notching (n = 8), were similar with a wear rate of 47 mm^3/year and 0.12 mm/year, and 40 mm^3/year and 0.11 mm/year, respectively. As there were no incidences of grade 3/4 notching, we cannot make any conclusions about polyethylene wear and its effect on biological response in high notching cases.

It is interesting to note that there was no significant difference in volumetric or linear wear rate between quadrants. The Aequalis™ Reversed II has a 155° neck-shaft angle, measured as the angle between the long axis of the humeral stem and the perpendicular to the metaphyseal tray inclination line. More modern reverse shoulder designs, with neck-shaft angles of 145° or 135°, aim to minimize abutment of the polyethylene with the lateral pillar of the scapula. Compared to reverse shoulders with a lower neck-shaft angle, a 155° neck-shaft angle places the contact of the glenosphere within the polyethylene equally between quadrants rather than more inferiorly at low abduction angles when the same glenosphere positioning is employed.[21] Further studies ought to compare the effects of neck-shaft angle on wear, as this variable may change the observed wear patterns.

The wear recorded from different arm positions was distributed among quadrants for individual arm positions, and no single arm position was capable of capturing all recorded wear. This is important because it emphasises that RSA wear is multidirectional, and multiple wear vectors are associated with different activities of daily living. Fluoroscopic imaging of a patient's full range of motion may provide a more complete representation of such wear vectors.

There are a number of limitations to this study. We do not have postoperative baseline measurements of these patients, which would allow for the calculation of bias. Our method also does not distinguish between creep and wear of the polyethylene liner. In future studies, prospective imaging following surgery would allow for a measure of bias,

and imaging between six months and one year would likely provide a measure of creep. Further, although we used muscle contraction to minimize joint distraction, we had no way to ensure that the articulating components were contacting each other for all arm positions, and this may have underestimated the recorded wear rates.

The imaging technique is not capable of identifying extra-articular wear, and for this reason is incapable of quantifying polyethylene damage due to scapular notching. Retrieval analysis has highlighted that damage to the inferior rim is common,[4,17,22,24] and though only 33% of our cases had evidence of low-grade notching, it is still likely that being unable to record this may have underestimated the total polyethylene volume loss.

The proposed measurement method relies on the use of either CAD or reverse engineered models of the implants and liners under investigation. Implant manufacturers may be hesitant to provide such models, limiting the widespread use of this technique. Lastly, we did not correlate wear rate with clinical function and pain because of our small sample size. We encourage future studies with larger numbers to assess any relationships between these parameters.

Despite these limitations, we have presented the first study investigating the in vivo wear rates of the reverse shoulder. Based on our preliminary results, we have shown that in vivo RSA wear is appreciable, and that further studies of different RSA designs, different polyethylene preparations, increased patient numbers, and longer terms-of-service (10 to 15 years) are required.

7.5   Conclusion

The results from this in vivo study show a volumetric wear rate of approximately 40 mm^3/year and linear wear rate of approximately 0.1 mm/year for 36 mm polyethylene liners. Results from the 42 mm liners show higher volumetric and linear wear rates, although a greater number of subjects is required for conclusive results. In vivo wear of reverse total shoulder arthroplasty is multidirectional and perceptible.

7.6 References

1. Bragdon CR, Greene ME, Freiberg AA, Harris WH, Malchau H. Radiostereometric analysis comparison of wear of highly cross-linked polyethylene against 36- vs 28-mm femoral heads. J Arthroplasty. 2007;22(6 SUPPL. 2):125–129. doi:10.1016/j.arth.2007.03.009

2. Brorson S, Rasmussen JV, Olsen BS, Frich LH, Jensen SL, Hróbjartsson A. Reverse shoulder arthroplasty in acute fractures of the proximal humerus: A systematic review. Int J Shoulder Surg. 2013;7(2):70–78. doi:10.4103/0973-6042.114225

3. Carpenter S, Pinkas D, Newton MD, Kurdziel MD, Baker KC, Wiater JM. Wear rates of retentive versus nonretentive reverse total shoulder arthroplasty liners in an in vitro wear simulation. J Shoulder Elb Surg. 2015;24(9):1372–1379. doi:10.1016/j.jse.2015.02.016

4. Day JS, MacDonald DW, Olsen M, Getz C, Williams GR, Kurtz SM. Polyethylene wear in retrieved reverse total shoulder components. J Shoulder Elb Surg. 2012;21(5):667–674. doi:10.1016/j.jse.2011.03.012

5. Day JS, Paxton ES, Lau E, Gordon VA, Abboud JA, Williams GR. Use of reverse total shoulder arthroplasty in the Medicare population. J Shoulder Elb Surg. 2015;24(5):766–772. doi:10.1016/j.jse.2014.12.023

6. Digas G, Kärrholm J, Thanner J, Herberts P. 5-Year experience of highly cross-linked polyethylene in cemented and uncemented sockets: Two randomized studies using radiostereometric analysis. Acta Orthop. 2007;78(6):746–754. doi:10.1080/17453670710014518

7. Digas G, Kärrholm J, Thanner J, Malchau H, Herberts P. Highly cross-linked polyethylene in cemented THA: Randomized study of 61 hips. Clin Orthop Relat Res. 2003;(417):126–138. doi:10.1097/01.blo.0000096802.78689.45

8. Dumbleton JH, Manley MT, Edidin AA. A literature review of the association between wear rate and osteolysis in total hip arthroplasty. J Arthroplasty. 2002;17(5):649–661. doi:10.1054/arth.2002.33664

9. Giles JW, Langohr GDG, Johnson JA, Athwal GS. Implant design variations in reverse total shoulder arthroplasty influence the required deltoid force and resultant joint load. Clin Orthop Relat Res. 2015;473(11):3615–3626. doi:10.1007/s11999-015-4526-0

10. Gill HS, Waite JC, Short A, Kellett CF, Price AJ, Murray DW. In vivo measurement of volumetric wear of a total knee replacement. Knee. 2006;13(4):312–317. doi:10.1016/j.knee.2006.04.001

11. Glyn-Jones S, Isaac S, Hauptfleisch J, McLardy-Smith P, Murray DW, Gill HS. Does highly cross-linked polyethylene wear less than conventional polyethylene in total hip arthroplasty? A double-blind, randomized, and controlled trial using Roentgen stereophotogrammetric analysis. J Arthroplasty. 2008;23(3):337–343. doi:10.1016/j.arth.2006.12.117

12. Haggart J, Newton MD, Hartner S, Ho A, Baker KC, Kurdziel MD, et al. Neer Award 2017: wear rates of 32-mm and 40-mm glenospheres in a reverse total

shoulder arthroplasty wear simulation model. J Shoulder Elb Surg. 2017;26(11):2029–2037. doi:10.1016/j.jse.2017.06.036

13. Jenny JY, Saragaglia D. No detectable polyethylene wear 15 years after implantation of a mobile–bearing total knee arthroplasty with electron beam– irradiated polyethylene. J Arthroplasty. 2019;34(8):1690–1694. doi:10.1016/j.arth.2019.03.054

14. Van de Kleut ML, Athwal GS, Faber KJ, Teeter MG. In vivo volumetric and linear wear measurement of reverse shoulder arthroplasty at minimum 5-year follow-up. J Shoulder Elb Surg. 2020;29(8):1695-1702. doi:10.1016/j.jse.2019.11.031

15. Van de Kleut ML, Yuan X, Athwal GS, Teeter MG. Validation of in vivo linear and volumetric wear measurement for reverse total shoulder arthroplasty using model-based radiostereometric analysis. J Orthop Res. 2019;37(7):1620–1627. doi:10.1002/jor.24294

16. Kohut G, Dallmann F, Irlenbusch U. Wear-induced loss of mass in reversed total shoulder arthroplasty with conventional and inverted bearing materials. J Biomech. 2012;45(3):469–473. doi:10.1016/j.jbiomech.2011.11.055

17. Kurdziel MD, Newton MD, Hartner S, Baker KC, Wiater JM. Quantitative evaluation of retrieved reverse total shoulder arthroplasty liner surface deviation and volumetric wear. J Orthop Res. 2018;36(7):2007–2014. doi:10.1002/jor.23849

18. Kwon YW, Forman RE, Walker PS, Zuckerman JD. Analysis of reverse total shoulder joint forces and glenoid fixation. Bull NYU Hosp Jt Dis. 2010;68(4):273–280. doi:PMID: 21162705

19. Langohr GDG, Athwal GS, Johnson JA, Medley JB. Wear simulation strategies for reverse shoulder arthroplasty implants. Proc Inst Mech Eng Part H J Eng Med. 2016;230(5):458–469. doi:10.1177/0954411916642801

20. Langohr GDG, Haverstock JP, Johnson JA, Athwal GS. Comparing daily shoulder motion and frequency after anatomic and reverse shoulder arthroplasty. J Shoulder Elb Surg. 2018;27(2):325–332. doi:10.1016/j.jse.2017.09.023

21. Langohr GDG, Willing R, Medley JB, Athwal GS, Johnson JA. Contact mechanics of reverse total shoulder arthroplasty during abduction: The effect of neck-shaft angle, humeral cup depth, and glenosphere diameter. J Shoulder Elb Surg. 2016;25(4):589–597. doi:10.1016/j.jse.2015.09.024

22. Lewicki KA, Bell J-E, Van Citters DW. Analysis of polyethylene wear of reverse shoulder components: A validated technique and initial clinical results. J Orthop Res. 2017;35(5):980–987. doi:10.1002/jor.23353

23. Livermore J, Ilstrup D, Morrey B. Effect of femoral head size on wear of the polyethylene acetabular component. J Bone Joint Surg. 1990;72–A(4):518–528.

24. Nam D, Kepler CK, Nho SJ, Craig EV, Warren RF, Wright TM. Observations on retrieved humeral polyethylene components from reverse total shoulder arthroplasty. J Shoulder Elb Surg. 2010;19(7):1003–1012. doi:10.1016/j.jse.2010.05.014

25. Peers S, Moravek JE, Budge MD, Newton MD, Kurdziel MD, Baker KC, et al. Wear rates of highly cross-linked polyethylene humeral liners subjected to alternating cycles of glenohumeral flexion and abduction. J Shoulder Elb Surg. 2015;24(1):143–149. doi:10.1016/j.jse.2014.05.001

26. Postacchini R, Carbone S, Canero G, Ripani M, Postacchini F. Reverse shoulder

prosthesis in patients with rheumatoid arthritis: a systematic review. Int Orthop. 2016;40(5):965–973. doi:10.1007/s00264-015-2916-2

27. Price A, Short A, Kellett C, Beard D, Gill H, Pandit H, et al. Ten-year in vivo wear measurement of a fully congruent mobile bearing unicompartmental knee arthroplasty. J Bone Joint Surg Br. 2005;87(11):1493–1497. doi:10.1302/0301-620X.87B11.16325

28. Schairer WW, Nwachukwu BU, Lyman S, Craig EV, Gulotta LV. National utilization of reverse total shoulder arthroplasty in the United States. J Shoulder Elb Surg. 2015;24(1):91–97. doi:10.1016/j.jse.2014.08.026

29. Schmalzried TP, Jasty M, Rosenberg A, Harris WH. Polyethylene wear debris and tissue reactions in knee as compared to hip replacement prostheses. J Appl Biomater. 1994;5(3):185–190. doi:10.1002/jab.770050302

30. Simovitch RW, Gerard BK, Brees JA, Fullick R, Kearse JC. Outcomes of reverse total shoulder arthroplasty in a senior athletic population. J Shoulder Elb Surg. 2015;24(9):1481–1485. doi:10.1016/j.jse.2015.03.011

31. Sirveaux F, Favard L, Oudet D, Huquet D, Walch G, Molé D. Grammont inverted total shoulder arthroplasty in the treatment of glenohumeral osteoarthritis with massive rupture of the cuff. Results of a multicentre study of 80 shoulders. J Bone Joint Surg Br. 2004;86–B(3):388–395. doi:10.1302/0301-620X.86B3.14024

32. Smith SL, Li BL, Buniya A, Ho Lin S, Scholes SC, Johnson G, et al. In vitro wear testing of a contemporary design of reverse shoulder prosthesis. J Biomech. 2015;48(12):3072–3079. doi:10.1016/j.jbiomech.2015.07.022

33. Teeter MG, Seslija P, Milner JS, Nikolov HN, Yuan X, Naudie DDR, et al. Quantification of in vivo implant wear in total knee replacement from dynamic single plane radiography. Phys Med Biol. 2013;58(9):2751–2767. doi:10.1088/0031-9155/58/9/2751

34. Terrier A, Merlini F, Pioletti DP, Farron A. Comparison of polyethylene wear in anatomical and reversed shoulder prostheses. J Bone Joint Surg Br. 2009;91–B(7):977–982. doi:10.1302/0301-620X.91B7.21999

35. Thomas GE, Simpson DJ, Mehmood S, Taylor A, McLardy-Smith P, Singh Gill H, et al. The seven-year wear of highly cross-linked polyethylene in total hip arthroplasty. J Bone Joint Surg Am. 2011;93(8):716–722. doi:10.2106/JBJS.J.00287

36. Vaupel ZM, Baker KC, Kurdziel MD, Wiater JM. Wear simulation of reverse total shoulder arthroplasty systems: Effect of glenosphere design. J Shoulder Elb Surg. 2012;21(10):1422–1429. doi:10.1016/j.jse.2011.10.024

37. Walker M, Willis MP, Brooks JP, Pupello D, Mulieri PJ, Frankle MA. The use of the reverse shoulder arthroplasty for treatment of failed total shoulder arthroplasty. J Shoulder Elb Surg. 2012;21(4):514–522. doi:10.1016/j.jse.2011.03.006

38. Wang A, Stark C, Dumbleton JH. Mechanistic and morphological origins of ultra-high molecular weight polyethylene wear debris in total joint replacement prostheses. Proc Inst Mech Eng Part H J Eng Med. 1996;210(3):141–155. doi:10.1243/PIME

39. Werner BS, Böhm D, Abdelkawi A, Gohlke F. Glenoid bone grafting in reverse shoulder arthroplasty for long-standing anterior shoulder dislocation. J Shoulder Elb Surg. 2014;23(11):1655–1661. doi:10.1016/j.jse.2014.02.017

8 Conclusions and future directions

8.1 Summary

As global populations age, the demand for joint replacement and the need for long-term survivorship of these artificial joints grows. Reverse total shoulder arthroplasty (RTSA) offers a solution for patients suffering from a number of shoulder pathologies, and while early-to-mid-term RTSA outcomes are promising, the current standard of care lacks long-term follow-up. Radiostereometric analysis (RSA) has proven valuable in orthopedics, enabling submillimeter measurements of implant migration, and measures of linear and volumetric wear not otherwise observable on 2D clinical radiographs.[11] At the time this thesis was completed, there were no prospective randomized clinical trials investigating different implant fixation methods, nor an in vivo assessment of polyethylene wear in RTSA. The purpose of this thesis, therefore, was to address these gaps in the orthopedic literature by providing an in vivo evaluation of the current RTSA state-of-art, utilizing RSA.

The work of this thesis began by completing a phantom study using a Sawbones reverse shoulder model to evaluate the bias and repeatability of RSA using the Aequalis™ Ascend™ Flex reverse shoulder system (Wright Medical-Tornier Group, Memphis, TN, USA) (Chapter 3). Phantom studies utilizing the proposed implants of investigation are recommended prior to clinical RSA examination in order to determine the random and systematic error of the imaging and analysis technique under ideal conditions. Relevant to our subsequent clinical trial, bias of the humeral stem relative to the tantalum bead fiducial cluster ranged from 0.05 ± 0.01 mm to 0.08 mm ± 0.02 mm along translation axes, and $0.11 \pm 0.03°$ to $0.79 \pm 0.25°$ along rotation axes. Repeatability ranged from 0.11 to 0.13 mm in translation, and 0.15 to $1.95°$ in rotation. Bias and repeatability were poorest along the out-of-plane translation axis and the internal-external rotation axis. Bias of the glenosphere relative to tantalum beads ranged from 0.02 ± 0.01 mm to 0.06 ± 0.02

mm in translation, and $0.21 \pm 0.10°$ to $0.24 \pm 0.12°$ in rotation, with repeatability ranging from 0.07 to 0.13 mm, and 0.07 to 0.14°. These results are comparable to the reported values of previous RSA studies, indicating that model-based RSA is appropriate for the evaluation of both humeral stem and glenosphere fixation in the reverse shoulder.[17]

Following the phantom study, a randomized clinical trial was conducted to evaluate, for the first time, the early migration patterns of reverse shoulder components using either cemented or press-fit humeral stem fixation (Chapter 4), and bony increased offset reverse shoulder arthroplasty (BIO-RSA) or porous titanium augmented glenospheres (Chapter 5), using model-based radiostereometric analysis. It was hypothesized that press-fit stems would migrate more than cemented stems prior to stabilizing, and that both BIO-RSA and augmented glenospheres would demonstrate immediate fixation. Results comparing humeral stem fixation demonstrated significant increases in total translation one year postoperatively (mean difference = 0.54, $P = 0.005$), and inferior stem migration six months (mean difference = 0.40 mm, $P = 0.026$) and one year (mean difference = 0.75 mm, $P < 0.001$) postoperatively with the use of press-fit stems compared to cemented. While press-fit stems showed initial evidence of migration, supporting our hypothesis, the cohort stabilized from six months to one year. There were no significant differences in patient range of motion, pain, or functional outcomes between groups at one year.

Comparing glenosphere lateralization using either BIO-RSA or the porous titanium augment, no measurable differences were observed between groups at any time point along any axis, or within groups at any time point after three months. There were no significant differences between groups in pain or functional metrics at one year, though the metal augment cohort demonstrated greater flexion and abduction. Compared to preoperative values, however, both groups improved with comparable gain – 53 vs. 48° in flexion, and 39 vs. 46° in abduction, for BIO-RSA and metal augment cohorts, respectively. Overall, our hypothesis was supported, as both groups demonstrated stable fixation through one year.

Similar to validating the use of radiostereometric analysis for migration of RTSA components, the technique was then validated for linear and volumetric polyethylene wear measurements (Chapter 6). The inherent limitation of using radiographic techniques in wear estimation is that the polyethylene liner is radiolucent. For this reason, supplementary analysis methods need to be developed to address this limitation. This validation study used the previously proposed pipeline of acquiring position and orientation information of the radiopaque metallic components (glenosphere and humeral stem) from model-based RSA, and in a separate external software, virtually inserting the appropriate polyethylene 3D model into the stem. The apparent intersection of the glenosphere into the liner was then taken as wear. A Sawbones shoulder phantom was again used, fitted with the Aequalis™ Reversed II shoulder system (Wright Medical-Tornier Group, Memphis, TN, USA). Instead of the manufactured polyethylene liner, additively manufactured liners with artificial wear patterns were inserted into the metaphyseal tray, representing the "true" accepted reference. Following the wear analysis pipeline, a linear wear precision of 0.21 mm and bias of 0.36 ± 0.13 mm were reported, with volumetric precision of 49.3 mm^3 and bias of 48.9 ± 24.3 mm^3. These results suggest that in vivo polyethylene wear can be measured without the need for reference markers or baseline radiographs, though it is limited to measuring articular wear and does not differentiate between creep and wear.

These wear analysis techniques were then applied to a reverse shoulder patient population to evaluate, for the first time, in vivo wear (Chapter 7). It was hypothesized that the wear of these liners, composed of ultra-high molecular weight polyethylene, would be measurable and correlated with time in vivo. Fifteen Aequalis™ Reversed II shoulders with minimum five-year term-of-service were assessed. Because the shoulder has six degrees of motion, wear patterns from activities of daily living may not be captured from analysis of a single arm position, and therefore multiple positions were acquired. Each patient was imaged at the extent of their range of motion in internal and external rotation, forward flexion, lateral abduction, and with the arm at the side. The mean volumetric and linear wear rates for the 36 mm liners (n = 13) were 42 ± 22 mm^3/year and 0.11 ± 0.03 mm/year, respectively. Volumetric (r = 0.688, P = 0.009) and linear (r = 0.767, P =

0.002) wear were both significantly moderately correlated with term-of-service, supporting our hypothesis. Only two patients had 42 mm liners and therefore a greater sample size is required for conclusive results, however this preliminary assessment demonstrated volumetric and linear wear rates approximately double that of the 36 mm liners. Overall, the results are comparable to that of a simulation study utilizing the same implant components and demonstrate that reverse shoulder wear is multidirectional and perceptible.[16]

8.2   Future directions

This work has provided a foundation for the assessment of reverse total shoulder arthroplasty, leaving many directions for future research studies. At the validation level, phantom studies can be conducted to assess tantalum bead placement within the bone, minimizing condition number by optimizing bead dispersion and limiting bead occlusion. Though eight beads were inserted in the bone surrounding each glenosphere and humeral stem, bead occlusion on the RSA radiographs was common and condition numbers relatively high. To this effect, in small osseous structures such as the glenoid and proximal humerus in which bead dispersion may be difficult to achieve, guides could be developed to facilitate bead insertion. Advances in medical-grade metal additive manufacturing may enable patient-specific guides in the future. Further studies could be conducted to assess the influence of patient positioning and x-ray tube angle on radiograph and RSA quality, as was previously completed in a study of the glenosphere.[8]

In terms of measuring implant migration, model-based RSA requires no modification to the implant prior to use. While this is advantageous compared to traditional marker-based RSA, the need for beads in the host bone limits the use of RSA to prospective investigations, and still suffers from the aforementioned potential bead occlusion. The further unique requirements of RSA such as calibration cages, simultaneous x-ray exposure, and proprietary analysis software limits the technique to dedicated research facilities. Advances in computed tomography (CT) such as improved resolution and lower radiation doses, in addition to its inherent 3D output and routine clinical use in

arthroplasty, have recently led a number of groups to explore its feasibility as an alternative to conventional RSA in measuring implant migration. Studies investigating the use of CT with bone markers or 3D surface anatomy (completely markerless analysis) report no difference in accuracy and precision of the technique compared to conventional RSA, suggesting that markerless RSA has the potential to measure early implant migration.[1,3,4,15] Further advances in intensity-based registration techniques could overcome potential changes in bone morphology over time by using only the internal bone information common in each scan.[4] Reducing the current restrictions imposed by RSA can increase the number of participants and subsequently implant designs assessed in the critical early postoperative period.

Specific to Chapters 4 and 5, it has been highlighted that these are the first results comparing implant fixation in RTSA. The purpose of evaluating implant migration in hip and knee replacement is that early migration has been associated with later loosening requiring revision.[12,13] The results of Chapters 4 and 5 will therefore provide foundational migration values for the specific fixation methods and implant designs used. Ideally, these patients will be recruited again at long-term (10+ years) follow-up for further assessment, to determine the effect of early migration on long-term radiographic and clinical outcomes. As different implants come to market, RSA, or potentially a CT-based alternative, should be used to evaluate their respective migration patterns and magnitudes. Results from early and long-term follow-up can then be taken together to influence future implant design, structure, and materials.

With respect to polyethylene wear, a number of investigations can be conducted to further understand wear behaviour in a complex joint such as the shoulder. Though the quasi-static RSA approach taken in Chapter 7 has been applied previously in total knee arthroplasty,[9] dynamic imaging such as single plane fluoroscopy may provide a more complete picture of wear patterns, especially when performing common activities of daily living. An in vivo method of assessing extra-articular wear, such as that induced by scapular notching, would also address a limitation of the current analysis framework. Further, though analysis at a single time point postoperatively is attractive from a patient

recruitment and feasibility perspective, baseline imaging and at three to six months postoperatively would provide measurement bias for each individual patient, in addition to the measurement effect of creep.[7] Acquiring double examinations would also provide a measure of clinical precision of the current technique. From a materials perspective, it would be interesting to compare differences in wear with the use of a highly cross-linked polyethylene, or of that with an antioxidant such as vitamin E. Finally, it is important to address the clinical impact of such findings. The study presented in Chapter 7 had few patients, only two of whom had the larger 42 mm bearing diameter. Evaluating wear rates in a larger population with different implant designs and sizes and correlating these with clinical outcomes will provide a more comprehensive understanding of the effects of long-term wear.

8.3   Significance

Advances in computational power and wear testing apparatus over the past decade have contributed to a growing number of simulation studies investigating the effects varying parameters such as bone quality, applied loads, and implant designs have on fixation and wear. These studies have the benefit of being cost-effective, fast, and easily repeated, though are limited in their representation of the true variability of the in vivo environment. For RTSA, the fastest growing joint replacement, it is imperative that in vitro and in silico simulations are supported by in vivo studies with both quantitative and qualitative outcome measures.[6,14]

This work presents the first prospective randomized clinical trial investigating humeral stem and glenosphere fixation in RTSA. Accordingly, these results will influence the future standard of care in surgical practice and the design of next-generation shoulder implants. Chapter 4 shows that short press-fit humeral stems are no different from standard length cemented stems in terms of range of motion, pain, and functional outcome, and that while they demonstrate early inferior migration, stabilize within six months postoperatively. At one year, neither cohort demonstrated radiographic evidence of loosening. The results from Chapter 5 show that both BIO-RSA and porous titanium

augmented baseplates stabilize immediately, with neither cohort exhibiting radiographic evidence of glenoid loosening or scapular notching. Similarly, both cohorts had a comparable improvement in clinical outcomes.

The first assessment of in vivo RTSA polyethylene wear has also been performed. These results are significant as they demonstrate RTSA wear is measurable and multidirectional, with wear rates an order of magnitude greater than what is observed with highly cross-linked polyethylene in the hip.[2,5,10] Consequently, these results may direct a change from using conventional to highly cross-linked polyethylene in the reverse shoulder, if future studies demonstrate a correlation between polyethylene wear and poorer clinical outcomes.

Using radiostereometric analysis, methods for the in vivo evaluation of RTSA have been presented. The tools used in these studies are generalizable to different implant designs, enabling the in vivo study of future changes to not only RTSA, but other joint replacements.

8.4 References

1. Boettner F, Sculco P, Lipman J, Renner L, Faschingbauer M. A novel method to measure femoral component migration by computed tomography: a cadaver study. Arch Orthop Trauma Surg. 2016;136(6):857–863. doi:10.1007/s00402-016-2442-8
2. Bragdon CR, Doerner M, Martell J, Jarrett B, Palm H, Multicenter Study Group, et al. The 2012 John Charnley Award: Clinical multicenter studies of the wear performance of highly crosslinked remelted polyethylene in THA. Clin Orthop Relat Res. 2013;471(2):393–402. doi:10.1007/s11999-012-2604-0
3. Brodén C, Olivecrona H, Maguire GQ, Noz ME, Zeleznik MP, Sköldenberg O. Accuracy and precision of three-dimensional low dose CT compared to standard RSA in acetabular cups: An experimental study. Biomed Res Int. 2016;2016. doi:10.1155/2016/5909741
4. Brodén C, Sandberg O, Sköldenberg O, Stigbrand H, Hänni M, Giles JW, et al. Low-dose CT-based implant motion analysis is a precise tool for early migration measurements of hip cups: a clinical study of 24 patients. Acta Orthop. 2020;3674. doi:10.1080/17453674.2020.1725345
5. Campbell DG, Field JR, Callary SA. Second-generation highly cross-linked X3™ polyethylene wear: A preliminary radiostereometric analysis study. Clin Orthop Relat Res. 2010;468(10):2704–2709. doi:10.1007/s11999-010-1259-y

6.   Chalmers PN, Salazar DH, Romeo AA, Keener JD, Yamaguchi K, Chamberlain AM. Comparative utilization of reverse and anatomic total shoulder arthroplasty. J Am Acad Orthop Surg. 2018;26(24):504–510. doi:10.5435/JAAOS-D-17-00075

7.   Deng M, Latour RA, Ogale AA, Shalaby SW. Study of creep behavior of ultra-high-molecular-weight polyethylene systems. J Biomed Mater Res. 1998;40(2):214–223. doi:10.1002/(sici)1097-4636(199805)40:2<214::aid-jbm6>3.0.co;2-o

8.   Fraser AN, Tsukanaka M, Fjalestad T, Madsen JE, Röhrl SM. Model-based RSA is suitable for clinical trials on the glenoid component of reverse total shoulder arthroplasty. J Orthop Res. 2018;36(12):3299–3307. doi:10.1002/jor.24111

9.   Gill HS, Waite JC, Short A, Kellett CF, Price AJ, Murray DW. In vivo measurement of volumetric wear of a total knee replacement. Knee. 2006;13(4):312–317. doi:10.1016/j.knee.2006.04.001

10.   Glyn-Jones S, McLardy-Smith P, Gill HS, Murray DW. The creep and wear of highly cross-linked polyethylene: A three-year randomised, controlled trial using radiostereometric analysis. J Bone Jt Surg Br. 2008;90(B):556–561. doi:10.1302/0301-620X.90B5.20545

11.   Kärrholm J, Gill RHS, Valstar ER. The history and future of radiostereometric analysis. Clin Orthop Relat Res. 2006;448(448):10–21. doi:10.1097/01.blo.0000224001.95141.fe

12.   Pijls BG, Plevier JWM, Nelissen RGHH. RSA migration of total knee replacements: A systematic review and meta-analysis. Acta Orthop. 2018;89(3):320–328. doi:10.1080/17453674.2018.1443635

13.   Ryd L, Albrektsson BE, Carlsson L, Dansgard F, Herberts P, Lindstrand A, et al. Roentgen stereophotogrammetric analysis as a predictor of mechanical loosening of knee prostheses. J Bone Joint Surg Br. 1995;77(3):377–383.

14.   Schairer WW, Nwachukwu BU, Lyman S, Craig EV, Gulotta LV. National utilization of reverse total shoulder arthroplasty in the United States. J Shoulder Elb Surg. 2015;24(1):91–97. doi:10.1016/j.jse.2014.08.026

15.   Scheerlinck T, Polfliet M, Deklerck R, Van Gompel G, Buls N, Vandemeulebroucke J. Development and validation of an automated and marker-free CT-based spatial analysis method (CTSA) for assessment of femoral hip implant migration In vitro accuracy and precision comparable to that of radiostereometric analysis (RSA). Acta Orthop. 2016;87(2):139–145. doi:10.3109/17453674.2015.1123569

16.   Terrier A, Merlini F, Pioletti DP, Farron A. Comparison of polyethylene wear in anatomical and reversed shoulder prostheses. J Bone Joint Surg Br. 2009;91–B(7):977–982. doi:10.1302/0301-620X.91B7.21999

17.   Valstar ER, Nelissen RGHH, Reiber JHC, Rozing PM. The use of Roentgen stereophotogrammetry to study micromotion of orthopaedic implants. ISPRS J Photogramm Remote Sens. 2002;56(5–6):376–389. doi:10.1016/S0924-2716(02)00064-3

Appendices

Appendix A   Glossary

Definitions adapted from the Merriam-Webster Medical Dictionary
(https://www.merriam-webster.com/medical)

Abduction	To draw (a limb) away from a position near or parallel to the median axis of the body
Adduction	To draw (a limb) toward or past the median axis of the body
Anterior	Situated before or toward the front
Arthroplasty	The operative formation or restoration of a joint
Coronal plane	An anatomic plane dividing the body into front and back, perpendicular to the transverse and sagittal planes
Cortical (bone)	Dense outer surface bone
Diaphysis	The shaft or central part of a long bone
Distal	Situated away from the center of the body or from the point of attachment
Extension	Increasing the angle between two body parts
Flexion	Decreasing the angle between two body parts
Fossa	An anatomical pit, groove, or depression
Glenoid version	The angular orientation of the axis of the glenoid articular surface relative to the transverse axis of the scapula; an anterior angle is referred to as anteversion, a posterior angle as retroversion
Inferior	Below or toward the feet
Lateral	Away from the midline of the body
Medial	Toward the midline of the body
Metaphysis	The narrow portion of a long bone between the epiphysis and diaphysis, containing the growth plate

Osteophyte	An abnormal bony outgrowth or projection
Osteoporotic	Decreased bone mass density with enlargement of trabecular spaces
Periprosthetic	Referring to the structure in close relation to/around an implant
Posterior	Situated behind or toward the back
Proximal	Situated next to or nearest the point of attachment, located toward the center of the body
Radiograph	X-ray image
Radiolucent	Partly or wholly permeable to radiation (including x-rays)
Ream	To enlarge, shape, or smooth a hole/surface (by removing material)
Sagittal plane	An anatomic plane dividing the body into left and right parts, perpendicular to the coronal and transverse planes
Stress	Force per unit area
Subluxation	A partial dislocation
Superior	Above or toward the head
Trabecular (bone)	Porous sponge-like inner bone
Transverse plane	An anatomic plane dividing the body into superior and inferior parts, perpendicular to the coronal and sagittal planes

Appendix B   Ethics approval

Chapters 4, 5

Western Research

Research Ethics

Western University Health Science Research Ethics Board
HSREB Full Board Initial Approval Notice

Principal Investigator: Dr. George Athwal
Department & Institution: Schulich School of Medicine and Dentistry\Surgery, St. Joseph's Health Care London

HSREB File Number: 105908
Study Title: Evaluation of implant fixation in reverse total shoulder arthroplasty
Sponsor: Lawson Health Research Institute

HSREB Initial Approval Date: January 09, 2015
HSREB Expiry Date: January 09, 2016

Documents Approved and/or Received for Information:

Document Name	Comments	Version Date
Instruments	DASH	
Instruments	SF12	
Instruments	American Shoulder and Elbow Surgeon's Self-report Form	
Other	NCT # 102305966	2015/01/09
Western University Protocol	(received Nov.28/14)	
Letter of Information & Consent	Clean copy	2015/01/05

The Western University Health Science Research Ethics Board (HSREB) has reviewed and approved the above named study, as of the HSREB Initial Approval Date noted above.

HSREB approval for this study remains valid until the HSREB Expiry Date noted above, conditional to timely submission and acceptance of HSREB Continuing Ethics Review. If an Updated Approval Notice is required prior to the HSREB Expiry Date, the Principal Investigator is responsible for completing and submitting an HSREB Updated Approval Form in a timely fashion.

The Western University HSREB operates in compliance with the Tri-Council Policy Statement Ethical Conduct for Research Involving Humans (TCPS2), the International Conference on Harmonization of Technical Requirements for Registration of Pharmaceuticals for Human Use Guideline for Good Clinical Practice Practices (ICH E6 R1), the Ontario Personal Health Information Protection Act (PHIPA, 2004), Part 4 of the Natural Health Product Regulations, Health Canada Medical Device Regulations and Part C, Division 5, of the Food and Drug Regulations of Health Canada.

Members of the HSREB who are named as Investigators in research studies do not participate in discussions related to, nor vote on such studies when they are presented to the REB.

The HSREB is registered with the U.S. Department of Health & Human Services under the IRB registration number IRB 00000940.

Ethics Officer, on behalf of Dr. Marcelo Kremenchutzky, HSREB Vice Chair

Ethics Officer to Contact for Further Information

Erika Basile	Grace Kelly	Mina Mekhail	Vikki Tran
ebasile@uwo.ca	grace.kelly@uwo.ca	mmekhail@uwo.ca	vikki.tran@uwo.ca

This is an official document. Please retain the original in your files.

Western University, Research, Support Services Bldg., Rm. 5150
London, ON, Canada N6A 3K7 t. 519.661.3036 f. 519.850.2466 www.uwo.ca/research/services/ethics

Chapter 7

Western Research

Date: 12 July 2018

To: Dr. George Athwal

Project ID: 111295

Study Title: Evaluation of wear in reverse total shoulder arthroplasty

Application Type: HSREB Initial Application

Review Type: Delegated

Full Board Reporting Date: August 7, 2018

Date Approval Issued: 12/Jul/2018

REB Approval Expiry Date: 12/Jul/2019

_____

Dear Dr. George Athwal

The Western University Health Science Research Ethics Board (HSREB) has reviewed and approved the above mentioned study as described in the WREM application form, as of the HSREB Initial Approval Date noted above. This research study is to be conducted by the investigator noted above. All other required institutional approvals must also be obtained prior to the conduct of the study.

Documents Approved:

Document Name	Document Type	Document Date	Document Version
Data collection instruments, May 2018	Other Data Collection	Received July 10, 2018	
Letter of Information and Consent, June 25 2018	Written Consent/Assent	25/Jun/2018	2
Recruitment Script - RTSR wear study, June 28 2018	Telephone Script	28/Jun/2018	2
WREM Protocol, June 25 2018	Protocol	Received July 10, 2018	

No deviations from, or changes to, the protocol or WREM application should be initiated without prior written approval of an appropriate amendment from Western HSREB , except when necessary to eliminate immediate hazard(s) to study participants or when the change(s) involves only administrative or logistical aspects of the trial.

REB members involved in the research project do not participate in the review, discussion or decision.

The Western University HSREB operates in compliance with, and is constituted in accordance with, the requirements of the TriCouncil Policy Statement: Ethical Conduct for Research Involving Humans (TCPS 2); the International Conference on Harmonisation Good Clinical Practice Consolidated Guideline (ICH GCP); Part C, Division 5 of the Food and Drug Regulations; Part 4 of the Natural Health Products Regulations; Part 3 of the Medical Devices Regulations and the provisions of the Ontario Personal Health Information Protection Act (PHIPA 2004) and its applicable regulations. The HSREB is registered with the U.S. Department of Health & Human Services under the IRB registration number IRB 00000940.

Please do not hesitate to contact us if you have any questions.

Sincerely,

Karen Gopaul, Ethics Officer on behalf of Dr. Joseph Gilbert, HSREB Chair

Note: This correspondence includes an electronic signature (validation and approval via an online system that is compliant with all regulations).

Appendix C   Letters of information and consent

Chapters 4, 5

LETTER OF INFORMATION

Project Title:	**Evaluation of implant fixation in reverse total shoulder arthroplasty**
Investigators:	**Dr. George Athwal, MD Principal Investigator (Study Doctor)** Dr. Matthew Teeter Dr. Douglas Naudie Madeleine Van de Kleut, PhD Candidate
Location:	The Hand and Upper Limb Centre. Robarts Research Institute. London, Ontario, Canada.

What is the purpose?

You are being invited to voluntarily participate in a research study designed for patients undergoing primary reverse total shoulder arthroplasty (replacement) surgery at St. Joseph's Health Care, London. This letter of information describes the research study and your role as the participant. Please read this form carefully. Do not hesitate to ask anything about the information provided. Your doctor will describe the study and answer your questions.

Study Purpose

Total shoulder replacement arthroplasty is a well-established surgery for restoring comfort and function to the arthritic shoulder. In this procedure the arthritic ball is replaced by a smooth metal ball fixed to the arm bone (humerus) by a stem that fits within it. The arthritic socket (glenoid) is resurfaced with high-density polyethylene prosthesis. Surgeons have two different options when implanting the components of a reverse total shoulder replacement, to ensure that the implants will remain well-fixed within the bone. First is to use an implant designed to be "cemented" into the bone, using specially designed bone cement. This bone cement acts like grout in a tile floor, interfacing between the implant and the bone to ensure the implants stay in place. The second option is to use an "uncemented" or "press-fit" implant designed to have bone grow into the implant itself to keep it from moving. Both types of implants have demonstrated good clinical success. However, no studies have ever measured exactly how securely these two different fixation options are within the bone. All implants are expected to move a small amount ("micromotion" of less than 1 mm) soon after they are implanted, just like a house settles after it is built. Too much motion can mean that the implant is loose and will eventually need to be replaced. For hip and knee replacements,

the amount and pattern of these micromotions has already been established for both cemented and uncemented implants, both of which have good long-term track records.

The purpose of this study is to examine this micromotion in cemented and uncemented reverse total shoulder replacement implants, to determine the amount and pattern of any motion over time with Tantalum marker beads and also to determine how motion throughout the patient's daily activity affects implant migration and wear The Tantalum beads consist of 1mm spherical x-ray markers made of commercially pure, unalloyed tantalum. At the time of surgery, Tantalum marker beads are implanted in the bone surrounding the implant

How many people will be in this study: There will be 40 local participants in this study.

Procedure

If you decide to participate in this study, you will first be randomly assigned like the flip of a coin to one of two study groups. You and your surgeon will not be able to choose which group you will be in. If you are randomized into the first group, you will receive an implant put in place using bone cement. If you are randomized into the second group, you will receive and implant that is "uncemented" and is held in place by bone ingrowth onto the implant. In addition the randomization will also happen within the groups creating one group with glenoid components that are lateralized using a bony-offset (bone graft) and one group with glenoid components that are lateralized using a porous metal (metal augmented) disk. As such, 4 randomization groups will be created: 1) pressfit humerus & bony-offset lateralized glenoid (2) pressfit humerus & metal-augmented lateralized glenoid (3) cemented humerus & bony-offset lateralized glenoid (4) cemented humerus & metal-augmented lateralized glenoid.

During the surgery all study patients will have 8 tantalum beads implanted in each of their scapula (shoulder blade) and humerus (upper arm bone). These beads are the size of the head of a pin and have no impact on how your shoulder will function after the surgery. The beads will be used as markers on x-ray to assess for any microscopic movement of the implant components. Patients will be x-rayed using a special type of x-ray called radiostereometric analysis (RSA). These x-rays will be after your normally scheduled orthopaedic clinic visits with your surgeon after surgery at 6 weeks, 3 months, 6 months, 1 year, and 2 years. The x-rays will be taken in the Musculoskeletal Imaging Laboratory on the 2nd floor of the Robarts Research Institute, beside University Hospital. This will take approximately 15-30 minutes per visit.

Post-operatively, you will receive the standard of care provided for all shoulder joint replacement patients. You will be seen by your surgeon at two, six weeks, three months, six months and one year visits after your shoulder replacement surgery. You will be asked to answer survey questions about your shoulder pre-operatively, at the three

months, and at your one and two year visits. The forms will be introduced by Katrina Munro (research Coordinator). These follow-up visits are standard of care for all shoulder joint replacement patients regardless of study participation.

To determine how motion throughout the patient's daily activity affects implant migration and wear, you will be asked to wear a tight-fitting shirt fitted with five sensors one month prior to the operation, at 3 months post-operation, and at 1 year post-operation. We will use five YEI 3-Space Sensors attached to a snug fitting long sleeved shirt and connected to a portable battery with USB cables. One sensor will be placed over the sternal area in a pocket on a shirt, one sensor will be placed laterally on the upper arm at the midpoint of both the right and left humerus and the last sensors will be placed on the dorsum of the distal forearm of both the left and right arms. These sensors will collect position data using an accelerometer and electromagnetic compass, and record position relative to one another in a continuous fashion. They are self-enclosed, devices in sealed plastic containers, meant for the purpose and designed for recreating human motion in the video game industry.

There will be minimal risks to the patient: the units have been designed to be worn close to the skin and emit no significant heat. The battery and units are sealed in plastic containers.

We will choose for you a shirt that fits snugly; we'll have most sizes available.
We will ask you to put on shirt, activate, and check the sensors and battery.
You will perform standard movements of shoulder and elbow ROM to ensure sensors are working and describe full active range of motion for each joint. Motions have to be done simultaneously with both the right and left side. Research support staff Katrina Munro will go through the movements with you and ask questions about your overall shoulder function. You will leave the clinic with the shirt on, collecting data and wear it throughout your normal daily activities. We encourage you to carry on with your normal activities, whatever they may be. The shirt should be taken off for showering, but left on for other activities, sports and travel as much as possible. The following day, we will ask you to return the shirt. You will be given a pre-addressed and pre-paid shipping envelope, to be couriered back to the HULC the next day after wearing the shirt. Later we will download sensor data to computer for further analysis.

Potential Study Risks

There is always a very slight chance of cancer from excessive exposure to radiation. Special care is taken during RSA x-ray examinations to use the lowest radiation dose possible while producing the best images for evaluation.

The scientific unit of measurement for radiation dose is the millisevert (mSv). People are exposed to radiation from natural sources all the time. The average person receives an effective dose of about 3 mSv per year from naturally occurring radioactive materials and cosmic radiation from outer space.

161

Each RSA examination of the shoulder will expose the patient to 0.1 mSv of ionizing radiation, or 3.3% of the background radiation we are all exposed to yearly. The sum total of radiation exposure across the multiple RSA exams (at 6 weeks, 3 months, 6 months, 1 year, and 2 years) is 1.3 mSv, equivalent to approximately 43% of yearly background radiation exposure.

There are no known risks associated with Tantalum marker beads. If there is an infection risk, these beads are easily accessible to be removed. These beads have been implanted into thousands of patients worldwide and in more than 200 patients here at LHSC with no complications.

Women pregnant or planning on getting pregnant will be excluded from the study.

Potential Benefits Associated with this Study

You may or may not benefit directly from participation in this study. The outcomes of this study may help increase the understanding of how cemented and uncemented shoulder implants perform. This could, in the future, help modify or enhance the care and treatment of patients undergoing reverse total shoulder replacement surgery.   There is no guarantee of benefit by participating in this study.

Voluntary Participation

Participation in the study is voluntary. You may refuse to participate, refuse to answer any questions or withdraw from the study at any time with no effect on your future care. Any new information obtained during the course of the research that may affect your willingness to continue participation in the study will be provided to you. You do not waive any legal right by signing the consent form.

Withdrawal from the study

If you decide to withdraw from the study, the information that was collected before you leave the study will still be used in order to help answer the research question. No new information will be collected without your permission.

Alternatives to Study Participation

If you choose not to participate, you will have your shoulder replacement surgically implanted using the technique and surgical instruments routinely used by your surgeon.

Compensation

You will be given a parking pass to cover the cost of parking while at your RSA imaging appointments.

Confidentiality

You will not be identified personally in any publication or communication resulting from this study. All information collected will be stored in a locked office and entered into a secure hospital computer on a server accessible by authorized individuals only. This information will be used solely for the advancement of medical science and any personal information will be kept confidential.

RSA image data will be processed at the Robarts Research Institute, a secure research facility. This data will be stored on password-protected computer, and will be made anonymous by coding it with a numeric identifier. Study data will be kept for 10 years (according to hospital standards).

A copy of this letter will be given to you. Representatives of the University of Western Ontario Health Sciences Research Ethics Board or/and representatives of Lawson Quality Assurance Education Program may require access to your study-related records or follow-up with you to monitor the conduct of this research.

If you have any questions about your rights as a research participant or the conduct of the study you may contact Dr. David Hill, Scientific Director, c/o Lawson Health Research Institute at █████████████

Whom may you contact to find out more about this study?

You will be given a copy of this letter. If you have questions about taking part in this study, you can directly contact:

Dr. George Athwal, MD
The Hand and Upper Limb Centre, St. Joseph's Health Centre
█████████████

Katrina Munro (Research Assistant)
The Hand and Upper Limb Centre, St. Joseph's Health Centre
█████████████████████

Consent To Participate In: **Evaluation of implant fixation in reverse total shoulder arthroplasty**

I have read the letter of information, have had the nature of the study explained to me and I agree to participate. All questions have been answered to my satisfaction

_____   _____   _____
Signature of Participant   Print Name   Date

_____   _____   _____
Signature of person   Print Name of person   Date
obtaining consent   obtaining consent

Chapter 7

LETTER OF INFORMATION

Project Title: **Evaluation of wear in reverse total shoulder arthroplasty**

Investigators:

Dr. George Athwal, MD Principal Investigator (Study Doctor)
Dr. Kenneth Faber, MD (Study Doctor)
Dr. Matthew Teeter
Madeleine Van de Kleut, PhD Candidate

Location: The Hand and Upper Limb Centre. Robarts Research Institute. London, Ontario, Canada.

What is the purpose?

You are being invited to voluntarily participate in a research study designed for patients having undergone reverse total shoulder arthroplasty (replacement) surgery at St. Joseph's Health Care, London. This letter of information describes the research study and your role as the participant. Please read this form carefully. Do not hesitate to ask anything about the information provided. Your doctor will describe the study and answer your questions.

Study Purpose

Reverse total shoulder replacement (RTSR) is a well-established surgery for restoring comfort and function to the arthritic shoulder with demonstrated good clinical success. The replacement is composed of a metal stem implanted into the humerus (upper arm bone) and a metal sphere implanted in the glenoid (part of the shoulder bone). Placed between these two metal components is a plastic cup to reduce friction and allow for smooth arm movement. Over time, the continuous contact of the metal sphere on the plastic component can lead to wear, similar to the wearing of tires on the road over time. It is important to measure this wear to identify how current implants perform, and to provide insight into future designs.

There have been a handful of studies looking at the wear from retrieved (failed) implants and using computer models, however, no studies have ever measured the wear of the plastic articulating component while still implanted in the body (*in vivo*).

The purpose of this study is to measure RTSR wear *in vivo*.

How many people will be in this study: There will be 20 local participants in this study.

Procedure

Patients will be x-rayed using a special type of x-ray called radiostereometric analysis (RSA). These x-rays will be after your normally scheduled orthopaedic clinic visit with your surgeon. The x-rays will be taken in the Musculoskeletal Imaging Laboratory on the 2nd floor of the Robarts Research Institute, beside University Hospital. You will be accompanied from St. Joseph' Hospital to the Robarts Research Insitute. Five RSA x-ray exposures will be taken, with the patient's arm at the limits of its active range of motion (maximum forward flexion, abduction, adduction, external rotation, and internal rotation). This visit will take approximately 30 minutes. Patients are not required to return to St. Joseph's hospital following the visit to Robarts Research Institute.

Potential Study Risks

There is always a very slight chance of cancer from excessive exposure to radiation. Special care is taken during RSA x-ray examinations to use the lowest radiation dose possible while producing the best images for evaluation.

The scientific unit of measurement for radiation dose is the millisevert (mSv). People are exposed to radiation from natural sources all the time. The average person receives an effective dose of about 3 mSv per year from naturally occurring radioactive materials and cosmic radiation from outer space.

Each RSA examination of the shoulder will expose the patient to 0.1 mSv of ionizing radiation, or 3.3% of the background radiation we are all exposed to yearly. With five exposures equating to 0.5 mSv, this amounts to approximately two months of background radiation.

Women pregnant or planning on getting pregnant will be excluded from the study.

Potential Benefits Associated with this Study

You may or may not benefit directly from participation in this study. The outcomes of this study may help increase the understanding of how shoulder implants perform. This could, in the future, help modify or enhance the care and treatment of patients undergoing reverse total shoulder replacement surgery. There is no guarantee of benefit by participating in this study.

Voluntary Participation

Participation in the study is voluntary. You may refuse to participate, refuse to answer any questions or withdraw from the study at any time with no effect on your future care. Any new information obtained during the course of the research that may affect your willingness to continue participation in the study will be provided to you. You do not waive any legal right by signing the consent form.

Withdrawal from the study

If you decide to withdraw from the study, you may choose to allow for the information that was collected before you leave to be used in order to help answer the research question, or you may choose to withdraw all collected information entirely. No new information will be collected without your permission.

Alternatives to Study Participation

If you choose not to participate, you will have your routine follow-up visit with your orthopedic surgeon and standard diagnostic x-rays.

Compensation

You will be given a parking pass to cover the cost of parking while at your RSA imaging appointment.

Confidentiality

You will not be identified personally in any publication or communication resulting from this study. All information collected will be stored in a locked office and entered into a secure hospital computer on a server accessible by authorized individuals only. This information will be used solely for the advancement of medical science and any personal information will be kept confidential.

RSA image data will be processed at the Robarts Research Institute, a secure research facility. This data will be stored on password-protected computer, and will be made anonymous by coding it with a numeric identifier. Study data will be kept for 15 years (according to hospital standards).

A copy of this letter will be given to you. Representatives of the University of Western Ontario Health Sciences Research Ethics Board or/and representatives of Lawson Quality Assurance Education Program may require access to your study-related records or follow-up with you to monitor the conduct of this research.

If you have any questions about your rights as a research participant or the conduct of the study you may contact the St. Joseph's Health Care London Patient Relations Consultant at 519-646-6100 x64727.

St Joseph's HEALTH CARE LONDON

Whom may you contact to find out more about this study?

You will be given a copy of this letter. If you have questions about taking part in this study, you can directly contact:

Dr. George Athwal, MD
The Hand and Upper Limb Centre, St. Joseph's Health Centre
████████████

Dr. Kenneth Faber, MD
The Hand and Upper Limb Centre, St. Joseph's Health Centre
████████████

Madeleine Van de Kleut
Robarts Research Institute, Imaging Research Laboratories
████████████████████████

Consent To Participate In: **Evaluation of wear in reverse total shoulder arthroplasty**

I have read the letter of information, have had the nature of the study explained to me and I agree to participate. All questions have been answered to my satisfaction

_____   _____   _____
Signature of Participant   Print Name   Date

_____   _____   _____
Signature of person   Print Name of person   Date
obtaining consent   obtaining consent

Appendix D   Patient reported outcomes questionnaires

Subjective Shoulder Value

What is the overall percent value of your shoulder if a completely normal shoulder represents 100%?

_____%

ASES Shoulder Score

Name: _____   Date: _____

1) Usual work: _____

2) Usual sport/leisure activity: _____

3) Do you have shoulder pain at night?

   YES NO

4) Do you take painkillers such as paracetamol (acetaminophen), diclofenac, or ibuprofen?

   YES NO

5) Do you take strong painkillers such as codeine, tramadol, or morphine?

   YES NO

6) How many pills do you take on an average day? _____

7) Intensity of pain? (0 → no pain at all; 10 → pain as bad as it can be)

   0   1   2   3   4   5   6   7   8   9   10

8) Is it difficult for you to put on a coat?

   - o Unable to do
   - o Very difficult to do
   - o Somewhat difficult
   - o Not difficult

9) Is it difficult for you to sleep on the affected side?

   - o Unable to do
   - o Very difficult to do
   - o Somewhat difficult
   - o Not difficult

10) Is it difficult for you to wash your back/do up bra?

   - o Unable to do
   - o Very difficult to do
   - o Somewhat difficult
   - o Not difficult

11) Is it difficult for you to manage toileting?

- o Unable to do
- o Very difficult to do
- o Somewhat difficult
- o Not difficult

12) Is it difficult for you to comb your hair?

- o Unable to do
- o Very difficult to do
- o Somewhat difficult
- o Not difficult

13) Is it difficult for you to reach a high shelf?

- o Unable to do
- o Very difficult to do
- o Somewhat difficult
- o Not difficult

14) Is it difficult for you to lift 10 lbs (4.5 kg) above your shoulder?

- o Unable to do
- o Very difficult to do
- o Somewhat difficult
- o Not difficult

15) Is it difficult for you to throw a ball overhand?

- o Unable to do
- o Very difficult to do
- o Somewhat difficult
- o Not difficult

16) Is it difficult for you to do your usual work?

- o Unable to do
- o Very difficult to do
- o Somewhat difficult
- o Not difficult

17) Is it difficult for you to do your usual sport/leisure activity?

- o Unable to do
- o Very difficult to do
- o Somewhat difficult
- o Not difficult

UW Medicine

Bone and Joint Center – Shoulder and Elbow Team
4245 Roosevelt Way NE Seattle, WA 98105-6920 campus Box 354740

Simple Shoulder Test

Dominant Hand (*fill in only one circle*): Right ○   Left ○   Ambidextrous ○

Please answer YES or NO for both of your shoulders

		RIGHT		LEFT		
		YES	NO	YES	NO	
1	Is your shoulder comfortable with your arm at rest by your side?	○	○	○	○	1
2	Does your shoulder allow you to sleep comfortably?	○	○	○	○	2
3	Can you reach the small of your back to tuck in your shirt with your hand?	○	○	○	○	3
4	Can you place your hand behind your head with the elbow straight out to the side?	○	○	○	○	4
5	Can you place a coin on a shelf at the level of your shoulder without bending your elbow?	○	○	○	○	5
6	Can you lift one pound (a full pint container) to the level of your shoulder without bending your elbow?	○	○	○	○	6
7	Can you lift eight pounds (a full gallon container) to the level of your shoulder without bending your elbow?	○	○	○	○	7
8	Can you carry twenty pounds at your side with this extremity?	○	○	○	○	8
9	Do you think you can toss a softball under-hand twenty yards with this extremity?	○	○	○	○	9
10	Do you think you can toss a softball over-hand twenty yards with this extremity?	○	○	○	○	10
11	Can you wash the back of your opposite shoulder with this extremity?	○	○	○	○	11
12	Would your shoulder allow you to work full-time at your regular job?	○	○	○	○	12

Office Use Only – For Physician to Fill Out

	DJD	SDJD	RA	FS	PTSS	AVN	CA	CTA	SA	PTCL	RCT	TUBS	AMBRII
R	○	○	○	○	○	○	○	○	○	○	○	○	○
Other:													
	DJD	SDJD	RA	FS	PTSS	AVN	CA	CTA	SA	PTCL	RCT	TUBS	AMBRII
L	○	○	○	○	○	○	○	○	○	○	○	○	○
Other:													

Affix Pt Label Here

Name:
U Number:
DOB:
DOS:

1

THE

DASH

INSTRUCTIONS

This questionnaire asks about your symptoms as well as your ability to perform certain activities.

Please answer *every question*, based on your condition in the last week, by circling the appropriate number.

If you did not have the opportunity to perform an activity in the past week, please make your *best estimate* on which response would be the most accurate.

It doesn't matter which hand or arm you use to perform the activity; please answer based on your ability regardless of how you perform the task.
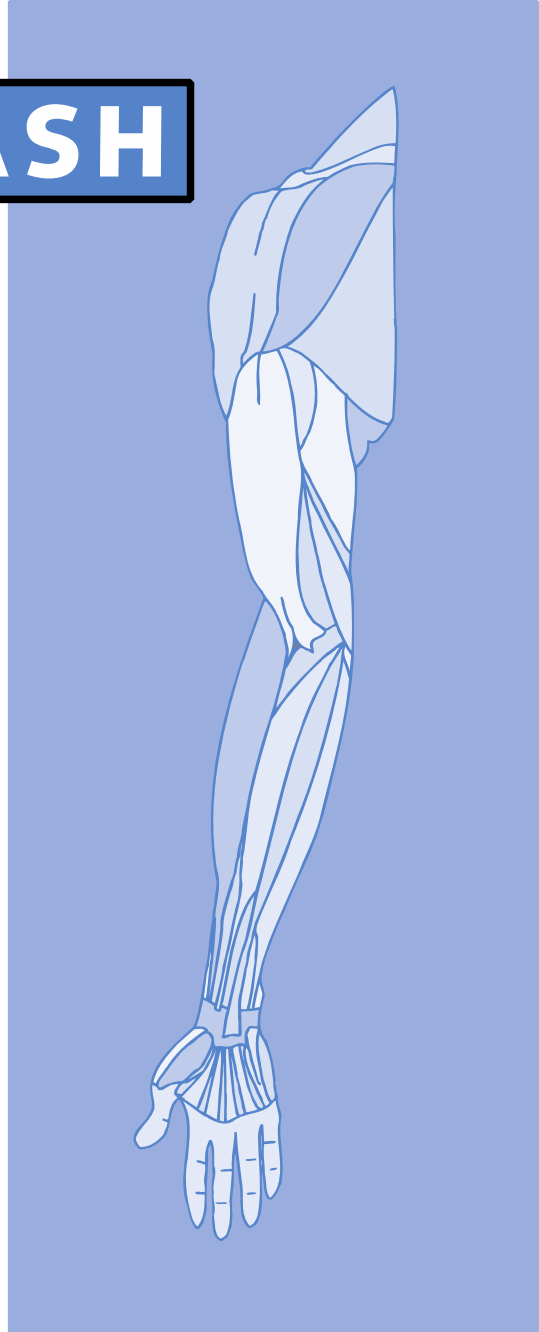
DISABILITIES OF THE ARM, SHOULDER AND HAND

Please rate your ability to do the following activities in the last week by circling the number below the appropriate response.

	NO DIFFICULTY	MILD DIFFICULTY	MODERATE DIFFICULTY	SEVERE DIFFICULTY	UNABLE
1. Open a tight or new jar.	1	2	3	4	5
2. Write.	1	2	3	4	5
3. Turn a key.	1	2	3	4	5
4. Prepare a meal.	1	2	3	4	5
5. Push open a heavy door.	1	2	3	4	5
6. Place an object on a shelf above your head.	1	2	3	4	5
7. Do heavy household chores (e.g., wash walls, wash floors).	1	2	3	4	5
8. Garden or do yard work.	1	2	3	4	5
9. Make a bed.	1	2	3	4	5
10. Carry a shopping bag or briefcase.	1	2	3	4	5
11. Carry a heavy object (over 10 lbs).	1	2	3	4	5
12. Change a lightbulb overhead.	1	2	3	4	5
13. Wash or blow dry your hair.	1	2	3	4	5
14. Wash your back.	1	2	3	4	5
15. Put on a pullover sweater.	1	2	3	4	5
16. Use a knife to cut food.	1	2	3	4	5
17. Recreational activities which require little effort (e.g., cardplaying, knitting, etc.).	1	2	3	4	5
18. Recreational activities in which you take some force or impact through your arm, shoulder or hand (e.g., golf, hammering, tennis, etc.).	1	2	3	4	5
19. Recreational activities in which you move your arm freely (e.g., playing frisbee, badminton, etc.).	1	2	3	4	5
20. Manage transportation needs (getting from one place to another).	1	2	3	4	5
21. Sexual activities.	1	2	3	4	5

DISABILITIES OF THE ARM, SHOULDER AND HAND

	NOT AT ALL	SLIGHTLY	MODERATELY	QUITE A BIT	EXTREMELY
22. During the past week, *to what extent* has your arm, shoulder or hand problem interfered with your normal social activities with family, friends, neighbours or groups? *(circle number)*	1	2	3	4	5

	NOT LIMITED AT ALL	SLIGHTLY LIMITED	MODERATELY LIMITED	VERY LIMITED	UNABLE
23. During the past week, were you limited in your work or other regular daily activities as a result of your arm, shoulder or hand problem? *(circle number)*	1	2	3	4	5

Please rate the severity of the following symptoms in the last week. *(circle number)*

	NONE	MILD	MODERATE	SEVERE	EXTREME
24. Arm, shoulder or hand pain.	1	2	3	4	5
25. Arm, shoulder or hand pain when you performed any specific activity.	1	2	3	4	5
26. Tingling (pins and needles) in your arm, shoulder or hand.	1	2	3	4	5
27. Weakness in your arm, shoulder or hand.	1	2	3	4	5
28. Stiffness in your arm, shoulder or hand.	1	2	3	4	5

	NO DIFFICULTY	MILD DIFFICULTY	MODERATE DIFFICULTY	SEVERE DIFFICULTY	SO MUCH DIFFICULTY THAT I CAN'T SLEEP
29. During the past week, how much difficulty have you had sleeping because of the pain in your arm, shoulder or hand? *(circle number)*	1	2	3	4	5

	STRONGLY DISAGREE	DISAGREE	NEITHER AGREE NOR DISAGREE	AGREE	STRONGLY AGREE
30. I feel less capable, less confident or less useful because of my arm, shoulder or hand problem. *(circle number)*	1	2	3	4	5

DASH DISABILITY/SYMPTOM SCORE = [(sum of n responses) − 1] x 25, where n is equal to the number of completed responses.
n

A DASH score may <u>not</u> be calculated if there are greater than 3 missing items.

Constant Shoulder Score

Clinician's Name: _____   Patie nt's Name: _____

Answer all questions, selecting just one unless otherwise stated

During the past 4 weeks......

1. Pain

- [ ] Severe
- [ ] Moderate
- [ ] Mild
- [ ] None

2. Activity Level (check all that apply)

- [ ] Unaffected Sleep
- [ ] Full Recreation/Sport
- [ ] Full Work

3. Arm Positioning

- [ ] Up to Waist
- [ ] Up to Xiphoid
- [ ] Up to Neck
- [ ] Up to Top of Head
- [ ] Above Head

4. Strength of Abduction [Pounds]

- [ ] 0
- [ ] 1-3
- [ ] 4-6
- [ ] 7-9
- [ ] 10-12
- [ ] 13-15
- [ ] 15-18
- [ ] 19-21
- [ ] 22-24
- [ ] >24

RANGE OF MOTION

5. Forward Flexion

- [ ] 31-60 degrees
- [ ] 61-90 degrees
- [ ] 91-120 degrees
- [ ] 121-150 degrees
- [ ] 151-180 degrees

6. Lateral Elevation

- [ ] 31-60 degrees
- [ ] 61-90 degrees
- [ ] 91-120 degrees
- [ ] 121-150 degrees
- [ ] 151-180 degrees

7. External Rotation

- [ ] Hand behind Head, Elbow forward
- [ ] Hand behind Head, Elbow back
- [ ] Hand to top of Head, Elbow forward
- [ ] Hand to top of Head, Elbow back -
- [ ] Full Elevation

8. Internal Rotation

- [ ] Lateral Thigh
- [ ] Buttock
- [ ] Lumbosacral Junction
- [ ] Waist (L3)
- [ ] T12 Vertebra
- [ ] Interscapular (T7)

The Constant Shoulder Score is: 0_____

Grading the Constant Shoulder Score

>30 Poor   21-30 Fair   11-20 Good   <11 Excellent

Appendix E   Humeral stem migration graphs (Chapter 4)
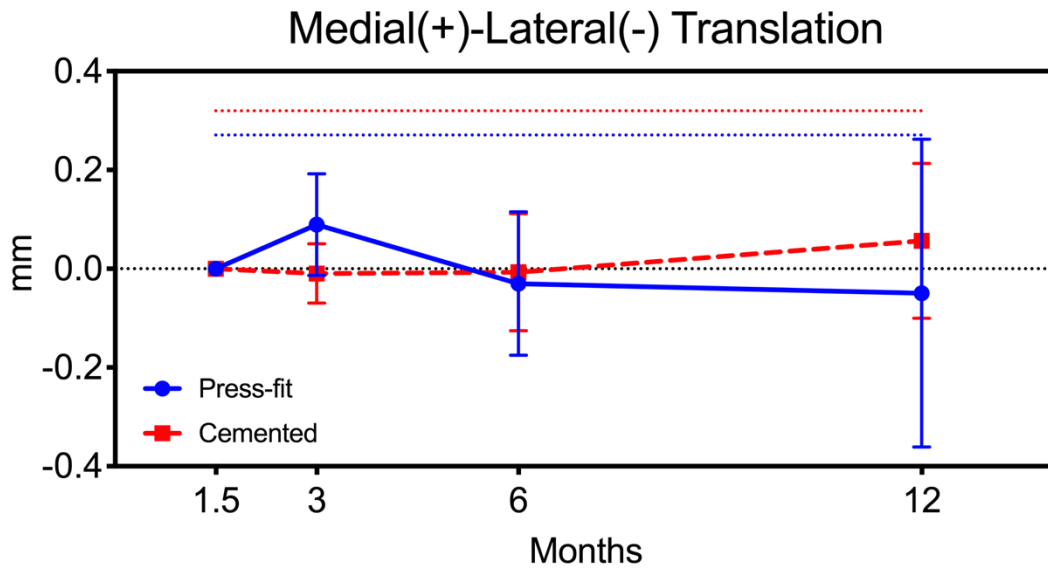
Figure E.1 Medial(+)-lateral(-) (T_x) humeral stem migration. Press-fit precision is represented as the fine blue dotted line, and cemented precision as the fine red dotted line.
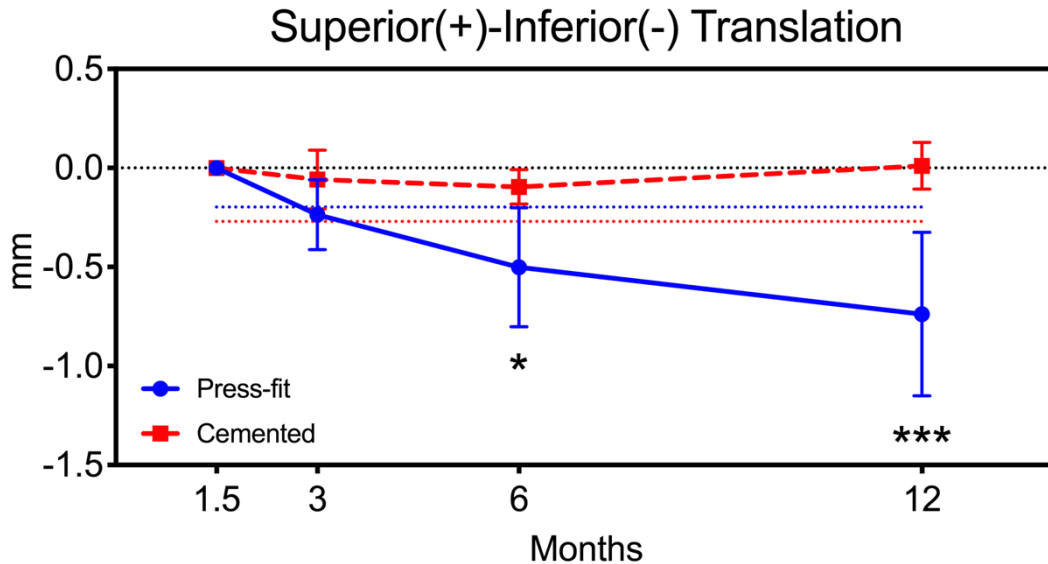
Figure E.2 Superior(+)-inferior(-) (T_y) humeral stem migration. Press-fit stems demonstrate significantly greater subsidence six months ($P = 0.026$) and one year ($P < 0.001$) postoperatively. Press-fit precision is represented as the fine blue dotted line, and cemented precision as the fine red dotted line.
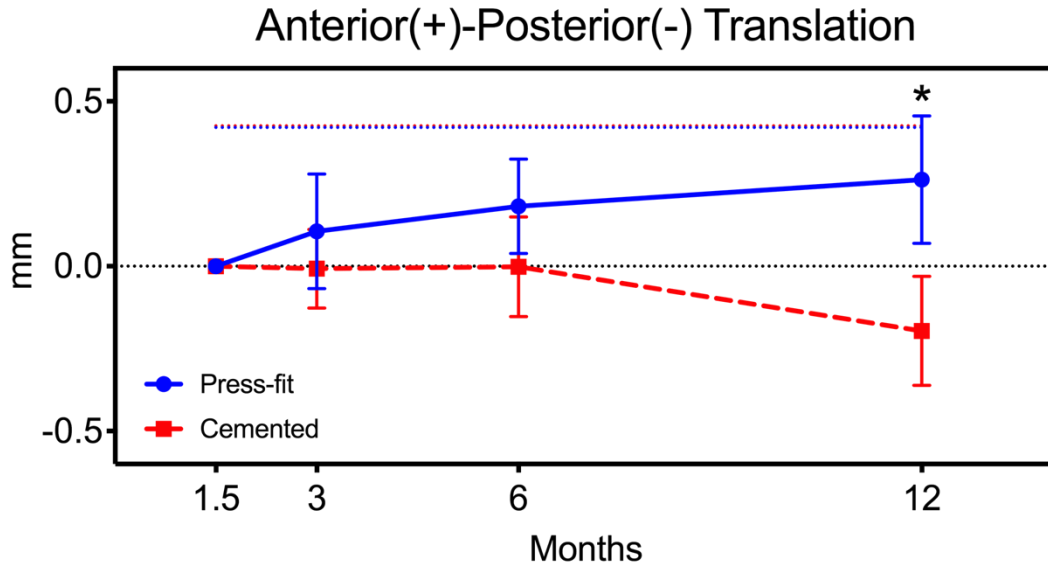
Figure E.3 Anterior(+)-posterior(-) (T_z) humeral stem migration. Press-fit stems demonstrate significantly greater anterior migration one year ($P = 0.002$) postoperatively. Press-fit precision is represented as the fine blue dotted line, and cemented precision as the fine red dotted line.
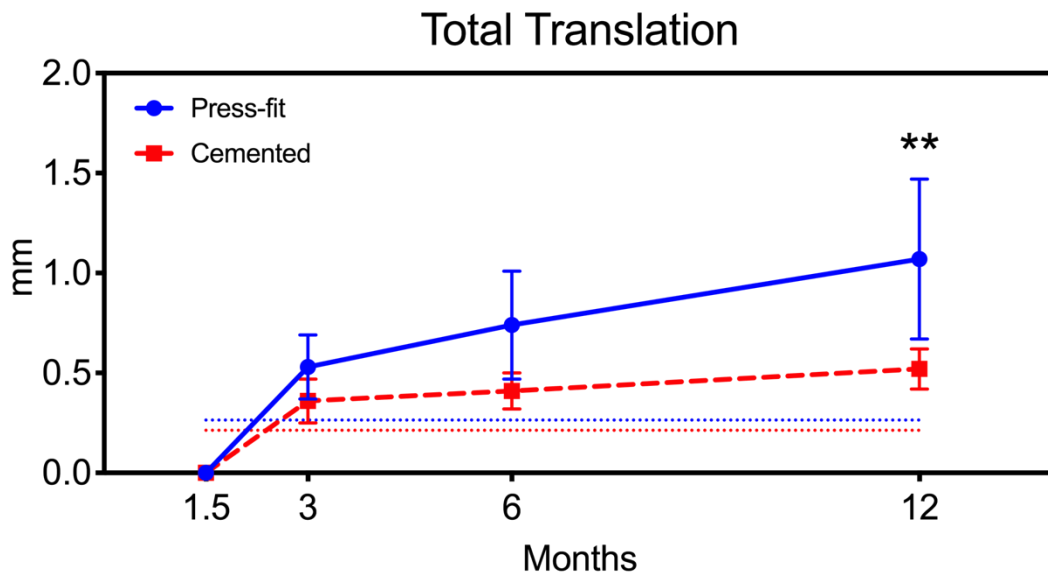
Figure E.4 Total translation (T_r) for humeral stem migration. Press-fit stems demonstrate significantly greater total translation one year ($P = 0.005$) postoperatively. Press-fit precision is represented as the fine blue dotted line, and cemented precision as the fine red dotted line.
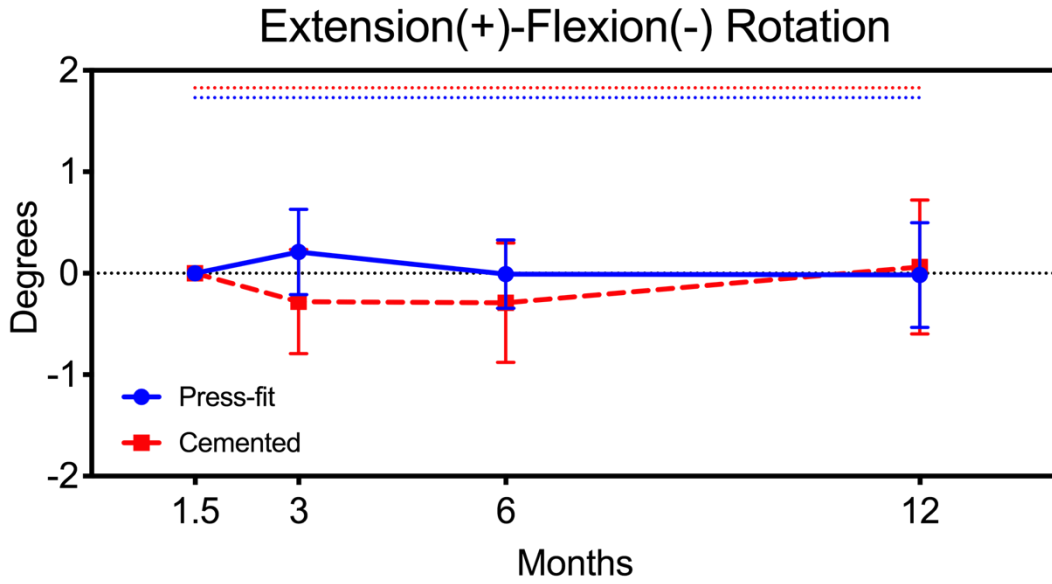
Figure E.5 Extension(+)-flexion(-) (R_x) humeral stem rotation. Press-fit precision is represented as the fine blue dotted line, and cemented precision as the fine red dotted line.
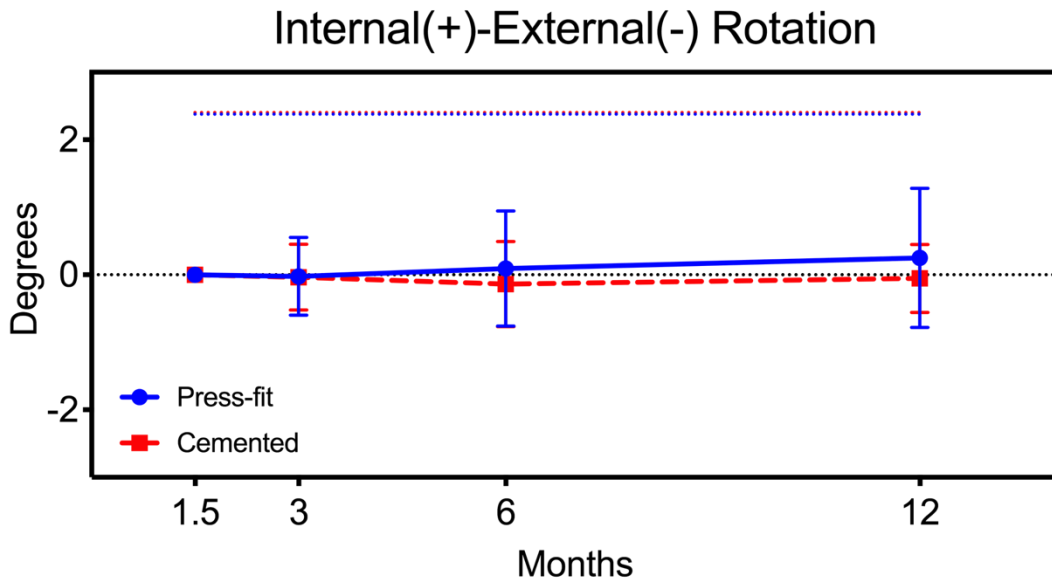
Figure E.6 Internal(+)-external(-) (R_y) humeral stem rotation. Press-fit precision is represented as the fine blue dotted line, and cemented precision as the fine red dotted line.
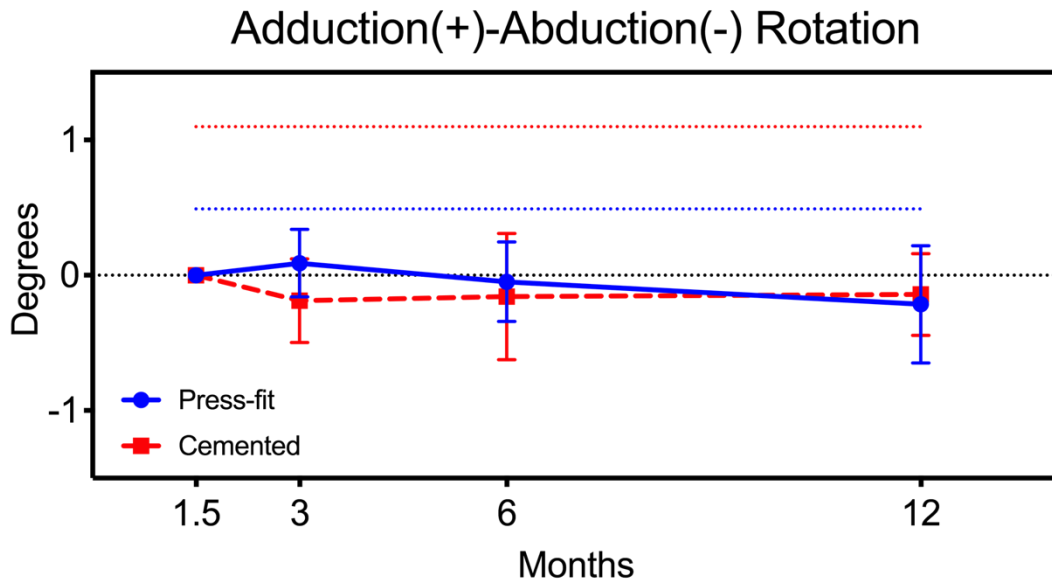
Figure E.7 Adduction(+)-abduction(-) (R_z) humeral stem rotation. Press-fit precision is represented as the fine blue dotted line, and cemented precision as the fine red dotted line.

Appendix F   Glenosphere migration graphs (Chapter 5)

Medial(+)-Lateral(-) Translation
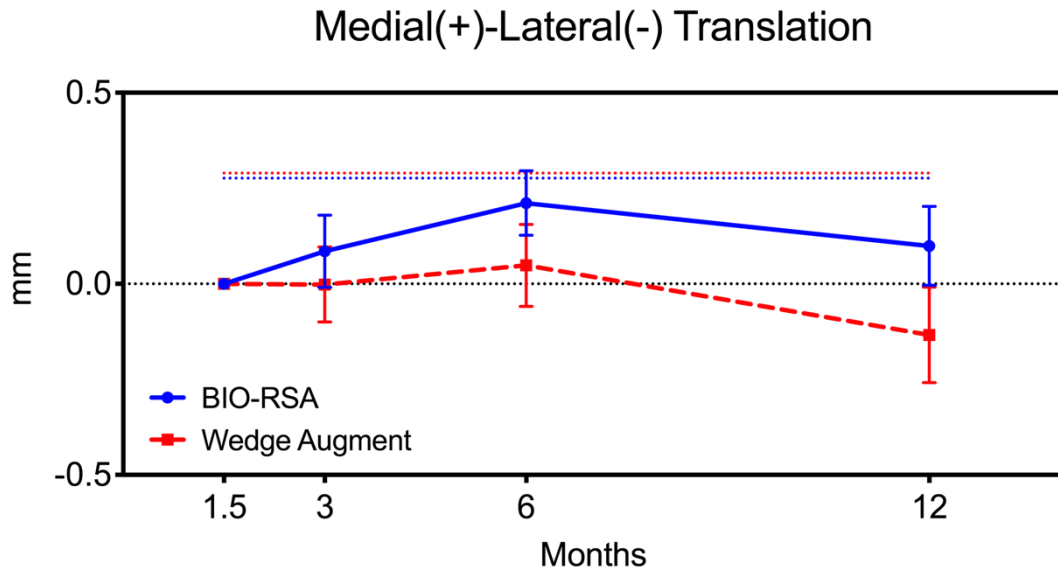
Figure F.1 Medial(+)-lateral(-) (T_x) glenosphere migration. BIO-RSA precision is represented as the fine blue dotted line, and wedge augment precision as the fine red dotted line.

Superior(+)-Inferior(-) Translation
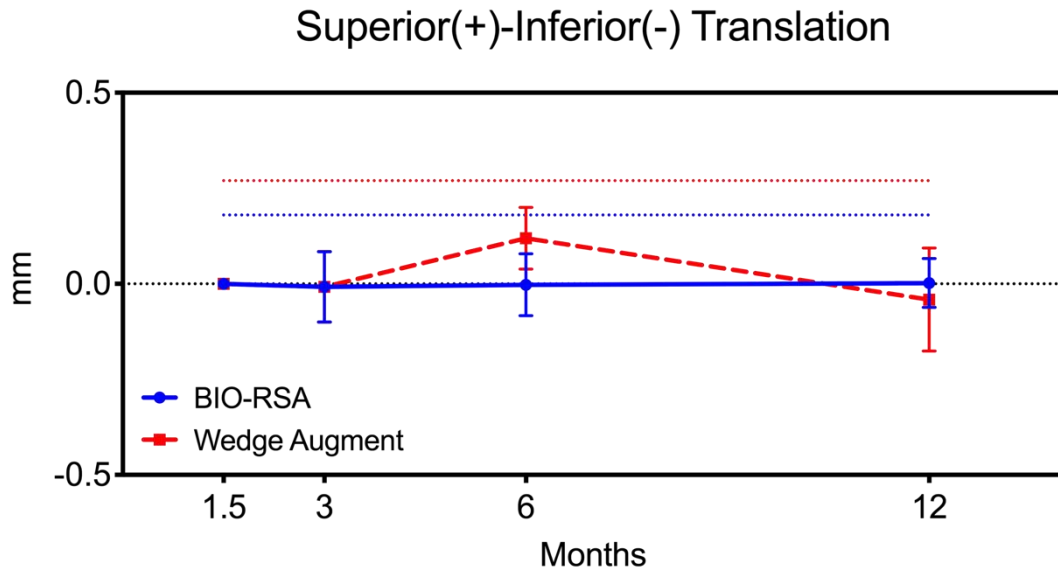
Figure F.2 Superior(+)-inferior(-) (T_y) glenosphere migration. BIO-RSA precision is represented as the fine blue dotted line, and wedge augment precision as the fine red dotted line.
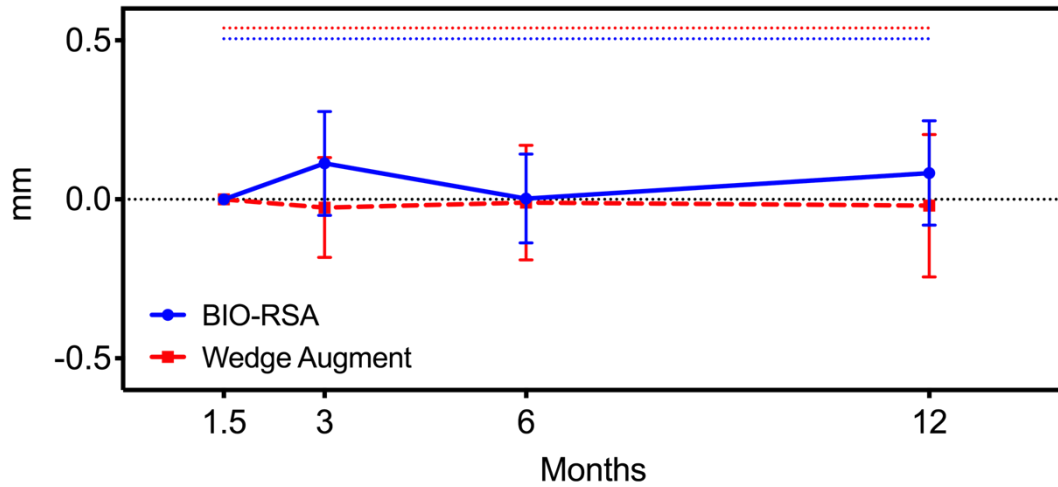
Figure F.3 Anterior(+)-posterior(-) (T_z) glenosphere migration. BIO-RSA precision is represented as the fine blue dotted line, and wedge augment precision as the fine red dotted line.
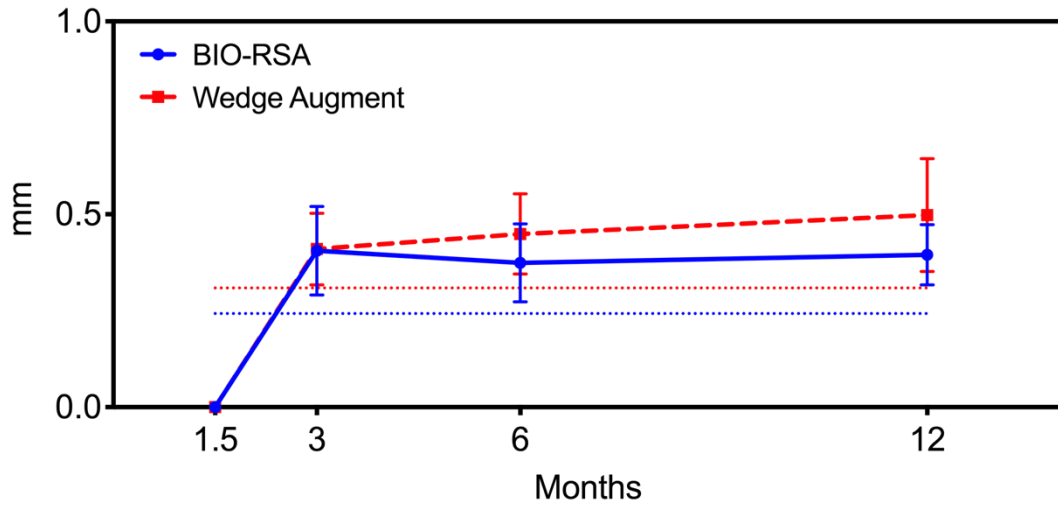
Figure F.4 Total translation (T_r) for glenosphere migration. BIO-RSA precision is represented as the fine blue dotted line, and wedge augment precision as the fine red dotted line.
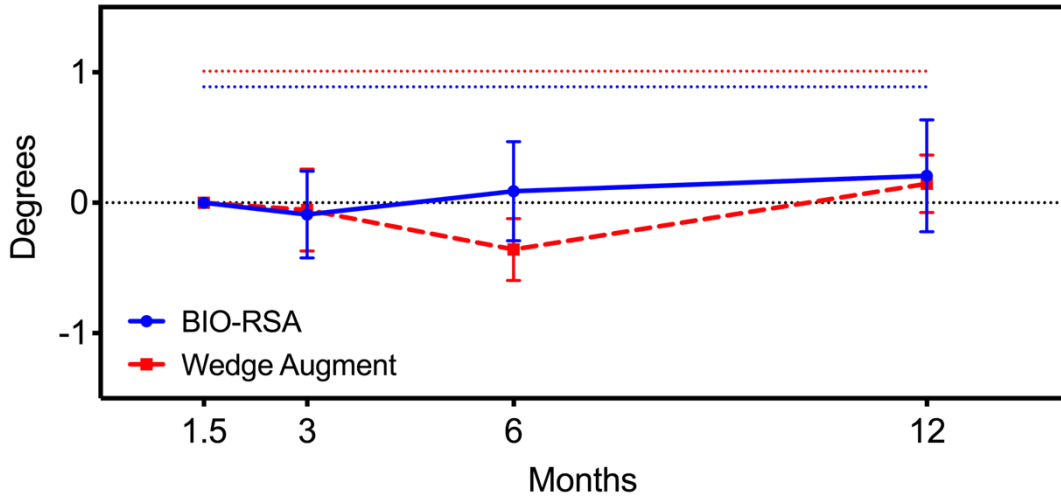
Figure F.5 Ante(+)-retro(-) glenosphere version (R_x). BIO-RSA precision is represented as the fine blue dotted line, and wedge augment precision as the fine red dotted line.
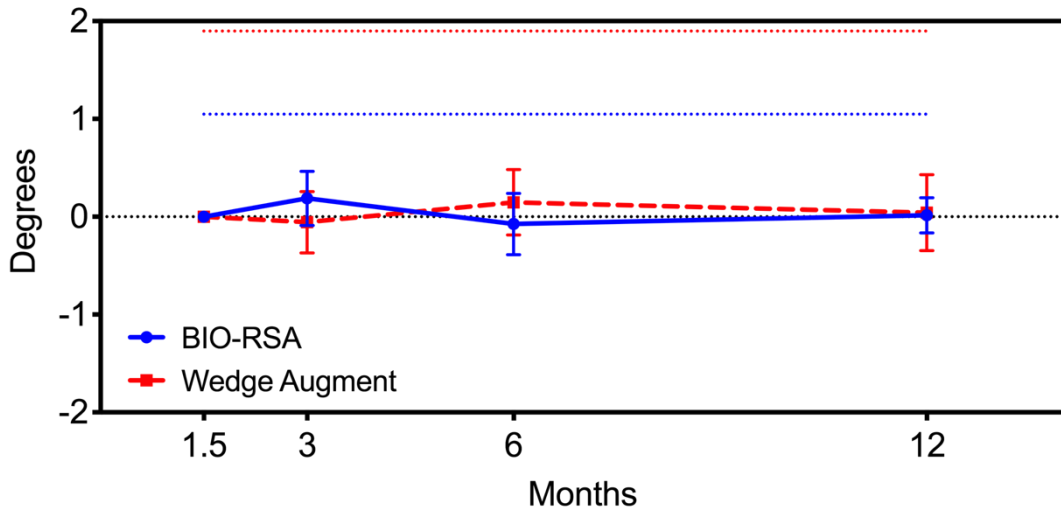
Figure F.6 Glenosphere inclination(-)-declination(+) (R_z). BIO-RSA precision is represented as the fine blue dotted line, and wedge augment precision as the fine red dotted line.

Appendix G   Simple effects analysis

Simple effects analysis is a measure of multiple comparisons, used to determine whether differences are observed within study cohorts for a repeated measure – in this case, time.

Table G.1 Within stem fixation cohorts, a significant difference was observed between the six and twelve month time points for total translation ($P = 0.026$). No significant differences were observed within the cemented cohort at any time point.

	Cemented (*P*-values)		Press-fit (*P*-values)	
	3-6 Months	*6-12 Months*	*3-6 Months*	*6-12 Months*
Medial(+)-Lateral(-) (T_x)	> 0.999	> 0.999	0.862	> 0.999
Superior(+)-Inferior(-) (T_y)	> 0.999	0.776	0.059	0.188
Anterior(+)-Posterior(-) (T_z)	> 0.999	0.290	> 0.999	> 0.999
Total Translation (T_r)	> 0.999	0.387	0.374	**0.026**
Flexion(-)-Extension(+) (R_x)	> 0.999	> 0.999	> 0.999	> 0.999
Internal(+)-External(-) (R_y)	> 0.999	> 0.999	> 0.999	> 0.999
Adduction(+)-Abduction(-) (R_z)	> 0.999	> 0.999	> 0.999	0.593

Table G.2 Within glenosphere lateralization cohorts, the metal wedge augment cohort demonstrated significant differences between time points in translation and rotation, though the magnitude of the observed difference was within the precision of the technique and therefore of little clinical value. No statistical difference was observed within the BIO-RSA cohort.

	BIO-RSA (*P*-values)		Augment (*P*-values)	
	3-6 Months	*6-12 Months*	*3-6 Months*	*6-12 Months*
Medial(+)-Lateral(-) (T_x)	0.115	0.184	0.894	**0.021**
Superior(+)-Inferior(-) (T_y)	>0.999	>0.999	**0.002**	**0.013**
Anterior(+)-Posterior(-) (T_z)	0.759	>0.999	>0.999	>0.999
Total Translation (T_r)	>0.999	>0.999	>0.999	>0.999
Anteversion(+)-Retroversion(-) (R_x)	>0.999	0.644	0.238	**0.006**
Inclination(-)-Declination(+) (R_z)	0.708	>0.999	>0.999	>0.999

Appendix H   Interaction between randomization groups

This study was effectively set up as a 2x2 factorial design randomized clinical trial, in order to evaluate both humeral stem and glenosphere fixation within the same patient group, minimizing the number of patients needed for recruitment while maintaining statistical power. Applying a three-way mixed effects model (effect of stem fixation, effect of glenosphere fixation, effect of time), we can assess whether there was any interaction between the effects. *P*-values from this analysis are presented in Table H.1, highlighting that stem fixation does not influence glenosphere fixation, and therefore the assumption of treating these patient groups as independent studies holds.

Table H.1 *P*-values from the three-way mixed effects model.

Effect	T_x	T_y	T_z	T_r	R_x	R_z
Time point	0.814	0.010	0.831	<0.001	0.847	0.598
Stem fixation	0.857	0.003	0.011	0.013	0.424	0.969
Glenosphere fixation	0.811	0.871	0.656	0.759	0.821	0.154
Time point x Stem fixation	0.349	0.002	0.096	0.110	0.399	0.132
Time point x Glenosphere fixation	0.720	0.789	0.725	0.856	0.188	0.246
Stem fixation x Glenosphere fixation	**0.568**	**0.913**	**0.271**	**0.980**	**0.820**	**0.868**
Time point x Stem fixation x Glenosphere fixation	0.572	0.934	0.081	0.476	0.800	0.318

Appendix I   Copyright licenses

Chapter 3: Validation of radiostereometric analysis in six degrees of freedom for use with reverse total shoulder arthroplasty

Chapter 6: Validation of in vivo linear and volumetric wear measurement for reverse total shoulder arthroplasty using model-based radiostereometric analysis

Licensed Content Issue	7
Licensed Content Pages	8
Type of use	Dissertation/Thesis
Requestor type	Author of this Wiley article
Format	Electronic
Portion	Full article
Will you be translating?	No
Title of your thesis / dissertation	Radiostereometric techniques in the evaluation of reverse total shoulder arthroplasty
Expected completion date	Jul 2020
Expected size (number of pages)	200
Requestor Location	Madeleine Van de Kleut Attn: Madeleine Van de Kleut
Publisher Tax ID	EU826007151

Total   0.00 CAD

Terms and Conditions

TERMS AND CONDITIONS

This copyrighted material is owned by or exclusively licensed to John Wiley & Sons, Inc. or one of its group companies (each a"Wiley Company") or handled on behalf of a society with which a Wiley Company has exclusive publishing rights in relation to a particular work (collectively "WILEY"). By clicking "accept" in connection with completing this licensing transaction, you agree that the following terms and conditions apply to this transaction (along with the billing and payment terms and conditions established by the Copyright Clearance Center Inc., ("CCC's Billing and Payment terms and conditions"), at the time that you opened your RightsLink account (these are available at any time at http://myaccount.copyright.com).

Terms and Conditions

- The materials you have requested permission to reproduce or reuse (the "Wiley Materials") are protected by copyright.

- You are hereby granted a personal, non-exclusive, non-sub licensable (on a stand-alone basis), non-transferable, worldwide, limited license to reproduce the Wiley Materials for the purpose specified in the licensing process. This license, **and any CONTENT (PDF or image file) purchased as part of your order,** is for a one-time use only and limited to any maximum distribution number specified in the license. The first instance of republication or reuse granted by this license must be completed within two years of the date of the grant of this license (although copies prepared before the end date may be distributed thereafter). The Wiley Materials shall not be used in any other manner or for any other purpose, beyond what is granted in the license. Permission is granted subject to an appropriate acknowledgement given to the author, title of the material/book/journal and the publisher. You shall also duplicate the copyright notice that appears in the Wiley publication in your use of the Wiley Material. Permission is also granted on the understanding that nowhere in the text is a previously published source acknowledged for all or part of this Wiley Material. Any third party content is expressly excluded from this permission.

- With respect to the Wiley Materials, all rights are reserved. Except as expressly granted by the terms of the license, no part of the Wiley Materials may be copied, modified, adapted (except for minor reformatting required by the new Publication), translated, reproduced, transferred or distributed, in any form or by any means, and no derivative works may be made based on the Wiley Materials without the prior permission of the respective copyright owner.**For STM Signatory Publishers clearing permission under the terms of the STM Permissions Guidelines only, the terms of the license are extended to include subsequent editions and for editions in other languages, provided such editions are for the work as a whole in situ and does not involve the separate exploitation of the permitted figures or extracts,**

190

- Should any provision of this Agreement be held by a court of competent jurisdiction to be illegal, invalid, or unenforceable, that provision shall be deemed amended to achieve as nearly as possible the same economic effect as the original provision, and the legality, validity and enforceability of the remaining provisions of this Agreement shall not be affected or impaired thereby.

- The failure of either party to enforce any term or condition of this Agreement shall not constitute a waiver of either party's right to enforce each and every term and condition of this Agreement. No breach under this agreement shall be deemed waived or excused by either party unless such waiver or consent is in writing signed by the party granting such waiver or consent. The waiver by or consent of a party to a breach of any provision of this Agreement shall not operate or be construed as a waiver of or consent to any other or subsequent breach by such other party.

- This Agreement may not be assigned (including by operation of law or otherwise) by you without WILEY's prior written consent.

- Any fee required for this permission shall be non-refundable after thirty (30) days from receipt by the CCC.

- These terms and conditions together with CCC's Billing and Payment terms and conditions (which are incorporated herein) form the entire agreement between you and WILEY concerning this licensing transaction and (in the absence of fraud) supersedes all prior agreements and representations of the parties, oral or written. This Agreement may not be amended except in writing signed by both parties. This Agreement shall be binding upon and inure to the benefit of the parties' successors, legal representatives, and authorized assigns.

- In the event of any conflict between your obligations established by these terms and conditions and those established by CCC's Billing and Payment terms and conditions, these terms and conditions shall prevail.

- WILEY expressly reserves all rights not specifically granted in the combination of (i) the license details provided by you and accepted in the course of this licensing transaction, (ii) these terms and conditions and (iii) CCC's Billing and Payment terms and conditions.

- This Agreement will be void if the Type of Use, Format, Circulation, or Requestor Type was misrepresented during the licensing process.

- This Agreement shall be governed by and construed in accordance with the laws of the State of New York, USA, without regards to such state's conflict of law rules. Any legal action, suit or proceeding arising out of or relating to these Terms and Conditions or the breach thereof shall be instituted in a court of competent jurisdiction in New York County in the State of New York in the United States of America and each party hereby consents and submits to the personal jurisdiction of such court, waives any objection to venue in such court and consents to service of process by registered or certified mail, return receipt requested, at the last known address of such party.

WILEY OPEN ACCESS TERMS AND CONDITIONS

Chapter 7: In vivo volumetric and linear wear measurement of reverse shoulder arthroplasty at minimum five-year follow-up

ELSEVIER

Reversion of rights

Articles may sometimes be accepted for publication but later rejected in the publication process, even in some cases after public posting in "Articles in Press" form, in which case all rights will revert to the author (see https://www.elsevier.com/about/our-business/policies/article-withdrawal).

Revisions and Addenda

I understand that no revisions, additional terms or addenda to this Journal Publishing Agreement can be accepted without Journal of Shoulder and Elbow Surgery Board of Trustees's express written consent. I understand that this Journal Publishing Agreement supersedes any previous agreements I have entered into with Journal of Shoulder and Elbow Surgery Board of Trustees in relation to the Article from the date hereof.

Author Rights for Scholarly Purposes

I understand that I retain or am hereby granted (without the need to obtain further permission) the Author Rights (see description below), and that no rights in patents, trademarks or other intellectual property rights are transferred to Journal of Shoulder and Elbow Surgery Board of Trustees.

The Author Rights include the right to use the Preprint , Accepted Manuscript and the Published Journal Article for Personal Use and Internal Institutional Use . They also include the right to use these different versions of the Article for Scholarly Sharing purposes, which include sharing:

- the Preprint on any website or repository at any time;

- the Accepted Manuscript on certain websites and usually after an embargo period;

- the Published Journal Article only privately on certain websites, unless otherwise agreed by Journal of Shoulder and Elbow Surgery Board of Trustees.

In the case of the Accepted Manuscript and the Published Journal Article the Author Rights exclude Commercial Use (unless expressly agreed in writing by Journal of Shoulder and Elbow Surgery Board of Trustees), other than use by the author in a subsequent compilation of the author's works or to extend the Article to book length form or re-use by the author of portions or excerpts in other works (with full acknowledgment of the original publication of the Article).

Author Representations / Ethics and Disclosure / Sanctions

I affirm the Author Representations noted below, and confirm that I have reviewed and complied with the relevant Instructions to Authors, Ethics in Publishing policy, Declarations of Interest disclosure and information for authors from countries affected by sanctions (Iran, Cuba, Sudan, Burma, Syria, or Crimea). Please note that some journals may require that all co-authors sign and submit Declarations of Interest disclosure forms. I am also aware of the publisher's policies with respect to retractions and withdrawal (https://www.elsevier.com/about/our-business/policies/article-withdrawal).

For further information see the publishing ethics page at https://www.elsevier.com/about/our-business/policies/publishing-ethics and the journal home page. For further information on sanctions, see https://www.elsevier.com/about/our-business/policies/trade-sanctions

Author representations

- The Article I have submitted to the journal for review is original, has been written by the stated authors and has not been previously published.

- The Article was not submitted for review to another journal while under review by this journal and will not be submitted to any other journal.

- The Article and the Supplemental Materials do not infringe any copyright, violate any other intellectual property, privacy or other rights of any person or entity, or contain any libellous or other unlawful matter.

- I have obtained written permission from copyright owners for any excerpts from copyrighted works that are included and have credited the sources in the Article or the Supplemental Materials.

- Except as expressly set out in this Journal Publishing Agreement, the Article is not subject to any prior rights or licenses

and, if my or any of my co-authors' institution has a policy that might restrict my ability to grant the rights required by this Journal Publishing Agreement (taking into account the Author Rights permitted hereunder, including Internal Institutional Use), a written waiver of that policy has been obtained.

- If I and/or any of my co-authors reside in Iran, Cuba, Sudan, Burma, Syria, or Crimea, the Article has been prepared in a personal, academic or research capacity and not as an official representative or otherwise on behalf of the relevant government or institution.

- If I am using any personal details or images of patients, research subjects or other individuals, I have obtained all consents required by applicable law and complied with the publisher's policies relating to the use of such images or personal information. See https://www.elsevier.com/about/our-business/policies/patient-consent for further information.

- Any software contained in the Supplemental Materials is free from viruses, contaminants or worms.

- If the Article or any of the Supplemental Materials were prepared jointly with other authors, I have informed the co-author(s) of the terms of this Journal Publishing Agreement and that I am signing on their behalf as their agent, and I am authorized to do so.

Governing Law and Jurisdiction

This Agreement will be governed by and construed in accordance with the laws of the country or state of Journal of Shoulder and Elbow Surgery Board of Trustees ("the Governing State"), without regard to conflict of law principles, and the parties irrevocably consent to the exclusive jurisdiction of the courts of the Governing State.

For information on the publisher's copyright and access policies, please see http://www.elsevier.com/copyright.
For more information about the definitions relating to this agreement click here.

☑ **I have read and agree to the terms of the Journal Publishing Agreement.**

7 January 2020   T-copyright-v22/2017

Curriculum Vitae

MADELEINE L. VAN DE KLEUT PhD(C)

EDUCATION AND TRAINING

09/16 – Present **PhD Biomedical Engineering (Biomechanics)**

Doctoral Thesis: The migration and wear of reverse total shoulder arthroplasty

Supervisor: Matthew G. Teeter

Collaborative Training Program in Musculoskeletal Health Research, Bone and Joint Institute

University of Western Ontario, London, Canada

Expected: July 2020

09/12 – 04/16 **BMSc (Honours) Medical Biophysics (Clinical Physics Concentration)**

With distinction
University of Western Ontario, London, Canada

RESEARCH EXPERIENCE

2016 – Present **Research Assistant to Matthew G. Teeter, PhD**
Imaging Research Laboratories, Robarts Research Institute

University of Western Ontario

2014 – 2016 **Research Assistant to Jeffrey J. L. Carson, PhD**
Optics and Photonics Laboratory, Lawson Health Research Institute

University of Western Ontario

AWARDS AND DISTINCTIONS

2019 – 2020 **Queen Elizabeth II Graduate Scholarship in Science and Technology** ($15,000)
University of Western Ontario

2018 – 2020 **Transdisciplinary Bone and Joint Training Award** ($9,000 annually)
Bone and Joint Institute, University of Western Ontario

2018 – 2019	**Ontario Graduate Scholarship** ($15,000)	
	University of Western Ontario	
2017 – 2018	**Ontario Graduate Scholarship** ($15,000)	
	University of Western Ontario	
2016 – 2018	**Transdisciplinary Bone and Joint Training Award** ($10,000 annually)	
	Bone and Joint Institute, University of Western Ontario	
2016 – 2017	**Canada Graduate Scholarship – Master's** ($17,500)	
	Canadian Institutes of Health Research	
2016	**Strik Couprie Inch Cancer Research Course Prize** ($300)	
	University of Western Ontario	
2015	**Reinhard Konrad Memorial Award in Science** ($1,500)	
	Faculty of Science, University of Western Ontario	
2014	**Cancer Research and Technology Transfer (CaRTT) Summer Studentship** ($7,148)	
	Schulich School of Medicine and Dentistry, University of Western Ontario	
2013 – 2016	**Dean's Honour List**	
	Faculty of Science, University of Western Ontario	
2012 – 2016	**Continuing Admission Scholarship** ($2,500 annually)	
	University of Western Ontario	

PEER REVIEWED PUBLICATIONS

1. **Van de Kleut, M. L.**, Bloomfield, R. A., Teeter, M. G., & Athwal, G. S. (2020). Monitoring daily shoulder activity before and after reverse total shoulder arthroplasty using inertial measurement units. *Journal of Shoulder and Elbow Surgery*. Accepted.

2. **Van de Kleut, M. L.**, Nair, C., Milner, J. Holdsworth, D., Athwal, G. S., & Teeter, M. G. (2020). In vivo reverse total shoulder arthroplasty contact mechanics. *Journal of Shoulder and Elbow Surgery*. Epub ahead of print.

3. **Van de Kleut, M. L.**, Athwal, G. S., Faber, K. J., Yuan, X., & Teeter, M. G. (2020). In vivo volumetric and linear wear measurement for reverse total shoulder arthroplasty with minimum five-year follow-up. *Journal of Shoulder and Elbow Surgery. 29(8),* 1695-1702.

4. **Van de Kleut, M. L.**, Athwal, G. S., Yuan, X., & Teeter, M. G. (2019). Validation of in vivo linear and volumetric wear measurement for reverse total shoulder arthroplasty using model-based radiostereometric analysis. *Journal of Orthopaedic Research, 37(7),* 1620–1627.

5. **Van de Kleut, M. L.**, Yuan, X., Athwal, G. S., & Teeter, M. G. (2018). Additively manufactured implant components for imaging validation studies. *Proceedings of the Institution of Mechanical Engineers, Part H: Journal of Engineering in Medicine*, *232*(7), 690–698.

6. **Van de Kleut, M. L.**, Yuan, X., Athwal, G. S., & Teeter, M. G. (2018). Validation of radiostereometric analysis in six degrees of freedom for use with reverse total shoulder arthroplasty. *Journal of Biomechanics*, *68*, 126–131.

PUBLISHED CONFERENCE PROCEEDINGS

1. **Van de Kleut, M. L.**, Athwal, G. S., Yuan, X., & Teeter, M. G. (2020). Glenosphere and humeral stem fixation in reverse total shoulder arthroplasty: A prospective, randomized clinical trial. *Orthopaedic Proceedings, 102-B, SUPP_1*, 22.

2. **Van de Kleut, M. L.**, Athwal, G. S., Yuan, X., & Teeter, M. G. (2020). Polyethylene wear measurement following reverse total shoulder arthroplasty: An in vivo pilot study with minimum six-year follow-up. *Orthopaedic Proceedings, 102-B, SUPP_1*, 23.

3. **Van de Kleut, M. L.**, Athwal, G. S., Yuan, X., & Teeter, M. G. (2019). Evaluation of implant fixation in reverse total shoulder arthroplasty: A prospective, randomized clinical trial. *Orthopaedic Proceedings, 101-B, SUPP_4*, 14.

REFEREED CONFERENCE ABSTRACTS AND PRESENTATIONS

1. **Madeleine L. Van de Kleut**, George S. Athwal, Xunhua Yuan, Matthew G. Teeter. Cemented vs uncemented humeral stem fixation in reverse total shoulder arthroplasty: A prospective, randomized clinical trial. *American Academy of Orthopaedic Surgeons*, Orlando, United States. March 24-28, 2020.

2. **Madeleine L. Van de Kleut**, Xunhua Yuan, Matthew G. Teeter, George S. Athwal. BIO-RSA versus augmented baseplates in reverse shoulder arthroplasty: A prospective, randomized clinical trial utilizing radiostereometric analysis. *American Academy of Orthopaedic Surgeons*, Orlando, United States. March 24-28, 2020.

3. **Madeleine L. Van de Kleut**, George S. Athwal, Kenneth J. Faber, Matthew G. Teeter. In vivo polyethylene wear measurement following reverse total shoulder arthroplasty: A minimum 6-year follow-up. *American Academy of Orthopaedic Surgeons*, Orlando, United States. March 24-28, 2020.

4. **Madeleine L. Van de Kleut**, George S. Athwal, Xunhua Yuan, Matthew G. Teeter. Glenosphere and humeral stem fixation in reverse total shoulder arthroplasty: A prospective, randomized clinical trial. *The International Society for Technology in Arthroplasty*, Toronto, Canada. October 2-5, 2019.

5. **Madeleine L. Van de Kleut**, George S. Athwal, Kenneth, J. Faber, Xunhua Yuan, Matthew G. Teeter. Polyethylene wear measurement following reverse total shoulder arthroplasty: An in vivo pilot study with minimum six-year follow-up. *The International Society for Technology in Arthroplasty*, Toronto, Canada. October 2-5, 2019.

6. **Madeleine L. Van de Kleut**, George S. Athwal, Xunhua Yuan, Matthew G. Teeter. In vivo contact kinematics following reverse total shoulder arthroplasty: An RCT comparing glenosphere fixation technique. *London Health Research Day*, London, Canada. April 30, 2019.

7. **Madeleine L. Van de Kleut**, George S. Athwal, Xunhua Yuan, Matthew G. Teeter. Validation of in vivo linear and volumetric wear measurement for reverse total shoulder arthroplasty using model-based radiostereometric analysis. *6th International Radiostereometric Analysis Conference*, Aarhus, Denmark. April 4-6, 2019.

8. **Madeleine L. Van de Kleut**, Xunhua Yuan, George S. Athwal, Matthew G. Teeter. Implant fixation in reverse total shoulder arthroplasty: A prospective, randomized clinical trial. *6th International Radiostereometric Analysis Conference*, Aarhus, Denmark. April 4-6, 2019.

9. **Madeleine L. Van de Kleut**, George S. Athwal, Xunhua Yuan, Matthew G. Teeter. In vivo polyethylene wear measurement in reverse total shoulder arthroplasty. *Imaging Network Ontario*, London, Canada. March 28-29, 2019.

10. **Madeleine L. Van de Kleut**, George S. Athwal, Xunhua Yuan, Matthew G. Teeter. Evaluation of implant fixation in reverse total shoulder arthroplasty: A prospective, randomized clinical trial. *The International Society for Technology in Arthroplasty*, London, United Kingdom. October 10-13, 2018.

11. **Madeleine L. Van de Kleut**, George S. Athwal, Xunhua Yuan, Matthew G. Teeter. Reverse total shoulder arthroplasty and implant migration: Does arm activity play a role? *Canadian Bone and Joint Conference*, London, Canada. May 11, 12 2018.

12. **Madeleine L. Van de Kleut**, George S. Athwal, Xunhua Yuan, Matthew G. Teeter. Arm activity and implant migration analysis following reverse total shoulder arthroplasty. *Imaging Network Ontario*, Toronto, Canada. March 28, 29 2018.

13. **Madeleine L. Van de Kleut**, Xunhua Yuan, George S. Athwal, Matthew G. Teeter. Validation of radiostereometric analysis for use with reverse total shoulder arthroplasty. *Australia New Zealand Orthopedic Research Society & Radiostereometric Analysis Joint Conference*, Adelaide, Australia. October 6-8, 2017.

14. Lawrence C. M. Yip, Parsa Omidi, **Madeleine L. Van de Kleut**, Ivan Kosik, Astrid Chamson-Reig, Jeffrey J. L. Carson. Development of a photoacoustic imaging system for intraoperative breast tumour margin assessment: Initial results. *Oncology Research and Education Day*, London, Canada. June 16, 2017.

15. **Madeleine L. Van de Kleut**, Xunhua Yuan, George S. Athwal, Matthew G. Teeter. 3D printed components for phantom validation studies of imaging measurements. *London Health Research Day*, London, Canada. March 28, 2017.

16. Lawrence C. M. Yip, **Madeleine L. Van de Kleut**, Ivan Kosik, Astrid Chamson-Reig, Jeffrey J. L. Carson. A photoacoustic solution for tumour margin assessment: Reducing repeat lumpectomies. *London Health Research Day*, London, Canada. March 28, 2017.

17. **Madeleine L. Van de Kleut**, Xunhua Yuan, George S. Athwal, Matthew G. Teeter. Validation of radiostereometric analysis for use with reverse total shoulder arthroplasty. *Imaging Network Ontario Symposium*, London, Canada. March 15, 16 2017.

18. Lawrence C. M. Yip, **Madeleine L. Van de Kleut**, Ivan Kosik, Astrid Chamson-Reig, Jeffrey J. L. Carson. Intraoperative breast tumour margin assessment: A photoacoustic solution. *Imaging Network Ontario Symposium*, London, Canada. March 15, 16 2017. **2nd place Poster Award Winner.**

19. Lawrence C. M. Yip, **Madeleine L. Van de Kleut**, Ivan Kosik, Astrid Chamson-Reig, Jeffrey J. L. Carson. Novel hybrid imaging system to aid in surgical decision making. *Western Research Forum*, London, Canada. March 10, 2017.

20. **Madeleine L. Van de Kleut,** Philip Wong, Ivan Kosik, Jeffrey J. L. Carson. Investigating the use of 3D photoacoustic imaging for imaging the human hand. *London Health Research Day*, London, Canada. March 29, 2016.

21. Lawrence C. M. Yip, **Madeleine L. Van de Kleut**, Ivan Kosik, Astrid Chamson-Reig, Jeffrey J. L. Carson. Development of an intraoperative photoacoustic imaging system for ex vivo breast tissue margin assessment. *London Health Research Day*, London, Canada. March 29, 2016.

22. **Madeleine L. Van de Kleut,** Avery Raess, Philip Wong, Ivan Kosik, Jeffrey J. L. Carson. The effect of matching layers as an acoustic lens in a staring transducer array in photoacoustic imaging. *Imaging Network Ontario Symposium*, London, Canada. March 30, 31 2015.

INVITED PRESENTATIONS

1. **Madeleine L. Van de Kleut**. Radiostereometric analysis for the evaluation of reverse total shoulder arthroplasty. *Innovation in Motion – Health Sciences/Biomedical Engineering Collaborative Research Day*, London, Canada. June 3, 2019.

SUPERVISION, MENTORING, AND TEACHING ACTIVITIES

Winter 2020   **Teaching Assistant**

Engineering Science 1050: Foundations of Engineering Practice (YR1)

Faculty of Engineering
University of Western Ontario

Fall 2019   **Teaching Assistant**

Electrical and Computer Engineering 4445: Introduction to Digital Image Processing (YR4/Graduate)

Faculty of Engineering
University of Western Ontario

Summer 2019   **Project Mentor**

Mentee: Chaithanya Nair (YR2 Undergraduate)

Research Project: *Reverse total shoulder arthroplasty implant retrieval analysis*

University of Western Ontario

Winter 2019   **Teaching Assistant**

Electrical and Computer Engineering 3331: Introduction to Signal Processing (YR3)

Faculty of Engineering
University of Western Ontario

Summer 2018   **Project Mentor**

Mentee: Fay Zhuang (YR1 Undergraduate)

Research Project: *In vivo contact mechanics following reverse total shoulder arthroplasty*
University of Western Ontario

Fall 2018   **Teaching Assistant**

Electrical and Computer Engineering 4445: Introduction to Digital Image Processing (YR4/Graduate)

Faculty of Engineering
University of Western Ontario

Winter 2018   **Teaching Assistant**

Electrical and Computer Engineering 4438: Advanced Digital Image Processing (YR4/Graduate)

Faculty of Engineering
University of Western Ontario

Fall 2017	**Teaching Assistant**
	Electrical and Computer Engineering 4445: Introduction to Digital Image Processing (YR4/Graduate)
	Faculty of Engineering University of Western Ontario
Fall 2016 – Winter 2017	**Teaching Assistant**
	Engineering Science 1050: Introduction to Design and Innovation Studio (YR1)
	Faculty of Engineering University of Western Ontario
2016	**Project Mentor**
	Mentee: Laura Feldstein (YR3 Undergraduate)
	Research Project: *Photoacoustic Imaging of the Human Hand*
	University of Western Ontario

SERVICE AND LEADERSHIP EXPERIENCE

2019 – Present	**Student Reviewer, Biomedical Imaging Research Center (BIRC)**
	London, Canada
2019	**Student Reviewer**, **External review for the School of Biomedical Engineering** University of Western Ontario
2018 – Present	**Chair, Biomedical Engineering Graduate Student Committee**
	University of Western Ontario
2018 – Present	**Department Representative, Schulich Graduate Student Council**
	University of Western Ontario
2018	**Member, The Health Research Journal Club Ivey International Center for Health Innovation**
	University of Western Ontario
2016 – 2017	**Social Representative, Biomedical Engineering Graduate Student Committee**
	University of Western Ontario
2015 – 2016	**Vice President Events, Making Waves London**
	Making Waves Canada, London Chapter

2015 – 2016	**Co-Founder, Biophysics Network for Students (BONeS)**
	Schulich School of Medicine and Dentistry, University of Western Ontario
2015 – 2016	**Secretary, Science Students' Council**
	Faculty of Science, University of Western Ontario

COMMUNITY OUTREACH

2019 – Present	Let's Talk Science teacher partnership program – Paired with Grade 1 classroom to conduct scientific workshops once per unit (~bimonthly), Tecumseh Public School, London, Canada
2019	Judge – London Health Research Day, London, Canada
2019	Invited presentation – International Day for Women in Science, St. Paul Catholic Elementary School (Grade 7 and 8 classes), London, Canada

PROFESSIONAL DEVELOPMENT COURSES AND WORKSHOPS*

*In collaboration with the Collaborative Training Program in Musculoskeletal Health Research and the Ivey Business School – International Centre for Health Innovation

University of Western Ontario

2020	**Managerial Accounting**
	Presented by: Christopher Sturby, MBA
2019	**Consulting in Life Sciences**
	Presented by: Lisa Purdy
2019	**Introduction to Negotiations for Leaders**
	Presented by: Fernando Olivera, PhD
2019	**Introduction to Strategy**
	Presented by: Michael Rouse, PhD
2019	**Engaging with Leaders in Health Care**
	Presented by: Ivey International Center for Health Innovation Advisory Council Members
2018	**Learning How to Read Financial Statements for MSK Students**
	Presented by: Mary Gillett, MBA, HBA, CPA

2018	**Capacity Planning in Healthcare: Historical Approaches and Future Directions**
	Presented by: Matthew Myer, PhD
2017	**Design-Driven Innovation**
	SGPS 9101. Course instructor: Darren Meister, PhD
2017	**Health Systems Structure and Trends**
	Presented by: Vania Sakelaris
2017	**Small and Medium Enterprises – Building the Case for Commercialization and Venture Capital Investment**
	Presented by: Brent Norton, PhD
2017	**Introduction to Pharmaceuticals and Medical Devices**
	Presented by: Michael Rouse, PhD